Synthesis and Evaluation of Carbohydrate Based Cationic Polymers for siRNA Delivery and Tracking

Dissertation submitted to faculty of

University of Minnesota, Twin Cities in partial

fulfillment of the requirements for the degree of

Doctor of Philosophy (Ph.D.)

By

Lian Xue

July 2014

Advisor: Dr. Theresa M. Reineke

Published July 2014

ACKNOWLEDGEMENT

Hereby I thank my advisor Dr. Theresa M. Reineke for her great effort in training me to think critically and independently as a chemist. Her patience, insistence and striving for excellence will keep encouraging me for the rest of my career.

I thank my parents and my younger sister for their great support for my study. Their caring and optimistic spirit will always make my gloomy days shining. I thank Shengjie Yu for not making me angry.

I thank Dr. Nilesh Ingle for his training on the new flowcytometor. I thank Dr. Antons Sizov for a lot of discussion on synthetic problems. I thank Dr. Karina Kizjakina for her training in a lot of carbohydrate chemistry. Special thanks to Cocoa Wang from Virginia Tech for the measurement of relaxivity of the Gd containing compound for theronostic project, to Evan Weitz from Dr. Valérie C. Pierre's group for the training on Uv-vis for luminescence lifetime measurement, to Dr. Sneha Sanjay Kelkar for training on dynamic light scattering instrument.

I would like to thank my committee members in University of Minnesota, Twin Cities Dr. Michael Bowser, Dr. Timothy P Lodge and Dr. Wei-Shou Hu for their valuable advice and inspiring comments. I would also thank my committee members back in Virginia Tech Dr. Judy Riffle, Dr. Webster Santos and Dr. David G.I. Kingston for their help and their advice on my projects.

I also would like to thank my group and fellow colleagues for their great support. Thank to Yaoying Wu and Dustin Spouse for help during moving from Virginia Tech. Many thanks to the department officials Nancy Thao, Dr. Philippe Buhlmann for a lot of

supportive work and documentation works. Thanks to the ISSS for their efficient and supportive work for the international students.

Lastly and importantly, thanks to all my roommates I have ever lived with and their kindness to share a lot of joyful moments.

Abstract

Biocompatible and biodegradable macromolecules have been intensively used in pharmaceutical industries in various formulation preparations to fulfill different requirements. In the last two decades, RNA interference (RNAi) gene regulation has attracted a lot of attention for its high potency in medical applications. However, inadequate delivery of RNA molecules to intracellular target sites has become the bottleneck in both laboratory use and clinical therapy in the future. In general, the small interfering RNA molecules as well as other RNA molecules have poor pharmacokinetic profiles, can easily be hydrolyzed or degraded, cause serious immunogenic response and can be toxic to particular cell types and organs. To fulfill the demands, a variety of polymeric vehicles have been synthesized and investigated, and various chemical reactions have endowed the delivery systems with properties like high membrane permeability, low toxicity and tunable size and surface functionalities for anti-aggregation, etc. In our research, we have explored the major parameters that influenced the efficiency of siRNA delivery based on the experiments using carbohydrate based cationic polymers as successful biocompatible polymer models. Structure-property relationship has been studied from many perspectives, including the carbohydrate units, length of the polymers, dose response, and topology of the polymer-siRNA polyplexes in this study.

Herein, two series of carbohydrate-based polycations were synthesized and examined that varied in the degree of polymerization (n)—one containing trehalose [Tr4(n) series: Tr4(23), Tr4(55), Tr4(77)] and the other containing beta-cyclodextrin [CD4(n) series: CD4(10), CD4(26), CD4(39), CD4(143), CD4(239)]. In addition, two

monosaccharide models were examined for comparison that contains tartaramidoamine (T4) and galactaramidoamine (G4 or Glycofect) repeats. Delivery profiles for pDNA were compared with those obtained for siRNA delivery and reveal that efficacy differs significantly as a function of carbohydrate type, nucleic acid type and dose, polymer length, and presence of excess polymer in the formulation. The Tr4 polymers yielded higher efficacy for pDNA delivery, yet, the CD4 polymers achieved higher siRNA delivery and gene down regulation. The T4 and Glycofect derivatives, while efficient for pDNA delivery, were completely ineffective for siRNA delivery. A strong polymer length and dose dependence on target gene knockdown was observed for all polymers tested. Also, free polymer in solution (uncomplexed) was demonstrated to be a key factor in promoting siRNA uptake and gene down regulation.

The carbohydrate family has been systematically studies in biochemistry. Inspired by the nature, carbohydrates have been a platform that polymer chemists have gained ideas from to improve stability and biocompatibility of nanosystems, for example, by incorporating them as degradable domains or using them as new coating materials. Herein, we have examined nanosystems that have been coated with synthetic polycarbohydrates: poly(glucose) and poly(trehalose), as coating materials aimed to improve the profile of siRNA delivery into brain cancer cells. The poly(trehalose) coated nanocomplexes were demonstrated to be substantially effective for quantitative siRNA delivery in presence of high salt concentrations and serum proteins. The ability of trehalose to lower phase transition energy associated with water freezing and protective properties have shown that poly(trehalose) has great promise to serve as an important component in formulation of effective nanomedicines.

In order to fulfill the requirement for tracking the nanoparticles, studying the intracellular unpacking mechanism as well as pharmacokinetic studies in future, we have also developed series of cationic polymers combining lanthanide ion chelating domains. To improve the biocompatibility and the performance of the polymers in facilitating the dissociation of the nanoparticles, we have incorporated the α,α-(D)-trehalose, a naturally abundant disaccharide into the polymer chains. The trehalose has been known for its potency in protecting biological materials from dehydration and aggregation. The so-formed trehalose containing polymers have shown to be effective material to facilitate siRNA mediated target gene knockdown. The complexation and dissociation with siRNA can also be monitored via FRET (Förster resonance energy transfer) by chelating the polymers with luminescent lanthanide ions (Eu^{3+} and Tb^{3+}) and labeling the siRNA with organic dyes (Cy5 and TMR). On the other hand, compared with the currently commercially-available MRI contrast agent Magnevist, the polymers have achieved twice the relaxivity in two different magnetic fields.

In summary, by combining the carbohydrate moieties and oligoamines, we have systematically examined the structure-property relationship of various well designed polymers on siRNA delivery profiles using glioblastoma cells as model. On the other hand, we have successfully incorporated the trehalose moieties into the lanthanide chelating polymers to increase the biocompatibility and performance of the polymers for both siRNA delivery and imaging. By incorporating different lanthanide ions, we can potentially use these well structured polymers as theranostic models in fundamental biological research.

List of Content

Acknowledgement----------**i**

Abstract----------**iii**

List of Content----------**iv**

List of Figures----------**ix**

List of Tables----------**xii**

List of Schemes----------**xiii**

List of Abbreviations----------**xiv**

List of Publications---------- **-xvii**

Chapter 1: Introduction: Polymeric Materials for siRNA delivery and tracking----1

1. Cellular mechanism and barriers for siRNA delivery----------2

2. Versatile synthetic strategies for siRNA delivery----------6

3. Targeted delivery systems for siRNA----------21

4. siRNA delivery tracking and theranostics development----------31

Chapter 2: Carbohydrate Based Cationic Polymers for siRNA Delivery-- Role of Polymer Length, Carbohydrate Size, and Nucleic Acid Type----------44

1. Background----------45

2. Introduction----------45

3. Experimental section----------50

Materials and methods----------50

Synthesis and characterization of the carbohydrate-containing monomers and Polymers----------51

Polymer siRNA binding studies via gel electrophoresis shift assays----------55

Polyplex formation and analysis via dynamic light scattering (DLS)----------56

Cell culture studies----------56

Luciferase assay and protein assay----------57

Cellular uptake measurement by flow cytometry----------58

MTT assay----------59

4. Results----------60

Preparation and characterization of polymer vehicles----------60

Gel electrophoresis study of polymer-siRNA complexation----------63

Dynamic light scattering (DLS) study----------66

Effect of polyplex formulation on siRNA delivery to cultured glioblastoma cells ----------69

Promotion of siRNA-mediated gene down regulation by addition of free Polymers----------72

Influence of polymer length on polyplex uptake and efficacy----------75

Comparison of pDNA and siRNA delivery profiles----------77

MTT assay to evaluate the cytotoxicity----------79

5. Discussion----------80

Chapter 3. Promotion and stabilization effect of poly carbohydrates coating for nanosystems in siRNA delivery into cancer cells.----------94

1. Background----------95

2. Introduction----------96

3. Materials----------100

4. Polymer Synthesis----------102

5. Material preparation and properties study----------115

Polyplex formulation of diblock copolymer with siRNA----------115

Polyplex lyophilization----------116

Gel electrophoresis of polyplexes----------116

Dynamic light scattering measurements----------117

Evaluation of phase transitions of the polytrehalose and trehalose solutions with differential scanning calorimetry (DSC)----------118

6. Biological studies to evaluate the copolymers on siRNA delivery----------120

Cell culture experiments----------120

Cellular uptake measurement by flow cytometry----------121

Cellular uptake study via cell confocal microscopy----------126

Luciferase assay and protein assay----------128
Assessment of toxicity via MTT assay----------135
7. Discussion and conclusion----------136
Chapter 4. Trehalose containing lanthanide click polycations for siRNA delivery and tracking ----------141
1. Background----------142
2. Introduction----------143
3. Experiments and results----------147
Materials----------147
Synthesis of monomers and polymers----------150
Investigation on properties of polymers----------161
Determination of the number of water coordinate sites----------161
Inductively coupled plasma optical emission spectroscopy----------162
Polymer siRNA binding assay----------163
Relaxivity of Gd chelated polymers----------164
Dynamic light scattering study----------166
Stability of polyplexes upon addition of heparin----------167
FRET(Fluorescence resonance energy transfer) of polymer/siRNA complexation----------168
Cellular uptake of polyplexes and target gene knockdown in brain cancer cells----------172
Cellular uptake for polyplexes via flowcytometry----------172
Luciferase assay for siRNA mediated gene knockdown----------173
Cytotoxicity study via MTT assay----------175
4. Conclusion----------177
Chapter 5. Conclusions----------183
Reference----------189

List of Figures

Chapter 1

Figure 1. (a). Structure of siRNA (b). The exogenous dsRNA induced gene silencing pathway.--4

Figure 2. Common sites of chemical modification on siRNA backbones----------7

Figure 3. A. Aptamer-conjugated siRNA B. cholesterol-conjugated siRNA.----------8

Figure 4. Lac-PEG-siRNA conjugates.----------8

Figure 5. Stable nucleic acid-lipid particles (SNALPs).----------11

Figure 6. Structure of PEI.----------12

Figure 7: A. PEGylation of siRNA via SPDP linker. B.The formation of siRNA-PEG/PEI polyelectrolyte.----------13

Figure 8: A. Synthetic scheme of graft copolymer of PEI and PEG.----------14

Figure 9: The structure of chitosan, only the deacetylated units are shown in the figure.----------16

Figure 10: A.The structure of bis-(guanidinium)-tetrakis-(β-cyclodextrin) dendrimeric tetrapod.17

Figure 11: The self assembly of cyclodextrin linear polymer with adamantane terminated polymeric chains.----------18

Figure 12: Structure of cyclodextrin linear click copolymers.----------19

Figure 13: Examples of PGAAs (Poly(glycoamidoamine)s).----------19

Figure 14: Structure of trehalose click copolymers.----------20

Figure 15: The diagrammatic structure of IgG.----------23

Figure 16: The conjugation of antibodies to polymers.----------24

Figure 17: The synthetic route of conjugating RGD to PEI.----------26

Figure 18: Sequence of the modified LHRH, structure of CPT and LHRH-PEG-CPT conjugate.27

Figure 19: Synthesis of siRNA-PEG-LHRH conjugates and self assembly of polyelectrolyte.---28

Figure 20: The structure of folic acid and synthetic route of polymer.----------29

Figure 21: Conjugating lactose to the block copolymer via reductive coupling.----------31

Figure 22. Schematic representation of siRNA absorption and Dox loading onto L-amino acid β-CD modified QDs.----------33

Figure 23. Structures of polycations containing lanthanide chelates.----------35

Chapter 2

Figure 1. Schematic structures of the carbohydrate-containing cationic polymers.----------47

Figure 2. Schematic showing the different delivery destination of siRNA (cytoplasm) and pDNA (nucleus).----------47

Figure 3: 1H-NMR characterization of polymers Tr4 and CD4.----------62

Figure 4: SEC characterization for trehalose polymer Tr4(77).----------63

Figure 5. The binding of polymers with siRNA examined by agarose gel electrophoresis shift assays.----------64

Figure 6. Dynamic light scattering study to monitor complexation of siRNA.----------67

Figure 7. Influence of siRNA concentration and N/P ratio on polyplex-induced target gene (luciferase) down-regulation.----------71

Figure 8. Enhancement of siRNA delivery by polymer vehicles Tr4(77) and CD4(143).---------72

Figure 9. siRNA-mediated gene down regulation with U87-luc2 cells as a function of polyplex type.----------75

Figure 10. Comparison of pDNA and siRNA delivery efficiency.----------77

Figure 11: MTT assay to measure the cytotoxicity of siRNA-containing complexes.----------80

Chapter 3.

Figure 1. Schematic illustration of polyplexes formation from diblock copolymers complexed with siRNA.----------99

Figure 2. Characterization of the glycopolymers.----------104

Figure 3. Gel electrophoresis assay.----------117

Figure 4 a. Hydrodynamic radii and ζ-potentials of polyplexes in water over the period of 4 h.118

Figure 5. Physical properties of polytrehalose and polyplexes.----------119

Figure 6. (a) Cell viability by MTT assay of polytrehalose (b) Cellular uptake at siRNA concentration of 100 nM (c) Dependence of cellular uptake on siRNA concentration in (c) or (d) DMEM with 10% FBS (e) The rate of the uptake at 100 nm siRNA concentration in (e) OptiMEM or (f) DMEM with 10% FBS.----------123

Figure 7. Confocal microscopy of U-87 cells transfected with Cy5-labeled siRNA.----------127

Figure 8. Luciferase gene expression and cell viability observed in HeLa cells.----------129

Figure 9. Luciferase gene knockdown in luciferase-expressing U-87 cells.----------131

Figure 10 A-B. Confocal microscopy images obtained at various time points for cells transfected with polyplexes.----------134

Figure 11. MTT assay in U-87 cell line with various polyplex formulations.----------135

Chapter 4.

Figure 1. Structures of trehalose containing lanthanide click polycations and illustration of FRET for polymer and siRNA.----------147

Figure 2. Structural determination of 2,3,4,2',3',4'-hexa-O-acetyl-6,6'-diazido-6,6'-dideoxyl-D-trehalose.----------151

Figure 3. ESI-MS characterization of compound 1-alkyne-6-carboxybenzyl-2,3,4,5-tetra (tert-butyloxycarbonyl) pentaethylenetetraamine. ----------155

Figure 4. 1HNMR characterization of di-carboxylbenzyl-di-pentaethylenetetraamine click trehalose macromonomers.----------156

Figure 5. 1HNMR characterization of DTPA-BA.----------157

Figure 6. a). 1HNMR spectra of trehalose pentaethylene polymers with lanthanide chelation domain. b). The SEC analysis of the polymer. ----------159

Figure 7. Gel electrophoresis analysis of TrN4Ln(Ln=Eu, Gd, Tb).----------164

Figure 8. Relaxivity measurement of TrN4Gd.----------165

Figure 9. Dynamic light scattering study of polyplexes formed by lanthanide containing polymers with siRNA.----------166

Figure 10. Stability of polyplexes upon addition of heparin.----------167

Figure 11. Illustration of monitoring polyplex formation via FRET.----------169

Figure 12. FRET study on the TrN4Eu/Cy5-siRNA and TrN4Tb/TMR-siRNA complexation and heparin mediated dissociation.----------170

Figure 13. Cellular uptake and target gene knockdown studies of polyplexes formed from lanthanide polymers with siRNA.----------174

Figure 14. Cytotoxicity examined via MTT assay.----------176

List of Tables

Chapter 2.

Table 1. GPC characterization of the click polymers.----------61

Chapter 3.

Table 1. Determining molecular weight and composition of diblock copolymers by aqueous size exclusion chromatography.----------103

Chapter 4.

Table 1. Determination of number of water coordination sites.----------161

Table 2. ICP-OES analysis of the lanthanide content of polymers TrN4Eu, TrN4Gd and TrN4Tb respectively. ----------162

List of Schemes

Chapter 2.

Scheme 1. Synthesis of trehalose pentaethylene click polymer and cyclodextrin pentaethylene click polymer.----------55

Chapter 3.

Scheme 1. Synthesis of P(MAG46-b-AEMAx) via RAFT Polymerization.----------102

Scheme 2. Synthesis of 6-methacrylamido-6-deoxytrehalose (MAT).----------105

Scheme3. Polymer synthesis via RAFT polymerization. ----------105

Chapter 4.

Scheme 2: Synthesis the Trehalose Pentaethyleneamine click macromonomer.----------151

Scheme 3. Synthetic scheme of diethylenetriaminepentaacetic acid bisanhydride.----------157

Scheme 4. Synthetic scheme of trehalose based lanthanide containing polymers.----------158

List of Abbreviations

Boc	***tert*-butoxylcarbonyls**
BSA	**bovine serum albumin**
Cbz	**carboxylbenzyl**
CD4	**poly(β-cyclodextrin click pentaethylenetetraamine)**
Cy5	**cyanine dye 5**
Đ (Mw/Mn):	**polydispersity index.**
DCC	**di cyclohexylcarbodiimide**
DCM	**dichloromethane**
DEPC	**Diethylpyrocarbonate**
DLS	**Dynamic light scattering**
DMEM	**Dulbecco's modified eagle medium**
DMSO	**dimethylsulfoxide**
D_2O	**deuterium oxide**
DTPA	**diethylenetriaminepentaacetic acid**
DTPA-BA	**diethylenetriaminepentaacetic acid bisanhydride**
FACS	**fluorescent activated cell sorting**
FBS	**fetal bovine serum**
FRET	**Fluorescence resonance energy transfer**
G4	**galactaramidoamine**
GPC	**gel permeation chromatography**

HeLa	**human cervix adenocarcinoma cells**
IR	**infra red**
MHS	**Mark-Houwink-Sakurada**
M_n	**number average of molecular weight**
M_w	**weight average of molecular weight**
mRNA	**message ribonucleic acid**
MRI	**Magnetic Resonance Imaging**
MTT	**(3-[4,5-dimethylthiazol-2-yl]-2,5 diphenyl tetrazolium bromide)**
n	**degree of polymerization (number of repeating units)**
N4Gd	**poly(pentaethyleneamine-amidodiethylenetriaminetriaacetic gadolium)**
N4Tb	**poly(pentaethyleneamine-amidodiethylenetriaminetriaacetic terbium)**
NMR	**Nuclear Magnetic Resonance Spectroscopy**
N/P	**amines of polymer/phosphate on siRNA**
ICP-OES	**Inductively coupled plasma optical emission spectroscopy**
Opti-MEM	**reduced serum media**
pDNA	**plasmid DNA**
PEI	**Polyethylenimine**
RISC	**RNA-induced silencing complex**
RNAi	**RNA interference**
SEC	**Size-exclusion chromatography**
siRNA	**small interfering ribonucleic acid**

T4	**tartaramidoamine**
TAE	**Tris-Acetate-EDTA buffer**
TEM	**transmission electron microscopy**
TMR	**tetramethyl rhodamine**
Tr4	**poly(α,α-trehalose click pentaethylenetetraamine)**
U87	**Human glioblastoma-astrocytoma, epithelial-like cell line**

List of Publications

Lian Xue

2003.09-2007.07	B.S. in Pharmacy.
	Peking University
	Bachelor thesis: Design and synthesis of non-peptidomietics β-secretase inhibitors.
2008.08-2011.08	Ph.D. in Chemistry.
2011.08-2014.7	University of Minnesota, TC. MN
	Advisor: Theresa M. Reineke
	Doctoral Thesis:Synthesis and Evaluation of Carbohydrate Based Cationic Polymers for siRNA Delivery and Tracking

Publications and Presentations:

1. *A. E. Smith, A. Sizovs, G. Grandinetti, L. Xue, T. M. Reineke*, "Diblock Glycopolymers Promote Colloidal Stability of Polyplexes and Effective pDNA and siRNA Delivery under Physiological Salt and Serum Conditions" *Biomacromolecules*, **2011**, 12 ,3015–3022
2. *N. P. Ingle, L. Xue, T. M. Reineke*, "Spatio-Temporal Cellular Imaging of Polymer-pDNA Nanocomplexes Affords In Situ Morphology and Trafficking Trends" *Mol. Pharm.*, **2013**, *Article ASAP*.
3. *L. Xue, N. Ingle, T. M. Reineke*, "Highlighting the Role of Polymer Length, Carbohydrate Size, and Nucleic Acid Type in Potency of Glycopolycation Agents for pDNA and siRNA Delivery" *Biomacromolecules*, **2013**, *Article ASAP*.
4. *A. Sizovs, L. Xue, Z. Tolstyka, N. Ingle, Y. Wu, M. Cortez, T. M. Reineke*, "Poly(trehalose): Sugar-Coated Nanocomplexes Promote Stabilization and Effective Polyplex-Mediated siRNA Delivery" *J. Am. Chem. Soc.*, **2013**, 135, 15417–15424.
5. *Sneha S. Kelkar, Lian Xue, S. Richard Turner and Theresa M. Reineke*, Lanthanide-Containing Multi-functional Polymers for Monitoring Polyplex Dynamics via Lanthanide Resonance Energy Transfer. *Manuscript submitted to Biomacromolecules.*
6. *Lian Xue, Sneha S. Kelkar, Theresa M. Reineke*, Trehalose Containing Lanthanide Click Polycations for siRNA Delivery and Tracking . *Manuscript in preparation.*

7. *Lian Xue, Theresa M. Reineke.* Trehalose cationic polymers for siRNA delivery into glioblastoma cells. 8th National Graduate Research Polymer Conference, June 6 - 9, 2010.
8. *Lian Xue, Theresa M. Reineke*. Structure-property relationship of click polycations for siRNA delivery. MII Technical Conference and Review of Virginia Tech, 2010.
9. *Lian Xue, Theresa M. Reineke.* Carbohydrate-based click polycations for siRNA delivery. Oral presentation, 243rd ACS National Meeting & Exposition March 25- 29 2012, San Diego, California.
10. *Lian Xue, Anliang Li.* Chapter 14. Bioavailability—Targeted delivery and Prodrugs. 2008.02. ISBN: 978-122-01735-2.

Chapter 1

Introduction: Polymeric Materials for siRNA delivery and tracking

Background

RNA interference gene regulation has been investigated intensively in medical applications in last two decades. However, inadequate delivery of RNA molecules to intracellular target sites has become the bottleneck in both laboratory use and clinical therapy. Generally, the small interfering RNA molecules as well as other RNA molecules have poor pharmacokinetic profiles, can be hydrolyzed or degraded easily, cause serious immunogenic response and can be toxic to particular cell types as well. Several strategies have been developed to improve the pharmacokinetics of siRNA, including chemical modification, virus vectors, lipid and polymer complexation, etc. In order to achieve desirable properties with variations, developing biocompatible and biodegradable materials to successfully deliver siRNAs to targets has become a main strategy. In recent years, a variety of polymeric vehicles have been extensively synthesized and investigated; several of them have been developed from benchtop to bedside. The diversity of chemical reactions endows the delivery systems with various properties like high efficiency, low toxicity, and tunable sizes and surface properties for targeted delivery. Tracking the siRNA delivery becomes important as to understand the dynamic of the polyplexes, to elucidate the mechanism of interactions with cells, to provide a platform for potential theranostics development.

1. Cellular mechanism and barriers for siRNA delivery

1.1 Cellular mechanism of post-transcriptional gene regulation by siRNA

It was a milestone that Fire and Mello[1] discovered that mixing the sense and antisense strands of small RNAs achieved approximately tenfold more efficiency in gene

silencing than either strand alone. They named such double stranded RNA-induced gene down-regulation “RNA interference” or RNAi.

RNA interference is an RNA-dependent gene regulation method to help control gene activity. In living cells, RNAi can play an important role in defense against parasitic genes to minimize viral infections, secure genome stability and repress protein synthesis to regulate the development of organisms. In research, it provides a powerful tool to study the function of specific genes and pathways, and this may revolutionize drug discovery in the future.

In the classical view of the Central Dogma, genetic information is transcribed from DNA into RNA, and then translated from mRNA to proteins. Generally, there are two types of RNA molecules that are central to RNAi, and these are micro RNA (miRNA) and small interfering RNA (siRNA). In the exogenous dsRNA-initiated RNAi pathway (shown in Figure 1b), the ribonuclease III-like nuclease (so-called Dicer[2]) in the cytoplasm is responsible for processing of exogenous dsRNA to short RNA. The short double-stranded nucleotide fragments are called small interfering RNAs (siRNA). The siRNAs usually comprise 21-25 base pairs of double strand RNAs with 2-3 unpaired overhanging bases on each end[1]. Then, they are bound to RNA-binding proteins and transferred to an RNA-Induced Silencing Complex (RISC). However, only one of the double strands, the antisense strand, can guide the gene silencing, and the other strand (antisense strand) will be degraded while the activation of RISC[3]. Subsequently, the activated RISC complex binds to a messenger RNA (mRNA) molecule complementarily and induces the cleavage of the mRNA. In this manner, the translation to protein is inhibited due to diminishment of the templates.

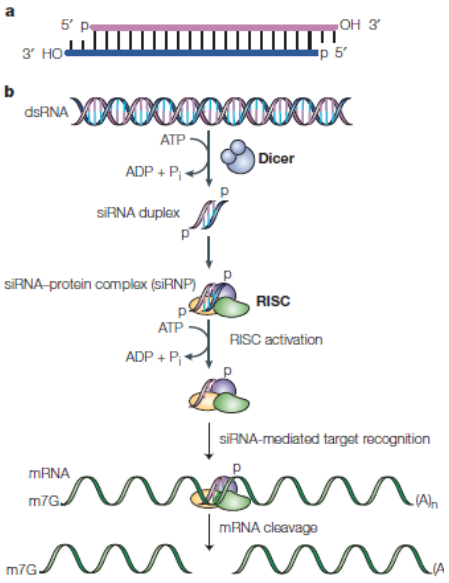

Figure 1: This shows the (a). Structure of siRNA (b). The exogenous dsRNA induced gene silencing pathway. This image was copied from reference Dykxhoorn, D. M.; Novina, C. D.; Sharp, P. A. *Nat Rev Mol Cell Biol* **2003**, *4*, 457-467[4].

1.2 Barriers in systemic and local delivery of siRNA nanoparticles

The potency of siRNA in therapeutic applications is versatile from central nervous systems therapeutics, antiviral and anticancer agents, inflammation to cardiovascular therapeutics. Theoretically, siRNA can act on target mRNAs and their correlated proteins are considered to be untreatable by small molecules or monoclonal antibodies.[5] From 1989 to March 2014 (according to http://www.wiley.com/legacy/wileychi/genmed/clinical/), over 1996 gene therapy clinical trials have been completed or are in progress. Among these, 12 are for siRNA, most of the vectors used in these trials were viral-based. However, nonviral vectors are recognized as important components for oligonucleotide therapeutics.

Delivery strategies for siRNA nanoparticles depend on accessibility of the target sites. Typically for eyes, skin, mucus membranes, lung diseases as well as local tumors, local delivery will be sufficient. However, for most pathologic sites, systemic administration is still the major delivery route. Physiological barriers for siRNA delivery can be classified into instability in serum, poor permeability through vascular endothelium and extracellular matrix, unexpected lymphatic clearance, poor cellular uptake and endosome escape. Firstly, siRNAs have short half lives and low stability in serum. They can easily undergo hydrolysis as compared to pDNA, and even cause immunogenic responses. Therefore, siRNAs are incorporated into nanoparticles for systemic delivery to improve the pharmacokinetic profiles. Post injection, the nanoparticles (NPs) must avoid filtration, phagocytosis and degradation in the blood stream. The survivability of the NPs depends on both size (5-250 nm) and surface characteristics. The surface properties and functionalities are also important to avoid aggregation and unwanted enzymatic degradation.[6]

Secondly, it is desirable for the NPs to cross the vascular endothelial cell barrier and avoid lymphatic clearance. There are certain tissues like solid tumors, the liver and spleen that allow entry of particles as large as 200 nm in diameter. In solid tumors, there is a enhanced permeability and retention (EPR) effect that allows relatively large nanoparticles to accumulate in tumor tissue. The EPR effect can be attributed to progressive angiogenesis and high vascular density, defective vascular structure, over excretion of different vascular dilators as well as impaired lymphatic clearance in solid tumors[7]. Targeting solid tumors through the EPR effect is still a major design objective for nanosized delivery systems.

More importantly, naked natural siRNA is not readily taken up by cells. Therefore, compensating for the negative charge of siRNA or shielding the charge is crucial to facilitate the internalization process. Once taken up by the cells via endocytosis, the siRNA –vector complexes have to escape the endosome to reach the cytoplasm where the RISC machinery is located[8]. The main hypothesis supporting cationic polymers for gene delivery is the "proton sponge" theory, which states that polycations can buffer acidic conditions by absorbing protons in the endosome. The drop in proton concentration in the endosome will trigger the influx of protons together with chloride, and this leads to osmotic influx of water to disrupt the endosomes and release the polyplexes into the cytoplasm.[9] Lastly, the siRNA must be released from vectors or formulations to reach the RNAi machinery RISCs.

2. Versatile synthetic strategies for siRNA delivery

Generally, to improve the delivery efficacy of siRNA, these polynucleotides can be chemically modified or incorporated into non-viral vectors. Conjugating delivery materials with siRNA via covalent linkage is another approach to overcoming the delivery difficulties.

2.1 Chemical modifications on siRNA backbones

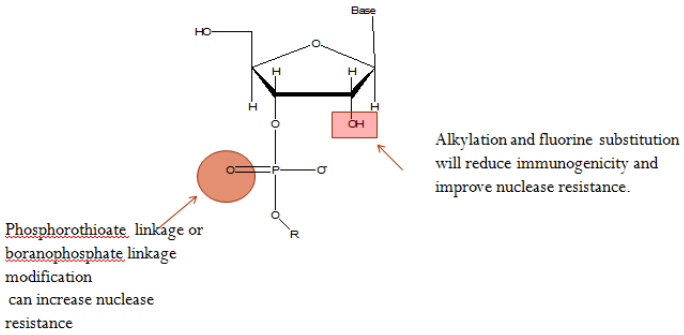

Figure 2: Common sites of chemical modification on siRNA backbones

Chemical modification of siRNA can improve the pharmacokinetic properties, activity and reduce side effects such as immunogenic responses and kidney toxicity[10]. The plasma stability and in vitro potency can be dramatically improved by fully modifying the 2'-OH. A siRNA with 2'-OH alkylation and fluorine substitution in an alternating manner has shown >500-fold improvement in potency.[11] Also 4'-thio-modified siRNA exhibits improved activity and nuclease stability in some systems.[12]

2.2 ***siRNA conjugates***

Conjugating the siRNA sense strand to small molecules, peptides, aptamers (in Figure 3A) and polymers can increase the efficacy of siRNA to target specific cell types or to improve the stability and solubility in serum. Cholesterol-modified siRNA (in Figure 3B) can significantly facilitate the accumulation of siRNA in the liver and silence apolipoprotein B in mice liver and jejunum to reduce blood cholesterol[13]. It was also reported that conjugating siRNA via a disulfide bond to penetratin or transportan, which are two kinds of peptide transduction domains (PTDs), can help siRNA penetrate into almost 100% of cell populations with 8% toxicity[14].

A B

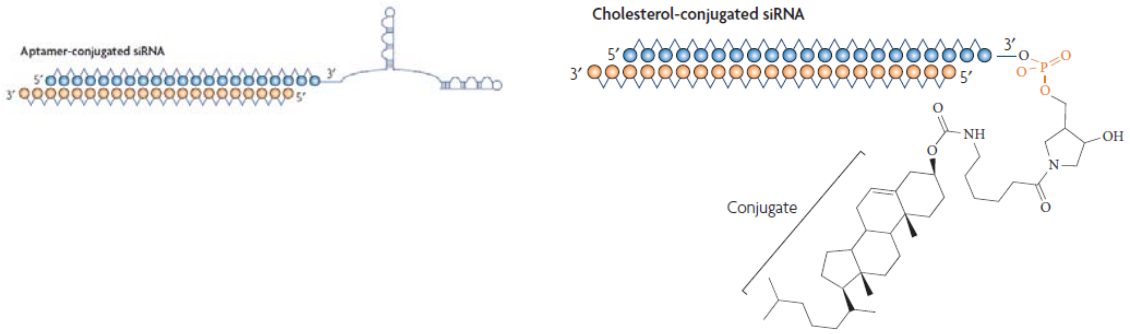

Figure 3: A. Aptamer-conjugated siRNA B. cholesterol-conjugated siRNA. The sense strand and anti-sense strand are represented as blue and orange circles respectively.[14] This figure was copied from reference "de Fougerolles, A.; Vornlocher, H. P.; Maraganore, J.; Lieberman, J. *Nature Reviews Drug Discovery* **2007**, *6*, 443-453"[14].

It is noteworthy that a class of nanometer-scale covalent carriers of siRNA can be prepared through self-assembly of PEG-based block ionomers. One example is conjugation of siRNA with lactosylated PEG (shown in Figure 4) through acid-labile linkages, and followed by incorporated with cationic poly(L-lysine) to form micelles. The micelles were reported to remarkably enhance RNAi in cultured hepatoma cells[15].

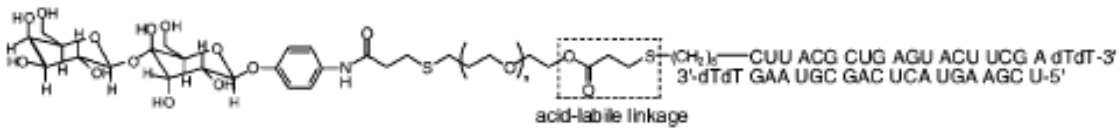

Figure 4: Lac-PEG-siRNA conjugates. This figure was copied from reference "Oishi, M.; Nagasaki, Y.; Itaka, K.; Nishiyama, N.; Kataoka, K. *Journal of the American Chemical Society* **2005**, *127*, 1624-1625"[15].

2.3 Synthetic vehicles for siRNA delivery

Common features of synthetic nanoparticles[16]

Generally, delivery vectors are designed to facilitate the uptake of siRNA into the target cells. In systemic delivery, the vectors should also protect siRNA from enzymatic degradation and immune system recognition and also avoid non-specific delivery. By survey of the existing nanoparticles, there are several common features that are useful for successful nano system design.

2.3.1 Surface properties

In colloidal systems like those containing siRNA nanoparticles, zeta potentials are widely used for quantifying the magnitude of the electrical charge at the Debye layer, which is a few nanometers from the surfaces in water. A vehicle bearing positive charge can facilitate the cellular uptake process, but at the same time it can increase the probability for adsorption onto surfaces and aggregation with serum proteins which are usually negatively charged. For example, polyethyleneimine (PEI) which is cationic polymer not only neutralizes the intense negative charge of the nucleic acids, but also condenses the complexes into a much smaller particle to facilitate endocytosis, the major way of cellular internalization[17].

For in vivo siRNA delivery, coating the surface of the nanoparticles with hydrophilic blocks like poly(ethylene glycol) (PEG) allows formation of core-shell structures to increase the solubility of the particle, to shield the charge, and to prevent aggregation. This approach can also protect the particles against degradation and immune system recognition, and provide longer circulation times in the blood stream. PEG has

been extensively used in drug delivery, and it can be utilized to control and tune the particle size[18].

2.3.2 Biodistribution and toxicity

Systemic administration of synthetic nanoparticles will usually lead to accumulation in organs like the liver, spleen, kidneys, lungs and tumors. Excretion from the kidney is size dependent, and usually polymers with less than 50 kDa in molecular weight can easily be excreted through the kidneys[19]. Also the enhanced permeability and retention effect as mentioned in 1.4 plays an important role in accumulating nanoparticles in solid tumors.

Safety is a primary concern for design of siRNA delivery vehicles. For example, viral vectors, which were widely applied in gene delivery a decade ago, can induce lethal immune responses and infection[20]. Therefore, biodegradable and biocompatible synthetic materials have great potential to achieve lower toxicity with high transfection efficacy.

2.3.3 Synthetic materials for siRNA delivery

Non-viral vectors have many advantages for oligonucleotide delivery. They are relatively safe, offer tunable properties and one can incorporate a wide range of ligands with this approach. Nanosized siRNA vectors can range from lipid based materials, polycations, gold nanoparticles, functionalized carbon nanotubes and quantum dots. Among all these types of delivery vectors, lipid based and cationic polymers are predominant in various applications.

2.3.3.1 Lipid based materials

Lipid based materials have been incorporated in many pharmaceutical formulations over the last two decades. Cationic lipid materials such as Lipofectamine 2000 or its analogs have been used for in vitro pDNA or siRNA delivery[21]. The history of cationic lipid based gene vectors can be traced back to the discovery of the ability of DOTMA (N-[1-(2,3-dioleyloxy)propyl]-N,N,N-trimethylammonium chloride) (shown in Figure 5b) to delivery both DNA and RNA.[22]

In a recent study, siRNAs were incorporated into stable nucleic acid lipid particles (SNALP) (shown in Figure 5a) and intravenously administrated to non-human primates. Successful apo-B knock down was observed in 24 hours.[23]

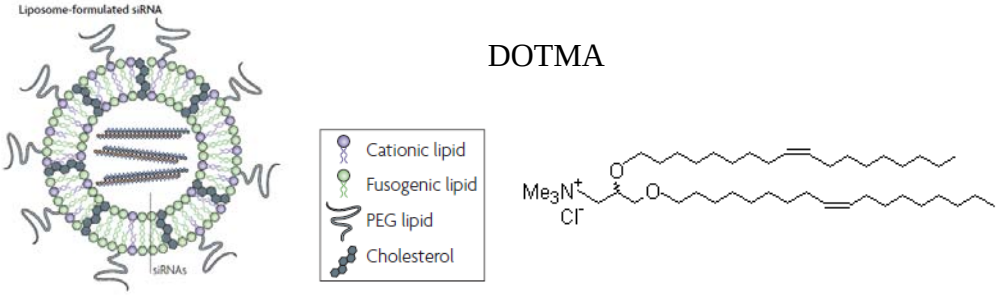

Figure 5: A. Stable nucleic acid-lipid particles (SNALPs) formed from cationic lipid, non cationic lipids and PEG chains. This figure was copied from reference" Whitehead, K. A.; Langer, R.; Anderson, D. G. *Nature Reviews Drug Discovery* **2009**, *8*, 516-516".[16] B. structure of DOTMA.

Positively charged lipids incorporate with negatively charged siRNA to form "lipoplexes". It has been reported that a stealth lipoplex can be taken up by the reticuloendothelial system (RES), where Kupffer cells in the liver could engulfed the lipoplexes which bound to blood proteins[24]. This resulted in low transfection efficiency in vivo. Toxicities of cationic lipids are an issue that must be addressed. In response to

this issue, PEGylated liposomes were developed to overcome non-specific accumulation[25]..

2.3.3.2 Polymer based vehicles

Cationic polymers, linear or branched, have been developed and used as efficient transfection agents in vitro and in vivo[26]. Usually the cationic polymers can bind with nucleic acids through electrostatic interactions and hydrogen bonding to neutralize the negative charge and further condense the large nucleic acids into smaller sized stable nanoparticles. Polyelectrolyte self-assembled nanoparticles (termed polyplexes) are the dominant type of polymeric delivery systems used for siRNA delivery. Usually the cationic polymer contains amine---including primary, secondary, tertiary and quaternary amines, as well as other positively charged groups like amidines and guanidines[27]. In physiological conditions, the cationic polymers can interact with the negatively charged phosphate groups on nucleic acid backbones, although the substructure of a polyplex is still under study. The charge ratio refers to the N:P ratio, which is often applied as a parameter to demonstrate the efficacy of the cationic polymer in transfection experiments.

2.3.3.2.1 PEIs (polyethyleneimines)

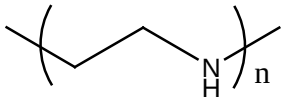

Poly(ethyleneimine)

Figure 6: Structure of PEI

PEI has been extensively investigated in nuleotide delivery including DNA and siRNA. It has been reported the low molecular weight PEI can efficiently stabilize siRNAs and successfully deliver siRNA into tumors via systemic administration in a mouse model, resulting in a remarkable reduction of target receptor c-erbB2/neu (HER-2) expression[28]. The intraperitoneal administration of polyplexes formed with PEI and siRNA has successfully achieved knock down of the target, the NMDA (N-methyl-D-aspartate) receptor NR2B which is related to chronic pain[29]. To stabilize siRNA in the polyplex, PEGylated siRNA was also used for anti-angiogenic gene therapy (shown in Figure 7)[30]. The siRNA was covalently bound to PEG via cleavable disulfide bonds that were introduced by the crosslinking reagent N-succinimidyl 3-(2-pyridyldithio)propionate (SPDP). The siRNA-PEG conjugates interact with PEI to form polyelectrolyte complex micelles through self-assembly.

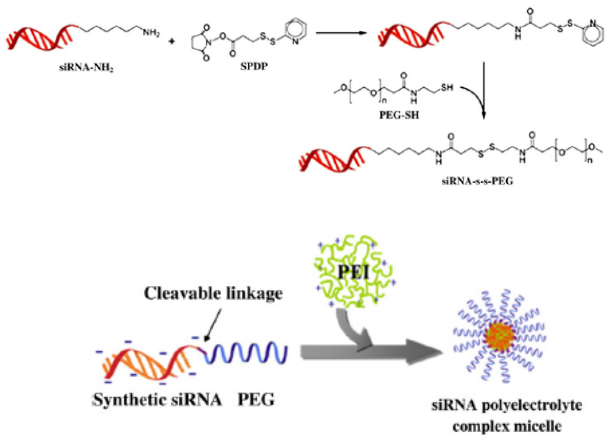

Figure 7: A. PEGylation of siRNA via SPDP linker. B.The formation of siRNA-PEG/PEI polyelectrolyte. This figure was copied from reference "Kim, S. H.; Jeong, J. H.; Lee, S. H.; Kim, S. W.; Park, T. G. *Journal of Controlled Release* **2008**, *129*, 107-116"[28].

Although PEI is efficient for nucleic acid delivery, it has serious cytotoxicity which appears to be molecular weight and concentration dependent[31]. To improve its biocompatibility, hydrophilic PEG was incorporated, and this was expected to reduce the cytotoxicity and improve the water solubility of PEI/DNA complexes. Therefore different PEGylation chemistries/architectures were developed, such as block and graft copolymers of PEI and PEG[31] (the synthetic schemes are shown in Figure 8).

A

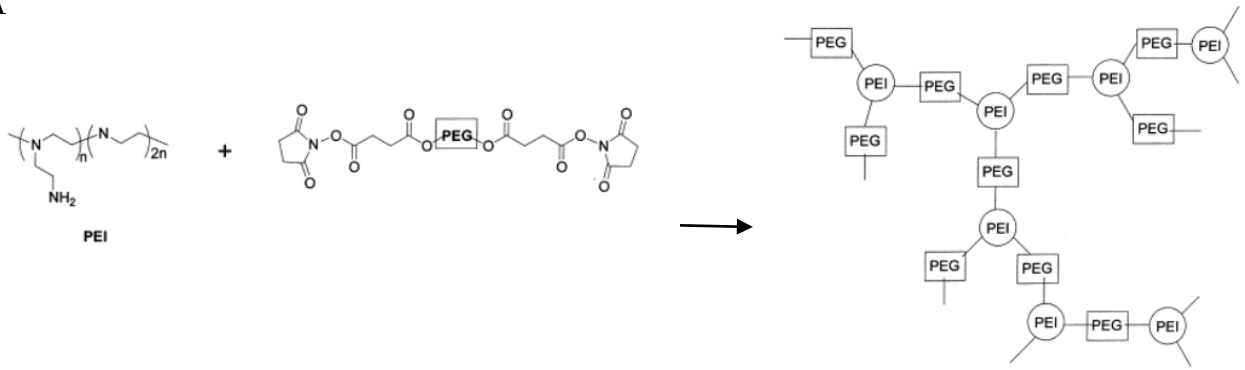

B

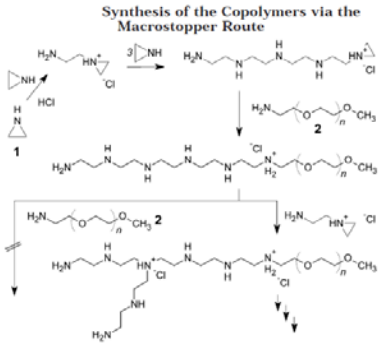

Figure 8: A. Synthetic scheme of graft copolymer of PEI and PEG. This figure was copied from reference "Ahn, C.-H.; Chae, S. Y.; Bae, Y. H.; Kim, S. W. *Journal of Controlled Release* **2002**, *80*, 273-282."[29]. B. Synthetic route of block copolymers of PEI and PEG. This figure was copied from reference "Petersen, H.; Martin, A. L.; Stolnik, S.; Roberts, C. J.; Davies, M. C.; Kissel, T. *Macromolecules* **2002**, *35*, 9854-9856".[32]

It has also been reported that PEG-b-PEI diblock copolymers can enhance DNA condensation better than multi-PEGylated PEIs.[32] Since siRNA and DNA behave quite differently in terms of their intracellular mechanisms of action, it is recommended that separate evaluations of the graft copolymers (PEG-g-PEI), which already have optimal molecular weight and N/P ratio for DNA, should be conducted.[33]

To reduce the toxicity of long chain PEI and increase the gene transfection efficiency of low molecular weight PEI, various degradable links were incorporated into short chain PEI, such as amides, acetals, esters and disulfides[34]. Transfection efficiencies of disulfide crosslinked PEI have also been investigated, and it was found that these depended strongly on both the degree of crosslinking and the precursor molecular weights[34].

2.3.3.2.2 Carbohydrate-based delivery systems

a. chitosan

Chitosan (shown in Figure 9) is a linear polysaccharide derived from deacetylation of chitin which is fully acetylated β-(1-4)-linked poly(N-acetyl-D-glucosamine). Chitosan consists of randomly distributed β-(1-4)-linked D-glucosamine (deacetylated unit) and N-acetyl-D-glucosamine (acetylated unit), depending on the degree of deacetylation. It has been widely used in controlled release formulations because it is biocompatible and biodegradable at a slow rate[35]. Chitosan also increases transcellular and paracellular transport across the muscosal epithelium[36].

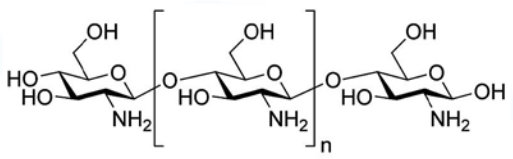

Figure 9: The structure of chitosan, only the deacetylated units are shown in the figure.

Due to the cationic nature from the protonated primary amine, chitosan had been investigated for nucleic acid delivery. It has been used in oral delivery of DNA to intestinal epithelial cells to produce IgA and serum IgG2a which are two forms of antibodies[37]. The efficacy of chitosan/siRNA in gene silencing in vitro is strongly dependent on the molecular weight and degree of deacetylation. High MW and high degree of deacetylated chitosan perform better, but the effective N/P ratio was as high as 50:1[38].

b. cyclodextrin based delivery systems

There are three kinds of cyclodextrins (CD)- α, -β, and –γ, constituted by 6 to 8 glucopyranoside units respectively. The three dimensional structure of β-CD endows it with proper ring size for optimal H-bonding, and due to the special cup like shape and relatively hydrophobic cavity, it can dramatically enhance the water solubility of hydrophobic moieties. Also the CDs are quite biocompatible and extremely water soluble, and can provide 6-8 reactive sites for easily performed chemical modifications. More interestingly, the adamantane has one of the highest binding affinity to β-CD (association constant on the order of 10^4-10^5 M^{-1} for adamantane carboxylate) in aqueous solution, the property can be utilized for self assembly of macromolecules and design of biosensors[39] .

Cyclodextrin itself does not have cationic center to complex with siRNA, therefore different cation containing cyclodextrin derivatives were synthesized for oligonucleotide delivery. In Marsura's group, a bis-(guanidinium)-tetrakis-(β-cyclodextrin) dendrimeric tetrapod (shown in Figure 10) has been synthesized and shown the potency in siRNA delivery to embryonic lung fibroblasts[40]. Also, a series of polycationic β-Cyclodextrin "Click Clusters" with monodispersity and size range of 80-130nm were developed by Dr. Reineke's group and from the preliminary study, the ones containing three to four secondary amine groups were most promising vehicles for DNA delivery, but the re evaluation of the vehicles for siRNA delivery is still required[41].

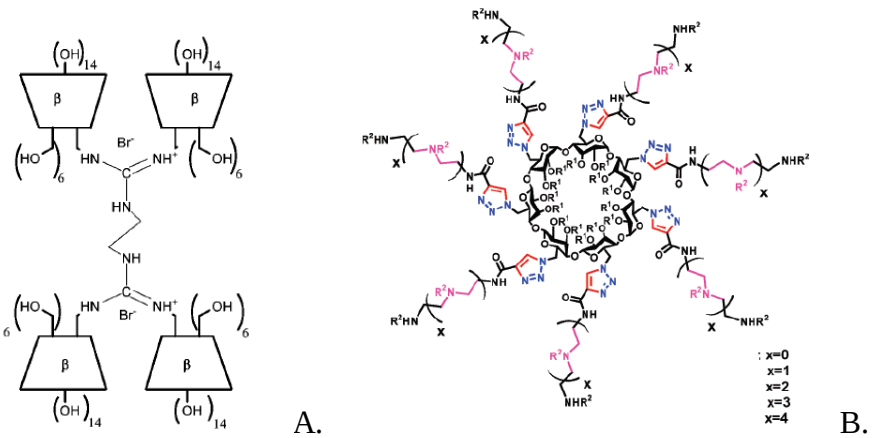

Figure 10: A.The structure of bis-(guanidinium)-tetrakis-(β-cyclodextrin) dendrimeric tetrapod. The figure was copied from reference"[40]". B. Structure of β-Cyclodextrin "Click Clusters. The figure was copied from reference "[41]".

Dr. Davis' group has performed extensive investigation on the CD containing polymers for drug and nucleic acid delivery for many years. And from the all investigations so far, the CD-containing polycations show low toxicities in vitro and in vivo, and they hadn't been observed to enter the nucleus of cells, which is a feature

beneficial for siRNA delivery[42]. The linear CD-containing polycations can be decorated by PEG by terminating the chain with adamantane, which can form inclusion complexes with cyclodextrin through self assembly[42]. The PEG moiety was terminated with adamantine, and a targeting moiety can be incorporated on the other end. And this kind of formulation has been brought from benchtop to bedside to achieve the first targeted delivery of siRNA in human[43]. In this formulation, the targeting component transferrin (Tf), which can specifically bind to transferrin receptors that are over expressed in tumor cells, was conjugated at the end of PEG chain opposite to adamantane. The four components (siRNA, CDP, PEG-AD, Tf-PEG-AD) then formed nanoparticles via self assembly when mixed together[43] (shown in Figure 11).

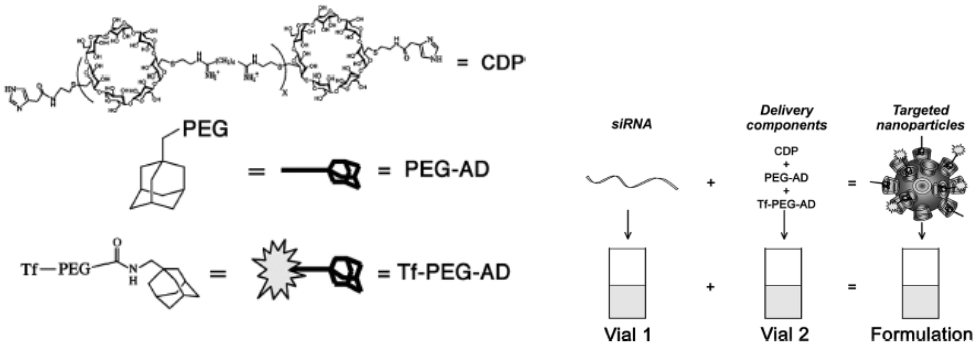

Figure 11: The self assembly of cyclodextrin linear polymer with adamantane terminated polymeric chains [43].

The Reineke's group has developed a series of cyclodextrin click copolymers (shown in Figure 12) with different oligoethyleneamines for pDNA delivery into HeLa cells[44]. The cell viability was quite high through all the structures and the transfection efficiency depended on the number of amines in each repeating unit and the degree of

polymerization. Among them, $Cd3_{49}$ (with three amines in each unit and degree of polymerization is 49) and $Cd4_{93}$ showed the most efficient reporter gene expression.

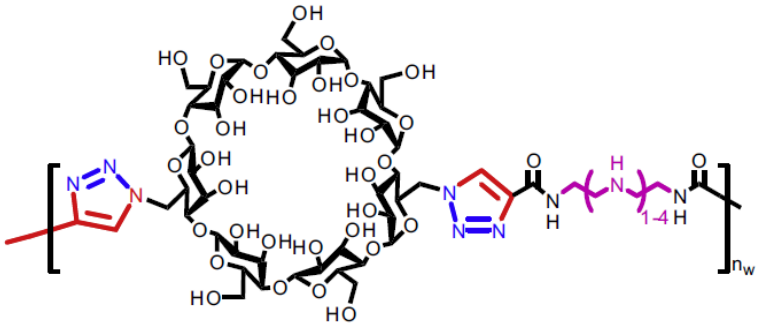

Figure 12: Structure of cyclodextrin linear click copolymers with different oligoethyleneamine analogues. The figure was copied from reference "[44]"

c. poly(glycoamidoamine)s

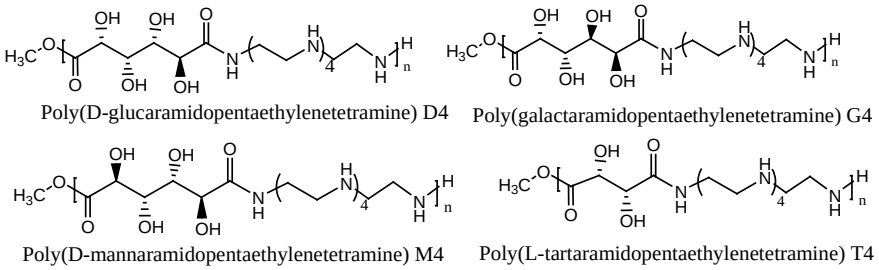

Figure 13: Examples of PGAAs (Poly(glycoamidoamine)s). In this figure, the polymers contain four secondary amines and either two or four hydroxyl groups per repeat unit with differing stereochemistry. This figure was copied from reference "[45]".

Inspired by the transfection agents PEI and chitosan, The Reineke's group has explored the polymers with carbohydrate moieties along with linear amino backbone linked via amide groups. Initially, the synthesis of these polymers proceeds by polycondensation of carbohydrate diesters with diamines. They found out that both the

number and the stereochemistry of hydroxyl units remarkably affect the biological properties of the polymers. Interestingly, the galactarate-based polymers showed higher transfection efficiency despite the lower binding affinity to pDNA compared with tartarate polymers in HeLa cells[45].

In the later studies, they concluded that the higher number of amine groups in repeating units would facilitate greater cellular uptake, and this may because the stronger interaction with cell surface proteoglyans as well as with endosomes. The carbohydrate components also affect gene expression level, and this could be attributed to the different buffering capacities. Also, the higher amine density (T series polymers have shorter molecular distance between oligoamines) could probably cause release via membrane defect formation. The different amine spacer could influence buffering capacity dramatically, but the decreased buffering capacity leads to an increase on gene expression, this finding also indicated the contradiction between the relation of buffering capacity and gene delivery[46].

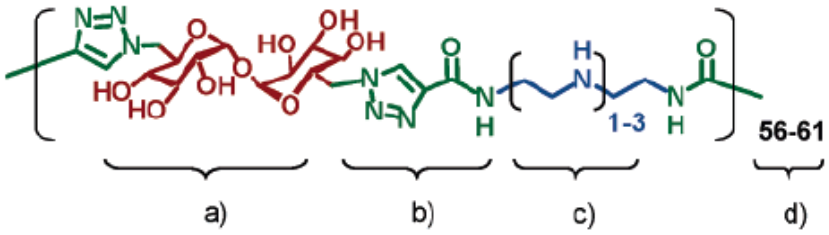

Figure 14: Structure of trehalose click copolymers. The figure was copied from reference "[47]".

The trehalose based copolymers (shown in Figure 14), represent another series of promising transfection reagents were designed and synthesized in The Reineke group via copper(I) catalyzed alkyl-azide cycloaddition polymerization. The initial concern about

incorporating a trehalose unit was its potency of water retention and great water solubility, protein stabilization, anti-aggregation properties, and its own stability against hydrolysis benefiting from an anomeric effect, also the rigid concave shape of the molecules may facilitate the nanoparticle formation. The click polymerization is an efficient way to synthesize polymers of high degree of polymerization in mild conditions. Surprisingly, the polymers can efficiently compact DNA at quite low N/P ratios and the one with three secondary amine groups in a repeating unit appears to reduce serum-mediated polyplex aggregation[47]. Later on, the effect of trehalose polymers' length on the efficacy was studied by synthesis of polymers with different degree of polymerization. There were no apparent evidence observed of the length of the polymers affecting the pDNA binding affinity, cellular internalization and DNase resistance. The degree of polymerization of the polymers does influence the serum stability and gene expression[48].

Although all the studies were based on pDNA, the low toxicity and high transfection efficiency of PGAAs shows great potency for siRNA delivery in the future.

Apart from the polymers above, cationic peptides like cell membrane transduction peptides as well as other lysine rich and arginine rich polypeptides are utilized for transfection agents. The polymethacrylate with amine groups on side chains are also commonly used for oligonucleotide delivery. In addition, a variety of nanoparticles like functionalized quantum dots, gold nanoparticles, carbon nanotubes can be applied both to deliver siRNA and track the intracellular events by imaging.

3. Targeted delivery systems for siRNA

Ideally, if delivery of siRNA can be enhanced specifically to the tissue of interest, like liver, spleen or tumor tissues, infected cells, it can not only reduce the dose of siRNA but also lower the risk of toxicity and side effects caused by high concentrations of siRNA and off target effects. Although currently there are few reports on targeted delivery of siRNAs in vivo, the targeted delivery systems of other small drugs, ODNs and pDNAs can guide the rational design of targeted delivery systems for siRNA.

In solid tumors, enhanced permeability and retention (EPR) effect can be applied to facilitate the passively targeted delivery of therapeutics to tumor cells. In systemic delivery, to exhibit EPR effect, the particles must circulate at least 6 hours in blood. Another paradigm is to incorporate endocytosis related ligands that can be selectively recognized by tumor cells. This approach depends on the specificity of the interaction and binding affinity between the ligands and tumor cells, the accessibility of the location of the interaction, and the density of the receptors compared to normal cells.

In addition, tumor targeting via extracellular activation of nanocarriers is another paradigm that guides the design of targeted delivery systems. This strategy takes advantages of the special environment as a mean to trigger transformation of the stealth nanoparticles to a more active form of nanoparticles. The unique environment of tumor cells like slightly acidic and hypoxia condition as well as abundant proteinases can be used as selective mechanisms for tumor tissue[49]. Up to date, according to different targeting moieties used in delivery, the systems can be divided to several classes:

3.1 Antibody and antibody fragment mediated delivery

Antibodies are immunoglobulins that can bind to unique part of antigens in a highly specific manner. The huge diversity and availability of monoclonal antibodies endows them with the possibility as routine clinical treatment for cancer diseases and the potency for targeted delivery for therapeutics.

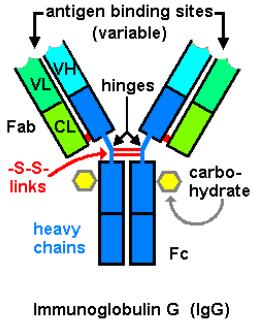

Figure 15: The diagrammatic structure of IgG. This figure was copied from website: http://www.bmb.leeds.ac.uk/teaching/icu3/selfdir/immunol/index.htm

Usually the antibodies, such IgGs (shown in Figure 15), are consisted of Fab fragments and Fc fragments, the later can be possibly recognized as antigen. In recent reports, fragment Fab and scFv have been used and more beneficial over the whole antibodies, because they are less bulky, easy to deal with and less immunogenic[50]. To this end, the antibodies are still of high cost.

It is challenging to conjugate antibodies or fragments to polymers, usually the glycosylated part has been considered as the ideal site for conjugation to maintain the activity of the antibodies, the schemes are shown as follows[51]:

a.

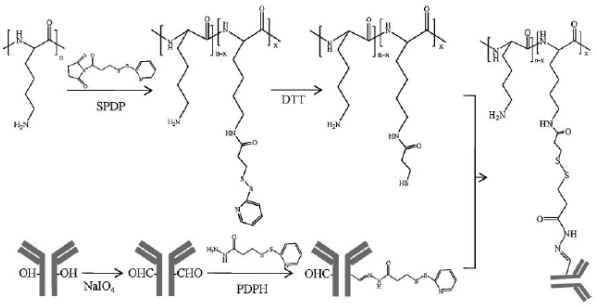

b.

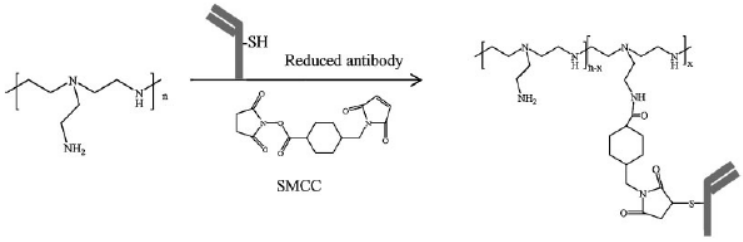

c.

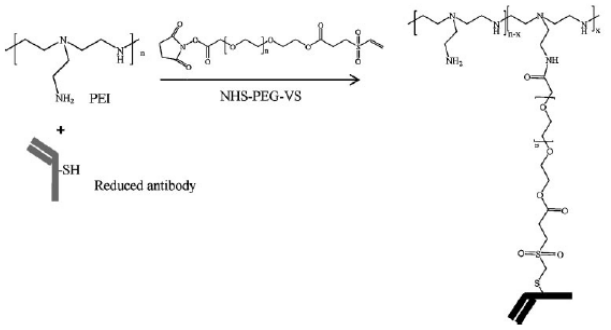

Figure 16: The conjugation of antibodies to polymers. a. antibody-polylysine conjugation via disulfide exchange b. antibody-PEI conjugation via thiol-ene reaction through linker SMCC. c. antibody-PEG-PEI conjugation via thiol-ene reaction. The figure was copied from the reference "[50,51,52]"(Mok, H.; Park, T. G. *Macromolecular Bioscience* **2009**, *9*, 731. Wu, G.; Barth, R. F.; Yang, W.; Chatterjee, M.; Tjarks, W.; Ciesielski, M. J.; Fenstermaker, R. A. *Bioconjugate Chemistry* **2003**, *15*, 185. Qian, Z. M.; Li, H.; Sun, H.; Ho, K. *Pharmacol Rev* **2002**, *54*, 561.).

3.2 Transferrin receptor mediated delivery

Transferrin receptor (TfR) is a kind of glycoprotein overexpressed in many cancer cell lines. It has also been verified that TfR can mediate endocytosis and be recycled without intracellular degradation[53]. Tf-PEI/DNA complexes can achieve 100-500 fold gene expression in tumor as adenovirus in mice. Although many peptide drugs are prevented from crossing blood brain barrier (BBB), therapeutics can be delivered to brain via BBB transporter such like TfR. While since the high endogenous plasma concentration of transferrin, the antibodies of TfR was applied to selective target BBB endothelium due to the high expression of TfR[53]. Also, as mentioned in last chapter, Davis group had incorporated the Tf into the cyclodextrin based polymers for the siRNA formulations.

3.3 Functional peptides mediated delivery

3.3.1 RGD and analog mediated delivery

Integrins are receptors sitting on cell membrane that mediate cell signaling and relate to adhesion, mobility and cell cycle. Arg-Gly-Asp (RGD) peptide has been intensively studied and applied in targeted delivery systems. It can be recognized by integrin receptor $\alpha v\beta 3/\alpha v\beta 5$ which are overexpressed in angiogenic endothelial cells of tumor tissues. Both linear (RGDC) and cyclic (cRGD) RGD like (CGRGDSPC) and (ACDCRGDCFCG) have been incorporated by conjugating to PEI (shown in Figure 17), poly(amido ester), modified PEG and other polymers via disulfide bond through cysteine.

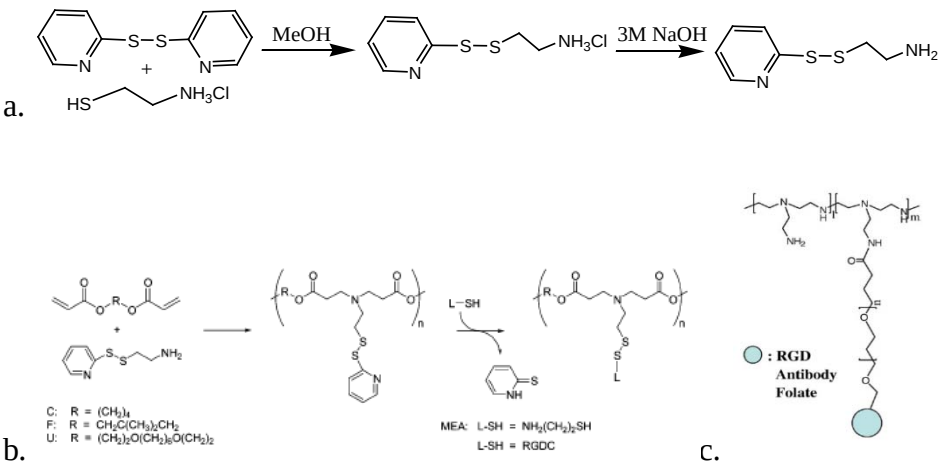

Figure 17: The synthetic route of conjugating RGD to PEI. The figures were copied from reference "[54],[55]"(Zugates, G. T.; Anderson, D. G.; Little, S. R.; Lawhorn, I. E. B.; Langer, R. *Journal of the American Chemical Society* **2006**, *128*, 12726.W Suh, S. H., L Yu, SW Kim *Molecular Therapy* **2002**, *6*, 664.).

One example showed above was the synthetic route of three kinds of polymers via Michael addition followed by linking to RGDC via disulfide exchange on the side chains[54]. The in vitro studies showed the RGD modified polymers exhibited higher efficiency in delivery pDNA to human heptatocellular carcinoma cell line than those not modified[54]. The PEI-g-PEG-RGD was observed to have high selectivity toward angiogenic endothelial cells and much less toxicity. Surprisingly, one RGD unit per PEI chain would be sufficient to show high affinity to integrin receptor.[55]

3.3.2 Luteinizing hormone-releasing hormone

It has been validated the luteinizing hormon-releasing hormone (LHRH) receptors are usually over-expressed in a variety of cancer cells. The LHRH has been used in the apoptosis-inducing agent camptothecin (CPT) formulation for tumor targeted delivery[56].

The sequence of the conjugates is shown below. The peptide LHRH was PEGylated through amine group at the end.

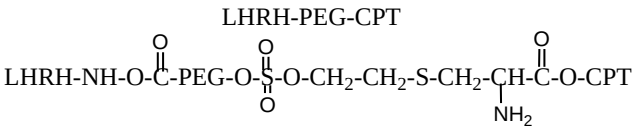

Figure 18: Sequence of the modified LHRH, structure of CPT and LHRH-PEG-CPT conjugate. This figure was copied from reference "[56]" (Dharap, S. S.; Wang, Y.; Chandna, P.; Khandare, J. J.; Qiu, B.; Gunaseelan, S.; Sinko, P. J.; Stein, S.; Farmanfarmaian, A.; Minko, T. *Proceedings of the National Academy of Sciences of the United States of America* **2005**, *102*, 12962.).

LHRH has also been used in targeted delivery for siRNA in the form of conjugating to sense strand of siRNA[57]. PEG was linked to siRNA via disulfide bond with the other ending group carboxylic acid reacted with amine in LHRH. The synthetic scheme is shown as follows:

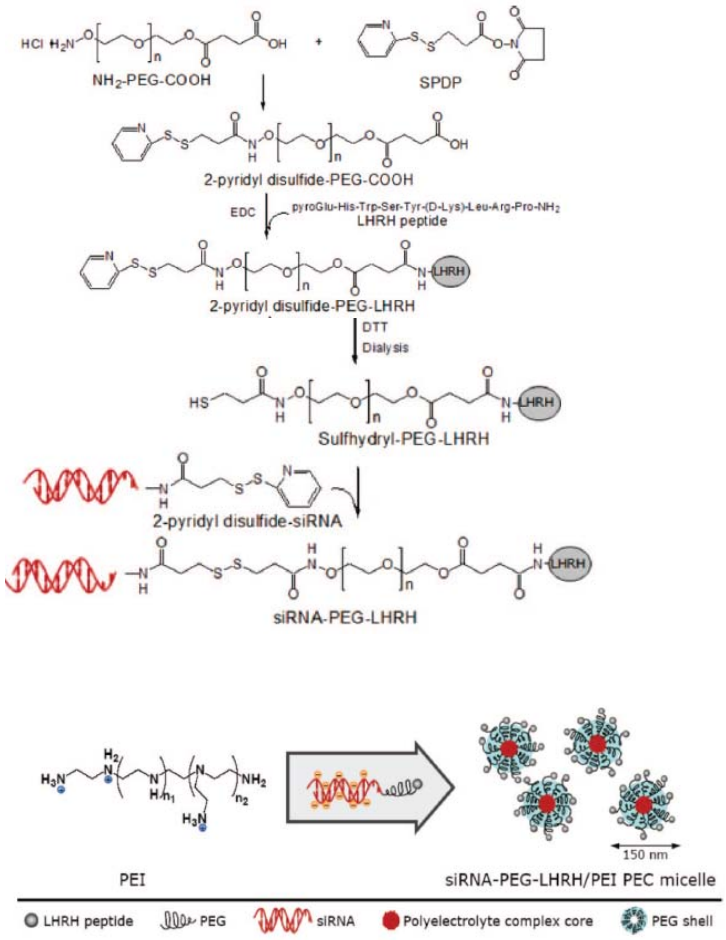

Figure 19: Synthesis of siRNA-PEG-LHRH conjugates and self assembly of polyelectrolyte. The figure was copied from reference "[57]"(Kim, S. H.; Jeong, J. H.; Lee, S. H.; Kim, S. W.; Park, T. G. *Bioconjugate Chemistry* **2008**, *19*, 2156.).

Then the so formed siRNA-PEG-LHRH conjugate associated with PEI via ionic interactions to form polyelectrolyte complex micelles. And they proposed the siRNA should sit in the core of the particle, and targeting groups will expose on the surface since the hydrophilic PEG chain will form outer shell structure.

3.3.3 Folate mediated delivery

It has been demonstrated that the folate receptor, which is glycosylphosphatidylinositol-anchored glycoprotein over expressed in several types of tumor cells, and the binding affinity to folate could be as high as K_d~10^{-9}M. Though there are two carboxylic acid groups that can be applied to conjugate to polymers, the binding affinity will be disrupted if reacting with α-carboxylic acid. In amine terminated PEG-Polylysines, the folate can conjugated to the end of PEG via DCC or NHS coupling. The formed folate-PEG-PLL complexes had shown significant enhance in gene transfection in KB cells but not in A549 cells which do not have folate receptors over-expressed[58]. Another in vitro folate mediated delivery system for siRNA was developed in McCormick's group by coupling the folate to side chain of APMA unit in the polymer. The poly(HPMA-stat-APMA)-b-DMAPMA was synthesized via reversible addition-fragmentation chain transfer (RAFT) polymerization with low polydispersity[59]. Synthetic scheme is shown as follows:

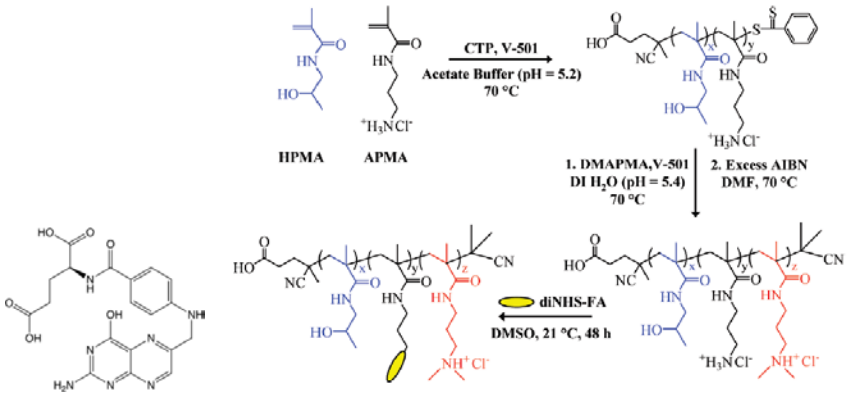

Figure 20: The structure of folic acid and synthetic route of polymer (HPMA-stat-APMA)-b-DMAPMA-folate conjugates. The figure was copied from reference "[59]"(Zhang, Y.; Holley, A. C.; Guo, Y.; Huang, F.; McCormick, C. L. *Biomacromolecules* **2009**, *10*, 936.).

3.3.4 Carbohydrate mediated delivery

Carbohydrate units play an important role in the molecular recognition on cell surface and immunological events, and usually oncogenic transformed cells will overexpress oligosaccharides which can be antigen to activate antigen presenting lymphocytes[60]. The strategy used in vaccine formulation can also be applied to lymphocyte targeting delivery. In Hanson' group, the mannose had been conjugated to polymers like polylysine as targeting moiety into macrophages and dendritic cells which have overexpressed mannose receptors. In contrast, the pDNA bound to galactosylated polylysine didn't show detectable gene expression in macrophages in vitro[61]. While, the monosaccharide galactose can be used to target hepatoma cell via asialoglycoprotein receptors, which can induce the receptor mediated endocytosis. The disaccharide lactose composed of β-D-galactose and β-D-glucose through 1,4 linkage used to be applied to specifically introduce the pDNA to hepatocyte via asialoglycoprotein receptor mediated pathway[62]. The DMAEMA and NVP were copolymerized though chain growth polymerization initiated by carboxyl containing azo-initiator, then the terminal carboxylic group was conjugated to PEG diamine after activated by NHS. The other terminal amine of the PEG block reacted with lactose by reductive coupling to yield a galactose containing transfection agents (shown in Figure 21)[62].

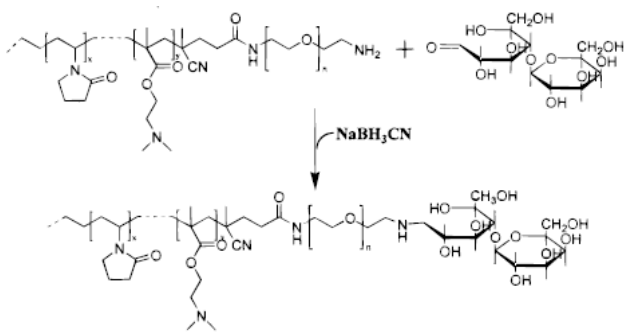

Figure 21: Conjugating lactose to the block copolymer via reductive coupling. The figure was copied from reference "[62]".

3.3.5 Aptamer mediated delivery

Aptamer is a sequence of nucleic acid or peptide that can specific bind to target molecules. It is usually selected by large random screening. In Giangrande's group, they used aptamer-siRNA chimeras to target prostate cancer cells via prostate specific membrane antigen (PSMA). In order to verify the binding of aptamer-siRNA chimeras to the receptor, they did competition studies using RNA free aptamers and antibodies. To further demonstrate the binding, they knocked down the expression of PSMA to see the delivery efficiency. The aptamer-siRNAs were also claimed to be substrates for Dicer[63].

4. siRNA delivery tracking and theranostics development

On top of traditional chemotherapeutic strategies, RNA interference becomes more promising as an alternative approach. Besides the advantages achieved by the RNAi strategy, the tracking of these molecules in vitro and in vivo in recent years has become more prominent and crucial to preclinical studies. The fundamental understanding of the mechanism of siRNA and vector complexation, stability, internalization, cellular

trafficking, dissociation and incorporation in to the RISC complexes, need to be addressed in order to lead to rational design of nano carriers. Among all the siRNA tracking methods, there are a few categories reported:

4.1 Quantum dots (QD) based systems

Quantum dots have been developed for a variety of purposes in biomedical applications due to its tunable optical properties and chemically stability. Quantum dots can be coated with functional motifs and used as drug loading platform or can be absorbed into the complexes as an inclusive unit. One successful example of co-delivery systems were developed by Mao et al[64], where they discovered that quantum dots were coated with beta-cyclodextrin coupled to amino acids such as L-Arg or L-His, and the drug doxorubicin (Dox) were encapsulated into the hydrophobic cavities of beta-cyclodextrin. Significant down-regulation of target genes was observed via RT-PCR and Western Blot. The organization of the system provided a successful approach to combine the chemotherapeutic strategy with siRNA delivery and tracking.

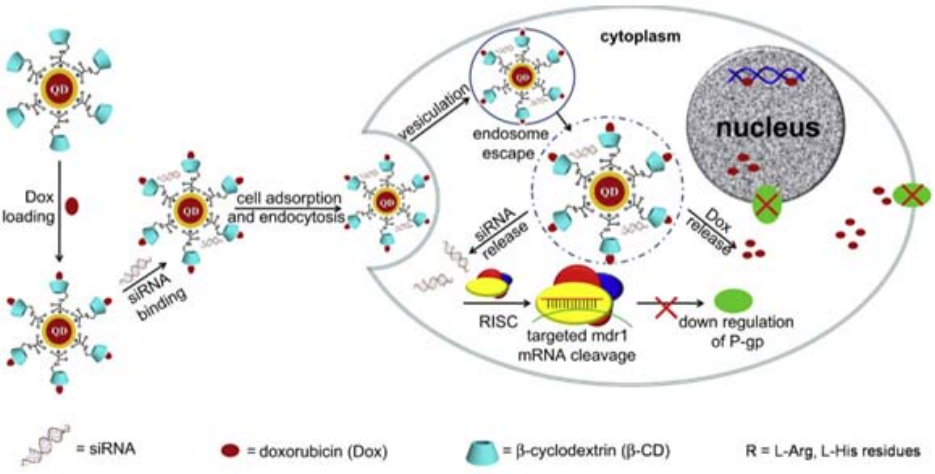

Figure 22. Schematic representation of siRNA absorption and Dox loading onto L-amino acid β-CD modified QDs and illustration of multifunctional QDs as co-delivery system developed by Mao's group. Figure adapted from publication: Li, J.-M.; Wang, Y.-Y.; Zhao, M.-X.; Tan, C.-P.; Li, Y.-Q.; Le, X.-Y.; Ji, L.-N.; Mao, Z.-W. *Biomaterials* **2012**, *33*, 2780.

Lee et. al. developed systems by covalently conjugating the QDs onto siRNA backbones via thiol linkage and non-reducible linkage, therefore to track the release of the siRNA by reducing the bond and keeping the siRNA intact in cellular circulation respectively[65] into the glioblamstoma cells U87. Also Gao et. al. reported the systems developed by using QDs and proton-absorbing polymeric coatings to monitor tracking in real-time during transfection[66].

4.2 Organic dyes based systems

Organic dyes are commonly used in various examinations and detections as these structures are flexible to incorporate into a variety of chemical structure systems. The choice can depend on the requirement of the systems and chemical structures. Also FRET(Fluorescent resonance energy transfer) is commonly used to detect the stability, disassembly of the systems in a different environment to help understand the physical properties of the systems. Anderson et. al. has developed a nanosystem containing siRNA labeled with two different organic dyes as FRET pairs, therefore the complexation and release of the siRNA chains from the systems can be reflected via FRET[67]. Yong et. al have developed Poly-L-lysine coated fluorescent upconversion nanoparticles for siRNA delivery, the tracking was performed to excite the candidate by NIR light to emit high signal-to-noise ratio light and enable imaging in deep tissue. Anna Moore's group labeled

the membrane translocation peptide with Cy5.5 and siRNA with Dy547 to monitor the delivery into CNS cells. The co-localization and dissociation were visualized via confocal microscopy[68] to demonstrate the release of the siRNA and the target gene knockdown was also observed and verified via imaging and qRT-PCR.

4.3 Lanthanide based systems

Lanthanide containing systems have provided another approach for the drug delivery (nucleic acid delivery) tracking and MRI contrast capability. The Gd chelates are commonly used for MRI (nuclear magnetic resonance imaging), which is a non-invasive approach for high resolution tomographic imaging technique. The MRI doesn't require ionizing radiation, and is the most reliable way to acquire soft tissue imaging. The Gd related magnetic resonance imaging is based on the T_1 relaxation. The T_1 relaxation times are different among different tissues, such as in lipid tissues, the relaxation rate is much higher than those in hydrophilic tissues and the vasculature; therefore the relaxation time is shorter. In order to obtain better imaging for the area of interest, the agent that is administrated has to increase the relaxation rate. One approach is to increase the water coordinate sites of the paramagnetic substance; therefore the water exchanging will be accelerated. If the tumbling rate of the environment is similar to the Larmor frequencies of proximal water protons, they will absorb these emitted photons and relax to equilibrium. There are several parameters to affect the relaxivity of bulk water, like distance of the proton from the paramagnetic ion (r), rotational motion (τ_r), time of proton localization in the proximity of the paramagnetic ion (τ_m), electron relaxation time in the paramagnetic ion (τ_e), and number of water coordinate sites to the paramagnetic center (q). Gd(III) and Mn(II) which are the commonly studied contrast agents, yet are

toxic towards biological objects, therefore chelates that can stably frame the ions are required for the design for the purpose of biological applications[69]. The Gd based nucleic acid delivery systems have been developed according to the criteria that combining the delivery and imaging into one nanoparticle. Bryson and Reineke synthesized step growth polymers by combining the oligoamines and DTPA into one polymer chain, therefore obtaining polycation structures containing lanthanide chelates[69].

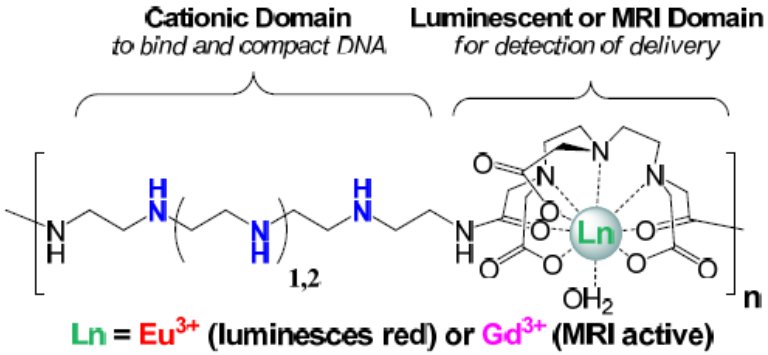

Figure 23. Structures of polycations containing lanthanide chelates. Two analogous structures that differ in the length of the ethyleneamine block in the repeat unit (3a or 3b containing 3 or 4 ethyleneamines, respectively). These two analogs can be chelated with either Eu^{3+} or Gd^{3+} for microscopy and MRI imaging respectively. Figure was used with permission from the publication: Bryson, J. M.; Fichter, K. M.; Chu, W.-J.; Lee, J.-H.; Li, J.; Madsen, L. A.; McLendon, P. M.; Reineke, T. M. *Proceedings of the National Academy of Sciences* **2009**.

The polymers were chelated with Eu^{3+} and Gd^{3+} respectively to achieve luminacent and MRI contrast properties. The oligoamines domains endowed the polymers with positive charges to electrostaticly bind to pDNA. The cellular uptake study

and confocal imaging showed the polyplexes were successfully uptaken by the HeLa cells. However, the target gene expression was not consistent with cellular uptake and showed no significant gene expression. In Sneha Kelkar et. al. study from Reineke's group, she had extended the oligoamine domain to include five and six secondary amines in an effort to improve the performance of the polymers on pDNA delivery. In the flowcytometry and luciferase studies, significant pDNA uptake and expression was observed to demonstrate the success of rational design of polymeric vectors[70].

Miller et. al. also developed Gd^{3+} containing liposomes that exhibited a size less than 100 nm. The particles were visualized to accumulated in tumor tissues via MRI. The capacity of pDNA transfection was also observed via fluorescence microscopy[71].

Apart from the examples listed above, there are many other advances in nanomedicines that have combined the therapeutic, targeting and diagnostic functions covalently or non-covalently into a single nanoscaled compartment. For example, gold nanoshells form multifunctional nanosystems, radio active labeled nanosystems, carbon nanotubes have been developed for multifunctional purposes.

Reference:

(1) Fire, A.; Xu, S.; Montgomery, M. K.; Kostas, S. A.; Driver, S. E.; Mello, C. C. *Nature* **1998**, *391*, 806.

(2) Bernstein, E.; Caudy, A. A.; Hammond, S. M.; Hannon, G. J. *Nature* **2001**, *409*, 363.

(3) Schwarz, D. S.; Hutvner, G.; Du, T.; Xu, Z.; Aronin, N.; Zamore, P. D. **2003**, *115*, 199.

(4) Dykxhoorn, D. M.; Novina, C. D.; Sharp, P. A. *Nat Rev Mol Cell Biol* **2003**, *4*, 457.

(5) Yu, B.; Zhao, X.; Lee, L. J.; Lee, R. J. *The American Association of Pharmaceutical Scientists.***2009**, *11*, 195.

(6) Alexis, F.; Pridgen, E.; Molnar, L. K.; Farokhzad, O. C. *Molecular Pharmaceutics* **2008**, *5*, 505.

(7) Maeda, H. *Adv Enzyme Regul* **2001**, *41*, 189.

(8) Gilmore, I. R.; Fox, S. P.; Hollins, A. J.; Akhtar, S. *Current Drug Delivery* **2006**, *3*, 147.

(9) Boussif, O.; Lezoualch, F.; Zanta, M. A.; Mergny, M. D.; Scherman, D.; Demeneix, B.; Behr, J. P. *Proceedings of the National Academy of Sciences of the United States of America* **1995**, *92*, 7297.

(10) Judge, A. D.; Bola, G.; Lee, A. C. H.; MacLachlan, I. *Molecular Therapy* **2006**, *13*, 494.

(11) Allerson, C. R.; Sioufi, N.; Jarres, R.; Prakash, T. P.; Naik, N.; Berdeja, A.; Wanders, L.; Griffey, R. H.; Swayze, E. E.; Bhat, B. *Journal of Medicinal Chemistry* **2005**, *48*, 901.

(12) Dande, P.; Prakash, T. P.; Sioufi, N.; Gaus, H.; Jarres, R.; Berdeja, A.; Swayze, E. E.; Griffey, R. H.; Bhat, B. *Journal of Medicinal Chemistry* **2006**, *49*, 1624.

(13) Soutschek, J.; Akinc, A.; Bramlage, B.; Charisse, K.; Constien, R.; Donoghue, M.; Elbashir, S.; Geick, A.; Hadwiger, P.; Harborth, J.; John, M.; Kesavan, V.;

Lavine, G.; Pandey, R. K.; Racie, T.; Rajeev, K. G.; Rohl, I.; Toudjarska, I.; Wang, G.; Wuschko, S.; Bumcrot, D.; Koteliansky, V.; Limmer, S.; Manoharan, M.; Vornlocher, H. P. *Nature* **2004**, *432*, 173.

(14) de Fougerolles, A.; Vornlocher, H. P.; Maraganore, J.; Lieberman, J. *Nature Reviews Drug Discovery* **2007**, *6*, 443.

(15) Oishi, M.; Nagasaki, Y.; Itaka, K.; Nishiyama, N.; Kataoka, K. *Journal of the American Chemical Society* **2005**, *127*, 1624.

(16) Whitehead, K. A.; Langer, R.; Anderson, D. G. *Nature Reviews Drug Discovery* **2009**, *8*, 516.

(17) Nguyen, H. K.; Lemieux, P.; Vinogradov, S. V.; Gebhart, C. L.; Guerin, N.; Paradis, G.; Bronich, T. K.; Alakhov, V. Y.; Kabanov, A. V. *Gene Ther* **2000**, *7*, 126.

(18) Auguste, D. T.; Furman, K.; Wong, A.; Fuller, J.; Armes, S. P.; Deming, T. J.; Langer, R. *Journal of Controlled Release* **2008**, *130*, 266.

(19) Rappaport, J.; Hanss, B.; Kopp, J. B.; Copeland, T. D.; Bruggeman, L. A.; Coffman, T. M.; Klotman, P. E. *Kidney International* **1995**, *47*, 1462.

(20) Barquinero, J.; Eixarch, H.; Perez-Melgosa, M. *Gene Therapy* **2004**, *11*, S3.

(21) Dalby, B.; Cates, S.; Harris, A.; Ohki, E. C.; Tilkins, M. L.; Price, P. J.; Ciccarone, V. C. *Methods* **2004**, *33*, 95.

(22) Malone, R. W.; Felgner, P. L.; Verma, I. M. *Proceedings of the National Academy of Sciences of the United States of America* **1989**, *86*, 6077.

(23) Frank-Kamenetsky, M.; Grefhorst, A.; Anderson, N. N.; Racie, T. S.; Bramlage, B.; Akinc, A.; Butler, D.; Charisse, K.; Dorkin, R.; Fan, Y.; Gamba-Vitalo, C.;

Hadwiger, P.; Jayaraman, M.; John, M.; Jayaprakash, K. N.; Maier, M.; Nechev, L.; Rajeev, K. G.; Read, T.; Rohl, I.; Soutschek, J.; Tan, P.; Wong, J.; Wang, G.; Zimmermann, T.; de Fougerolles, A.; Vornlocher, H. P.; Langer, R.; Anderson, D. G.; Manoharan, M.; Koteliansky, V.; Horton, J. D.; Fitzgerald, K. *Proceedings of the National Academy of Sciences of the United States of America* **2008**, *105*, 11915.

(24) Chonn, A.; Semple, S. C.; Cullis, P. R. *Journal of Biological Chemistry* **1995**, *270*, 25845.

(25) Papahadjopoulos, D.; Allen, T. M.; Gabizon, A.; Mayhew, E.; Matthay, K.; Huang, S. K.; Lee, K. D.; Woodle, M. C.; Lasic, D. D.; Redemann, C. *Proceedings of the National Academy of Sciences of the United States of America* **1991**, *88*, 11460.

(26) Oh, Y. K.; Park, T. G. *Adv Drug Deliv Rev* **2009**.

(27) Franchini, J.; Ranucci, E.; Ferruti, P.; Rossi, M.; Cavalli, R. *Biomacromolecules* **2006**, *7*, 1215.

(28) Urban-Klein, B.; Werth, S.; Abuharbeid, S.; Czubayko, F.; Aigner, A. *Gene Therapy* **2005**, *12*, 461.

(29) Tan, P. H.; Yang, L. C.; Shih, H. C.; Lan, K. C.; Cheng, J. T. *Gene Therapy* **2005**, *12*, 59.

(30) Kim, S. H.; Jeong, J. H.; Lee, S. H.; Kim, S. W.; Park, T. G. *Journal of Controlled Release* **2008**, *129*, 107.

(31) Ahn, C.-H.; Chae, S. Y.; Bae, Y. H.; Kim, S. W. *Journal of Controlled Release* **2002**, *80*, 273.

(32) Petersen, H.; Martin, A. L.; Stolnik, S.; Roberts, C. J.; Davies, M. C.; Kissel, T. *Macromolecules* **2002**, *35*, 9854.

(33) Malek, A.; Czubayk, F.; Aigner, A. *Journal of Drug Targeting* **2008**, *16*, 124.

(34) Peng, Q.; Hu, C.; Cheng, J.; Zhong, Z.; Zhuo, R. *Bioconjugate Chemistry* **2009**, *20*, 340.

(35) Kiang, T.; Wen, J.; Lim, H. W.; Leong, K. W. K. W. *Biomaterials* **2004**, *25*, 5293.

(36) Artursson, P.; Lindmark, T.; Davis, S. S.; Illum, L. *Pharmaceutical Research* **1994**, *11*, 1358.

(37) Roy, K.; Mao, H.-Q.; Huang, S. K.; Leong, K. W. *Nat Med* **1999**, *5*, 387.

(38) Liu, X. D.; Howard, K. A.; Dong, M. D.; Andersen, M. O.; Rahbek, U. L.; Johnsen, M. G.; Hansen, O. C.; Besenbacher, F.; Kjems, J. *Biomaterials* **2007**, *28*, 1280.

(39) Holzinger, M.; Bouffier, L.; Villalonga, R.; Cosnier, S. *Biosensors and Bioelectronics* **2009**, *24*, 1128.

(40) Menuel, S.; Fontanay, S.; Clarot, I.; Duval, R. E.; Diez, L.; Marsura, A. *Bioconjugate Chemistry* **2008**, *19*, 2357.

(41) Srinivasachari, S.; Fichter, K. M.; Reineke, T. M. *Journal of the American Chemical Society* **2008**, *130*, 4618.

(42) Davis, M. E.; Brewster, M. E. *Nat Rev Drug Discov* **2004**, *3*, 1023.

(43) Davis, M. E. *Molecular Pharmaceutics* **2009**, *6*, 659.

(44) Srinivasachari, S.; Reineke, T. M. *Biomaterials* **2009**, *30*, 928.

(45) Liu, Y.; Reineke, T. M. *Bioconjugate Chemistry* **2005**, *17*, 101.

(46) Liu, Y.; Reineke, T. M. *Bioconjugate Chemistry* **2006**, *18*, 19.

(47) Srinivasachari, S.; Liu, Y.; Zhang, G.; Prevette, L.; Reineke, T. M. *Journal of the American Chemical Society* **2006**, *128*, 8176.

(48) Srinivasachari, S.; Liu, Y.; Prevette, L. E.; Reineke, T. M. *Biomaterials* **2007**, *28*, 2885.

(49) Gullotti, E.; Yeo, Y. *Molecular Pharmaceutics* **2009**, *6*, 1041.

(50) Suh, W.; Chung, J.-K.; Park, S.-H.; Kim, S. W. *Journal of Controlled Release* **2001**, *72*, 171.

(51) Mok, H.; Park, T. G. *Macromolecular Bioscience* **2009**, *9*, 731.

(52) Wu, G.; Barth, R. F.; Yang, W.; Chatterjee, M.; Tjarks, W.; Ciesielski, M. J.; Fenstermaker, R. A. *Bioconjugate Chemistry* **2003**, *15*, 185.

(53) Qian, Z. M.; Li, H.; Sun, H.; Ho, K. *Pharmacol Rev* **2002**, *54*, 561.

(54) Zugates, G. T.; Anderson, D. G.; Little, S. R.; Lawhorn, I. E. B.; Langer, R. *Journal of the American Chemical Society* **2006**, *128*, 12726.

(55) W Suh, S. H., L Yu, SW Kim *Molecular Therapy* **2002**, *6*, 664.

(56) Dharap, S. S.; Wang, Y.; Chandna, P.; Khandare, J. J.; Qiu, B.; Gunaseelan, S.; Sinko, P. J.; Stein, S.; Farmanfarmaian, A.; Minko, T. *Proceedings of the National Academy of Sciences of the United States of America* **2005**, *102*, 12962.

(57) Kim, S. H.; Jeong, J. H.; Lee, S. H.; Kim, S. W.; Park, T. G. *Bioconjugate Chemistry* **2008**, *19*, 2156.

(58) Cho, K. C.; Kim, S. H.; Jeong, J. H.; Park, T. G. *Macromolecular Bioscience* **2005**, *5*, 512.

(59) Zhang, Y.; Holley, A. C.; Guo, Y.; Huang, F.; McCormick, C. L. *Biomacromolecules* **2009**, *10*, 936.

(60) Buskas, T.; Ingale, S.; Boons, G.-J. *Angewandte Chemie International Edition* **2005**, *44*, 5985.

(61) Ferkol, T.; Perales, J. C.; Mularo, F.; Hanson, R. W. *Proceedings of the National Academy of Sciences of the United States of America* **1996**, *93*, 101.

(62) Lim, D. W.; Yeom, Y. I.; Park, T. G. *Bioconjugate Chemistry* **2000**, *11*, 688.

(63) McNamara, J. O.; Andrechek, E. R.; Wang, Y.; Viles, K. D.; Rempel, R. E.; Gilboa, E.; Sullenger, B. A.; Giangrande, P. H. *Nat Biotech* **2006**, *24*, 1005.

(64) Li, J.-M.; Wang, Y.-Y.; Zhao, M.-X.; Tan, C.-P.; Li, Y.-Q.; Le, X.-Y.; Ji, L.-N.; Mao, Z.-W. *Biomaterials* **2012**, *33*, 2780.

(65) Jung, J.; Solanki, A.; Memoli, K. A.; Kamei, K.-i.; Kim, H.; Drahl, M. A.; Williams, L. J.; Tseng, H.-R.; Lee, K. *Angewandte Chemie* **2010**, *122*, 107.

(66) Yezhelyev, M. V.; Qi, L.; O'Regan, R. M.; Nie, S.; Gao, X. *Journal of the American Chemical Society* **2008**, *130*, 9006.

(67) Alabi, C. A.; Love, K. T.; Sahay, G.; Stutzman, T.; Young, W. T.; Langer, R.; Anderson, D. G. *ACS Nano* **2012**, *6*, 6133.

(68) Moore, A. and Z. Medarova *Methods Mol Biol* **2009,** *487*, 93-110.

(69) Bryson, J. M.; Fichter, K. M.; Chu, W.-J.; Lee, J.-H.; Li, J.; Madsen, L. A.; McLendon, P. M.; Reineke, T. M. *Proceedings of the National Academy of Sciences* **2009**.

(70) Kelkar, S. S.; Xue, L.; Turner, S. R.; Reineke, T. M. *Biomacromolecules* **2014**, *15*, 1612.

(71) Kamaly, N.; Kalber, T.; Ahmad, A.; Oliver, M. H.; So, P.-W.; Herlihy, A. H.; Bell, J. D.; Jorgensen, M. R.; Miller, A. D. *Bioconjugate Chemistry* **2007**, *19*, 118.

Chapter2:

Carbohydrate Based Cationic Polymers for siRNA Delivery-- Role of Polymer Length, Carbohydrate Size, and Nucleic Acid Type

This chapter is based on the publication:

L. Xue, N. Ingle, T. M. Reineke, "Highlighting the Role of Polymer Length, Carbohydrate Size, and Nucleic Acid Type in Potency of Glycopolycation Agents for pDNA and siRNA Delivery" *Biomacromolecules*, 2013, 14 (11), pp 3903–3915.

Background

While nucleic acids such as small interfering RNA (siRNA) and plasmid DNA (pDNA) are promising research tools and therapeutic modalities, their potential in medical applications is limited by a fundamental mechanistic understanding and inadequate efficiency. Herein, two series of carbohydrate-based polycations were synthesized and examined that varied in the degree of polymerization (n)—one containing trehalose [Tr4(n) series: Tr4(23), Tr4(55), Tr4(77)] and the other containing beta-cyclodextrin [CD4(n) series: CD4(10), CD4(26), CD4(39), CD4(143), CD4(239)]. In addition, two monosaccharide models were examined for comparison that contain tartaramidoamine (T4) and galactaramidoamine (G4 or Glycofect) repeats. Delivery profiles for pDNA were compared with those obtained for siRNA delivery and reveal that efficacy differs significantly as a function of carbohydrate type, nucleic acid type and dose, polymer length, and presence of excess polymer in the formulation. The Tr4 polymers yielded higher efficacy for pDNA delivery, yet, the CD4 polymers achieved higher siRNA delivery and gene down regulation. The T4 and Glycofect derivatives, while efficient for pDNA delivery, were completely ineffective for siRNA delivery. A strong polymer length and dose dependence on target gene knockdown was observed for all polymers tested. Also, free polymer in solution (uncomplexed) was demonstrated to be a key factor in promoting siRNA uptake and gene down regulation.

Introduction

The discovery of RNA interference by Fire and Mello[1] has been a milestone on the revolutionary journey of modern therapeutics. Dramatic attention has been drawn to the investigation and development of small interfering RNA (siRNA)-related gene

silencing techniques, both as research tools and potential therapeutic strategies.[2, 3] _ENREF_2 Currently, the major challenge to the translation of this discovery into novel therapeutics is the inadequate delivery of siRNA to target sites of therapeutic interest.[4] Once in the cytoplasm, siRNA is able to assemble with the components of the RNA-induced silencing complex (RISC) to initiate the cleavage and degradation of its corresponding mRNA. In this manner, the production of the corresponding protein is diminished.[2] However, the anionic nature of siRNA and its vulnerability to enzymatic degradation (when unmodified) limits the cellular internalization of 'naked' siRNA.[4, 5] Therefore, development of safe and effective systems for siRNA delivery has received extraordinary attention.

There are many different approaches currently being taken to the development of delivery vehicles for siRNA, including polymers, lipids, viruses, gold nanoparticles, carbon nanotubes, and other nanosystems.[4, 6-12] In particular, polymer-based delivery vehicles offer tunable structures and versatile combinations of different functionalities that allow achievement of desirable properties, including particle size, surface charge (zeta potential), and targeting ligand incorporation.[12] Cationic polymers can bind with anionic siRNA to form polyplexes via electrostatic interactions and hydrogen bonding, thereby neutralizing the siRNA negative charge and protecting it from degradation. An early example of an efficient nucleic acid delivery polymer is polyethylenimine (PEI), which has had limited use in the clinic due, in large part, to its high toxicity at effective doses.[13,14] Currently, there are some polymer-based candidate siRNA formulations at different stages of clinical trials.[4] The first targeted delivery of siRNA in humans, reported in 2009, is based upon the use of a cyclodextrin-containing cationic polymer.[15]

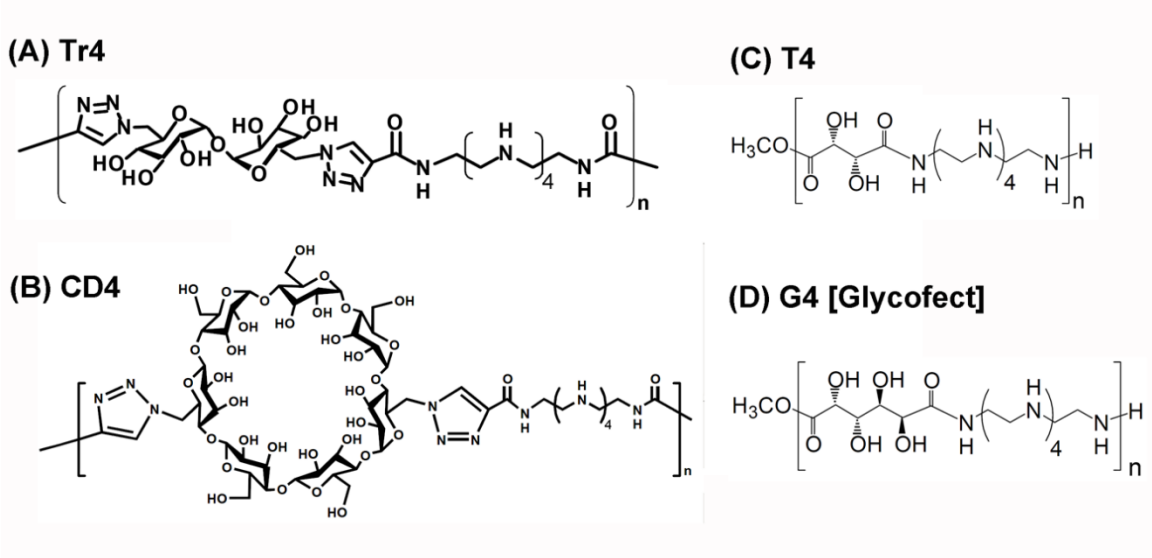

Figure 1. Schematic structures of the carbohydrate-containing cationic polymers [Tr4,[16] CD4,[17] T4,[18] and G4 (Glycofect)[18]] examined in this study, which span a large range in carbohydrate size (small to large).

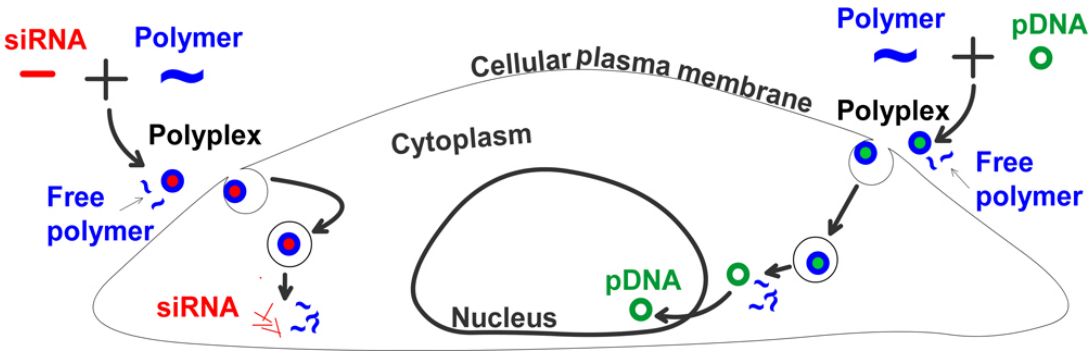

Figure 2. Schematic showing the different delivery destination of siRNA (cytoplasm) and pDNA (nucleus). In this study we also examine the role of free polymer, which also affects cellular entry and intracellular delivery.

Previously, we have developed several series of carbohydrate-based cationic polymers (Figures 1 and 2) that successfully deliver pDNA to various cell types *in vitro*.[16-21] By alternating the carbohydrate type (both mono-, di-, and oligo-saccharides) and oligoethyleneamine length (between 1-6 in the repeat unit) within the polymer backbone, efficient pDNA delivery has been achieved with generally low concomitant cytotoxicity.[16-21] The optimal structures for these series of polymers have mainly contained the pentaethylenetetramine moieties in the repeat unit. The structure-activity relationships have been extensively studied and shown to be strongly dependent on the type of carbohydrate and oligoethyleneamine length for pDNA delivery.[16-21] For example, when considering preliminary studies with cationic beta-cyclodextrin and trehalose click polymers (Figure 1A and 1B), the delivery efficiency of pDNA and toxicity profile has been shown to depend on the molecular weight (typically, longer polymers reveal higher delivery efficiency and toxicity); however this is highly dependent on cell and polymer type.[16, 17] Also, the trehalose analogs (Figure 1A) form stable polyplexes that have been found to remain mostly as discrete polyplexes in cell culture media containing fetal bovine serum, which could aid in cellular internalization and trafficking, promoting efficacy.[19] While many delivery vehicles have been examined for pDNA delivery and assessed for structure-activity relationships (SAR) in vitro for gene expression, results examining siRNA SAR will likely be divergent. Because of the significant differences between siRNA and pDNA, including molecular weight and subcellular target site, previously-derived structure-activity relationships cannot be directly translated from pDNA delivery to siRNA delivery.[22-24] ENREF 24 In a recent study by Salcher et. al., a series of branched four-armed oligomers with either terminal cysteine or alanine groups

affected polyplex stabilization and delivery efficiency of siRNA and pDNA.[25] Structures with terminal cysteines appeared to stabilize the complexes and promote high delivery of both nucleic acid types. However, the type of oligoethyleneamine in the branches yielded clear differences in efficacy for siRNA (tetraethylenepentamine was best for gene knockdown) versus pDNA (pentaethylenehexamine was best to promote transgene expression).[25] In addition, many new delivery systems are being developed and examined specifically for siRNA delivery. A related study by Frohlich et. al. has also reported the structure-activity relationships of a new family of oligo (ethane amino) amides with lipid modifications, which had different molecular shapes (described as 'i', 'T', and 'U' – shaped oligos); the oligo shape affected siRNA delivery and gene knockdown where C18 lipid modification appeared to play the largest role in increasing gene knockdown.[26]

Herein, a systematic evaluation of siRNA-mediated gene knockdown has been examined for a series of carbohydrate-containing 'click' polymers. The series of polymers were synthesized to contain either a trehalose [Tr4(n)] or beta-cyclodextrin [CD4(n)] moiety copolymerized with a oligoethyleneamine monomer via copper-catalyzed azide/alkyne cycloaddition. In addition, models containing galactaramidoamine (Glycofect) or tartaramidoamine (T4) repeats were also created for comparison, thus spanning a large range in saccharide size (small to large, Figure 1). The effects of saccharide type, polymer length, and nucleic acid type (pDNA and siRNA), and presence of free polymer on polyplex formation and cellular delivery were examined. We reveal that all of these parameters all play a large role in the formation of polyplexes and delivery efficacy of both pDNA and siRNA in cultured U-87 (glioblastoma) cells largely

due to chemical differences in the vehicles (Figure 1) and the inherent differences in mechanism/site of action for pDNA versus siRNA (Figure 2).

Experimental Section

Materials and Methods

General

U-87 MG-luc2 (U-87_luc2) cells, human glioblastoma cells genetically engineered to constitutively express luciferase, were obtained from Caliper LifeSciences, Inc. (Mountain View, CA). Luc2 siRNA, which targets luc2 luciferase, and a Cy5-labeled Luc2 siRNA were obtained from Integrated DNA Technologies, Inc. (Coralville, IA). The sequence of the sense strand of the Luc2 siRNA is 5'-GGACGAGGACGAGCACUUCUU-3', and the antisense strand sequence is 3'-UUCCUGCUCCUGCUCGUGAAG-5'. The Cy5 fluorophore within the Cy5-labeled Luc2 siRNA was conjugated to the 3' terminus of the sense strand (5'-GGACGAGGACGAGCACUUCUU-Cy5-3'). Scrambled siRNA (siCon) was purchased from Dharmacon, Inc (Lafayette, CO). DMEM+GlutaMAX^{TM}-I (DMEM), Opti-MEM I+GlutaMAX^{TM}-I (Opti-MEM), UltraPure^{TM} Agarose-1000, MTT (3-(4,5-dimethylthiazol-2-yl)-2,5-diphenyl tetrazolium bromide), propidium iodide (1.0 mg/mL solution in water), PBS pH=7.4, trypsin, antibiotic-antimycotic and Lipofectamine™2000 (Lipo) were obtained from Invitrogen, Inc. (Carlsbad, CA). DEPC-treated water for the RNA work was obtained from Fisher Scientific (Pittsburgh, PA). INTERFERin™ was a gift from Polyplus-Transfection (Strasbourg, France). jetPEI™ was purchased from Polyplus-Transfection (above). The Luciferase Assay System was obtained from

Promega Corporation (San Luis Obispo, CA). Bio-Rad DC Protein Assay Reagent A, Reagent B, and Reagent S were obtained from Bio-Rad Laboratories, Inc. (Hercules, CA). CellScrub™ Buffer was obtained from Genlantin, Inc. (San Diego, CA). Bovine albumin and all chemicals used in polymer synthesis were purchased from Sigma-Aldrich (St. Louis, MO). Spectra/Por® dialysis membranes (MWCO: 6,000-8,000 and MWCO: 3,500) were obtained from Spectrum Laboratories, Inc. (Rancho Dominguez, CA). Glycofect Transfection Reagent™, having a degree of polymerization of approximately 11 was donated by Techulon, Inc. (Blacksburg, VA). Polymer T4 (n_w=12) was synthesized by our previously published method. [21, 27].

Synthesis and characterization of the carbohydrate-containing monomers and polymers

The synthetic routes (scheme was listed at the end of this section and characterization in the results section) for the monomers and polymers have been reported in our previous publications,[16, 17, 19] with some slight modifications. In brief, the dialkyne-pentaethylenetetramine monomers were synthesized from pentaethylenehexamine by protecting the primary amines with trifluoroacetyl groups and secondary amines with *tert*-butoxylcarbonyls (Boc). The product was recrystallized twice from ethanol, followed by the deprotection of the primary amines by refluxing in aqueous methanol with potassium carbonate. The primary amines were then coupled to propiolic acid using dicyclohexyl carbodiimide (DCC). The dialkyne-pentaethylenetetramine monomer was purified by chromatography [silica gel, 5% (v:v) ethanol in dichloromethane (DCM)] and further recrystallized from ethyl acetate/hexane (1:3 v:v).

The total % yield from starting material to final dialkyneoligoethylene amine monomer product was 34%.

2,3,4,2',3',4'-hexa-O-acetyl-6,6'-diazido-6,6'-dideoxyl-D-trehalose was also synthesized according to a previously-published procedure.[19] The final product was purified on a silica gel column using 10% (v:v) diethyl ether in DCM. Fractions containing the product were collected, the solvent was evaporated, and the products were further recrystallized from 10% (v:v) ethyl acetate in diethyl ether to yield fine white crystals. The total % yield from starting materials to final product was 33%.

The protected (OAc) diazide-β-cyclodextrin monomers were synthesized and purified exactly according to our previously published procedure.[17] The total % yield from starting materials to final product was 10%. Generally, the polymerization of the trehalose and β-cyclodextrin monomers with the dialkyne-pentaethylenetetramine monomer was performed in a 1:1 (v:v) solution of tert-butyl alcohol and water under catalysis of copper(I), generated *in situ* from $CuSO_4$ and sodium ascorbate, at 50-70^{o}C to yield the protected (OAc and Boc) polymers. The product was dried under vacuum, followed by the deprotection of the acetal groups with sodium methoxide in methanol and deprotection of Boc with trifluoroacetic acid in dichoromethane. The final products were purified by dialysis against ultrapure water, then lyophilized and analyzed by NMR and GPC (Table 1). The total % yields from polymerization to deprotection of the trehalose polymers and cyclodextrin polymers were 23% and 18% respectively. Characterization data for these polymers are available in result sections.

Synthetic routes for the click polymers

1. Synthesis of acetylated diazido trehalose monomer

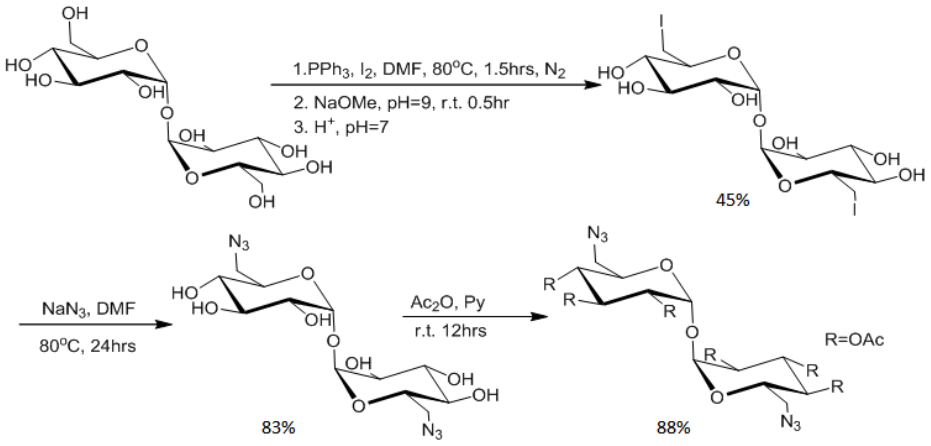

2. Synthesis of dialkyne pentaethyleneamine monomer

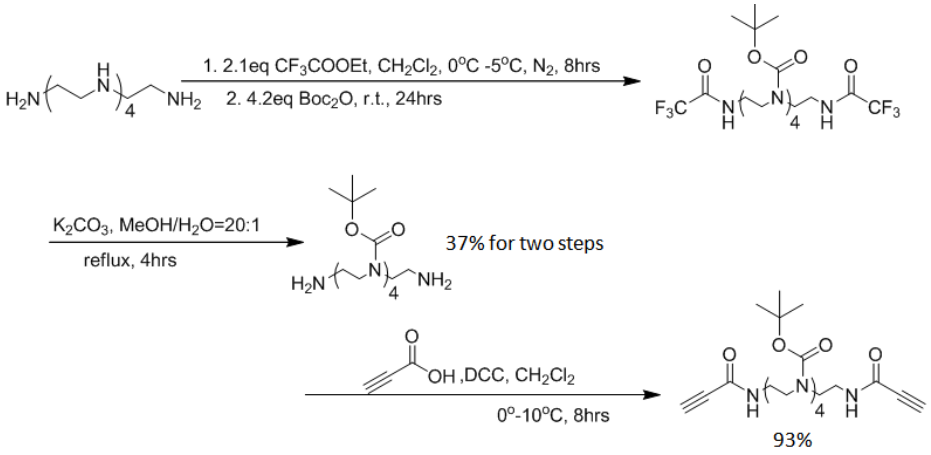

3. Synthesis of dialkyne cyclodextrin monomer

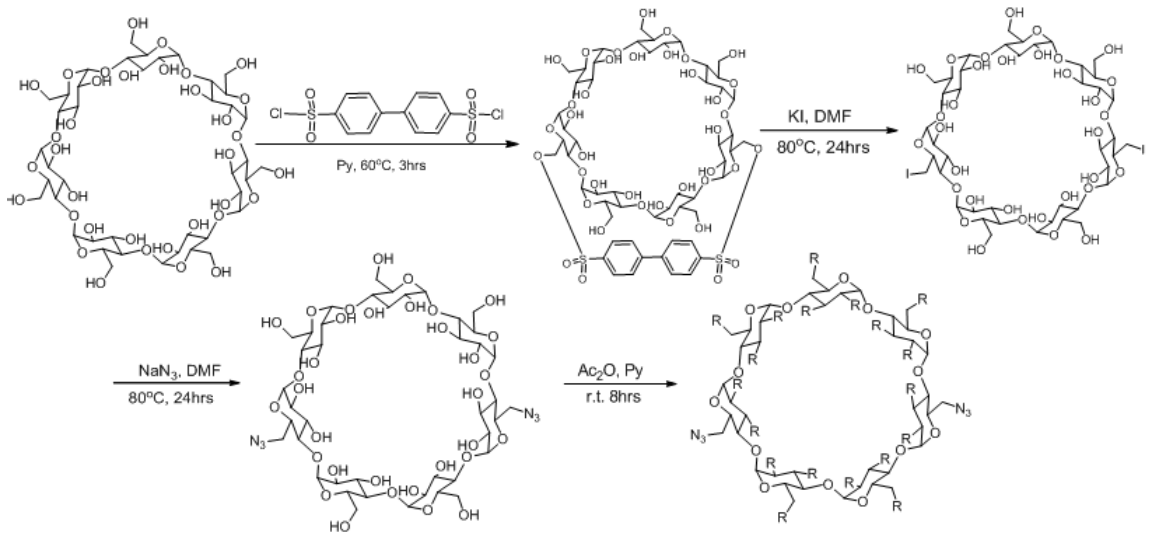

4. Copper(I) catalyzed azide alkyne click polymerization and polymer deprotection for trehalose polymers

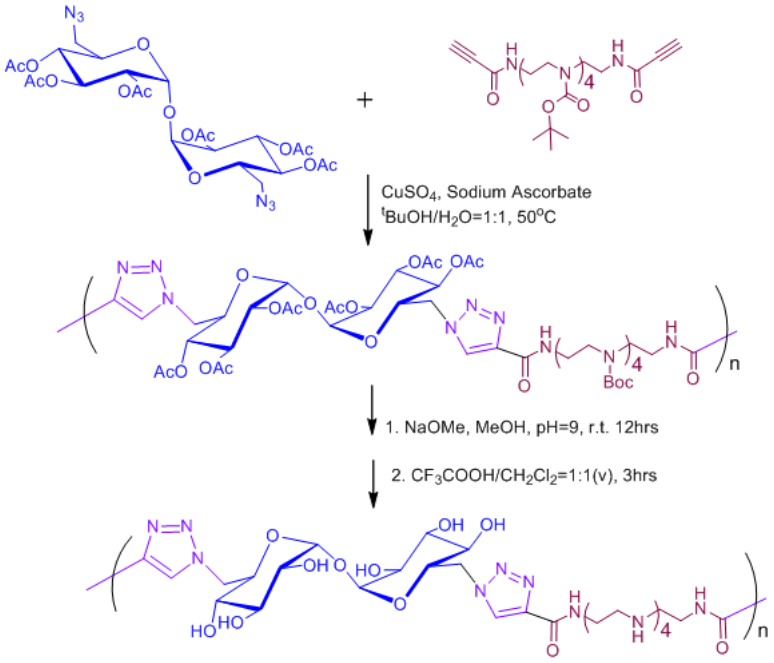

4. Copper(I) catalyzed azide alkyne click polymerization and polymer deprotection for cyclodextrin click polymers

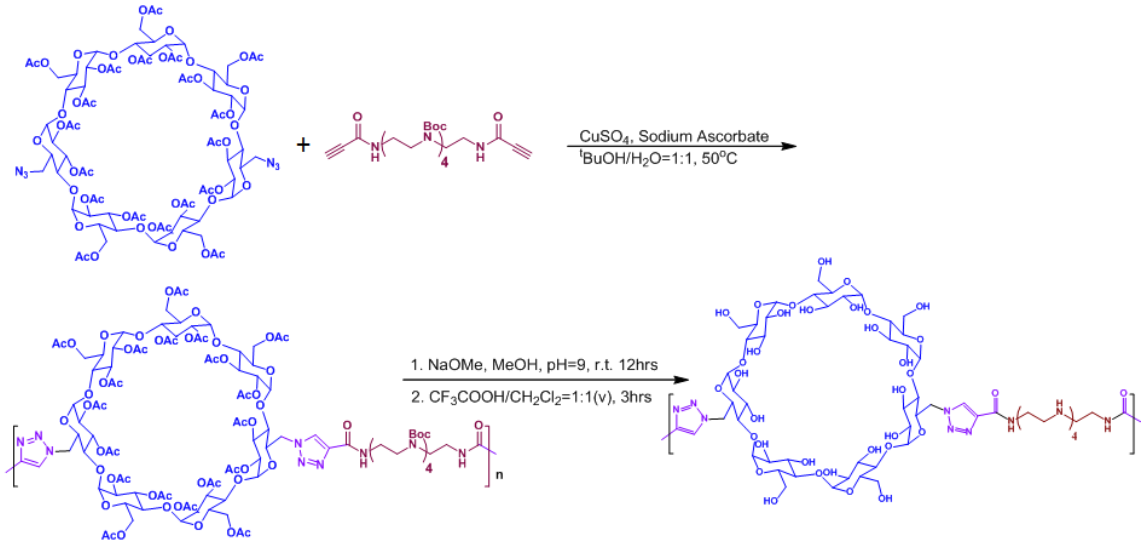

Scheme 1. Synthesis of trehalose pentaethylene click polymer and cyclodextrin pentaethylene click polymer.

Polymer siRNA binding studies via gel electrophoresis shift assays

Agarose gels [2% (w/v)] were prepared by dissolving 1 g agarose in 50 mL TAE buffer (40 mM Tris-acetate, 1 mM EDTA) while heating. Immediately before the gel solution was poured in the gel electrophoresis chamber and cooled to ambient temperature, 4 µL of ethidium bromide (10 mg/mL) was added. The polyplexes were formed by adding 10 µL of each polymer solution at various concentrations to 10 µL of 2 µM siRNA solution in RNase-free (DEPC-treated) water. The N/P ratio indicates the polymer/nucleic acid ratio for polyplex formulation (the number of secondary amines on polymer backbones to the number of phosphate groups on the nucleic acid backbones to form the polyplex solutions) as previously described.[16, 17, 19] The polyplexes were

incubated at room temperature for 30 min. 2 µL of BlueJuice™ loading buffer (Invitrogen) was added to each polyplex solution shortly before loading onto the gel. Electrophoresis was performed at 65 V for 45 min. The complexation of siRNA by the polymer was indicated by the lack of gel migration (or shift) of the siRNA-containing bands.

Polyplex formation and analysis via dynamic light scattering (DLS)

Hydrodynamic diameters of the polymer-siRNA polyplex formulations were determined by dynamic light scattering (DLS) using a ZetaSizer (Nano ZS) instrument from Malvern, Inc. (Worcestershire, United Kingdom) equipped with a 633-nm laser. For each size measurement, polyplexes were formulated by addition of 33 µL of polymer solution in RNase-free water to 33 µL of 2 µM siRNA solution in RNase-free water at room temperature forming complexes at various N/P ratios. The formation of polyplexes was monitored by performing DLS measurements at 0, 5, 10, 15, 30 and 60 min after solution mixing. Each polyplex solution was then diluted to a final volume of 750 µL with RNase-free water for zeta potential measurements of each sample in triplicate.

The stability of the polyplexes in transfection media was studied by adding Opti-MEM (70 µL) or serum-containing DMEM (70 µL) to polyplex solutions (66 µL) in RNase-free water 30 min after mixing of the polymer and siRNA solutions. DLS measurements were then performed at the indicated time points (up to 24 h).

Cell culture studies

In case of siRNA, luciferase-expressing glioblastoma cells (U-87_luc2) were used for target gene (luciferase) down-regulation efficiency experiments, cellular uptake

studies, and MTT assays for cell viability. In addition non-luciferase expressing glioblastoma cells (U87MG) were used in up-regulation efficiency experiments and cellular uptake with plasmid DNA. The cells were grown in complete DMEM (supplemented with 10% (v:v) fetal bovine serum (FBS) and 1% antibiotic-antimycotic solution (containing penicillin, streptomycin, and amphotericin B) at 37^{o}C and 5% CO_2.

Luciferase assay and protein assay

Luciferase-expressing glioblastoma cells (U-87_luc2) were seeded at 50,000 cells/well in 24-well plates 24 h prior to transfection. In general, anti-luciferase (Luc2) siRNA, control (siCon) siRNA, and polymer stock solutions were diluted with RNase-free water, and the polyplexes were formed by the addition of 33 µL of polymer solution to 33 µL of siRNA solution, followed by incubation for 30 min at room temperature. The resulting polyplex solutions were then added to pre-warmed Opti-MEM or DMEM to yield transfection solutions. Cells were washed with PBS before the addition of 200 µL of the transfection solution.

The formation of siRNA-containing lipoplexes using Lipofectamine™ 2000 and complexes with INTEFERin™ were performed according to the manufacturer's protocol. Polyplexes with the carbohydrate polymers were formulated at various N/P ratios as we previously described.[17, 18] The cells were incubated with polyplex/lipoplex solutions for 4 h before complete DMEM was added. Forty eight hours later, the cells were washed with 500 µL PBS and treated with 1x cell lysis buffer (Promega, Madison, WI) for 15 min at room temperature. Aliquots (5 µL) of cell lysate were examined on 96-well plates with a luminometer (GENios Pro, TECAN US, Research Triangle Park, NC) for luciferase

activity over 10 s. For each well, 100 µL of luciferase assay substrate (Promega, Madison, WI) was added. The average of duplicate measurements on each individual replicate was utilized for calculation. The amount of protein (mg) in cell lysates was calculated using a standard curve generated with bovine serum albumin by following the protocol included in Bio-Rad DC protein assay kit. The relative light unit (RLU)/mg protein was then calculated and averaged across replicate wells. The protein and luciferase levels of non-transfected cells were used for normalizing the data and calculating the extent of gene knockdown. Each treatment was tested in triplicate in 24-well plates.

For the experiments examining pDNA delivery, non-luciferase expressing U87MG cells were plated 24 hours prior to transfection at a cell density of 50,0000 cells/well in 24-well plates in DMEM culture media containing 10% FBS. Polyplexes were formulated with luciferase plasmid DNA (gWiz-luc) at respective N/P ratios and incubated at room temperature for 1 h prior to transfection. The cells were then transfected in the presence of either (1) serum-free a OptiMEM media or (2) DMEM media containing 10% FBS.

Cellular uptake measurement by flow cytometry

Flow cytometry was performed to examine the cellular uptake of Cy5-labeled siRNA with various formulations at 3 h post-transfection. In general, U-87_luc2 glioblastoma cells were seeded at 300,000/well in 6-well plates 24 h prior to transfection. To transfect, 33 µL of each polymer solution was added to 33 µL of 2 µM Cy5-labeled siRNA solution. After 30 min incubation at room temperature (to form the polyplexes), each polyplex solution was pipetted into 1584 µL of pre-warmed Opti-MEM to yield the

final transfection solution. Each well was treated with 500 µL of the obtained transfection solution. After 3 h, the media was removed and cells were washed with 500 µL/well CellScrub™ Buffer for 15 min at room temperature. The CellScrub™ Buffer was then aspirated and cells were exposed to trypsin (0.05% (w/v), 500 µL/well) for 3 min to provide detachment from the plate, then complete DMEM (500 µL/well) was applied to inhibit trypsin. The cell suspension was collected and centrifuged at 1000 rpm for 10 min at 4^{o}C. The supernatant was removed and cells were twice washed with 0.5 mL PBS and centrifuged to remove the extracellular polyplexes. Finally, 1 mL PBS was added and the suspensions were kept on ice prior to flow cytometry analysis. Propidium iodide (2.5 µL) was added prior to the analysis. The flow cytometer (FACSCalibur and FACSVerse, Becton Dickenson, San Jose, CA) equipped with a helium-neon laser to excite Cy5 at 633 nm was used to count twenty thousand events for each sample. The threshold fluorescence level was defined by manually adjusting the positive region such that <1% of negative control cells were positive for fluorescence. Each treatment was performed in triplicate. For pDNA delivery experiments, non-luciferase expressing cells (U87MG) were transfected with Cy5 labeled plasmid DNA and analyzed for uptake via flow cytometry analysis.

MTT assay

MTT reagent (3-(4, 5-dimethylthiazol-2-yl)-2, 5-diphenyltetrazolium bromide) was used to estimate the cytotoxicity of the formulations. Typically, U-87_luc2 glioblastoma cells were seeded at 50,000 cells/well in 24-well plates 24 h prior to transfection. The polyplexes were formed following the procedure described above. 200 µL of transfection media was added to each well; 4 h later, complete DMEM was added

at 1 mL/well. Then, 24 h later, the media was aspirated and the cells were washed with PBS (500 µL/well). 1 mL of serum-containing DMEM with 0.5 mg/mL of MTT was added to each well and cells were incubated for 1 h. The media was then replaced with 600 µL of DMSO for 15 min at room temperature. A 200 µL aliquot of the media was transferred to a well of a 96-well plate for analysis by colorimeter with wavelength at 570 nm. Samples of non-transfected cells were used for normalization.

Statistical Analysis

Statistical analysis was performed at alpha level of 0.05 using JMP software (SAS Campus Drive, Cary, NC). The Tukey-Kramer HSD (honestly significant difference) was used to test significant differences among all means. In addition, a Student's t-test was used to further find significant differences in cases where the differences were apparent but not detectable by Tukey's test. All significant differences are denoted by asterisk (*) mark.

Results

Preparation and characterization of polymer vehicles

We have previously published the main synthetic procedures for all of the model polymers examined in this study. T4 and Glycofect (G4) were examined at one length (degree of polymerization, n ~ 12) due to difficulties in the synthesis of these models at longer lengths.[18, 20, 27] For the click polymer models, we obtained two series of polymers that vary in the carbohydrate type (trehalose or beta-cyclodextrin) in the repeat unit and the polymer length (Table 1), which was obtained by varying the reaction conditions as

previously described.[16, 17,19, 28] Each novel polymer prepared for this study is referred to by a name indicating the carbohydrate (i.e. 'Tr' for trehalose, 'CD' for β-cyclodextrin, "T" for tartarate), number of secondary amines (4), and the weight-averaged number of repeat units (n_w).

Table 1. GPC characterization of the click polymers. M_w: weight-averaged molecular weight. M_n: number-averaged molecular weight. Đ (M_w/M_n): polydispersity index. n_w: weight-averaged number of repeat units. The degree of polymerization (n) for Glycofect is ~11 according to the manufacturer.

Polymer	M_w	M_n	Đ (M_w/M_n)	n_w
T4(12)	4.3kDa	3.9kDa	1.1	12
Tr4(23)	17.2 kDa	10.2 kDa	1.7	23
Tr4(55)	40.5 kDa	18.4 kDa	2.2	55
Tr4(77)	56.1 kDa	37.6 kDa	1.5	77
CD4(10)	15.7 kDa	12.6 kDa	1.2	10
CD4(26)	39.0 kDa	26.8 kDa	1.5	26
CD4(39)	58.7 kDa	34.2 kDa	1.7	39
CD4(143)	217.6 kDa	105.9 kDa	2.0	143
CD4(239)	363.5 kDa	177.5 kDa	2.0	239

NMR Measurements

^{1}H NMR measurements were performed with a temperature-controlled Varian 400-MR spectrometer operating at a frequency of 399.7 MHz. Samples were prepared in D_2O (HOD internal standard).

A).

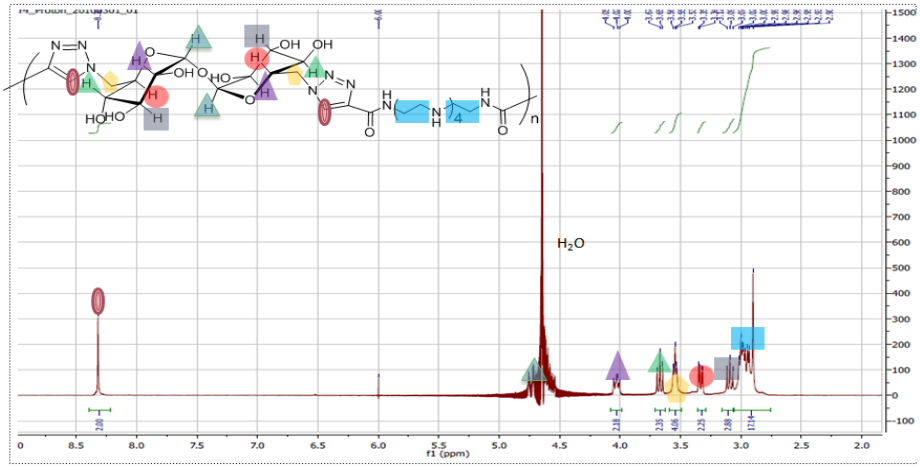

B).

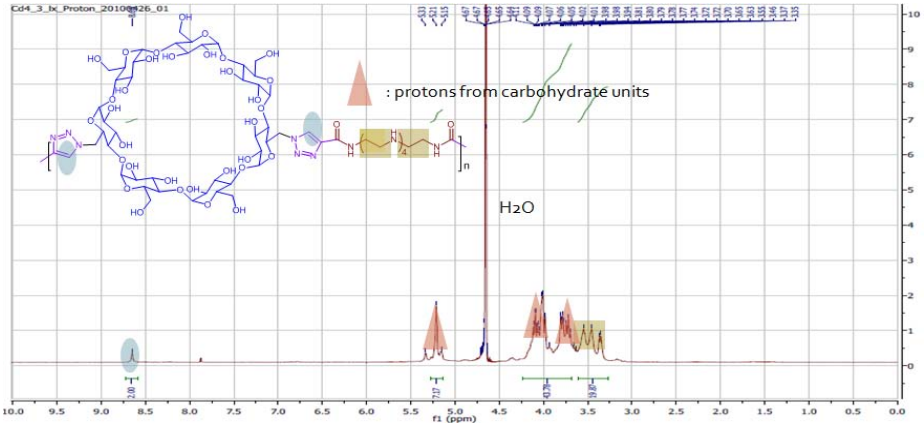

Figure 3: ^{1}H-NMR characterization of polymers Tr4 and CD4. A). Tr4(77): δ 2.90-3.05 m 17H, 3.05-3.12 t 2H, 3.30-3.35 dd 2H, 3.50-3.52 d 4H, 4.00-4.02 t 2H, 8.28 s 2H. The corresponding peaks were assigned according to 1H1H-COSY. B). 1H-NMR of CD4(26). δ 3.30-3.60 m 20H, 3.65-4.11 m 42H, 5.15-5.33 d 7H, 8.60 s 2H.

Size Exclusion Chromatography

Size exclusion chromatography (SEC) was applied to determine the number-average molecular weight (Mn) and polydispersity indices (PDIs) for trehalose polymers and

cyclodextrin polymers. The mobile phase for trehalose polymer is a solution of 0.5% sodium acetate (pH=5.5 with acetic acid) containing 20% acetonitrile. The mobile phase for cyclodextrin polymers is a solution of water: methanol: acetic acid (70:25:5).

A flow rate of 0.3 mL/min in the column (Eprogen Inc., IL), on a Wyatt HELEOS II (Santa Barbara, CA) light scattering detector (λ = 662 nm), and an Optilab rEX refractometer (λ = 658 nm) were used. The Mn, PDI, and dn/dc of the polymers were determined by Astra V (version 6.0, Wyatt Technologies).

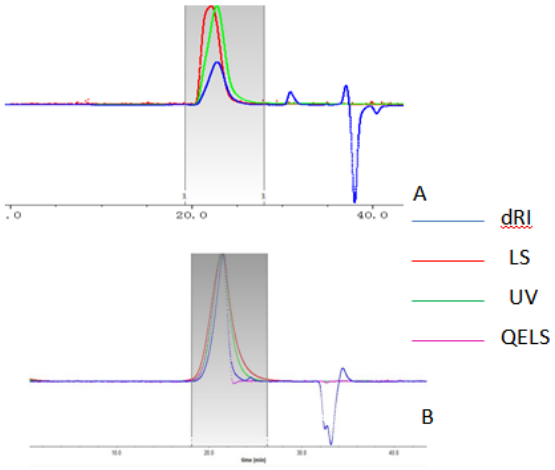

Figure 4: SEC characterization for trehalose polymer Tr4(77) (A) and cyclodextrin polymer CD4(26) (B).

Gel electrophoresis study of polymer-siRNA complexation

Formulations of siRNA at various N/P ratios (polymer-amines / siRNA-phosphates) were prepared with each of the ten different cationic polymers. Three trehalose-containing click polymers (Tr4(23), Tr4(55), and Tr4(77)) and five β-cyclodextrin-containing click polymers (CD4(10), CD4(26), CD4(39), CD4(143), and CD4(239)) were examined. In addition, the results here in were compared to two

polymers described previously; the poly(glycoamidoamine) structures containing four secondary amines per repeat group and either L-tartarate (T4) or meso-galactarate (G4 or "Glycofect").[18,20] These formulations were subjected to electrophoretic analysis in an agarose gel to assess polymer-siRNA interaction (Figure 5).

A).

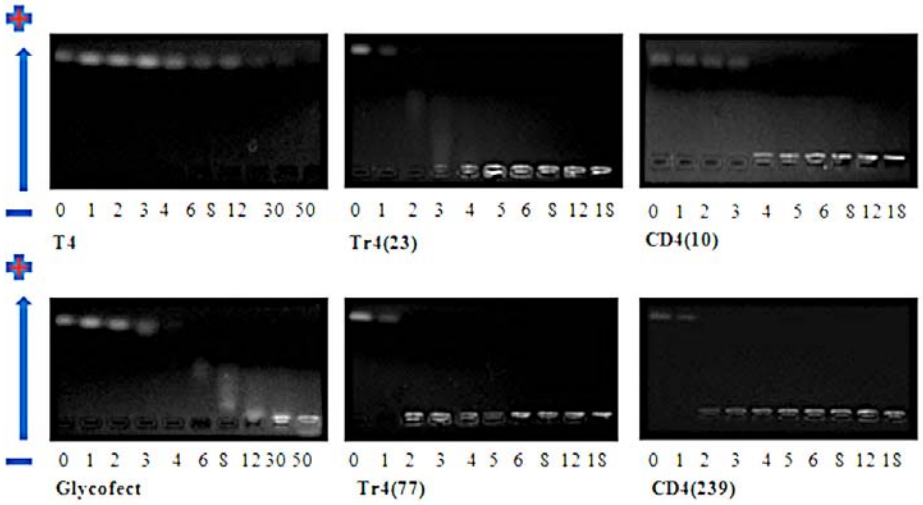

B).

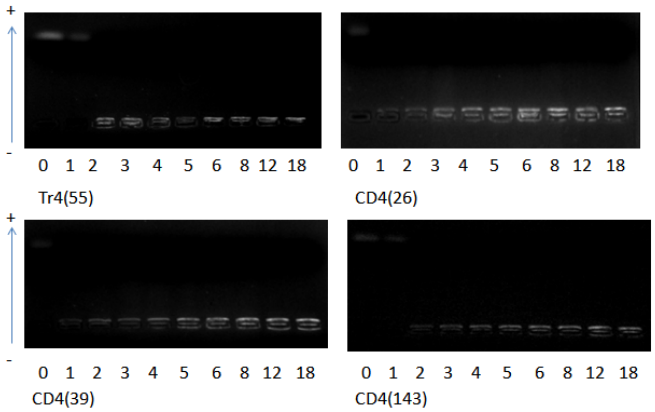

Figure 5. The binding of polymers with siRNA examined by agarose gel electrophoresis shift assays. A). Photographs of gels for T4, Glycofect, Tr4(23), Tr4(77), CD4(10) and CD4(239) at various N/P ratios. The wells where the gel was loaded is at the bottom of each gel photograph (near the - electrode) and the pDNA, if uncomplexed, migrates to the top of the gel photograph (towards the + electrode). B). Photographs of gels for T4(55), CD4(26), CD4(39) and CD4(143) at N/P ratios: 1, 2, 3, 4, 5, 6, 8, 12 and 18.

Polymer T4 containing 12 repeat units has been successfully used to complex pDNA at a low N/P ratio of 1 and effectively delivers pDNA to various cell lines at N/P ratios of 5-30; [27]; however, surprisingly, evidence of free siRNA in the gel is apparent for all N/P ratios tested that were at or below 30. At some N/Ps, blurred areas can be seen, which indicates some interaction between polymer and siRNA, but full complexation was not achieved even at the highest tested N/P ratio of 50. A similar affect was noticed with Glycofect (complexes pDNA at an N/P ratio of 2),[20] however, retardation of siRNA migration was noticed at a high N/P ratio of 30 and 50 (yet blurring of the pDNA band was still noticed). Binding of siRNA by all analogs of the trehalose and β-cyclodextrin polymers was noticed at significantly lower N/P ratios, with N/P=4 being sufficient to ensure the complete retardation of siRNA migration (thus indicating binding and

polyplex formation) for even the shortest versions of these polymers [Tr4(23) and CD4(10)]. This indicates that carbohydrate type plays a role in complex formation since the T4, Glycofect, CD4(10), and Tr4(23) polymers all had similar degrees of polymerization yet very different N/P ratios of binding siRNA. Comparing the binding ability among polymers of different length within the same series (Figure 5, no clear trend was observed; however, it should be noted that longer Tr4 and CD4 polymers tend to retard the migration of siRNA at somewhat lower N/P ratios than their shorter analogues. Because the siRNA-polyplexes with T4 and Glycofect did not appear to be stably complexed (Figure 5), the DLS data for these polymers was not reported in the subsequent section.

Dynamic light scattering (DLS) study

Particle size and zeta potential (surface charge) are two physical parameters that affect the performance of polyplexes both *in vitro* and *in vivo* for nucleic acid delivery. To study the complexation process, dynamic light scattering (DLS) measurements of polyplex hydrodynamic diameter were performed at 0, 5, 10, 15, 30 and 60 min time points after the addition of a polymer solution to siRNA solution (that were diluted with RNase free water). After 60 min, size measurement was made and the zeta potential of each formulation was also measured. The polyplexes were formulated at an N/P ratio of 50 as that was found to yield optimal gene down regulation in culture experiments (*vide infra*).

A).

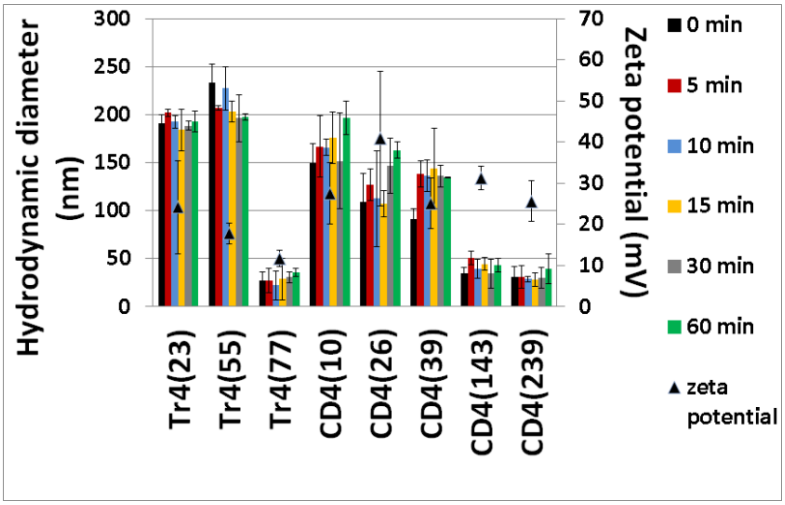

B). C).

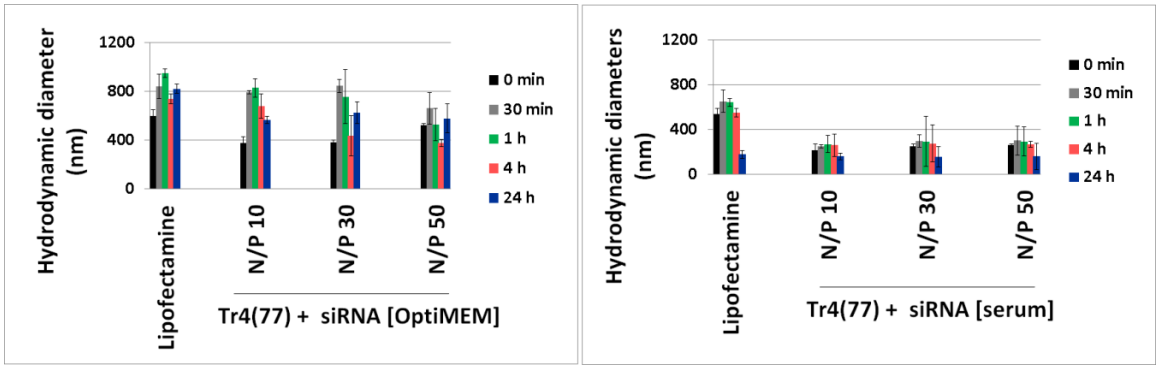

Figure 6. Dynamic light scattering study to monitor complexation of siRNA at different conditions**. A).** Polyplexes formed at N/P=50 in RNase-free water at 25 ^{o}C. Nanoparticle size (hydrodynamic diameter) was measured at the indicated timepoints from 0 min to 60 min. Zeta potential (triangles) was measured after the 60 min timepoint. All the experiments were completed in triplicate. It should be noted here that both T4 and Glycofect did not form polyplexes with siRNA according to DLS. **B). C).** Stability of polyplexes in two kinds of transfection media as measured by dynamic light scattering. Both (B) reduced-serum Opti-MEM and (C) complete DMEM (with 10% FBS) were applied to polyplexes as transfection media, and particle size was measured at indicated

time points through 24 h at room temperature. Tr4(77) was the polymer used in this study with three N/P ratios (10, 30, and 50) tested.

To study the stability of the polyplexes in reduced-serum and serum-containing transfection media, Tr4(77)-siRNA polyplex sizes were examined in both transfection media at selected timepoints up to 24 h at room temperature (Figure 6B-C). In Opti-MEM, the polyplexes were relatively large (~400-800 nm) and measurement results fluctuated significantly; however, most measured sizes were larger for all subsequent timepoints than they were for t=0 (this was true for Lipofectamine and for Tr4(77) at N/P=10 and N/P=30; only Tr4(77) at N/P=50 showed no apparent trend in size change over time). In serum-containing DMEM, particles formed with Lipofectamine decreased in size significantly (from ~600 nm to ~200 nm) at 24 h versus all prior timepoints. It is also should be noted that, in contrast to the particles formed with Lipofectamine, the size of polyplexes formed using Tr4(77) differs significantly between Opti-MEM (~400-800 nm) and complete DMEM (~150-300 nm). In addition, the relative amount of Tr4(77) in the formulation (N/P=10, 30, or 50) did not influence the size of nanoparticles in either transfection medium.

By monitoring the formation of polyplexes over 60 min (Figure 6), we did not observe any significant change in size over time. That is, the hydrodynamic diameter measured immediately after mixing the siRNA and polymer solutions (0 min) is essentially the same throughout 60 min of incubation, indicating that the polyplex formation is extremely rapid and that, once formed, the complexes do not change in size. For the Tr4 series of polymers, Tr4(23) and Tr4(55) form polyplexes with hydrodynamic diameters of around 200 nm; Tr4(77), however, yields significantly smaller (36 nm)

polyplexes. The same phenomenon was observed for the CD4 series: while shorter polymers (10, 26 and 39 repeat units) form polyplexes with siRNA of about 130-180 nm, the longer structures (143 and 239 repeat units) yielded polyplexes with hydrodynamic diameters around 40 nm. It is interesting to note that T4 and Glycofect "complexes" at N/P = 50 were also analyzed via DLS, however, these polymers did not form polyplexes with siRNA according to DLS measurements (also in line with the gel shift assay data).

All of the Tr4 and CD4 series of polymers tested form polyplexes with siRNA that have positive ζ-potentials. For the Tr4 series, a trend was observed where it was noticed that the ζ-potential decreased with increasing polymer length. The ζ-potential drops from +24 mV for polyplexes formed with Tr4(23) to +12mV for Tr4(77)-containing polyplexes. Surprisingly, a similar trend was not observed for the CD4 series. All of the CD4 polymers, with an exception of CD4(26), formed polyplexes with ζ-potential of +25 to +30 mV. Because of the high N/P ratio (50) used for all formulations tested, there is expected to be a significant amount of "free" polymer in solution (that is, polymer not complexed within the polyplexes), which may contribute to these results.

Effect of polyplex formulation on siRNA delivery to cultured glioblastoma cells

The N/P ratio and siRNA concentration were systematically examined in evaluation of siRNA sequence-specific target (luciferase) down-regulation (Figure 5). The siRNA concentrations were varied from 1 to 100 nM and N/P ratios from 8 to 50. As shown in Figure 5 for both polymer vehicles tested [Tr4(77) and CD4(143)], the most potent target gene down-regulation was observed at a siRNA concentration of 100 nM and N/P=50. Both polyplex types exhibited a dependence of luciferase down-regulation

on siRNA concentration; an inhibitory effect was observed at 30 nM, although to a lesser extent than at 100 nM, while no inhibitory effect was seen for siRNA concentrations of 10 nM and below. Similarly, dose dependence with respect to the amount of polymer (N/P ratio) was noticed for both polymers. The luciferase down-regulation was strongest at N/P=50 and was close to 60% for both vehicles. At an N/P ratio of 20, the down regulation was slightly reduced, and a biological effect was completely absent for the polyplexes at an N/P ratio of 8. Finally, all samples in which luciferase expression was reduced showed the expected siRNA sequence specificity, for example, the same polyplex siRNA concentration and N/P ratio, substitution of siCon for siLuc2 abrogated target down-regulation, which indicates that the gene knockdown was not due to off target effects or toxicity of the polymer vehicle. T4 and G4 were also examined for siRNA delivery (*vide infra*) and were completely ineffective for siRNA delivery (promotion of gene down regulation).

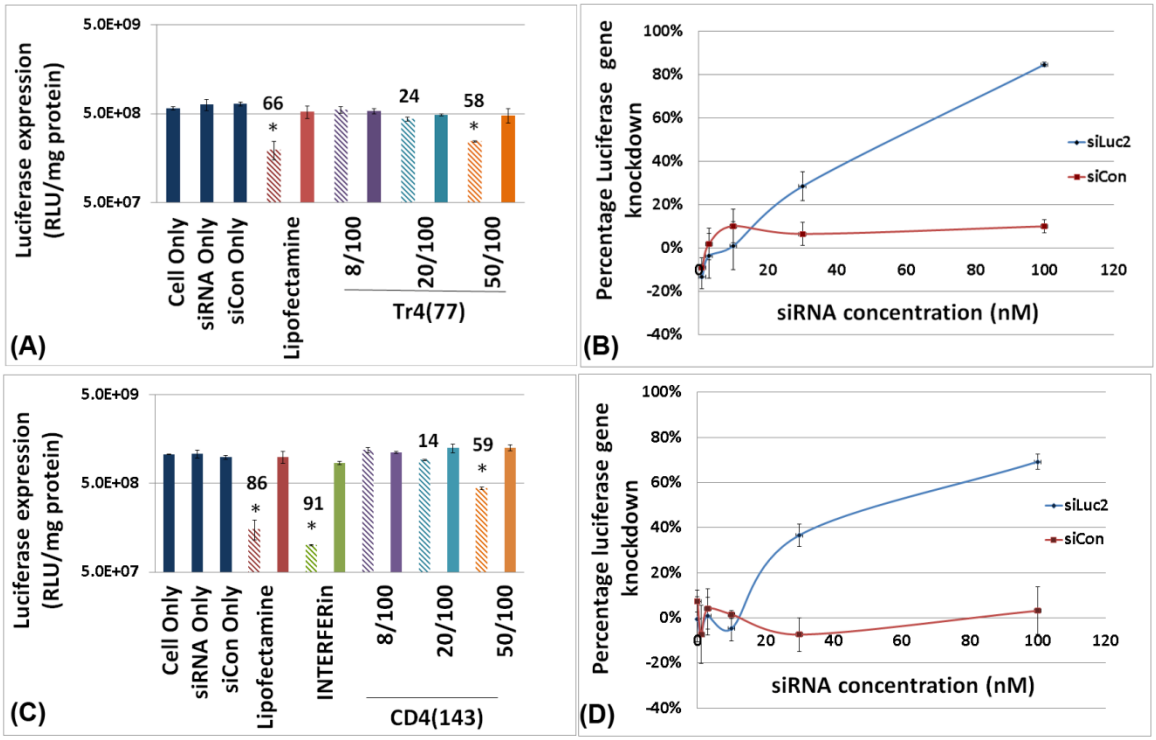

Figure 7. Influence of siRNA concentration and N/P ratio on polyplex-induced target gene (luciferase) down-regulation in U-87_luc2 glioblastoma cells. Notation is as follows: hashed bar (lighter color) indicates treatment with polyplexes containing siRNA and the solid bar (darker color) indicates treatment with polyplexes containing siCon. The numbers above the bars indicate percentage of gene down-regulation. The notation Tr4(77) 50/100 indicates that polyplexes were formulated with siRNA and Tr4(77) at an N/P ratio of 50 and with 100 nM siRNA concentration. "siLuc2" indicates anti-luciferase siRNA; "siCon" indicates scrambled siRNA negative control. (A) Knockdown efficiency response to polyplexes formed with Tr4(77) with 100 nM siRNA at differing N/P ratio, (B) Extent of knockdown response to Tr4(77) polyplexes formulated at an N/P ratio of 50 at siRNA concentrations from 1 nM to 100 nM. (C) Knockdown efficiency response to polyplexes formed with CD4(143) with 100 nM siRNA at differing N/P ratios, (D) Extent

of knockdown response to CD4(143) formulated at an N/P ratio of 50 at siRNA concentrations from 1 nM to 100 nM. [Note: The "*" symbol indicates significantly different values as compared to 'cells only' control ($p<0.05$)].

Promotion of siRNA-mediated gene down regulation by addition of free polymers

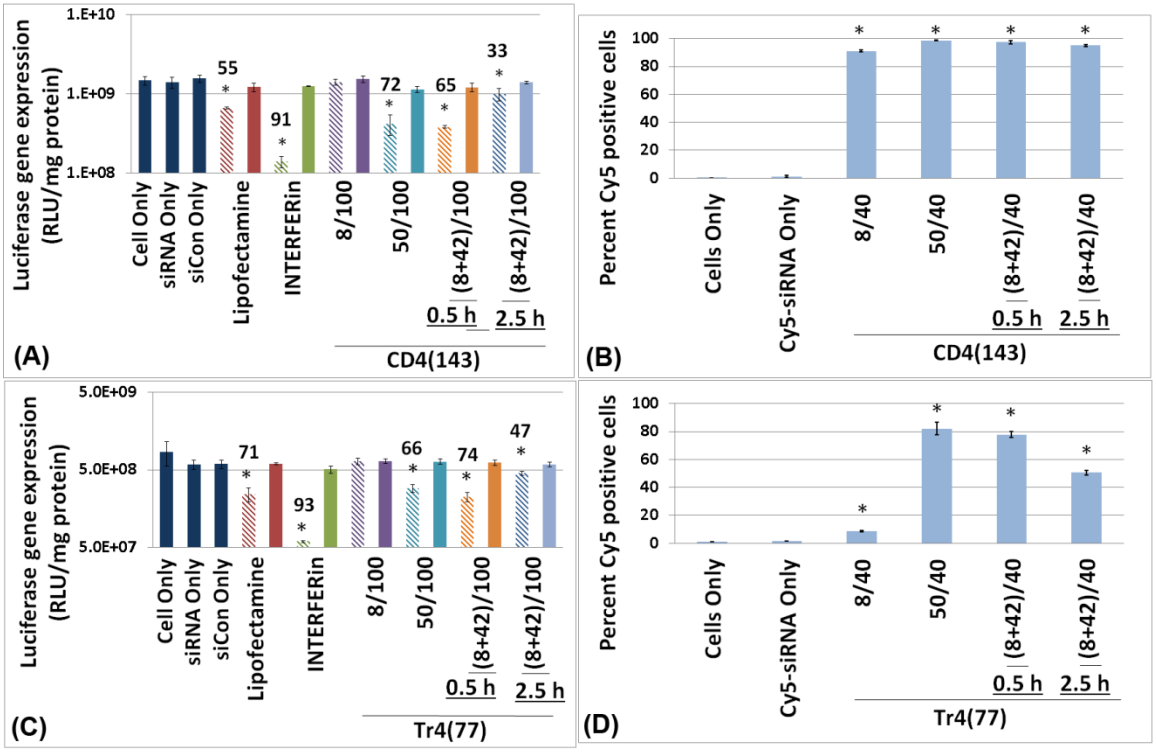

Figure 8. Enhancement of siRNA delivery by polymer vehicles Tr4(77) and CD4(143) upon the addition of free polymer to solution. To understand the role of free polymer in gene down regulation, polyplexes formed at N/P = 8 were added to cells, then at time points of 0.5 h or 2.5 h after initial transfection, a solution containing free polymer equivalent to N/P=42 was added to the wells (brining effective polymer-siRNA ratio to N/P=50 after a time delay). For luciferase gene down regulation (graphs A and C), the cells were transfected with 200 µL/well of siRNA or siCon (at a final RNA concentration

of 100 nM/well). For Cy5-siRNA cellular uptake (graphs B and D), the cells were transfected with 500 μL/well of Cy5-siRNA (at a final concentration 40 nM/well). (A) Luciferase gene down-regulation 48 h after transfection with CD4(143)-siRNA polyplexes. (B) Cellular uptake of Cy5-siRNA in the different polyplex formulations with CD4(143) 3 h after transfection. Data is reported as the percentage of live cells positive for Cy5. (C) Luciferase gene down-regulation 48 h after transfection with Tr4(77)-siRNA polyplexes. (D) Cellular uptake of Cy5-siRNA in the different polyplex formulations with Tr4(77) 3 h after transfection. Data is reported as the percentage of live cells positive for Cy5. Notation is as follows: hashed bar (lighter color) indicates treatment with polyplexes containing siRNA and the solid bar (darker color) indicates treatment with polyplexes containing siCon negative control. The numbers above the bars indicate percentage of gene down-regulation. [Note the * symbol indicates significantly different values as compared to the cells only control ($p<0.05$)].

To investigate the effect of free polymer, we treated U-87_luc2 glioblastoma cells with free polymer 0.5 h or 2.5 h after initial exposure of the cells to CD4(143)/siRNA or Tr4(77)/siRNA polyplexes that were formulated at an N/P ratio of 8 (Figure 8). The amount of free polymer added was such that the total amount of polymer to which cells were exposed (sum of polymer in polyplexes plus subsequently-added free polymer) was equivalent to N/P=50 (Figure 8). Addition of free polymers at the earlier time point (0.5 h after initiation of polyplex exposure), significantly increased siRNA internalization and gene down regulation for the Tr4(77) formulations but not as dramatically for the CD4(143) formulation, which was found to be very high at low N/P. There was close to a 10-fold increase (from 8% to 77%) in the percentage of Cy5 positive cells for Tr4(77)

polyplexes with addition of free polymer, however, for CD4(143) polyplexes, a smaller increase from 91% to 97% was noticed. Likewise, when comparing the extent of target gene down-regulation for these formulations, siRNA-mediated gene knockdown increased from 5% for CD4(143) and 25% for Tr4(77) at N/P of 8 to 65% and 74% in cells with free polymer 0.5 h after transfection for CD4(143) and Tr4(77) respectively, achieving an effect comparable to that obtained with polyplexes formulated at N/P=50. Addition of free polymer at a later time point (2.5 h after original polyplex exposure) was shown to promote cellular internalization of siRNA to a lesser degree for Tr4(77) from 8% to 50%, and for CD4(143) from 91% to 94%. The increase in luciferase gene knockdown was also lower for this time point for polyplexes formed with both Tr4(77) (increased from 25% to 47%) and for CD4(143) (increased from 5% to 33%). Overall, these results indicate that addition of free polymer during polyplex exposure increases uptake and potency, suggesting that free polymer within polyplexes formed at high N/P ratios contributes significantly to their efficacy and likely endosomal escape.

Influence of polymer length on polyplex uptake and efficacy

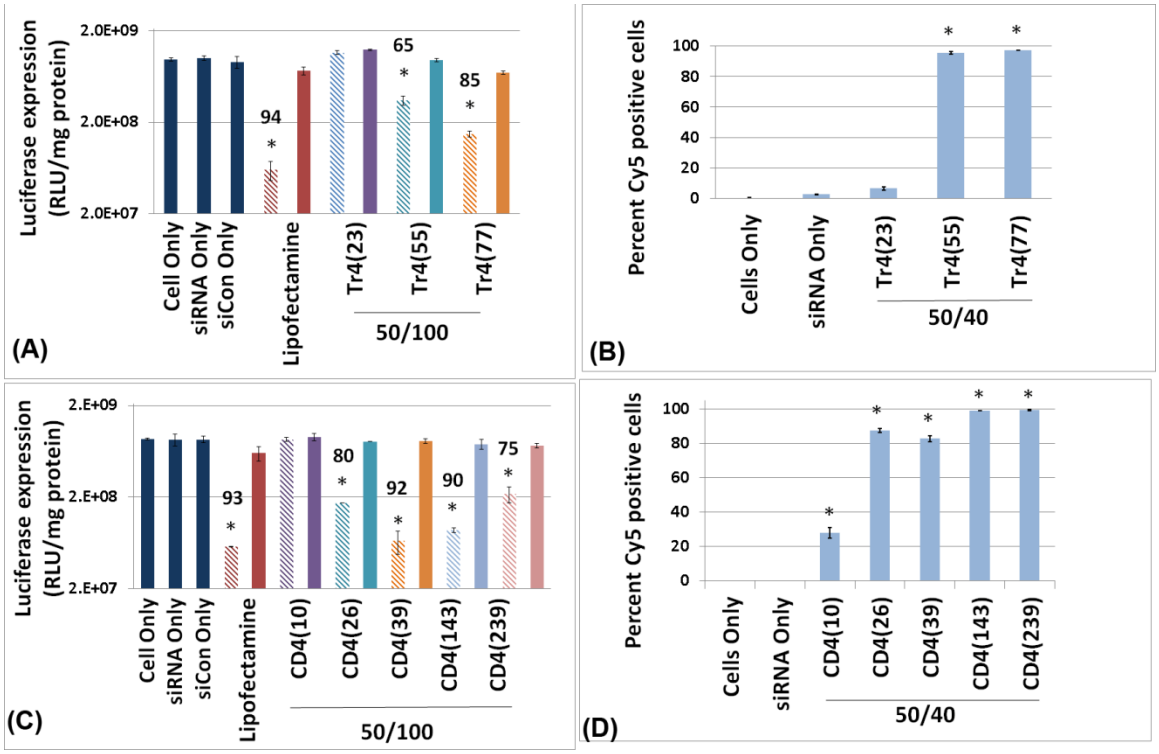

Figure 9. siRNA-mediated gene down regulation with U87-luc2 cells as a function of polyplex type (formed with either Tr4 or CD4 polymers) and polymer degree of polymerization. (A) Luciferase gene down-regulation facilitated by polyplexes formulated with polymer Tr4 (n_w =23, 55, 77) at an N/P = 50 using 100 nM siRNA (50/100). (B) Uptake of Cy5-labeled siRNA within Tr4-containing polyplexes formulated at an N/P = 50 with 40 nM of siRNA (50/40) as measured by flow cytometry 3 h after transfection. (C) Luciferase gene down-regulation facilitated by polyplexes formulated with polymer CD4 (n_w =10, 26, 39, 143, 239), at an N/P = 50 using 100 nM siRNA (50/100). (D) Uptake of Cy5-labeled siRNA within CD4-containing polyplexes formulated at an N/P = 50 with 40 nM of siRNA (50/40) as measured by flow cytometry 3 h after transfection. In graphs A and C, the hashed bars indicate data for cells treated

with siRNA-containing polyplexes and the solid bars indicate data for cells treated with siCon-containing polyplexes (control). The numbers above the bars indicate percentage of gene down-regulation. Note the * symbol indicates significantly different values as compared to the cells only sample ($p<0.05$).

The molecular weight of polymeric biomaterials may play a significant role in their properties. We investigated the influence of the molecular weight (polymer length) on the siRNA delivery efficiency and target gene down-regulation of polyplexes made with Tr4 or CD4 polymers (Figure 9). For the Tr4 series, an increase in polymer length improves the cell internalization (denoted by an increase in the percentage of cells positive for Cy5-siRNA Figure 9B and 9D) and the extent of luciferase down-regulation (Figure 9A and 9C). Interestingly, polyplexes made with Tr4(23) yield virtually no detectable siRNA internalization. However, Tr4(55) and Tr4(77) polyplexes deliver siRNA into 90%+ of the cells. The CD4 series also demonstrated a similar trend. Polyplexes created from the shortest polymer, CD4(10), were only internalized by about 30% of cells and did not reveal gene down regulation. Indeed, longer polymers were needed to achieve maximal siRNA uptake and target gene down-regulation up to a point, and then the highest molecular weight analog was not as effective. Interestingly, polyplexes formed with CD4(26) and CD4(39) were found to be internalized by about 80% of the cells and yielded significant gene knockdown (80% and 92% respectively). This result was surprising as Tr4(23) was completely inactive and Tr4(55) also was less potent than CD4(26). A similar result was found for CD4(143) were polyplexes were internalized by close to 100% of cells and 90% gene down regulation was found. Yet, while polyplexes formed with the longest system, CD4(239), were internalized by close

to 100% of cells, gene down regulation decreased to 75%. It should be noted that for all polymer-containing formulations examined in this study, no apparent cytotoxicity was observed 24 h after transfection according to MTT assays (for polyplexes formulated at an N/P=50 and siRNA concentration of 100 nM, as shown in Figure 11 in the later section.

Comparison of pDNA and siRNA delivery profiles

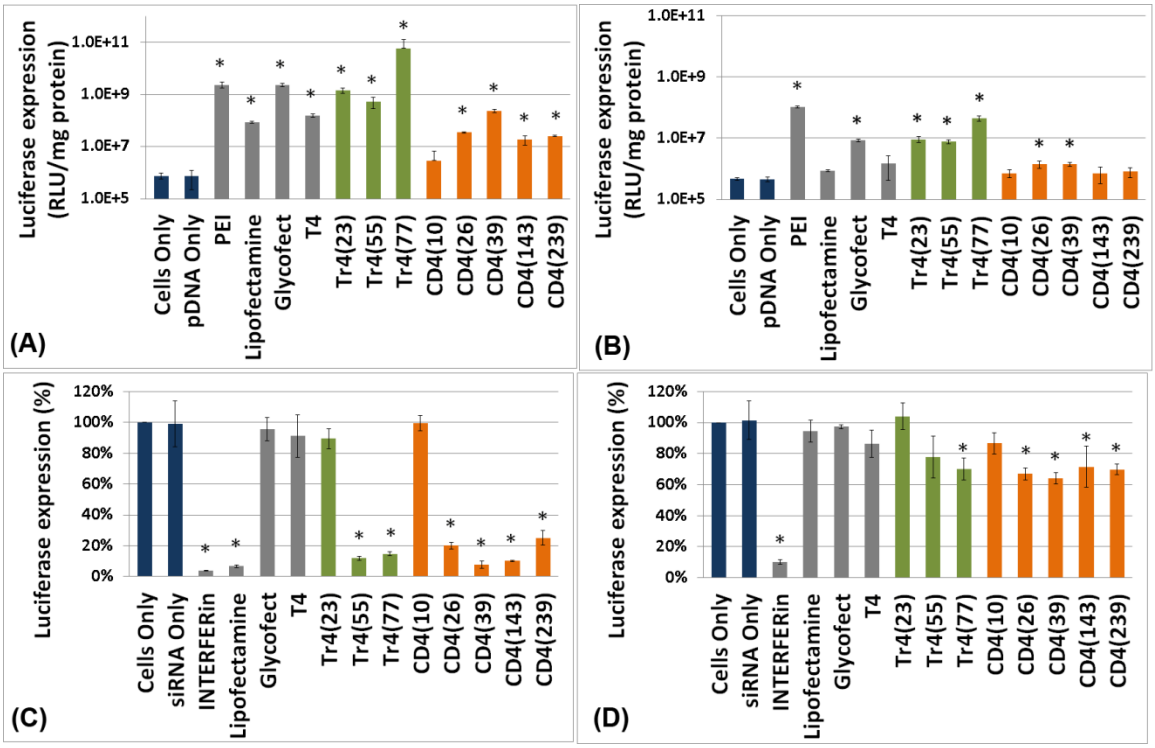

Figure 10. Comparison of pDNA and siRNA delivery efficiency for luciferase expression and down regulation respectively, in the absence and presence of serum. (A, B) Delivery of pDNA encoding the firefly luciferase reporter gene into U87 glioblastoma cells with the carbohydrate-containing polymers and controls in (A) OptiMEM and (B) DMEM. Trehalose (Tr4) or β-cyclodextrin (CD4)-containing polyplexes were formulated with pDNA at N/P=7, while pDNA complexes with T4 or G4 were

formulated at N/P=20 (maximum gene expression as previously published).[20, 27] (C, D) Delivery of anti-luciferase siRNA into U87-luc2 glioblastoma cells with the carbohydrate-containing polymers and controls in (C) OptiMEM and (D) DMEM. All of the carbohydrate-containing polymers were formulated at a siRNA concentration of 100 nM and N/P=50. Note the asterisk "*", symbol indicates significantly different values as compared to the 'cells only' sample ($p<0.05$).

As indicated in Figure 10A, polyplexes created from pDNA and all polymers in the Tr4 and CD4 series (and controls), delivered pDNA to U87 glioblastoma cells as significant luciferase activity is observed in cells transfected in OptiMEM. For cells transfected in DMEM supplemented with 10% fetal bovine serum (FBS), the luciferase activity was lower than in OptiMEM (Figure 10C). As published previously, both Glycofect and T4 yield high efficiency for pDNA delivery as indicated by high luciferase gene expression in H9c2(2-1) and HeLa cells.[18, 29] Also, initial work has shown the Tr4 and CD4 polymer vehicles were very active for pDNA delivery with these cell types _ENREF_17 and in some cases a trend was noticed that gene expression increased with increasing polymer molecular weight.[16, 17] However, these polymers have not been directly assessed for siRNA delivery and these data not directly compared for pDNA delivery. For the CD4 series, luciferase expression increased with polymer length from n_w=10 to n_w=39, but this trend did not continue for the high molecular weight versions n_w=143 or n_w=239. For the Tr4 series, the longest polymer tested (n_w=77) yielded the highest transgene expression (Figure 10A) out of any polymer and control in serum-free OptiMEM and second only to PEI in DMEM. When comparing siRNA delivery results, as shown in Figure 10C, polymers T4, Glycofect, Tr4(23) and CD4(10) failed to

effectively deliver anti-luciferase siRNA in U87_luc2 glioblastoma cells as a significant reduction in cellular bioluminescence was not observed. In contrast, for both the Tr4 and CD4 series, polymers of larger molecular weight—Tr4(55), Tr4(77), CD4(26), CD4(39), CD4(143) and CD4(239), all yielded significant luciferase down-regulation. The results in serum-free OptiMEM were dramatic, where 80-90% gene down regulation was found. Polymer CD4(39) yielded the highest gene down regulation of all the glycopolymers. In DMEM (contains 10% serum), the siRNA-mediated gene down regulation results were less dramatic (Figure 10D), where 60% gene knockdown was observed. Similar to the pDNA delivery results, maximum delivery efficacy was obtained for both pDNA and siRNA for both the Tr4(77) and CD4(39) polymers. Interestingly, while T4 and Glycofect are potent pDNA delivery vehicles, they are completely inactive for siRNA delivery. In addition, at similar N/P ratios, the Tr4 polymer series yielded higher delivery efficacy for pDNA (than the CD4 series); however, the opposite was true with siRNA, the CD4 series yielded the highest efficacy (Figures 9 and 10).

MTT assay to evaluate the cytotoxicity

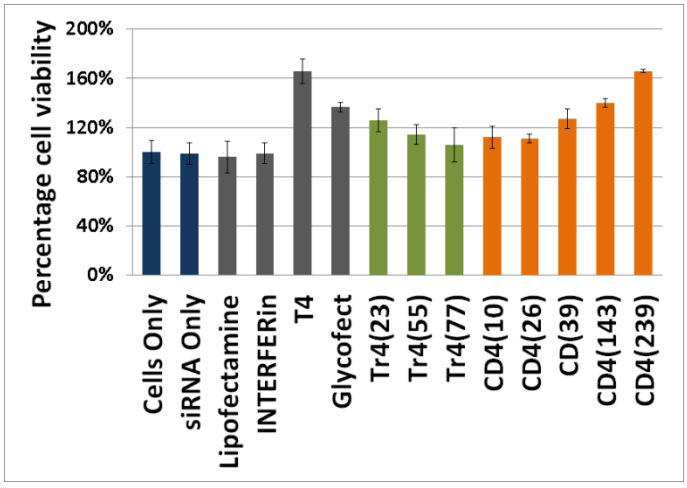

Figure 11: MTT assay to measure the cytotoxicity of siRNA-containing complexes in U87-luc2 glioblastoma cells 24 h after transfection at N/P=50 and a siRNA concentration of 100 nM. All the experiments were performed in triplicate. The y-axis label "Percentage cell viability" stands for the relative activity of mitochondria reductase compared with those without treatment.

As indicated in the Figure 11, all the formulations showed no cytotoxicity in the MTT study. The result indicates the polymers are promising for the future applications towards biomedical studies.

Discussion

In an effort to optimize the siRNA delivery performance with glycopolymer-based polyplexes and understand the polymer structure – siRNA delivery efficiency relationships, we assessed and compared how polyplex formation and nucleic acid delivery (pDNA versus siRNA) differed with a series of glycopolycation vehicles developed in our laboratory. The chemical structure of polymeric vehicles has a direct influence on its ability to deliver pDNA or siRNA.[23] Numerous studies have been published in the literature that are devoted to understanding the structure-activity relationships for pDNA delivery. For example, with PEI, both branched and linear versions of this polymer have been found to effectively deliver pDNA.[30] However, when considering siRNA delivery, that study also revealed that branched PEI was much more effective at siRNA-mediated gene down regulation (60% gene knockdown) when compared to linear PEI, which proved completely inactive.[30] It was hypothesized that the branched structure of PEI was able to form more stable polyplexes with siRNA.[30] The

current study herein was undertaken to investigate the influence of carbohydrate type, polymer length, dose response, and the presence of excess polymer on polyplex formation, and nucleic acid delivery efficiency with siRNA. With this family of polymer vehicles (Figure 1), we also sought to compare siRNA delivery to efficiency of pDNA delivery, which have much different intracellular locations and mechanisms of action (Figure 2). The polymer-siRNA binding was examined by gel electrophoresis (Figure 5). We observed that Glycofect can minimally retard siRNA migration at N/P ratios below 10, however, full binding of siRNA was still not observed until an extremely high N/P ratio of 50. Also, with polymer T4, there is no retardation of siRNA migration at N/P values below 30. These results are in stark contrast to what has been previously published by our group for pDNA delivery (where these polymers fully bind pDNA and retard migration on the gel at low N/P=2).[31, 32] These data indicate that these short oligomeric polymers (n ≈12) containing monosaccharides have very low relatively binding affinity to siRNA (but much stronger to pDNA). Molecular weight of both the polymer and the nucleic acid play a large role in polyplex formation. It should be noted that CD4(10), which has the same degree of polymerization as Glycofect and T4, exhibited a significant improvement in siRNA binding affinity (fully bound at N/P = 4, Figure 5) according to the gel shift assays. Despite having the same number of repeats, these polymers differ significantly in molecular weight due to the large difference in sizes of their carbohydrate units (and the presence of the triazole groups). Interestingly, this indicates that the carbohydrate size plays a role in polyplex formation and binding; previous studies from our group have shown that this is likely promoted through hydrogen bonding between the nucleic acid and the hydroxyl units in the polymerized carbohydrate monomer.[33, 34]

When comparing the CD4 and Tr4 polymer series, there was little to no difference in siRNA binding among the polymers of different lengths as all polymer analogs bound siRNA at low N/P ratios (between 2-4), which is similar to that previously published by our group for pDNA.[16, 17, 28] There is a possibility that such a difference could be observed for even shorter (n_w<10) polymers within these series; however, such shorter polymers are likely to be poor candidates for siRNA delivery, as can be seen from the trends observed in the gene knockdown experiments (*vide infra*).

To examine the polymer-siRNA complexation process in aqueous conditions, we monitored the sizes of species present over 60 min after mixing siRNA and polymer solutions. All of the Tr4 and CD4 polymers can readily form polyplexes (Figure 6). As observed with the gel experiments, T4 and Glycofect (G4) did not form well-defined polyplexes (not able to observe polyplex formation in DLS) likely due to their low molecular weight and low binding affinity. Again, this is in contrast to the ability of these polymers to form well defined polyplexes with pDNA.[16-21,31, 32] Similar to that observed with pDNA, rapid siRNA complexation was observed for all of the Tr4 and CD4 polymer series, and the dimensions of the polyplexes did not change significantly over 60 min incubation in water at room temperature. The size of the polyplexes formed with the Tr4 or CD4 polymers decreased with increasing polymer length; the shorter Tr4 and CD4 polymers yielded complexes having diameters of ~100 nm or above, while polymers Tr4(77), CD4(143), and CD4(239) yielded complexes of <50 nm (Figure6). It is also interesting to compare the siRNA polyplexes formed with the longer cyclodextrin polymers of ~50 nm diameter (N/P=50; CD4(143), CD4(239)) to that previously reported for pDNA, where polyplexes of ~100 nm diameter were formed with comparable

polymers of similar length (N/P=10; time = 45 min; CD4(93) and CD4(200)).[17] On the contrary, the smaller cyclodextrin polymers formed larger polyplexes with siRNA of ~150 to 200 nm diameter (CD4(26), CD4(39)), which is similar to the reported a size of ~70 to 100 nm for pDNA polyplexes (N/P=10; time = 45 min; CD4(27) and CD4(47)).[17]

These data suggest that the mechanism of polyplex formulation with long/flexible pDNA and short/rigid siRNA may be different. The plasmid DNA used in this study is several kilobase pairs, which ranges in size from 30 to 100 nm in solution. However, siRNA is typically 21-27 bp and is quite small, ranging in size from 2 to 7 nm.[23] Thus, the number of negative charges on each siRNA for electrostatic attraction of cationic polymers is substantially less than pDNA.[23] The short polymers n_w=23 to 55 do not seem to be optimal for wrapping siRNA strands into a compact polyplex. A small increase in the polymer length to n_w=77 seems to offer enough length for stable siRNA polyplex formation. A similar trend was observed with the CD4 polymer series. When considering these data along with that previously published for these polymers for pDNA, it appears that polymers with larger molecular weight are needed to serve as a "template" for stable siRNA polyplex formation. Yet, stable and compact polyplexes are able to be formed with short oligos/polymers and large plasmids, which may serve as the template.[16, 17, 19] Nucleic acid type (DNA versus RNA) could also drive differences in binding due to variances in helicity and the ribose sugar, which could affect complexation and H-bonding. Collectively, when considering the size, zeta potential, cellular uptake, and gene knockdown efficiency of different polyplex formulations, correlations relating size and Zeta potential to delivery efficiency were not observed. For example, polymeric vehicles Tr4(23) and CD4(10) failed to achieve significant siRNA delivery efficiency *in*

vitro, despite having similar polyplex size and Zeta potential to Tr4(55) and CD4(39), respectively, both of which demonstrated markedly improved cellular uptake and gene knockdown in U-87 glioblastoma cells (Figure 9).

The observation that gene knockdown was enhanced at higher N/P ratios despite being able to retard siRNA migration in the gel shift assays at lower N/P ratios, led us to hypothesize that the polyplex solutions contain significant free polymer, which may strongly influence delivery efficiency. To investigate the effect of addition of free polymer, transfection was performed with the timed addition of free polymer to the culture medium. As can be seen from Figure 7, transfection of U87_luc2 glioblastoma cells with CD4(143)-siRNA complexes at a low N/P=8 followed by the addition of free polymer into the transfection medium had a dramatic impact on the transfection efficiency. The addition of free polymer (up to a total polymer amount equivalent to N/P=50) at an early time point (0.5 h after the initiation of transfection) substantially improved the target gene (luciferase) down-regulation; the extent of down-regulation increased 7-fold compared to the polyplexes samples only formulated at N/P=8 (without free polymer addition). When free polymer was added at a later time point (2.5 h after the initiation of transfection), the efficiency improved to a lesser extent (2-fold increase in luciferase down-regulation). With the CD(143) delivery system, free polymer did not have a substantial effect on internalization as polyplex uptake was found to be above 80% at N/P ratios of 8, 50, and in the experiments with the timed polymer addition. A similar study was performed with Tr4(77) polymer and the results follow a similar trend as compared to CD4(143) polymer with some key differences. Polyplexes formulated at N/P = 8 did not show significant gene down regulation (Figure 8C). Significant luciferase

knockdown was observed at N/P=50 (Figure 8C). Similar to the CD4(143) polyplexes, addition of free polymer (up to a total polymer amount equivalent to N/P=50), increased the gene knockdown significantly (~ 74 %) for the earlier addition time point (0.5 h post transfection) and to a lower degree for the later time point. However, with Tr4(77) internalization was much lower at N/P=8 (~10% cells) but the cells positive for polyplex internalization did significantly improve at N/P= 50 and after free polymer addition, again indicating that the CD4 series yields more effective siRNA delivery. The results further indicate that for the free polymer to enhance gene knockdown, the free polymers needed to be present near the beginning of the transfection experiment (a longer duration time of 3.5 h incubation). The shorter incubation time of 1.5 h (for 2.5 h post transfection time point) showed lower (~ 47 %) gene knockdown (Figure 8C). This may be explained by the reduced uptake for Tr4(77) polyplexes at the 2.5 h post transfection time point. Taken together, these data validate the hypothesis that free polymer is necessary to achieve maximal siRNA delivery efficiency. Others have also shown this to be true, for example, Boeckle *et al.* revealed the effects of free polymer addition during transfection of CT 26 (fibroblast cells derived from colon of BALB/c mouse) cells with non-purified (contained free polymer) and purified PEI (did not contain free polymer) polyplexes at 1 h and 4 with varying concentrations of pDNA. They found that free polymer increased the luciferase expression by many fold as compared to purified PEI polyplexes.[35] When considering the data for CD4(143), although 90% of cells were positive for siRNA internalization at N/P 8, target gene down regulation was minimal at this low N/P ratio. However, when free polymer (equivalent to N/P = 42) was added to the culture media 0.5 hours after transfection at N/P 8, gene down regulation was equivalent to that observed

for polyplexes formulated at N/P =50. This was not the case for Tr4(77) at N/P 8, both internalization and gene down regulation was minimal. These results could indicate that free polymer aids in endosomal escape of siRNA formulations, which intern, aids gene knockdown and was particularly noticed with the cyclodextrin analogs. We speculate that the known affinity for cyclodextrin to extract cholesterol from cell membranes[36-39] could play a role in aiding endosomal disruption and polyplex release into the cytoplasm with the CD4 polymer series.

Despite the ability of Tr4(23) and CD4(26) to bind siRNA, Tr4(23) was unable to effectively deliver siRNA into glioblastoma cells, but CD4(26) was effective for siRNA internalization to a large fraction (80%) of U87 cells. Interestingly, at equivalent N/P ratios, the cyclodextrin polymers were found to be more potent than the analogous Tr4 polymer in terms of both cellular uptake and gene down regulation (Figures 8-10). These findings suggest that cyclodextrin, a larger carbohydrate unit, seems to be more suitable than trehalose for designing polymer vehicles that are active for siRNA delivery, in terms of both uptake and target gene down-regulation and could be related to more stable complex formation, enhanced endosomal release, and greater cytoplasm delivery.

When the polyplexes were collectively examined for transfection efficiency (Figure 10), the shortest polymers [including T4(10), Glycofect, CD4(10), as well as Tr4(23)] were completely inactive towards siRNA-mediated luciferase gene down regulation with U87_Luc cells, which is likely due, in part, to their inability to form stable complexes (Figure 7). Yet, the longer Tr4 and CD4 polymers achieved siRNA-mediated gene knockdown and a polymer length dependence on delivery efficacy was evident (Figure 9 and 10). Importantly, all but the short Tr4 and CD4 polymer analogs

were effective at promoting internalization of Cy5-labeled siRNA in 80%+ of U87 cells. In addition, while toxicity was not revealed according to MTT assays, the decrease in gene down regulation with increasing molecular weight could point towards an off target effect or decreased siRNA release.

Previously, we have shown with pDNA that the trehalose polymers reveal a distinct trend of an increase in gene expression with an increase in polymer length (n_w=35, 53, 75, 100) with HeLa cells.[16] However with H9c2(2-1) cells, such a trend was not observed, as the gene expression levels plateau with polymer lengths greater than n_w=35.[16] In the current study with U87MG cells, the observed gene expression was equivalent for pDNA being carried with Tr4 polymers n_w=23 to 55; however it then increased at n_w=77 (which is seen in both Opti-MEM and DMEM). Interestingly, for siRNA polyplexes formed with Tr4 polymers, gene down regulation was insignificant for Tr4(23) but drastically increased to ~90% for Tr4(55) and Tr4(77) in the presence of Opti-MEM. In the presence of DMEM containing 10% serum, a similar result was found but gene down regulation was dampened (~30% knockdown). Thus, the length of the trehalose and cyclodextrin polymers appears to be an important variable in cellular delivery of siRNA and pDNA. Many other reports have shown that varying polymer length affects delivery; for example Stand et. al. showed that the most efficient gene silencing was achieved using fully de-*N*-acetylated chitosans with intermediate chain lengths (DP_n 100–300).[40]

When directly comparing the efficacy of the T4, Glycofect, Tr4, and CD4 polymers for pDNA versus siRNA delivery, clear differences and trends in the combined data were observed (Figure 10). As we have previously published, both T4 and

Glycofect are effective pDNA delivery vehicles. Among all the polymers tested, Tr4(77) obtained the highest transgene expression in U87 glioblastoma cells, yielding over two orders of magnitude higher transgene expression for than CD4(39), the most potent cyclodextrin polymer for pDNA delivery. Also, Tr4(77) revealed over an order of magnitude higher gene expression than Glycofect. In contrast to their high potency for siRNA delivery, the CD4 polymers were shown to be less effective in the delivery of pDNA than the other polymers examined (Figure 10). A comparison of these carbohydrate-containing polymers for pDNA delivery revealed a slight correlation to the polymer length for both the Tr4 and CD4 series. As shown, the longest trehalose polymer revealed the highest gene expression, also, there was some correlation to the polymer length for the cyclodextrin polymers, where pDNA expression increased as the polymer molecular weight increased up to CD4(39), then the gene expression slightly decreased. In the presence of serum, however, gene expression was dampened. This is likely due to the presence of serum proteins in this media that may bind to the polyplexes. Because the CD4 series does promote nucleic acid delivery to a large amount of cells, the low gene expression efficacy could be due to two possible combined factors: i) the CD4 polymer series could promote higher delivery of nucleic acids to the cytoplasm than the Tr4 series (wrong destination for pDNA delivery), and ii) the CD4 polymers could bind very tightly to pDNA, discouraging release.

The dependence of potency on polymer type and length was more dramatic for siRNA delivery. We were surprised to discover that, despite the high potency of T4 and Glycofect for pDNA delivery, both of these polymers were completely ineffective at forming polyplexes with and delivering siRNA in vitro (Figure 5 and Figure 10D). Also,

a dramatic dependence on molecular weight was observed with the trehalose and cyclodextrin polymers. Both the low molecular weight versions of these systems [Tr4(23) and CD4(10)] revealed no activity for siRNA delivery. However, interestingly, as the degree of polymerization was further increased, the cyclodextrin polymers CD(26) and CD(39) were very active for siRNA delivery (80%, and 90% gene down regulation respectively), more so than the Tr4 polymer series. However, the two highest molecular weight analogs of the CD4 series were less effective for delivery. Collectively, these data reveal two very important trends: i) length of the polymer has an effect on gene expression and gene knockdown and ii) the carbohydrate type/size plays a clear role in siRNA binding, compaction, and delivery. The collective data for the CD4 series is particularly intriguing; the CD4 polymers clearly promote effective binding and encapsulation of both pDNA and siRNA, polyplex internalization into 90% of cells even at low N/P ratio, low gene expression but high siRNA-mediated gene knockdown. This points toward the direct role of the sugar in mediating both binding and delivery of nucleic acids. Cyclodextrin clearly promotes higher binding affinity, likely due to H-bonding via the hydroxyl groups and the polymerized nucleotides. In addition, cyclodextrin likely plays a role in promoting endosomal release of siRNA (as Tr4 analogs had lower affinity) possibly due to the known affinity of the hydrophobic cyclodextrin cup to extracting cholesterol out of the membrane, which could promote leaky endosomes. This was also clearly noticed when free polymer was added, which also clearly plays a role in promoting endosomal release of polyplexes carrying siRNA. Lastly, the efficacy was significantly reduced in serum, possibly due to the affinity of the cyclodextrin to binding serum proteins, which likely coat the polyplexes.

In conclusion, the observations with these polymers illustrate that, because of their structural differences and the difference in intracellular sites of action, indeed, knowledge based upon pDNA delivery cannot necessarily predict the performance of polymers for siRNA delivery. These findings also highlight the potential of utilizing the Tr4 and CD4 series of polymers as therapeutic pDNA and siRNA delivery agents and demonstrate the subtle effects of chemical structure on the activity of pDNA and siRNA delivery.

REFERENCES

1. Fire, A.; Xu, S.; Montgomery, M. K.; Kostas, S. A.; Driver, S. E.; Mello, C. C. *Nature* **1998,** 391, (6669), 806-811.

2. Dykxhoorn, D. M.; Novina, C. D.; Sharp, P. A. *Nat. Rev. Mol. Cell Biol.* **2003,** 4, (6), 457-467.

3. Hammond, S. M.; Caudy, A. A.; Hannon, G. J. *Nat. Rev. Genet.* **2001,** 2, (2), 110-119.

4. Whitehead, K. A.; Langer, R.; Anderson, D. G. *Nat. Rev. Drug Discov.* **2009,** 8, (2), 129-138.

5. Reischl, D.; Zimmer, A. *Nanomedicine* **2009,** 5, (1), 8-20.

6. Tseng, Y.-C.; Mozumdar, S.; Huang, L. *Adv. Drug Deliv. Rev.* **2009,** 61, (9), 721-731.

7. Herrero, M. A.; Toma, F. M.; Al-Jamal, K. T.; Kostarelos, K.; Bianco, A.; Da Ros, T.; Bano, F.; Casalis, L.; Scoles, G.; Prato, M. *J. Am. Chem. Soc.* **2009,** 131, (28), 9843-9848.

8. de Fougerolles, A.; Vornlocher, H.-P.; Maraganore, J.; Lieberman, J. *Nat. Rev. Drug Discov.* **2007,** 6, (6), 443-453.

9. Ding, W.; Hattori, Y.; Qi, X.; Kitamoto, D.; Maitani, Y. *Chem. Pharm. Bull.* **2009,** 57, (2), 138-143.

10. Gao, K.; Huang, L. *Mol. Pharm.* **2008,** 6, (3), 651-658.

11. Jiang, H.-L.; Kwon, J.-T.; Kim, E.-M.; Kim, Y.-K.; Arote, R.; Jere, D.; Jeong, H.-J.; Jang, M.-K.; Nah, J.-W.; Xu, C.-X.; Park, I.-K.; Cho, M.-H.; Cho, C.-S. *J Control Release* **2008,** 131, (2), 150-157.

12. Mintzer, M. A.; Simanek, E. E. *Chem. Rev.* **2008,** 109, (2), 259-302.

13. Boussif, O.; Lezoualc'h, F.; Zanta, M. A.; Mergny, M. D.; Scherman, D.; Demeneix, B.; Behr, J. P. *Proc. Natl. Acad. Sci. U.S.A.* **1995,** 92, (16), 7297-7301.

14. Werth, S.; Urban-Klein, B.; Dai, L.; Höbel, S.; Grzelinski, M.; Bakowsky, U.; Czubayko, F.; Aigner, A. *J Control. Release* **2006,** 112, (2), 257-270.

15. Davis, M. E. *Mol. Pharm.* **2009,** 6, (3), 659-668.

16. Srinivasachari, S.; Liu, Y.; Prevette, L. E.; Reineke, T. M. *Biomaterials* **2007,** 28, (18), 2885-2898.

17. Srinivasachari, S.; Reineke, T. M. *Biomaterials* **2009,** 30, (5), 928-938.

18. Lee, C. -C.; Liu, Y.; Reineke, T. M. Bioconjugate Chem. 2008, 19, 428-440.

19. Srinivasachari, S.; Liu, Y.; Zhang, G.; Prevette, L.; Reineke, T. M. *J. Am. Chem. Soc.* **2006,** 128, (25), 8176-8184.

20. Liu, Y.; Reineke, T. M. *J. Am. Chem. Soc.* **2005,** 127, (9), 3004-3015.

21. Liu, Y.; Wenning, L.; Lynch, M.; Reineke, T. M. *J. Am. Chem. Soc.* **2004,** 126, (24), 7422-7423.

22. Smith, A. E.; Sizovs, A.; Grandinetti, G.; Xue, L.; Reineke, T. M. *Biomacromolecules* **2011,** 12, (8), 3015-3022.

23. Scholz, C.; Wagner, E. *J Control Release* **2012,** 161, (2), 554-565.

24. Schallon, A.; Synatschke, C. V.; Jérôme, V.; Müller, A. H. E.; Freitag, R. *Biomacromolecules* **2012,** 13, (11), 3463-3474.

25. Salcher, E. E.; Kos, P.; Fröhlich, T.; Badgujar, N.; Scheible, M.; Wagner, E. J Controlled Release, 2012, 164, (3), 380-386.

26. Fröhlich, T.; Edinger, D.; Kläger, R.; Troiber, C.; Salcher, E.; Badgujar, N.; Martin, I.; Schaffert, D.; Cengizeroglu, A.; Hadwiger, P.; Vornlocher, H.-P.; Wagner, E. *J Control Release* **2012,** 160, (3), 532-541.

27. Liu, Y.; Wenning, L.; Lynch, M.; Reineke Theresa, M., Gene Delivery with Novel Poly(l-tartaramidoamine)s. In *Polymeric Drug Delivery I,* American Chemical Society: 2006; Vol. 923, pp 217-227.

28. Srinivasachari, S., Fichter, K. M., Reineke, T. M. *J. Am. Chem. Soc.* **2008,** 130, 4618-4627.

29. Grandinetti, G.; Reineke, T. M. *Mol. Pharm.* **2012,** 9, (8), 2256–2267.

30. Kwok, A.; Hart, S. L. *Nanomedicine* **2011,** 7, (2), 210-219.

31. Liu, Y., and Reineke, T. M. J. Am. Chem. Soc. 2005, 127, 3004-3015.

32. Reineke, T. M.; Davis, M. E., 9.26 - Nucleic Acid Delivery via Polymer Vehicles. In *Polymer Science: A Comprehensive Reference,* Editors-in-Chief: Krzysztof, M.; Martin, M., Eds. Elsevier: Amsterdam, 2012; pp 497-527.

33. Prevette, L. E., Kodger, T. E., Reineke, T. M., Lynch, M. L. *Langmuir* **2007,** 23, (19), 9773-9784.

34. Prevette, L. E.; Lynch, M. L.; Kizjakina, K.; Reineke, T. M. *Langmuir* **2008,** 24, (15), 8090-8101.

35. Boeckle, S.; von Gersdorff, K.; van der Piepen, S.; Culmsee, C.; Wagner, E.; Ogris, M. *J Gene Med* **2004,** 6, (10), 1102-1111.

36. Yancey, P. G.; Rodrigueza, W. V.; Kilsdonk, E. P. C.; Stoudt, G. W.; Johnson, W. J.; Phillips, M. C.; Rothblat, G. H. *J. Biol. Chem.* **1996,** 271, (27), 16026-16034.

37. Rodal, S. K.; Skretting, G.; Garred, O.; Vilhardt, F.; van Deurs, B.; Sandvig, K. *Mol. Biol. Cell* **1999,** 10, (4), 961-974.

38. van der Aa, M. A. E. M.; Huth, U. S.; Hafele, S. Y.; Schubert, R.; Oosting, R. S.; Mastrobattista, E.; Hennink, W. E.; Peschka-Suss, R.; Koning, G. A.; Crommelin, D. J. A. *Pharm. Res.* **2007,** 24, (8), 1590-1598.

39. Kline, M. A.; O'Connor Butler, E. S.; Hinzey, A.; Sliman, S.; Kotha, S. R.; Marsh, C. B.; Uppu, R. M.; Parinandi, N. L., Methods Mol. Biol. 2010, 610, 201-211.

40. Malmo, J.; Sørgård, H.; Vårum, K. M.; Strand, S. P. *J Controlled Release* **2012,** 158, (2), 261-268.

Chapter 3:

Promotion and stabilization effect of poly carbohydrate coating for the nanosystems in siRNA delivery into cancer cells.

This chapter is based on the publication:

1. Antons Sizovs, Lian Xue, Zachary P. Tolstyka, Nilesh P. Ingle, Yaoying Wu, Mallory Cortez, and Theresa M. Reineke. “Poly(trehalose): Sugar-Coated Nanocomplexes Promote Stabilization and Effective Polyplex-Mediated siRNA Delivery”. *Journal of the American Chemical Society* 2013 *135* (41), 15417-15424.
2. Adam E. Smith, Antons Sizovs, Giovanna Grandinetti, Lian Xue, and Theresa M. Reineke. "Diblock Glycopolymers Promote Colloidal Stability of Polyplexes and Effective pDNA and siRNA Delivery under Physiological Salt and Serum Conditions." *Biomacromolecules.* 2011 *12(8)*, 3015-3022.

Background

In the macromolecular interaction, the surface properties of nanosystems play a crucial role. In the biological environment, the biological recognition and transformation rely highly on the nature of the surface. The monosaccharide glucose and disaccharide trehalose are two of the most commonly used carbohydrate chemicals in biological research. The trehalose, known for its special biological stabilization effect, is well enriched in ocean creatures and used in supplementary treatment for Alzheimer's disease. In this chapter, two different strategies were investigated to evaluate the sugar coating effect on siRNA delivery as well as pDNA delivery. Two series of polymers have been synthesized via aqueous reversible addition-fragmentation chain transfer (RAFT) polymerization. Those composed of 2-deoxy-2-methacrylamido glycopyranose (MAG) with primary amine containing N-(2-aminoethyl) methacrylamide (AEMA) and those composed of 6-methacrylamido-6-deoxytrehalose with AEMA were investigated and evaluated to elucidate the coating effect on nucleic acid delivery. We demonstrate that the polyglucose and polytrehalose coating can ensure the colloidal stability of the polyplexes containing siRNA in the presence of high salt concentrations and serum proteins. The polytrehalose show the capability to lower the phase transition energy associated with freezing and protect the siRNA polyplexes during freeze-drying cycles and maintain the biological functions of the polyplexes after resuspension. The siRNA transfection efficiency facilitated by sugar coated polymers was conducted to show that the polytrehalose has exceptional cellular uptake and target gene knockdown while polyglucose coating doesn't show the same effect. Moreover, the cellular uptake of siRNA facilitated by polytrehalose polymers showed zero order kinetics. The amount of

siRNA copies delivered into the cells can be controlled by the siRNA concentration in cell culture media. The confocal microscopy has shown that trehalose-coated polyplexes undergo active trafficking in cytoplasm upon internalization and significant siRNA-induced target gene down-regulation was achieved with IC_{50} of 19 nM. While the polyglucose-coated polyplexes do not show significant siRNA delivery efficiency, the polymers can achieve successful pDNA delivery. The performance of the coated polymers on siRNA highly depends on the choice of sugar type. All the formulations tested show no cytotoxicity in cellular studies. These findings suggest that polytrehalose has the potential to serve as an important component of therapeutic nanoparticle formulations of nucleic acids and has great promise to be extended as a new coating approach for nanotechnologies in biomedical application.

Introduction

Polymers with proper charge and surface profile have been proven to be effective to complex with nucleic acids and facilitate the cellular uptake. In order to develop biocompatible materials for biological applications, coating materials that promote the stabilization of nanosystems from nonspecific interactions and colloidal aggregation are of high interest. To address this, several approaches have been proposed as PEG alternatives, such as poly-(amino acid)s, poly(glycerol), poly(2-oxazoline)s and vinyl polymers[1]. Inspired by their nature, the carbohydrate family offers abundant and sustainable alternatives to conventional stabilizing materials, among which, glucose and trehalose are two most representative candidates for monosaccharide and disaccharide. Synthetic glycopolymers have received broad interest as benefiting from the abundance

and ability of carbohydrate to initiate specific interaction and recognition with biological systems[2]. With emergence of controlled/living radical polymerization (CLRP) such as NMP (nitroxide-mediated polymerization)[3], ATRP (atom transfer radical polymerization)[4] and RAFT (reversible addition-fragmentation chain transfer polymerization)[5], researchers are capable of synthesizing the well defined structures of copolymers to study the structure- property relationships. Of all the techniques, RAFT is of particular significance because of the wide range of functional monomers and reliable conditions required for the reactions[6-8].

The glucose, as one of the most abundant carbohydrate, participate in a variety of biochemical reactions, signal pathways and energy metabolism[9]. The dysfunction of the glucose metabolism is associated with a variety of diseases such as diabetes and cardiovascular diseases[10]. The α,α-D-trehalose, a non-reducing disaccharide is very stable to acidic hydrolysis[11] and has been found to protect cells during oxidative stress[12] and freezing.[13,14] Trehalose is a known protective factor of autophagy, effectively shielding intracellular organelles from distortion during sudden environmental changes, such as aggregation and water crystallization. This has been readily observed and demonstrated in the plant called Selaginalla lepidophyll, known also as the resurrection plant or Rose of Jericho that contains about 12% of trehalose in dry mass. The restoration to normal metabolism is observed by exposing the lifeless resurrection plant to water within a few hours, which is a marvelous self protection against dryness and sudden dehydration environment[15]. Trehalose is also accumulated under stress in a number of animals and insects with cryptobiotic ability(for example, tardigrades[16,17]). In addition, trehalose has been reported to improve the cognitive and learning ability of patients with Alzheimer ’s

disease and reduce the Aβ deposit in hippocampus to show neural protective effect in clinical study.[18,19]

The property of trehalose has long been recognized, studied and utilized by cryobiologists and pharmacists to freeze, freeze-drying, and hypothermal storage of various bioactive molecules including proteins, antibodies, DNA, liposomes, DNA/lipid complexes, cells and even organs[20]. However, the human body does not biosynthesize trehalose but is able to metabolize it into two glucose molecules.

In previous studies, we have synthesized trehalose pentaethyleneamine click polymers with different polymer lengths. The preliminary studies have shown the trehalose containing click polymers can promote serum stability of the polyplexes and achieve significant pDNA delivery into cancer cells.[21] In the study of siRNA delivery, the trehalose click polymers also showed polymer length dependent efficacy for successful siRNA delivery[22]. Tseng et. al. have shown that the presence of free trehalose in cell culture media promotes plasmid DNA (pDNA) delivery by polyethyleneimine (PEI)-based complexes to various cell lines.[23] The neuroprotective effect of trehalose in Huntington, Parkinson, and prion diseases can attribute to the presence of polymers of trehalose in induction of autophagy in brain.[24-26] _ENREF_26 More recently Maynard et al. reported that *p*-formylpolystyrene modified with trehalose via an acetonide moiety is capable of imparting both lyo- and heat protectant properties to lysozyme when covalently attached to this enzyme.[27]

In this study, two series of RAFT block copolymers are synthesized, characterized and compared for siRNA delivery. For the family of diblock glycopolymers, the colloidal stabilizing block was formed by polymerizing 2-deoxy-2-methacrylamido glucopyranose

(MAG), followed by polymerization with aminoethylmethacrylate (AEMA) via RAFT polymerization. For the family of polytrehalose polymers, the colloidal stabilizing block was synthesized via polymerizing 6-methacryamido-6-deoxytrehalose via RAFT. In both approaches, we rationalized that a block copolymer comprised of densely-placed carbohydrate units would deter non-specific aggregation/adsorption and confer lyoprotective and cryoprotective properties as a surface layer on nanoparticles by insuring a high local concentration and significant topology. _ENREF_15Its polymeric nature would be expected to impart an increase in the local viscosity on the particle surface, thus enhancing vitrification of the surface-bound water and colloidal stability.[28] In addition, considering that the trehalose has neural protective effect, we reasoned that polytrehalose on the nanoparticle surface may significantly improve cellular internalization into glioblastoma cells, as the overexpress GLUT-1 is also reported.[29] For the first time, we demonstrate that synthetic polytrehalose motif enhances colloidal stability in salt, serum, and during lyophilization while still retaining high cellular internalization and effective payload delivery of inter-polyelectrolyte nanosystems.

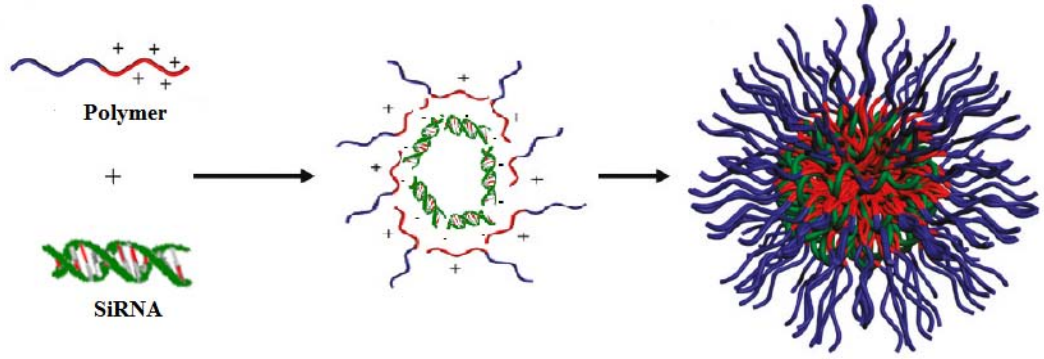

Figure 1. Schematic illustration of polyplexes formation from diblock copolymers complexed with siRNA.

Materials

All reagents for synthesis were obtained at the highest possible purity from Fisher Scientific Co (Pittsburgh, PA) or Sigma-Aldrich Co (St. Louis, MO) and used as received unless noted otherwise. N(2-aminoethyl)methacrylamide was purchased from Polysciences (Warrington, PA). JetPEI was obtained from PolyPlus Transfections (Illkirch, France). Dialysis membranes were obtained from Spectrum Laboratories, Inc. (Rancho Dominguez, CA). Dry methylene chloride, dimethyl formamide, methanol and tetrahydrofurane were obtained using an MBRAUN MB solvent purification system manufactured by M. Braun Inertgas-Systeme GmbH (Garching, Germany), using HPLC grade solvents obtained from Fisher Scientific Co (Pittsburgh, PA).

Thin layer chromatographies (TLC) were done using aluminum-backed silicagel plates (silicagel 60, F_{254}) obtained from Merck (Darmstadt, Germany) and visualized using UV light (254 nm) or staining agents: ninhydrin solution in ethanol for the visualization of amines, *p*-anisaldehyde solution in H_2SO_4/acetic acid/ethanol for the visualization of carbohydrates.

Preparative chromatographies were performed using a Buchi Separcore chromatography system, (Buchi Labortechnik AG, Switzerland) using Buchi plastic chromatography cartridges or homemade glass columns manually packed with 60-200 mesh Premium Rf silicagel (Sorbent Technologies Inc., Atlanta, GA). All solvents used for preparative chromatography were HPLC grade obtained from Fisher Scientific Co (Pittsburgh, PA).

LC-MS data was obtained with an Agilent system, Agilent Technologies (Santa Clara, CA) with a time-of-flight (TOF) analyzer coupled to a Thermo Electron TSQ-LC/MS ESI mass spectrometer.

NMR spectra were recorded using 400MR Varian-400 Hz spectrometer in deuterated solvents, namely D_2O, d_4-MeOD, d_6-DMSO, $CDCl_3$, CD_2Cl_2. All deuterated solvents were purchased from Cambridge Isotope Laboratories, Inc. (Andover, MA). ^{1}H-NMR spectra were recorded at 399.7 MHz and ^{13}C-NMR spectra were recorded at 101 MHz. Spectra were analyzed using MNova software (version 7.0.1-8414, Mestrelab Research S.L. (Santiago de Compostela, Spain)).

SEC was conducted using 1.0 wt% acetic acid/0.1 M Na_2SO_4 as the eluent at a flow rate 0.3 mL/min on size exclusion chromatography columns [CATSEC1000 (7μ, 50×4.6), CATSEC100 (5μ, 250×4.6), CATSEC300 (5μ, 250×4.6), and CATSEC1000 (7μ, 250×4.6)] obtained from Eprogen Inc. (Downers Grove, IL). Signals were acquired using Wyatt HELEOS II light scattering detector (λ = 662 nm) and an Optilab rEX refractometer (λ = 658 nm). SEC trace analysis was performed using Astra V software (version 5.3.4.18), Wyatt Technologies (Santa Barbara, CA). Biological sample fluorescence was measured with GENios Pro luminometer (TECAN US, Research Triangle Park, NC). Quartz Crystal Microbalance (QCM) experiments were performed on Q-Sense E4 QCM (Q-sense; Vastra Frolunda, Sweden) instrument. Differential scanning calorimetery (DSC) was conducted on a TA Instruments Q100 under nitrogen.

Polymer Synthesis

A. Synthesis of glucose containing RAFT polymer P(MAG_{46}-b-$AEMA_x$) (this work was accomplished by Dr. Adam Smith and Dr. Anton Sizovs).

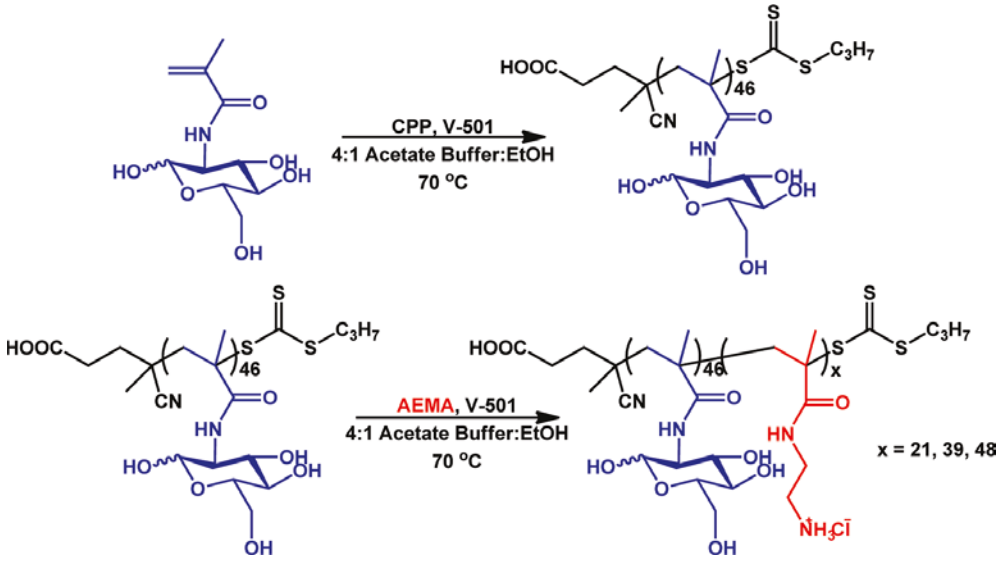

Scheme 1. Synthesis of P(MAG_{46}-b-$AEMA_x$) via RAFT Polymerization

The diblock copolymers of MAG and AEMA were synthesized according to Scheme 1. A trithiocarbonate, CPP, was used to mediate the aqueous RAFT polymerization of MAG in the presence of the free radical initiator V-501 to yield $PMAG_{46}$. The $PMAG_{46}$ macroCTA was subsequently chain-extended with AEMA to produce three diblock copolymers with varying AEMA block lengths. All polymerizations were performed in an aqueous acetate buffer to minimize hydrolysis and maintain the trithiocarbonate chain ends. SEC chromatograms of $PMAG_{46}$ and the three block copolymers, P1, P2, and P3, were unimodal with low PDIs (<1.25) indicating near-quantitative blocking efficiency and controlled polymerization (Figure 2-1). ^{1}H NMR studies of the glycopolymers (Figure 2-2) revealed compositions in agreement with those

calculated from SEC molecular weight measurements. The molecular weight and composition data of the diblock copolymer series are summarized in Table 1.

Polymer	M_n[a]	PDI[a](Đ)	MAG DP[b]	AEMA DP[b]
macroCTA	11700	1.24	46	
P1	14400	1.15	46	21
P2	16700	1.12	46	39
P3	17800	1.12	46	48

Table 1. As determined by aqueous size exclusion chromatography using a flow rate of 0.3 mL/min of 1.0 wt % acetic acid/0.1 M Na_2SO_4, Eprogen CATSEC100, CATSEC300, and CATSEC1000 columns, a Wyatt HELEOS II light scattering detector (λ = 662 nm), and an Optilab rEX refractometer (λ = 658 nm). b As determined by 1H NMR spectroscopy (1.5 mg/mL in D_2O at 65 ^oC).

1).

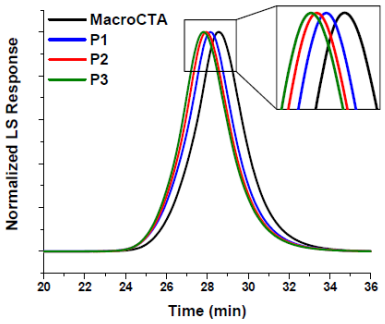

2).

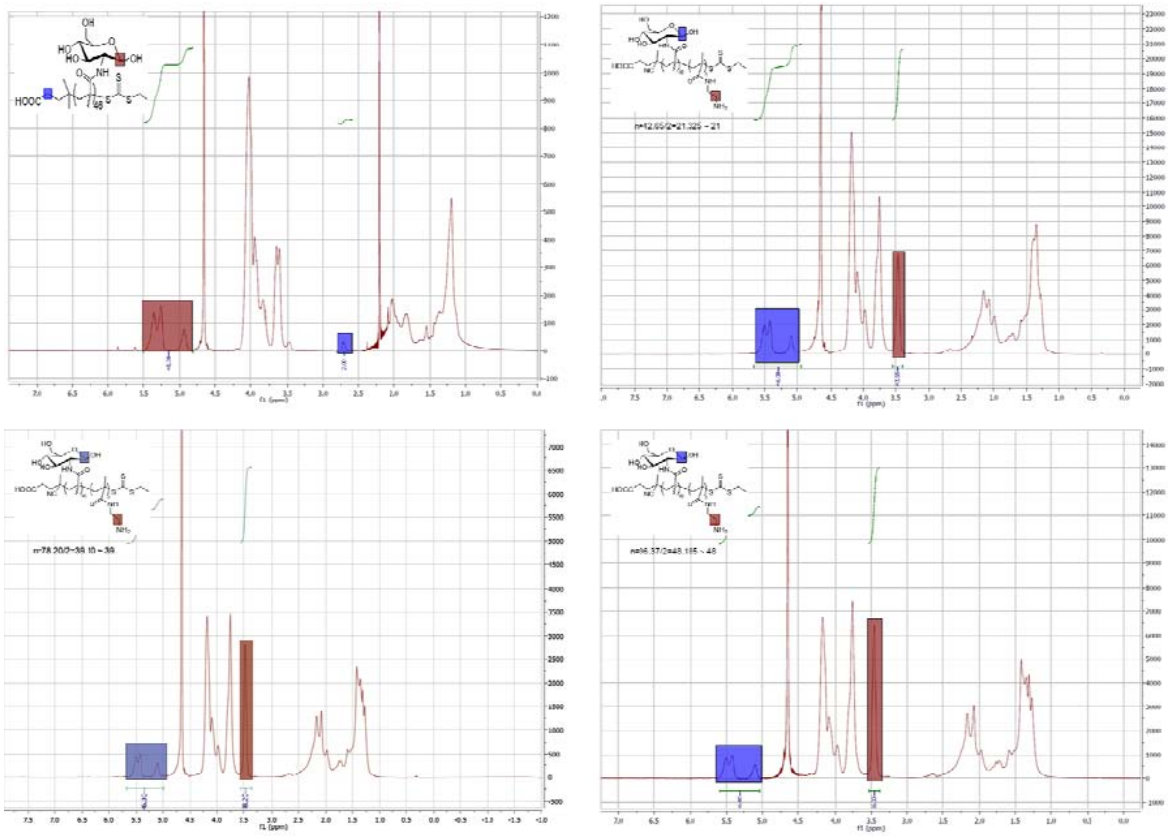

Figure 2. Characterization of the glycopolymers. 1). SEC trace for the PMAG macroCTA and the three diblock glycopolymers. 2). ^{1}H NMR spectra for (a) PMAG46, (b) P1, (c) P2, and (d) P3.

Synthesis of polytrehalose diblock copolymers

(This work was mainly accomplished by Anton Sizovs. Lian has contributed to the synthesis of 6-iodo-6-deoxy-2,3,4,5,2',3',4',5',6'-O-acetyl trehalose.)

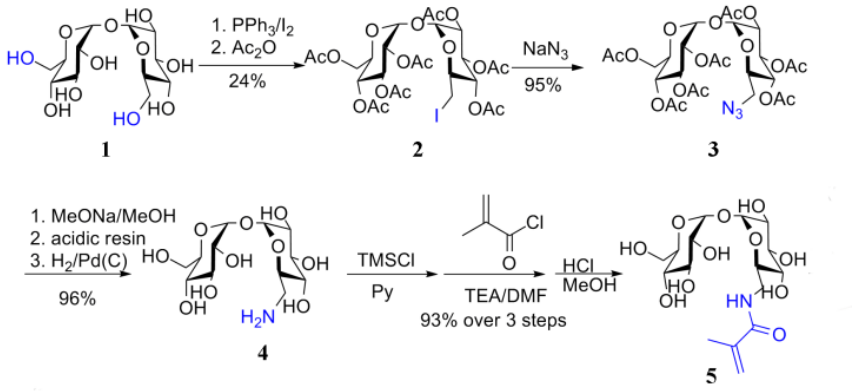

Scheme 2. Synthesis of 6-methacrylamido-6-deoxytrehalose (MAT).

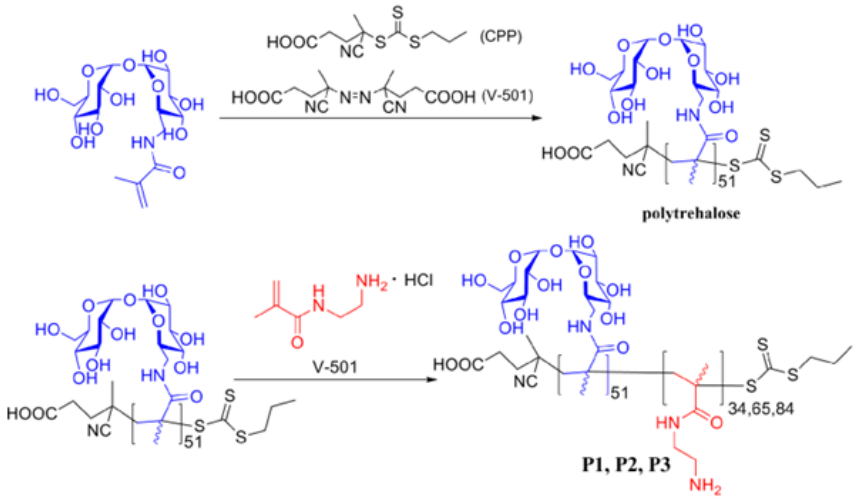

Scheme3. Polymer synthesis via RAFT polymerization.

In detail, typical procedure for the synthesis of 6-iodo-6-deoxy-2,3,4,5,2',3',4',5',6'-O-acetyl trehalose (2)

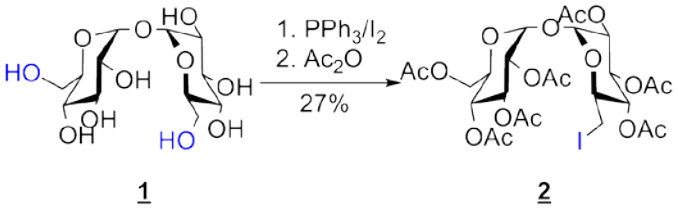

Iodine (47.50 g, 0.1871 mol) was placed in a flame-dried 1.5 L round-bottom flask and 800 mL of dry dimethylformamide (DMF) was added. Triphenylphosphine (51.55 g, 0.1965 mol) was dissolved in 150 mL of dry THF and added to iodine suspension. Anhydrous trehalose (42.64 g, 0.1246 mol, used as received) was added quickly via a funnel for solids. The reaction flask was closed with a septum, flushed with nitrogen, and placed in an oil bath. The reaction was allowed to proceed at 80 °C for 4 h. Solvents were removed under vacuum yielding a thick yellow oil.

The oil was poured into a 1 L solution of NaOMe in methanol through a funnel for liquids. The solution pH was measured by placing a drop of the methanolic solution on a piece of wet indicator paper. The pH was adjusted to 9 using NaOMe and the reaction mixture was then allowed to stir for 1h at room temperature. Acidic resin DOWEX-2H (H^+ form) was added to neutralize the solution and subsequently filtered off. Methanol was removed on a rotary evaporator yielding a yellow oil.

The oil was poured in 600 mL of water via a funnel for liquids causing PPh_3O precipitation. Importantly, a thin-tipped funnel was used to avoid the formation of large clumps of triphenylphosphine oxide. This solution was placed in a refrigerator at 4 °C for 12 h.

The aqueous solution was then filtered to remove PPh_3O. The filtrate was extracted with 2x50 mL of dichloromethane (DCM) to remove any remaining organic impurities (PPh_3O and PPh_3). Water was removed on a rotary evaporator, and the obtained oil was dried for 20 h over P_2O_5 at 500 mTorr.

The dry oil was dissolved in 800 mL of dry pyridine (Py) and the solution was placed in an ice-bath. Acetic anhydride (190 mL, 205 g (d=1.08 g/mL), 2.01 mol) were

added over ca. 15 min using an additional funnel. The reaction was allowed to stir at room temperature for 14 h. The reaction mixture was then poured on ice, forming a sticky precipitant. The ice was allowed to melt and the reaction mixture was extracted with 4x200 mL of DCM. The organic extracts were combined, washed with a dilute sulfuric acid solution to remove Py and dried over Na_2SO_4 overnight. It should be noted that washing with NaCl(sat) solution leads to halogen exchange ($RCH_2I \rightarrow RCH_2Cl$) and must be avoided.

Na_2SO_4 was filtered off and DCM was removed on a rotary evaporator yielding a yellowish oil. The oil was loaded on a silicagel column (300 g of silicagel, DCM) and mixture of per-O-acetylated 6-iodo-6-deoxy and 6,6´-diiodo-6,6´-deoxy trehalose was separated from the rest of the mixture using DCM/Et_2O=5/1 eluent.

This mixture of two products was separated by column chromatography (ca. 2 gram portions of mixture, 100 g of silicagel) using eluent gradient→DCM DCM/Et_2O(5/1) to yield 22.3 g (24.0%) of **2**.

^{1}H-NMR (400 MHz, $CDCl_3$) δ ppm: 5.56 – 5.45 (overlapping triplets, J = 10.2, 2H), 5.40 – 5.36 (d, 3.9 Hz, 1H), 5.36 – 5.33 (d, 1H), 5.22 – 5.15 (dd, J = 10.3, 3.9 Hz, 1H), 5.10 – 5.00 (m, 2H), 4.94 – 4.84 (dd, J = 10.0, 9.2 Hz, 1H), 4.27 – 4.19 (m, 1H), 4.08 – 3.98 (m, 2H), 3.97 – 3.89 (dd, J = 10.0, 9.0, 2.4 Hz, 1H), 3.30 – 3.20 (dd, J = 11.0, 2.6 Hz, 1H), 3.13 – 2.99 (m, 1H), 2.15 (s, 3H), 2.09 – 2.07 (m, 9H), 2.05 (s, 3H), 2.03 (s, 3H), 2.02 (s, 3H). ^{13}C-NMR (101 MHz, $CDCl_3$) δ ppm: 170.67, 170.00, 169.94, 169.67, 169.58, 169.57, 92.21, 91.68, 72.46, 70.31, 70.11, 69.84, 69.56, 69.27, 68.70, 68.38, 68.05, 61.91, 25.70, 21.28, 20.79, 20.74, 20.68, 20.63, 2.61. ESI-MS positive ion mode:

calculated m/z $[M+NH_4]^+$ 764.1257, found m/z: 764.1297; calculated m/z $[M+Na]^+$ 769.0811, found m/z: 747.0832.

Typical procedure for the synthesis of 6-azido-6-deoxy-2,3,4,5,2',3',4',5',6'-O-acetyl trehalose (3)

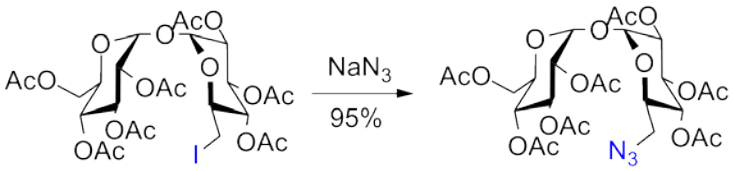

2 **3**

Compound **2** (16.56 g, 22.19 mmol) and NaN_3 (1.63 g, 25.07 mmol) were placed in a dry 500 mL flask equipped with a stir bar and capped with a septum. Next, 300 mL of dry DMF was added via cannula and nitrogen was bubbled through the solution for 20 min. The reaction mixture was brought to 60 °C and stirred for 4 h. The reaction mixture was cooled down and concentrated on a rotary evaporator to a final volume of ca. 150 mL. The resulting solution was poured into 700 mL of H_2O at 0 °C. It was extracted with 3x150 mL of ethyl acetate. Organic extracts were combined, washed with brine and dried over Na_2SO_4 overnight.

The solids were filtered off and the solvent was removed on a rotary evaporator yielding a white crystalline material. The product was recrystallized from ethylacetate/hexanes(1/3) to yield 11.94 g of **3** upon drying. The filtrate was placed in a freezer (-27 ^oC) resulting in precipitation of 1.62 g of **3**. The combined yield was 13.56 g (92.4%).

^{1}H-NMR (400 MHz, $CDCl_3$) δ ppm: 5.49 (ddd, J = 10.3, 9.3, 5.7 Hz, 2H), 5.35 – 5.30 (m, 2H), 5.04 (m, 4H), 4.25 (dd, J = 12.1, 5.6 Hz, 1H), 4.13 – 3.98 (m, 3H), 3.36 (dd, J = 13.3, 7.2 Hz, 1H), 3.17 (dd, J = 13.3, 2.5 Hz, 1H), 2.12 (s, 3H), 2.11 – 2.07 (2 overlapping

singlets, 6H), 2.06 (s, 3H), 2.05(s, 3H), 2.04 (2 overlapping singlets, 6H). ^{13}C-NMR (101 MHz, $CDCl_3$) δ ppm: 170.57, 169.97, 169.68, 169.53, 169.51, 92.82, 92.43, 70.03, 69.88, 69.86, 69.77, 69.70, 68.54, 68.26, 61.77, 50.94, 20.67, 20.65, 20.63, 20.61. ESI-MS positive ion mode: calculated m/z $[M+NH_4]^+$ 679.2318, found m/z: 679.2276; calculated m/z $[M+Na]^+$ 684.1872, found m/z: 684.1825.

Typical procedure for the synthesis of 6-amino-6-deoxy-trehalose (4)

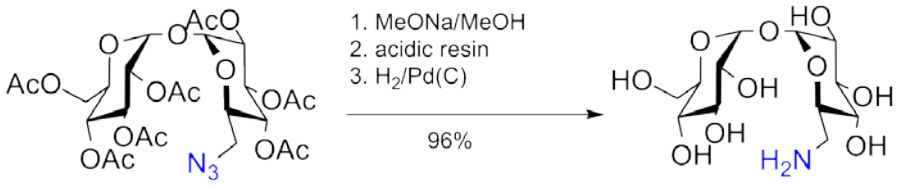

3 **4**

6-azido-6-deoxy-2,3,4,5,2',3',4',5',6'-O-acetyl trehalose **3** (11.81 g, 17.85 mmol) was dissolved in 450 mL of MeONa/MeOH (pH~9) and sonicated to assist dissolution. The reaction mixture was stirred at room temperature for 4h. The reaction progress was monitored by TLC/p-anisaldehyde stain (eluent: EtOAc/MeOH/H_2O=15/5/4). Ion exchange resin, DOWEX-50H, was added to reaction mixture, which was then stirred for 20 minutes (Note: DOWEX-50H might result in coloration of the reaction mixture, therefore it is advisable to wash the resin with methanol prior to use). The resin was removed by filtration and the solvent evaporated to yield the crude produce, 6-azido-6-deoxy-trehalose as amorphous solid.

The crude 6-azido-6-deoxy-trehalose was dissolved in methanol. The reaction mixture was deoxygenated by bubbling nitrogen through the solution for 30 min. Palladium on carbon (5% dispersion, 499 mg, 0.234 mmol) was added and hydrogen gas was bubbled through the solution for 20 h using a gas diffuser. After 20 h, nitrogen was

bubbled through the solution to remove the remaining dissolved hydrogen. The Pd(C) was filtered off using Celite and the solvent was removed using a rotary evaporator to yield the title compound **4** (5.83 g, 95.8% yield). ^{1}H-NMR (400 MHz, D_2O) δ ppm: 5.10 – 4.97 (two doublets, J = 4.4 Hz, 2H), 3.73 – 3.54 (m, 6H), 3.54 – 3.44 (dd, J = 9.9, 3.8 Hz, 2H), 3.34 – 3.23 (t, J = 9.4 Hz, 1H), 3.21 – 3.10 (t, J= 9.4 Hz, 1H), 2.91 – 2.79 (dd, J = 13.7, 2.5 Hz, 1H), 2.64 – 2.53 (dd, J = 13.8, 7.8 Hz, 1H). ^{13}C-NMR (101 MHz, D_2O) δ ppm: 93.03, 92.91, 72.35, 72.30, 72.01, 71.26, 70.99, 70.89, 69.53, 60.35, 48.73, 41.32. ESI-MS positive ion mode: calculated m/z $[M+H]^+$ 342.14, found m/z: 342.10.

Synthesis of 6-methacrylamido-6-deoxy trehalose (5)

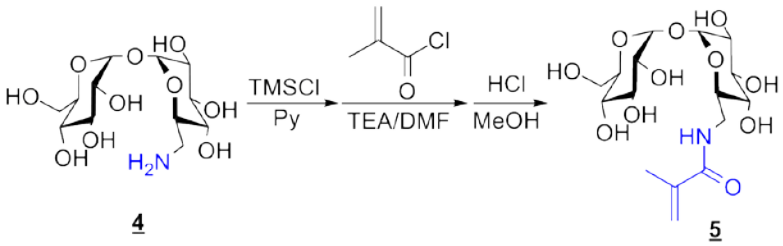

2-Deoxy-2-aminotrehalose **4** (3.74 g, 11.0 mmol) was suspended in 200 mL of dry pyridine. The reaction mixture was placed in an ice bath and trimethylsilyl chloride (TMSCl, 10.0 g, 92.0 mmol, 1.2 eq per -OH) was added using an addition funnel. The reaction mixture was allowed to slowly warm to room temperature, and the reaction was allowed to proceed overnight.

The reaction mixture was cooled down to ca. 0 ºC and poured into 600 mL of ice-cold carbonate buffer (pH=9). The aqueous suspension was extracted with 3x150 mL of hexanes. The extracts were combined and washed with water, followed by brine and finally dried over Na_2SO_4.

The solid was filtered off and hexanes were removed under reduced pressure on a rotary evaporator. A white crystalline material was obtained upon evaporation and was then dried at 500 mTorr over P_2O_5 to yield 8.83 g (95.2%) of the 6-amino-6-deoxy-2,3,4,5,2´,3´,4´,5´,6´-nano-*O*-trimethylsilyl trehalose. ^{1}H-NMR (400 MHz, CD_2Cl_2) δ ppm: 4.87 – 4.74 (two overlapped doublets J = 3.2 Hz, 2H), 3.90 – 3.77 (td, J = 9.0, 3.2 Hz, 2H), 3.73 – 3.52 (m, 4H), 3.44 – 3.26 (m, 4H), 2.87 – 2.78 (dd, J = 13.2, 3.0 Hz, 1H), 2.68 – 2.57 (dd, J = 13.2, 5.4 Hz, 1H).

The TMS protected aminotrehalose (1.687 g, 1.993 mmol) was dissolved in 2 mL of DCM and 35 mL of DMF. This solution was cooled down in an ice bath and triethylamine (0.55 mL, 0.40 g (d=0.726 g/mL), 3.9 mmol) was added. Freshly distilled methacryloyl chloride (0.22 mL, 0.24 g (d=1.07 g/mL) 2.3 mmol) was dissolved in 5 mL of dry DCM and was slowly (over ca. 10 min) added to the reaction mixture. The reaction was allowed to proceed at 0 ºC for 1H and, additionally, 3h at room temperature.

The reaction mixture was then cooled in an ice bath and poured into 200 mL of the ice-cold carbonate buffer (pH~8) that contained ice. The resulting suspension was extracted with 3x30 mL of hexanes. The organic extracts were combined and washed with water, followed by a brine wash, and finally the solution was dried over Na_2SO_4 overnight.

The solids were filtered off and the hexanes were removed under vacuum to yield a colorless oil. This oil was dissolved in 20 mL of dry methanol and placed in an ice bath. Next, 0.2 mL of a ~1.25M HCl solution in methanol was added and the reaction was allowed to warm to room temperature and further stirred for additional 10 min. Methanol was removed under vacuum using a rotary evaporator (the rotovap water bath

temperature was kept at 25 °C), yielding 0.765 g (93.3%) of the title compound (**5**) as a white solid foam. ^{1}H-NMR (400 MHz, CD_3OD) δ ppm: 5.77 – 5.61 (t, J = 0.9 Hz, 1H), 5.40 – 5.35 (t, J = 1.4 Hz, 1H), 5.13 – 5.03 (dd, J = 16.1, 3.8 Hz, 2H), 3.98 – 3.90 (dt, J = 9.7, 4.8 Hz, 1H), 3.86 – 3.74 (m, 4H), 3.72 – 3.64 (dd, J = 11.9, 5.4 Hz, 1H), 3.57 – 3.52 (d, J = 4.8 Hz, 2H), 3.52 – 3.44 (td, J = 9.8, 3.8 Hz, 2H), 3.36 – 3.31 (dd, J = 9.8, 9.0 Hz, 1H), 3.20 – 3.13 (dd, J = 9.8, 9.0 Hz, 1H), 2.00 – 1.84 (m, 3H).

Synthesis of polytrehalose 6 ($pMAT_{51}$)

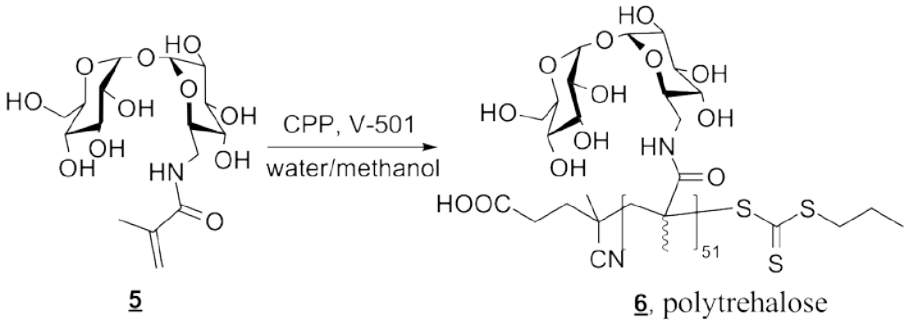

5 **6**, polytrehalose

6-Methacrylamido-6-deoxy trehalose **5** (0.765 g, 1.867 mmol, 65 eq) was dissolved in 7.00 mL of acetate buffer in D_2O. CPP (7.97 mg, $2.87x10^{-2}$ mmol, 1 eq) was dissolved in 645 µL of MeOD and added to the solution of **5**, followed by V-501 (0.805 mg, $2.87x10^{-3}$ mmol, 0.1 eq) in 244 µL of MeOD. Finally, 861 µL of MeOD was added to a final volume of 1.75 mL of MeOD in the mixture. The reaction flask was capped with a septum and connected to an NMR tube via cannula. The setup was deoxygenated by bubbling nitrogen through the solution for 45 min. At that time, 0.50 mL of reaction solution was transferred into the NMR tube. Polymerization was conducted in an NMR instrument at 70 °C while spinning the reaction tube at 20 Hz for 9 h. ^{1}H-NMR spectra were acquired at various time points. The rest of the reaction mixture was kept in the refrigerator overnight.

Once the polymerization kinetics was established, the reaction mixture was removed from the refrigerator and deoxygenated by bubbling nitrogen through the solution for 45 min. The flask was placed in an oil bath pre-heated to 70 ^{o}C. The reaction was allowed to proceed for 6 h to yield 77% monomer consumption and a targeted degree of polymerization of 50. The reaction was stopped by removing the septum and cooling the reaction mixture on ice. The reaction mixture was then transferred to a dialysis bag having a 3500 Da molecular weight cut-off. It was dialyzed against ultra-pure water acidified to pH 4-5 with HCl. Water changes were performed every 8-10 h. After 3 d of dialysis, the polymer solution was frozen and lyophilized to yield 490 mg of white, fluffy material.

SEC (eluent: 1.0 wt% acetic acid/0.1 M Na_2SO_4). A flow rate of 0.3 mL/min, light scattering detector (λ = 662 nm) and refractometer (λ = 658 nm). M_n=21.0 kDa, dp_n=50.7~51, PDI=1.04.

^{1}H-NMR (400 MHz, D_2O) δ ppm: 5.76 – 5.28 (bs, 100H), 4.39 – 3.50 (m, 600H), 2.78 – 2.66 (bs, 2H), 2.53 – 0.68 (m, 264H).

Synthesis of diblock copolymers P1, P2 and P3

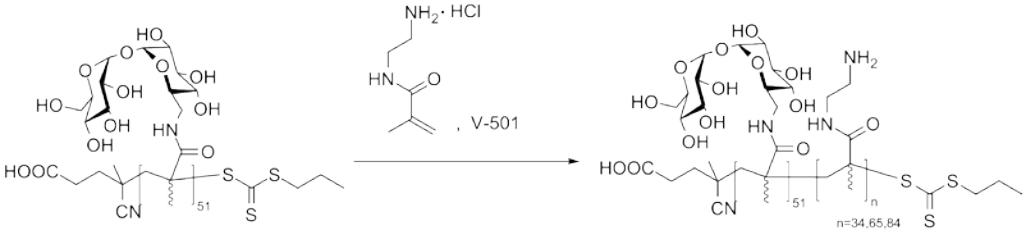

6, polytrehalose

P1, P2, P3

Polytrehaloes **6** (327 mg, 1.56x10^{-2} mmol, 1.00 eq) was dissolved in 3.00 mL of acetate buffer and the resulting solution was placed in a flask that contained aminoethylmethacrylamide hydrochloride (AEMA·HCl, 311 mg, 1.89 mmol, 121 eq). To

this, 0.780 mL of a solution containing V-501 radical initiator (0.44 mg, $1.56x10^{-3}$ mmol, 0.10 eq) was added and the flask was capped with a septum. The solution was deoxygenated by bubbling nitrogen through the reaction solution for 45 minutes. The flask was then placed in an oil bath preheated to 70 ^{o}C for polymerization. Two 1.25 mL samples were taken with a syringe at 30 min (**P1**) and 60 min (**P2**) of reaction time. Each sample was sprayed into a vial which was immediately cooled on ice. After 90 min (**P3**), the reaction was stopped by removing the septum and placing the reaction flask on ice. All three samples were placed in dialysis bags having a 3500 Da molecular weight cut-off and dialyzed against 3x4L of 0.5 M NaCl solution, followed by 3x4L 0.1 M NaCl and finally 6x4L of ultra-pure water. All dialysis media were acidified with HCl to pH 4-5.

Upon completion of dialysis, polymer solutions were lyophilized to yield white, fluffy powders.

MAT_{51}-*b*-$AEMA_{34}$(**P1**), 113 mg. SEC (eluent: 1.0 wt% acetic acid/0.1 M Na_2SO_4). A flow rate of 0.3 mL/min, light scattering detector (λ = 662nm) and refractometer (λ = 658 nm). M_n=23.4 kDa, PDI=1.04.

MAT_{51}-*b*-$AEMA_{65}$(**P2**), 141 mg. SEC (eluent: 1.0 wt% acetic acid/0.1 M Na_2SO_4). A flow rate of 0.3 mL/min, light scattering detector (λ = 662nm) and refractometer (λ = 658 nm). M_n=29.4 kDa, PDI=1.05.

MAT_{51}-*b*-$AEMA_{84}$(**P3**), 181 mg. SEC (eluent: 1.0 wt% acetic acid/0.1 M Na_2SO_4). A flow rate of 0.3 mL/min, light scattering detector (λ = 662nm) and refractometer (λ = 658 nm). M_n=31.8 kDa, PDI=1.06.

Synthesis of MAT_{51}-*b*-($AEMA_{33}$-*s*-AEMA-$fluorescein_1$) (P1-FITC)

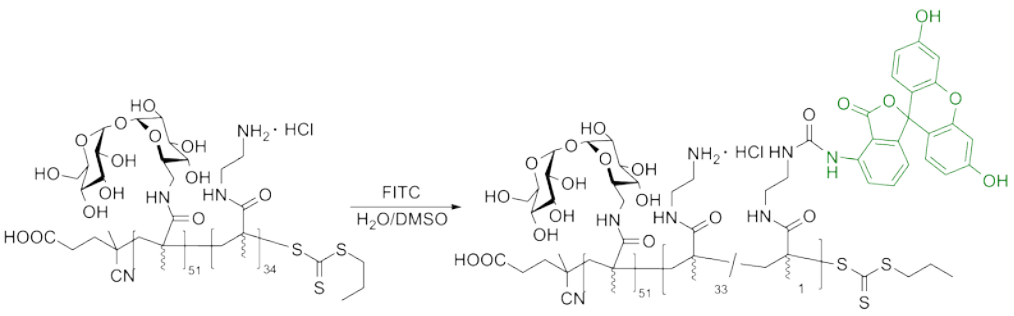

P1 (MAT_{51}-*b*-$AEMA_{34}$·34HCl, 12.0 mg, 34 eq) was dissolved in 850 µL of 0.1 M $NaHCO_3$, which was previously deoxygenated (bubbling N_2 though the solution for 30 min). The flask was placed in an ice bath and 20.0 µL of a DMSO solution containing fluorescein isothiocyanate (FITC, 0.18 mg, 1 eq) was added with a pipette. The reaction mixture was allowed to slowly reach RT. After 12 H of stirring the reaction mixture, it was placed in a dialysis bag (3500 Da molecular weight cut-off) and dialyzed for 8 h (in the dark) against each of the following aqueous solutions: 0.1 M NaCl (4 L x 2), 0.07 M NaCl (4L), 0.03 M NaCl (4L), H_2O (4 x 3). The content of the dialysis bag was then transferred into a vial and lyophilized, yielding P1-FITC (11.1 mg (91.1%) as a bright yellow powder.

Material preparation and properties study (this section is based on polytrehalose diblock copolymers. It was accomplished by Dr. Anton Sizovs and Lian Xue).

Polyplex formulation of diblock copolymer with siRNA

To a 2 µM solution of siRNA in RNase-free an equal volume of polymer solution at an appropriate concentration was added via autopipette. The solution was mixed well

by injecting/ejecting the solution with the pipette several times. The polyplexes were allowed to incubate undisturbed at room temperature for 1 h prior to transfection.

Polyplex lyophilization

Polyplexes formed with polytrehalose copolymers and siRNA were prepared in 1-mL microfuge tubes according to the procedure described above using 35μL of a 2 μM siRNA solution and 35 μL of the corresponding polymer solution. Once formed, the polyplexes were allowed to incubate for 1h at room temperature. Microfuge tubes containing solutions of polyplexes were placed in a freezer at -27 $^{\circ}$C for ca. 2 h. Lyophilization was performed by placing the microfuge tubes in a 1L lyophilization jar at room temperature and 10-30 mTorr vacuum for 24 h. To re-dissolve polyplexes, 70 μL of RNase free water was added to lyophilized material and solution was allowed to incubate at room temperature for 1h.

Gel electrophoresis of polyplexes

A 0.6% w/w agarose gel was prepared by dissolving 0.3 g of agarose in 50 mL of TAE buffer while heating. The resulting agarose solution was allowed to cool to ca. 40-45 ^{o}C and 3 μL of ethidium bromide solution was added.

The polyplex solutions (20 μL) were prepared by following the protocol for polyplex formulation described above. Loading buffer (2 μL of Blue juice^{TM}) was added to each sample. The polyplex solutions (10 μL) were each loaded into the wells of the gel, and electrophoresis was performed at 60V for 45 min.

Images of gels are obtained using 312 nm UV light to detect ethidium bromide.

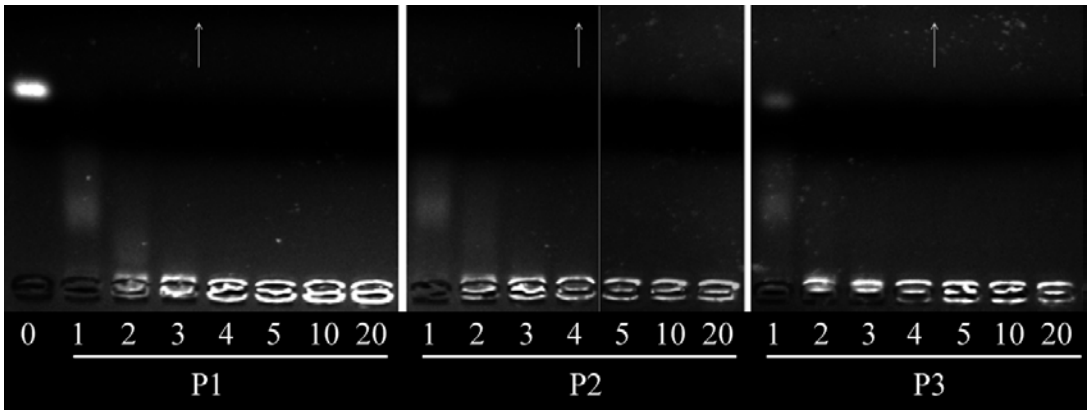

Figure 3. Gel electrophoresis assay. Numbers under each well correspond to polymer amine/siRNA phosphate (N/P) ratio. Arrows point towards anode(+).

Dynamic light scattering measurements

Polyplexes were prepared according to the standard protocol using 20 µL of a 2 µM siRNA solution and 20 µL of polymer P1, P2 or P3 solution of appropriate concentration to yield polyplexes at N/P ratios of 5, 10 and 20. After 1 h incubation at room temperature, polyplex solutions were diluted with water, OptiMEM, or DMEM with 10% serum to a final siRNA concentration of 400 nM. Solutions were transferred into cuvettes and particle sizes were measured at 25 ºC using 173º detection angle at various time points.

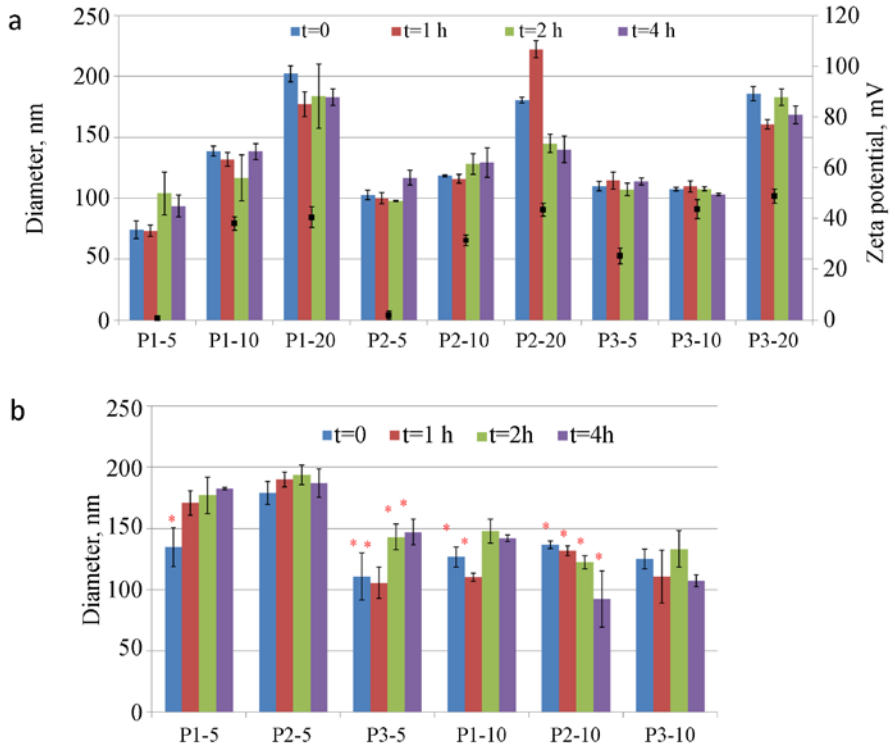

Figure 4 a. Hydrodynamic radii and ζ-potentials of polyplexes in water over the period of 4 h. Labels signify "polymer_name-N/P" b. Hydrodynamic radii of polyplexes after lyophilization and resuspension in water. A star (*) denotes cases in which a second population of larger particles was present (500-1000 nm). Labels signify "polymer-N/P".

Evaluation of phase transitions of the polytrehalose and trehalose solutions with differential scanning calorimetry (DSC)

Aqueous solutions of trehalose (0.58 mol%, 1.30 mol%, 2.21 mol%, 3.39 mol%, and 5.00 mol%) and polytrehalose (0.58 mol%, 1.30 mol%, 2.85 mol%, 3.39 mol%, 5.00 mol%, and 6.19 mol%) were prepared by weight using ultrapure water and trehalose dihydrate (obtained from Fisher Scientific, used as received) and polytrehalose correspondingly. Solutions were incubated for 12 h at 40 ºC in closed containers to ensure the complete dissolution of the materials. Solutions were cooled down to room

temperature and 7-12 mg samples were immediately transferred into aluminum pans and hermetically sealed. An empty aluminum pan with a lid was used as a reference. Heating and cooling was done at 5 ºC/min rate. Isothermal conditioning was applied for 10 min at both highest temperature (70 ºC) and lowest temperature (-65 ºC). The data was recorded for the second heat/cool/heat cycle and analyzed using TA Instruments Universal Analysis 2000 software, version 4.5A (Waters Corporation, Milford, MA).

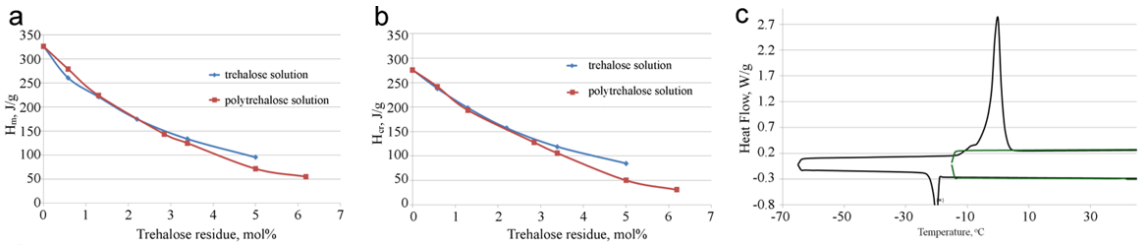

Figure 5. Physical properties of polytrehalose and polyplexes. (a) Depression in heats of ice melting, H_m and (b) water crystallization, H_{cr}, of trehalose and polytrehalose solutions at various concentrations. Data was not obtained for trehalose solutions above 5 mol% due to solubility limitations. (c) Differential scanning colorimetry of a 34 mol% solution of polytrehalose. Isothermal conditioning was applied for both cool-heat cycles at the lowest temperature for 30 min. The graphical representation of the exothermic peak does not display a 'loop' (*) which results from overcooling.

The aforementioned lyoprotective properties of trehalose have been largely attributed to its ability to decrease water crystallization around biological membranes and proteins and to decrease the energy associated with phase transitions of H_2O (crystallization and melting).[30] To examine whether polytrehalose retained this property, we analyzed both trehalose and polytrehalose solutions of various concentrations via differential scanning calorimetry (DSC). Polytrehalose was similar to trehalose in

depressing both the heat of ice melting (H_m) and the heat of water crystallization (H_{cr}), up to a concentration of 2.2 mol%, and was even more effective than trehalose itself at higher solution concentrations (Figures 5a and 5b). At 5 mol%, *poly*trehalose lowers H_m by an additional 24 J/g and H_{cr} by an additional 35 J/g compared to trehalose; that concentration corresponds to about 23 water molecules per trehalose residue, which is nearly twice as many water molecules as are present in the hydration sphere of trehalose alone.[31] It is known that high viscosity favors glass formation over crystallization and the observed enhanced efficiency is likely a result of the increased viscosity of the *poly*trehalose solution compared to that of a solution of trehalose.[32,33] Importantly, it was also discovered that if the polytrehalose solution is cooled significantly below 0°C but at least 5°C above the temperature at which the onset of water crystallization is observed, no crystallization occurs even after storage (Figure 5c). These data pointed toward the promising attributes of utilizing polytrehalose as a barrier to increase payload stability and decrease nanocomplex aggregation.

Biological studies to evaluate the copolymers on siRNA delivery (this section was accomplished by Lian Xue)

Cell culture experiments

Diethylpyrocarbonate (DEPC)-treated water for experiments involving the use of siRNA was obtained from Fisher Scientific (Pittsburgh, PA). Propidium iodide, Lipofectamine™2000, UltraPure™ Agarose-1000, trypsin, (3-(4,5-dimethylthiazol-2-yl)-2,5-diphenyl tetrazolium bromide (MTT), phosphate buffer saline (PBS), modified essential minimum eagle medium (Opti-MEM®) and Dulbecco's modified eagle medium

(DMEM) were purchased from Invitrogen, Inc. (Carlsbad, CA). CellScrub™ Buffer was obtained from Genlantin, Inc. (San Diego, CA). Bovine albumin was purchased from Sigma-Aldrich (St. Louis, MO). The Luciferase Assay Kit and cell lysis buffer were obtained from Promega (Madison, WI). Bio-Rad DC Protein Assay Reagent A, Reagent B and Reagent S were obtained from Bio-Rad Laboratories, Inc. (Hercules, CA). Anti luc2 luciferase siRNA (sense strand sequence 5´-GGACGAGGACGAGCACUUCUU-3´; antisense strand sequence 3´-UUCCUGCUCCUGCUCGUGAAG-5´) and Cy5-labeled anti Luc2 siRNA (sense strand sequence 5´-GGACGAGGACGAGCACUUCUU-Cy5-3´; antisense strand sequence 3´-UUCCUGCUCCUGCUCGUGAAG-5´) was purchased from Integrated DNA Technologies (Coralville, Iowa). Scrambled siRNA was obtained from Dharmacon, Inc (Lafayette, CO). Luciferase expressing human glioblastoma cells U-87 MG-luc2 (U-87_luc2) were obtained from Caliper LifeSciences, Inc. (Mountain View, CA). Luciferase-expressing glioblastoma cells (U-87_luc2) were used for target gene (luciferase) down-regulation efficiency experiments, cellular uptake studies, and MTT assays for cell viability. The cells were grown in complete DMEM [supplemented with 10% (v:v) fetal bovine serum, 1% antibiotic-antimycotic solution (containing penicillin, streptomycin, and amphotericin B)] at 37 ºC and 5%.

Cellular uptake measurement by flow cytometry

Flow cytometry was performed to examine the cellular uptake of fluorescently-labeled siRNA within various formulations at 3 h post-transfection. In general, luciferase-expressing U-87_luc2 glioblastoma cells were seeded at 300,000/well in 6-well plates 24 h prior to transfection. To transfect, 66 µL of polyplex solutions were prepared following the protocol described above. Each polyplex solution was pipetted into 1584 µL of pre-

warmed Opti-MEM to yield the final transfection solution, of which 500 µL was added to each well. After 3 h, the media was removed and cells were washed with 500 µL/well CellScrub™ Buffer for 15 min at room temperature to remove any surface-bound polyplexes (and to ensure that the signal was coming only from internalized polyplexes). The CellScrub™ Buffer was then aspirated and cells were exposed to trypsin (0.05% (w/v), 500 µL/well) for 3 min to provide detachment from the plate, then complete DMEM (500 µL/well) was applied to inhibit trypsin. The cell suspension was collected and centrifuged at 1000 rpm for 10 min at 4^{o}C. The supernatant was removed and cells were twice washed with 0.5 mL PBS and centrifuged to remove any remaining the extracellular polyplexes. Finally, 1 mL PBS was added and the suspensions were kept on ice prior to flow cytometry analysis. Propidium iodide (1.0 mg/mL, 2.5 µL) was added prior to the analysis. The flow cytometer (FACSCalibur, Becton Dickinson, San Jose, CA) equipped with a helium-neon laser to excite Cy5 at 633 nm was used to count twenty thousand events for each sample. The threshold fluorescence level was defined by manually adjusting the positive region such that <1% of negative control cells were positive for fluorescence. Each treatment was performed in triplicate.

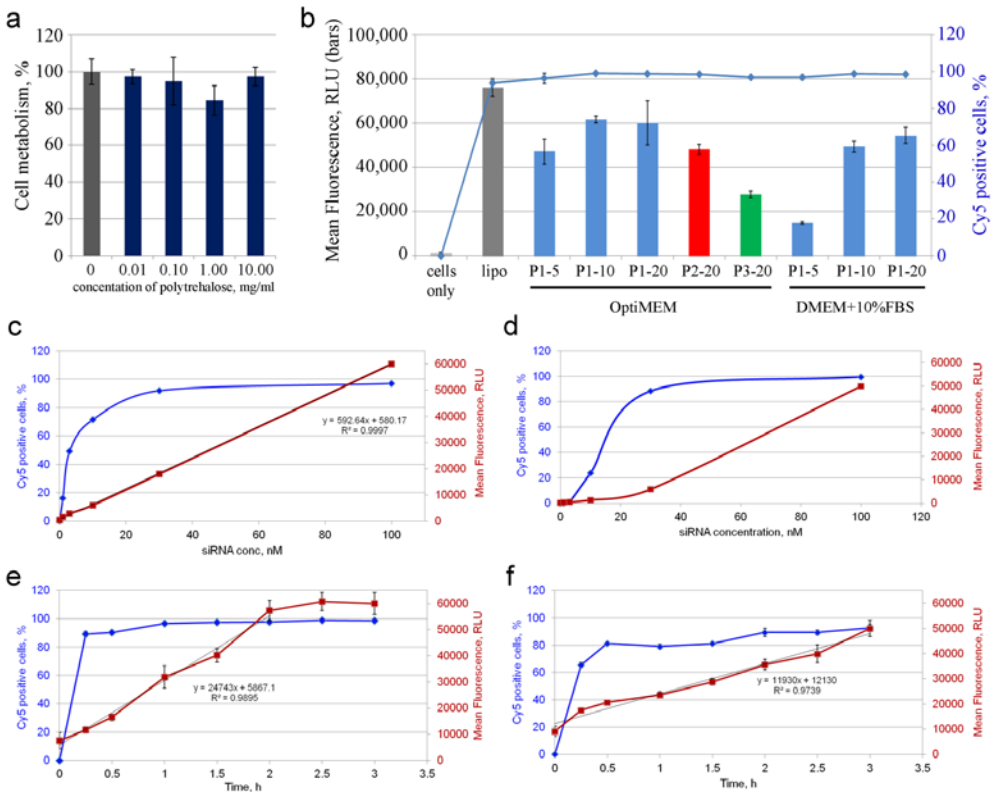

Figure 6. (a) Cell viability assessed by MTT assay after the incubation with various concentrations of polytrehalose (mean ± s.d., n = 3). (b) Cellular uptake by U-87 cells at siRNA concentration of 100 nM (mean ± s.d., n = 3). (c) Dependence of cellular uptake by U-87 cells on siRNA concentration using polymer P1 at N/P of 10 in (c) OptiMEM (mean ± s.d., n = 3) or (d) DMEM with 10% FBS (mean ± s.d., n = 3). (e) The rate of the uptake of P1−P10 polyplexes at 100 nm siRNA concentration in (e) OptiMEM (mean ± s.d., n = 3) or (f) DMEM with 10% FBS (mean ±s.d., n = 3). Red lines indicate Mean Cy5 intensity data; blue lines denote Cy5-positive cells (%).

Upon administration and biodistribution, cellular internalization is the first barrier that polyplexes encounter during the delivery process. To a large degree, this is defined by the interactions between the nanoparticle surface and cell membranes. We have reported previously that incorporation of another glycopolymer, polyglucoseamine into

nanoparticle formulations improves cellular uptake by glioblastoma cells.[34] It is also known that glioblastoma cells not only overexpress GLUT-1[29] but also that this glucose transporter can be employed by nanoparticles (virus) for cellular entry.[35] Trehalose is composed of two glucose units linked via an α,α-glycosidic bond, therefore, the ability of polytrehalose-coated polyplexes to undergo cellular internalization in glioblastoma cells was studied in detail.

Polyplexes were formulated with fluorescently-labeled siRNA, and the extent of their internalization by U-87 glioblastoma cells was measured with flow cytometry. All three polymers yielded efficient delivery of siRNA to cells and did so homogeneously across the cell population. More than 90% of the cells tested positive for siRNA with all formulations studied (Figure 4b). Polymer P1 was the most efficient among the three polymers tested, delivering the greatest number of siRNA copies per cell (as indicated by the greatest mean cellular fluorescence). It is important to note that polyplexes formed with each of the three polymers at N/P of 20 have similar sizes and ζ-potentials (Figure 4). However, the principle difference between the formulations is that the polytrehalose content. Polymer P1 contains 83% of polytrehalose by mass, whereas P2 and P3 contain 71% and 66%, respectively) which suggests that polytrehalose has a direct positive impact on the efficiency of U-87 uptake of these nanoparticles. Based on these initial uptake results, polymer P1 at N/P ratio 10 was chosen for further investigations.

The influence of siRNA concentration in the media on uptake (Figures 6c and 6d) was assessed. It was observed that the number of siRNA molecules that are internalized by cells is linearly proportional to the concentration of siRNA in serum containing DMEM (Figure 6d), and with nearly perfect linearity (R^2>0.99) in serum-free OptiMEM

(Figure 6c). The deviation from the linear dependence in serum containing DMEM is likely due to uptake in the presence of serum being slower. This finding shows that the amount of siRNA delivered to the cells can be controlled by altering the siRNA concentration in the media. Importantly, delivery is not saturated even at 100 nM siRNA concentration, meaning that this polymer can deliver higher doses of siRNA if necessary. The rate of the uptake was studied at 100 nM siRNA concentration and revealed interesting phenomena (Figure 6e and 6f). First, it is clear that polytrehalose coated nanoparticles internalize homogeneously across the cell population: more than 80% of U-87 cells are transfected with siRNA within the first 30 minutes. More importantly, the amount of siRNA delivered is linearly dependent on time in both serum-free and serum containing media, with R^2 values of 0.99 and 0.97 respectively. Thus, the rate of internalization is constant with time (zero order). In addition, in serum-free media, the fluorescence reaches a plateau after 2h, indicating that uptake is complete. These observations attest to the saturation of the internalization pathway. At this point, we are speculating specific receptor involvement in the uptake of the polytrehalose–coated polyplexes. It is worth noting that GLUT-1 operates in a saturated mode at physiological conditions,[36] it is overexpressed in glioblastoma cells[29] and is used by viruses (a nanoparticle-sized object) for cellular entry.[35] Considering the obtained uptake results and the known correlation between GLUT-1 and poor response to treatment in several types of cancer,[37-39] further investigation into polytrehalose promoted cellular entry is warranted.

Cellular uptake study via cell confocal microscopy *(this work was accomplished by Nilesh Ingle*)

Live cell imaging experiments were performed at 1, 3, 6, 12, 24, 36 and 48 h post transfection. The cells were plated in 35 mm glass bottom dishes with coverslip number 1.5 (MatTek Corporation, Ashland, MA). The cells were plated at a density of 80000 cells/dish at 24 hours prior to transfection in 4 mL DMEM supplemented with 10 % FBS and 1 % AB/AM and incubated at 37 ^{o}C and 5 % CO_2. Polyplexes were formulated by adding 15 µL of FITC-polymer P1 at 10 N/P ratio to 15 µL of Cy5-siRNA at 2 µM in DEPC treated water and then incubated for 1 h at room temperature. Prior to transfection, the polyplex solution was diluted by adding 270 µL of OptiMEM® to make a final volume of 300 µL (final siRNA concentration of 100 nM). The cells were transfected by adding 300 µL/dish of diluted polyplex solution. The cells were allowed to transfect for 3 h at 37 ºC and 5 % CO_2. For the timepoints of 1 and 3 h, the cells were washed with PBS and 4 mL of phenol red-free DMEM was added to each dish and imaged directly. For time points 6, 12, 24, 36 and 48 h, the cells were washed with PBS and 4 mL of 10 % FBS DMEM was added to the dish and further incubated for subsequent time points prior to imaging. In addition, for time points 36 and 48 h, the media was replaced with 4 mL of fresh 10 % FBS-containing DMEM at 24 hours post transfection. The controls were: (1) cells only, where the cells were not transfected, (2) FITC only, where the cells were transfected with polyplexes (where the only the polymer was labeled with FITC), (3) Cy5 only control cells were transfected with polyplexes where only the siRNA was labeled with Cy5.

Olympus FluoView FV1000 inverted confocal microscope was used for imaging. The image size was 1024*1024 pixels (12 bits). Sampling speed was 2.0 µs/pixel. The oil immersion objective used was PLAPON 60X O NA:1.42. The fluorophores used were FITC (fluorescein isothiocyanate) and Cy5 (Cyanine 5). The polymer was labeled with FITC in our laboratory as described above, and the Cy5 labeled siRNA was ordered from Integrated DNA Technologies (Coralville, Iowa). The FITC fluorophore was excited by a 488 nm laser and the Cy5 fluorophore was excited by 633 nm laser and all the images were acquired at the same laser settings and analyzed using Olympus FLUOVIEW software.

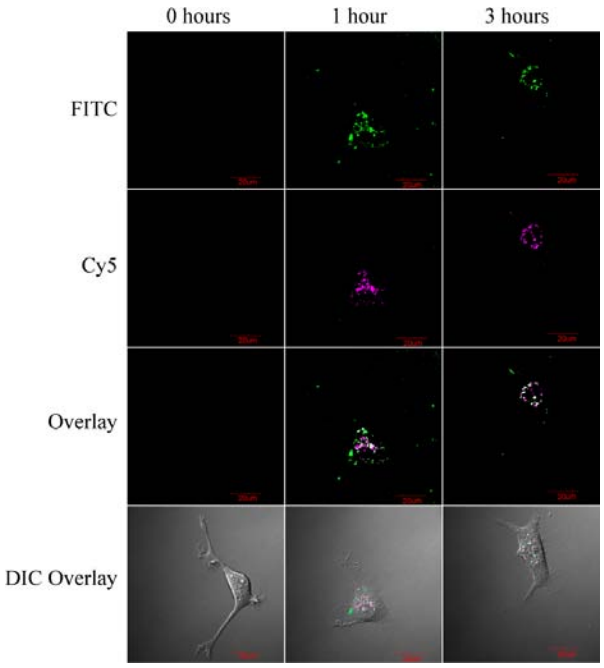

Figure 7. Confocal microscopy of U-87 cells transfected with Cy5-labeled siRNA (magenta) and FITC-labeled P1 (green) at N/P ratio 10. Cells were images at 0, 1, and 3 h after transfection (the time point of 0 = cells only).

Efficient uptake was also observed with confocal microscopy using Cy5-labeled siRNA and FITC labeled polymer P1 (Figure 7). After the first hour of incubation, the

punctuate nature of the fluorescence was observed in both Cy5 and FITC distributed throughout the cytoplasm. Distribution of the polyplexes inside the whole cell, rather than near the cellular membrane, indicates that trafficking of the particles is a rapid process. To visualize this polyplex trafficking, live cell imaging was used to compile a 6 minute video of P1polyplex (formulated at N/P 10) trafficking in U-87 cells 2 hours after transfection (see SI for the time-lapse video). The video reveals that the polymer and siRNA are associated as discrete polyplexes and active trafficking appears to take place as the polyplexes are shuttled around the cytoplasm.

Luciferase assay and protein assay

Luciferase-expressing glioblastoma cells (U-87_luc2) were seeded at 50,000 cells/well in 24-well plates 24 h prior to transfection. The anti-luciferase (Luc2) siRNA, control (siCon) siRNA, and polymer stock solutions were diluted with RNase-free water, and polyplexes were prepared following the protocol. The polyplex solution was diluted to a desired siRNA concentration (1 nM, 3 nM, 10 nM, 30 nM, 100 nM) with pre-warmed Opti-MEM or DMEM with 10% FBS to yield the transfection solutions. Cells were washed with PBS before the addition of 200 µl of the transfection solution. The formation of siRNA-containing lipoplexes using Lipofectamine2000 was performed according to the manufacturer's protocol.

The cells were incubated with polyplex/lipoplex solutions for 4 h before complete DMEM was added. After 48 h, the cells were washed with 500 µL PBS and treated with 1x cell lysis buffer for 15 min at room temperature. Aliquots (5 µl) of cell lysate were examined on 96-well plates with a luminometer for luciferase activity over 10 s with 100 µL of luciferase substrate added in each well immediately prior to relative light unit

(RLU) determination. The average of duplicate fluorescence measurements was utilized for calculation.

The amount of protein (mg) in cell lysates was calculated using a standard curve generated with bovine serum albumin by following the protocol included in Bio-Rad DC protein assay kit. The relative light unit (RLU)/mg protein was then calculated and averaged across replicate wells for comparison. The protein and luciferase levels of non-transfected cells were used for normalizing the data and calculating the extent of gene knockdown. Each treatment was tested in triplicate in 24-well plates.

1. Luciferase assay to evaluate the pDNA and siRNA delivery facilitated by polyglucose diblock copolymers.

A) B)

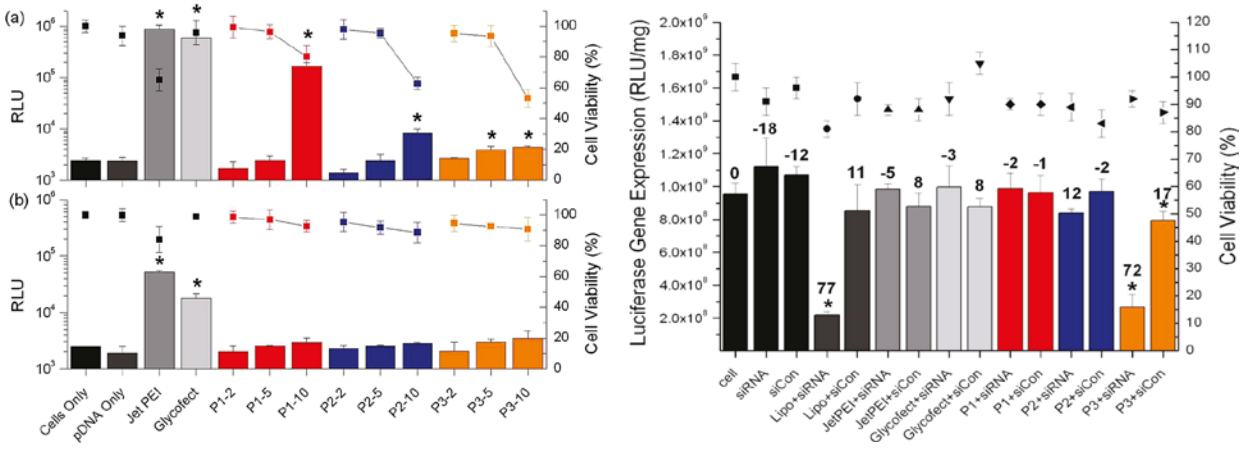

Figure 8. A) Luciferase gene expression and cell viability observed in HeLa cells transfected with polyplexes formed at N/P ratios of 2, 5, and 10 with pDNA and P1, P2, and P3 in (a) Opti-MEM and (b) DMEM. Error bars represent the standard of deviation of analyzed data from three replicates. Measurements found to be statistically significant

($p < 0.05$) compared with cells only marked with an asterisk. B). Luciferase gene expression (bars, left y axis) and cell viability (points, right y axis) in U-87 cells that stably express luciferase. The cells treated with polyplexes formed at an N/P ratio of 20 with an antiluciferase siRNA (100 nM) and glycopolymers P1, P2, and P3 in Opti-MEM. The percentage gene knockdown compared with the cells only control is given as numbers above the corresponding bars. Measurements found to be statistically significant ($p < 0.05$) compared with cells only are marked with an asterisk. Error bars represent the standard of deviation of analyzed data from three replicates.

As indicated in Figure 8A, the pDNA delivery was conducted in two different media. For most of the formulations, there is no significant gene expression observed, while for polyplexes P1/pDNA at N/P=10, dramatic luciferase expression was observed in the tranfection conducted in Opti-MEM. Cells treated with polyplexes formed with the glycopolymers P1 and P2 and the antiluciferase siRNA did not show significant gene knockdown compared with the negative controls. Remarkably, glycopolymer P3 demonstrated luciferase gene knockdown on par with Lipofectamine 2000 (72% for P3 and 77% for Lipofectamine 2000). The polyplexes composed of P3 + siCon also demonstrated statistically significant gene knockdown (17%), potentially due to the positive charge on P3 after releasing siCon leading to increased off target effects. As denoted in Figure 8B (right y axis), the cell viability was very high at these polyplex dose ratios, and thus the toxic effects were minimal. These results demonstrate how small differences in the polymer structure can have a large impact on delivery and efficacy of both pDNA (to the nucleus for gene expression) and siRNA (to the cytoplasm for gene knockdown).

2. Luciferase gene knockdown via siRNA facilitated by polytrehalose diblock copolymers.

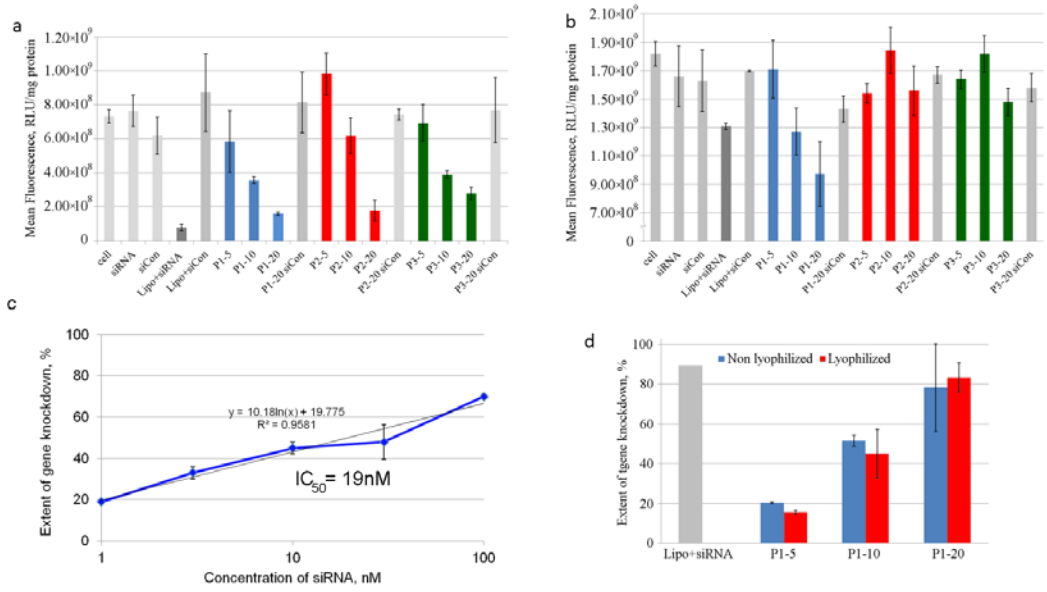

Figure 9. Luciferase gene knockdown in luciferase-expressing U-87 cells. Cells were transfected in a. OptiMEM and b. serum-containing DMEM (mean ±s.d., n=3). c. Evaluation of the efficiency of gene down regulation on siRNA concentration. Transfections were performed in OptiMEM (mean ±s.d., n=3). d. Comparison of target gene down-regulation in luciferase-expressing U-87 cells between freshly-prepared P1 polyplexes and previously-lyophilized P1 polyplexes. Transfections were performed at an siRNA concentration of 100 nM in OptiMEM (mean ±s.d., n=3). Labels signify "polymer name-N/P ratio", Lipo=Lipofectamine, siCon=siRNA with scrambled sequence (negative control), "cells" = no treatment was applied to cells (negative control).

The major goal of the biological investigation was to establish cellular internalization properties of the polytrehalose containing nanoparticles and cationic block was not optimized for siRNA release, but it was also important to investigate the ability

of polyplexes to down-regulate a target gene. The evaluation was performed in U-87 glioblastoma cells that stably express luciferase. The extent of gene down-regulation was assessed by the decrease in light production via luciferase assay. All three polymers promoted significant gene knockdown in OptiMEM (Figure 9a). The efficiency of gene down-regulation increased with an increase in N/P ratio and at an N/P of 20 was similar to that of Lipofectamine. In serum-containing DMEM, only polymer P1 was capable of promoting gene knockdown. We also investigated the dose response of the gene down-regulation. In contrast to the uptake response, which was linearly dependent on siRNA concentration (Figures 6c and 6d), the dependence of the extent of gene knockdown exhibited a logarithmic dependence on siRNA concentration (Figure 9c). The IC_{50} value for luciferase gene down-regulation promoted by P1 at N/P 10 with siRNA was calculated to be 19 nM.

It was of interest to probe the ability of the polytrehalose containing nanoparticles to retain siRNA-mediated gene down regulation after lyophilization and subsequent resuspension. Polymer P1 was chosen for these studies because it contains the largest amount of polytrehalose among three polymers and it was found to promote the optimal polyplex resuspension after lyophilization and also revealed to be the most effective at siRNA delivery. Therefore, we hypothesized that it would impart the greatest ability to preserve the biological activity of polyplexes.

Formulations of P1-siRNA polyplexes were lyophilized, and the dry powder was resuspended in RNase-free water. Gene down-regulation by the resuspended polyplexes was compared to freshly-prepared polyplexes made with the same polymer (Figure 9d). The extent of luciferase gene down-regulation induced by the lyophilized/resuspended

polyplexes was identical to that observed with the freshly-prepared analogs. This result shows that this polytrehalose motif displayed on the surface of the polyplexes indeed retains the lyoprotective property of trehalose in inter-polyelectrolyte siRNA nanoparticles during the freeze-drying process.

Using confocal microscopy we have investigated fluorescently-labeled polyplexes after uptake into U-87 cells for 48 hrs when gene down-regulation was measured (Figures 10 A-B).

A).

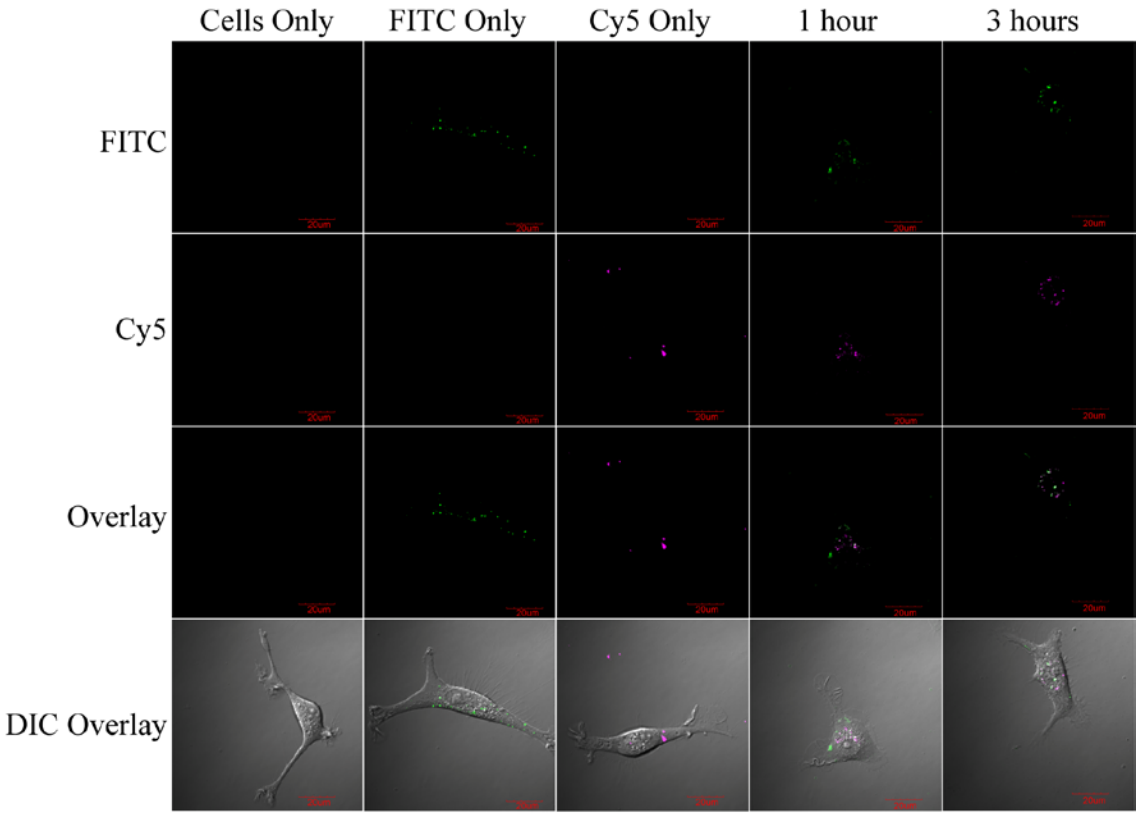

B).

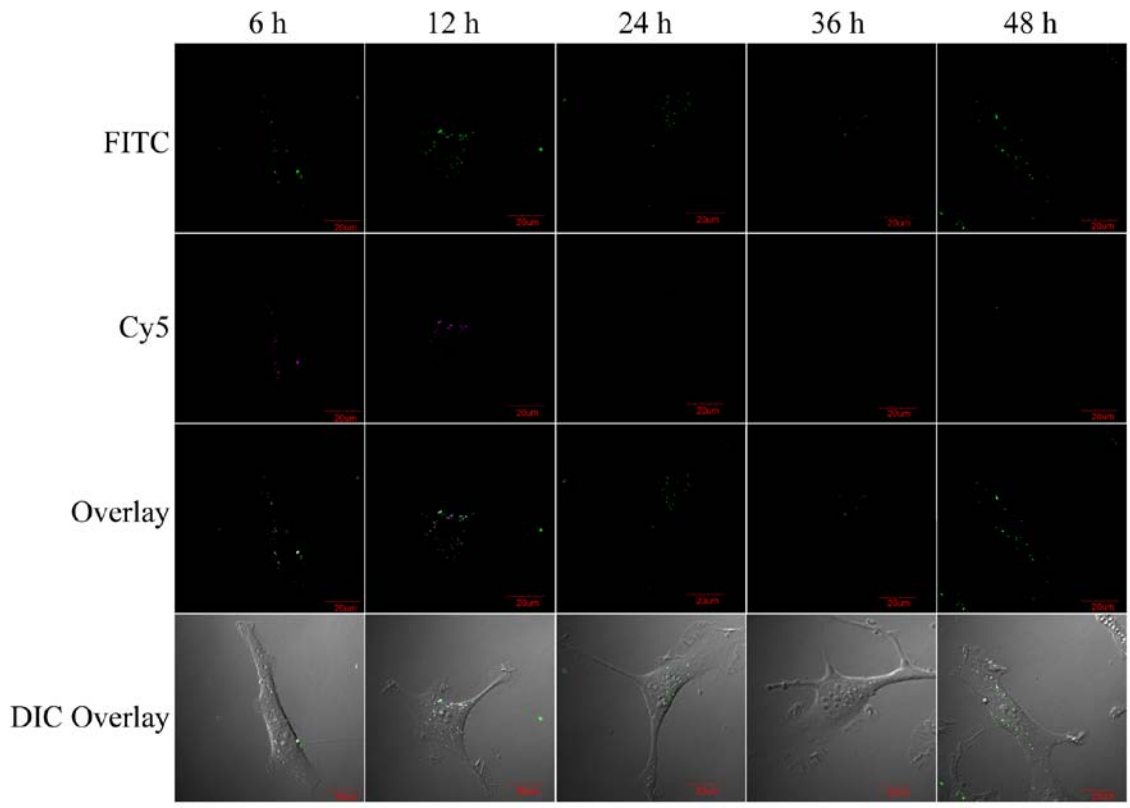

Figure 10 A-B. Confocal microscopy images obtained at various time points for cells transfected with polyplexes that were prepared with P1-FITC and Cy-siRNA at N/P ratio 10 and siRNA concentration 100 nM.

Despite the active trafficking observed immediately following the uptake as discussed above, the punctuate nature of the fluorescence remains visually unchanged up to 12 h (Figure 7). At 24 h, however, there is a sharp drop in Cy5 fluorescence, indicating that siRNA release takes place between 12 and 24 hours post transfection. At the same time FITC fluorescence that corresponds to the polymer FITC-P1 is maintained throughout the microscopy experiment (up to 48 h, Figure 10B) and remains punctuate.

Assessment of toxicity via MTT assay

MTT reagent (3-(4, 5-dimethylthiazol-2-yl)-2, 5-diphenyltetrazolium bromide) was used to estimate the cytotoxicty of the formulations. MTT can be reduced to purple formazan in living cells under the catalysis of mitochondrial reductase. Typically, U-87_luc2 glioblastoma cells were seeded at 50,000 cells/well in 24-well plates 24 h prior to transfection. The polyplexes were formed following the procedure described above. Transfection media (200 µL) was added to each well; 4 h later, complete DMEM was added at a concentration of 1 mL/well. Twenty four hours later, the media was aspirated and the cells were washed with PBS (500 µL/well). Serum-containing DMEM (1 mL) with 0.5 mg/mL of MTT was added to each well and the cells were incubated for 1 h. The media was then replaced with 600 µL of DMSO for 15 min at room temperature. A 200 µL aliquot of the media was transferred to a well of a 96-well plate for analysis by colorimeter with wavelength at 570 nm. Samples of non-transfected cells were used for the normalization.

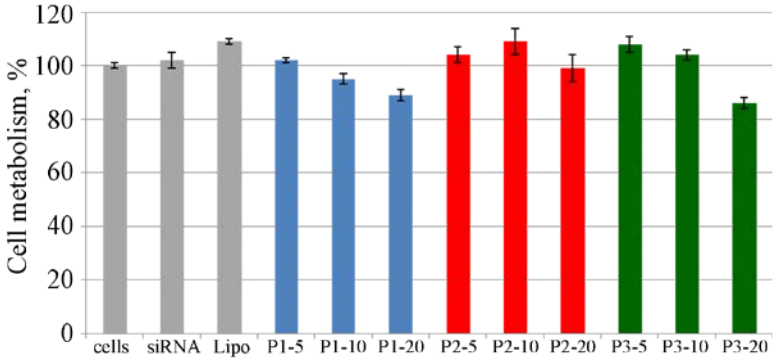

Figure 11. MTT assay in U-87 cell line with various polyplex formulations. Bars indicate cellular metabolism (mean ±s.d., n=3). siRNA concentration was 100 nM in all cases. Labels signify “polymer–N/P ratio (e.g. P1-10).

As indicated in Figure 11, all the polyplexes in the test didn't show cytotoxicity at selective N/P values through MTT assay.

Discussion and conclusion

The siRNA-based therapeutics has great potential although there are still a lot of challenges to be addressed. From the luciferase gene knockdown experiments for polyglucose copolymers, we have observed the P3 with longest chain length of AEMA achieved significant target gene knockdown whereas P1 and P2 didn't show any effect on siRNA mediated gene knockdown. Therefore the length of primary amine block on the polymer chains plays an important role in search of effective polymers for siRNA delivery. On the other hand, the polytrehalose motif presented in this study has many valuable and interesting properties that make it a candidate for inclusion within the outer layer of macromolecules and nanosystems.

Both series of polymers can be readily synthesized via RAFT polymerization. The monomers for polyglucose can be readily synthesized, but trehalose monomer preparation requires several steps to prepare and can be achieved on a multigram scale starting with trehalose. Additionally, aided by RAFT polymerization, polyglucose, polytrehalose and polyglucose/polytrehalose containing diblock polymers can be synthesized with a predefined length and low polydispersity via polymerization without use of protecting groups.

It was demonstrated that *poly*trehalose, similar to trehalose itself lowers the energy of phase transition (liquid to solid, and solid to liquid) of an aqueous solution, and this property allowed us to lyophilize siRNA polyplexes without loss of biological

function. Moreover, the polytrehalose did not exhibit cytotoxicity at all concentrations tested (up to 10 mg/ml).

Polytrehalose was shown to promote polyplex internalization by U-87 glioblastoma cells. The cellular uptake had zero order kinetics in both tested cell culture media and is directly proportional to the concentration of polytrehalose containing polyplexes in the media. Based on the results of the uptake experiments, we speculate that a carbohydrate-binding receptor may be responsible for the high efficiency of uptake. The successful use of polytrehalose in polymers for siRNA delivery was demonstrated in luciferase expressing U-87 glioblastoma cells. This activity was preserved following the lyophilization of polyplexes, potentially enabling the storage of the therapeutic siRNA formulations as dry powders and simplifying transportation. The remarkable properties demonstrated by polytrehalose make it particularly interesting stabilizing structure for study in macromolecule and nanoparticle formulations including micelles, liposomes, proteins, gold nanoparticles, and quantum dots.

REFERENCES

(1) Knop, K.; Hoogenboom, R.; Fischer, D.; Schubert, U. S. *Angewandte Chemie International Edition* **2010**, *49*, 6288.

(2) Ting, S. R. S.; Chen, G.; Stenzel, M. H. *Polymer Chemistry* **2010**, *1*, 1392.

(3) Götz, H.; Harth, E.; Schiller, S. M.; Frank, C. W.; Knoll, W.; Hawker, C. J. *Journal of Polymer Science Part A: Polymer Chemistry* **2002**, *40*, 3379.

(4) Matyjaszewski, K.; Xia, J. *Chemical Reviews* **2001**, *101*, 2921.

(5) Moad, G.; Rizzardo, E.; Thang, S. H. *Australian Journal of Chemistry* **2005**, *58*, 379.

(6) Ahmed, M.; Deng, Z.; Liu, S.; Lafrenie, R.; Kumar, A.; Narain, R. *Bioconjugate Chemistry* **2009**, *20*, 2169.

(7) Albertin, L.; Stenzel, M.; Barner-Kowollik, C.; Foster, L. J. R.; Davis, T. P. *Macromolecules* **2004**, *37*, 7530.

(8) Wu, Y.; Wang, M.; Sprouse, D.; Smith, A. E.; Reineke, T. M. *Biomacromolecules* **2014**, *15*, 1716.

(9) Roy, A.; Kim, Y.-B.; Cho, K. H.; Kim, J.-H. *Biochimica et Biophysica Acta (BBA) - General Subjects*.

(10) Paneni, F.; Costantino, S.; Cosentino, F. *Curr Atheroscler Rep* **2014**, *16*, 1.

(11) Teramoto, N.; Sachinvala, N.; Shibata, M. *Molecules* **2008**, *13*, 1773.

(12) Benaroudj, N.; Lee, D. H.; Goldberg, A. L. *J. Biol. Chem.* **2001**, *276*, 24261.

(13) Hagen, S. J.; Hofrichter, J.; Eaton, W. A. *Science* **1995**, *269*, 959.

(14) Clegg, J. S.; Seitz, P.; Seitz, W.; Hazlewood, C. F. *Cryobiology* **1982**, *19*, 306.

(15) Adams, R. P.; Kendall, E.; Kartha, K. *Biochem. Syst. Ecol.* **1990**, *18*, 107.

(16) Ramlov, H.; Westh, P. *Cryobiology* **1992**, *29*, 125.

(17) Sømme, L. *Eur. J. Entomol.* **1996**, *93*, 349.

(18) Du, J.; Liang, Y.; Xu, F.; Sun, B.; Wang, Z. *Journal of Pharmacy and Pharmacology* **2013**, *65*, 1753.

(19) Autiero, I.; Langella, E.; Saviano, M. *Molecular BioSystems* **2013**, *9*, 2835.

(20) Crowe, J. H.; Crowe, L. M.; Oliver, A. E.; Tsvetkova, N.; Wolkers, W.; Tablin, F. *Cryobiology* **2001**, *43*, 89.

(21) Srinivasachari, S.; Liu, Y.; Zhang, G.; Prevette, L.; Reineke, T. M. *J. Am. Chem. Soc.* **2006**, *128*, 8176.

(22) Xue, L.; Ingle, N. P.; Reineke, T. M. *Biomacromolecules* **2013**, *14*, 3903.

(23) Tseng, W. C.; Tang, C. H.; Fang, T. Y.; Su, L. Y. *Biotechnol. Prog.* **2007**, *23*, 1297.

(24) Sarkar, S.; Davies, J. E.; Huang, Z.; Tunnacliffe, A.; Rubinsztein, D. C. *J. Biol. Chem.* **2007**, *282*, 5641.

(25) Casarejos, M.; Solano, R.; Gómez, A.; Perucho, J.; de Yébenes, J.; Mena, M. *Neurochem. Int.* **2011**.

(26) Wada, M.; Miyazawa, Y.; Miura, Y. *Polym. Chem.* **2011**, *2*, 1822.

(27) Mancini, R. J.; Lee, J.; Maynard, H. D. *J. Am. Chem. Soc.* **2012**, *134*, 8474.

(28) Crowe, J. H.; Carpenter, J. F.; Crowe, L. M. *Annu. Rev. Physiol.* **1998**, *60*, 73.

(29) Jensen, R. L.; Chkheidze, R. *Tumors of the Central Nervous System* **2011**, *1*, 99.

(30) MacLaughlin, F. C.; Mumper, R. J.; Wang, J.; Tagliaferri, J. M.; Gill, I.; Hinchcliffe, M.; Rolland, A. P. *J Control Release* **1998**, *56*, 259.

(31) Branca, C.; Magazù, S.; Maisano, G.; Migliardo, F.; Migliardo, P.; Romeo, G. *J Phys Chem B* **2001**, *105*, 10140.

(32) Freed, K. F.; Edwards, S. *J Chem Phys* **1974**, *61*, 3626.

(33) Uhlmann, D. *J Non Cryst Solids* **1972**, *7*, 337.

(34) Buckwalter, D. J.; Sizovs, A.; Ingle, N. P.; Reineke, T. M. *ACS Macro Lett* **2012**, *1*, 609.

(35) Manel, N.; Kim, F. J.; Kinet, S.; Taylor, N.; Sitbon, M.; Battini, J. L. *Cell* **2003**, *115*, 449.

(36) Elsas, L. J.; Longo, N. *Annu. Rev. Med.* **1992**, *43*, 377.

(37) Airley, R.; Loncaster, J.; Davidson, S.; Bromley, M.; Roberts, S.; Patterson, A.; Hunter, R.; Stratford, I.; West, C. *Clin. Cancer Res.* **2001**, *7*, 928.

(38) Airley, R. E.; Loncaster, J.; Raleigh, J. A.; Harris, A. L.; Davidson, S. E.; Hunter, R. D.; West, C. M. L.; Stratford, I. J. *Int. J. Cancer* **2003**, *104*, 85.

(39) Jensen, R. L. *J. Neurooncol.* **2009**, *92*, 317.

Chapter 4.

Trehalose Containing Lanthanide Click Polycations for siRNA Delivery and Tracking

This chapter is based on the manuscript:

1. Lanthanide-Containing Polycations for Monitoring Polyplex Dynamics via Lanthanide Resonance Energy Transfer. Sneha S. Kelkar, Lian Xue, S. Richard Turner, and Theresa M. Reineke *Biomacromolecules* 2014 15 (5), 1612-1624

2. Trehalose containing lanthanide click polycations for siRNA delivery and tracking into glioblastoma cells. Lian Xue, Nilesh Ingle and Theresa M. Reineke. *Manuscript in preparation for ACS publication.*

Background

Lanthanide containing polymers have driven increasing attention in search of effect MRI contrast agents and sensors for biomedical applications. Trehalose, known for its preservation and stabilization effects, has been found to be prevalent in natural living beings and used broadly in pharmaceutical industries. Previously, we had demonstrated the effectiveness of incorporating trehalose into polymers to promote siRNA delivery profile. Here, we have developed the alternating polymers that combine the structures of trehalose, lanthanide-chelating domains and oligoamines. By chelating with europium, gadolinium and terbium ions, the polymers offered the corresponding properties for luminescence and MRI contrast capabilities. The presence of trehalose in the polymers has greatly increased the effectiveness of siRNA mediated gene knockdown in glioblastoma cells. The polymer chelates were calculated to show that there is approximately one water coordination site per chelate according the Horrock's equation upon measuring luminescent lifetimes of Terbium containing polymers. Compared with commercially available MRI contrast agent Magnevist®, gadolinium-chelating polymers are found to achieve more than twice longitudinal relaxivities (r1 per Gd) in two different magnetic fields. Dynamic light scattering study shows that sizes of polyplexes formed with siRNA are all below 100 nm and zeta potentials are above 25 mV, which are significantly different from those polymers without trehalose domains. From flowcytometry and luciferase gene knockdown experiments, the trehalose containing polymers achieved efficiency in siRNA delivery than those polymers without trehalose domains. Fluorescence resonance energy transfer (FRET) studies were applied to monitor polyplexes association and dissociation. The donor-acceptor pairs in the two systems are europium-chelating polymers with cyanine dyes (Cy5)-labeled siRNA and terbium-

chelating polymers with tetramethyl rhodamine (TMR)-labeled siRNA. All the polyplexes formed with siRNA have shown no cytotoxicity. This preliminary research has provided the evidence for effectiveness of trehalose containing lanthanide polymers as both siRNA delivery and monitoring materials. The trehalose domain has been demonstrated to play an important role in effective siRNA delivery.

Introduction

Nucleic acid based therapeutics has been emerging in the last two decades as a new approach in addition to traditional small molecular drugs[1,2]. The small interference RNA (siRNA) has been studied and optimized to be suitable for RNA interference (RNAi) both in laboratory and clinical trials[3-5]. The major challenge for developing siRNA delivery is the negatively charged nature of siRNA that prevents it from cellular uptake[6,7] and immunogenicity[8] _ENREF_6. In addition, siRNA is more vulnerable to enzymatic degradation compared with pDNA[7,9]. A variety of vehicles have been developed to help encapsulate siRNA into nanoparticles for cellular uptake[10-13]. The nanoparticles then will be released into cytoplasma from endosomes/lysosomes to reach the RISC (RNA intermediated silencing complex), which is the machinery responsible for siRNA processing and binding to corresponding mRNA to initiate the degradation[2,7,14]. The non-virus delivery vectors, they can be categorized into two types, the lipid based and polymer based. There are two pioneer polymer based materials: poly(ethylene) imines (PEI) and chitosan. Inspired by the two pioneers in nucleic acid delivery, PEI and chitosan, we had developed the trehalose click cationic polymers by combining the disaccharide trehalose with oligoamines via copper(I) catalyzed click reaction to balance the pros and cons of the two materials. Trehalose as a non-reducing disaccharide is stable

to acidic hydrolysis and protects the cells from dehydration and oxidative stress. The preliminary research has shown that the trehalose click polycations could successfully form nanoparticles with siRNA and effectively deliver them into glioblastoma cells with no toxicity found. Several researches also showed that the trehalose could have an anti-aggregation effect for pathological proteins and prevent nanoparticles from aggregation in serum media[15,16]. During the freezing cycles and dehydration, the trehalose can help preserve the biological structures of the creatures as well as biological products in these extreme conditions[17-20]. It is also reported that in the presence of trehalose, the delivery efficiency of PEI for pDNA can be improved through a variety of cell lines[21]. By coating the poly(trehalose) block to polycationic block, the diblock copolymers can be applied to deliver siRNA into glioblastoma cells in a dose dependent manner[22]. The poly(trehalose) block also showed lyoprotective and cryoprotective properties.

The interdisciplinary research in fields of nanomaterials and biomedical sciences has led to the increasing demands for smart materials that can combine therapeutic and imaging into one functional entity[23]. Visualizing the pathological tissues and guiding the drug delivery is challenged by many biological barriers. To reduce the multiple dosage of drug administration for diagnosis and real-time drug delivery monitoring, the theranostic materials are required. There are a variety of imaging agents involved to monitor delivery process, including fluorescent markers[24-27], MRI contrast components[28,29] and radio-labeled domains[30]. FRET(Förster resonance energy transfer)[31,32], which indicates non-radioactive energy transfer between two chromophores in a distance dependent manner, has been applied in a variety of biomaterials to monitor gene delivery profiles by functionalizing the delivery system with organic dyes [33,34] . Two chromospheres with an

emission and excitation spectra closely overlap and spatial proximity of 1-10 nm can act as "FRET" pairs[31]. The complexation and dissociation of the drugs and vehicles will trigger the FRET signal diminishment and restoration, and in this way, the researchers can monitor the drug delivery profile[35]. Also, FRET was found to be a sensitive method to measure the transition of monomer-dimer transition in biological studies[36]. A variety of studies have shown that FRET with organic dyes have issues, such as photobleaching, short fluorescence lifetime, and emission spectral overlaps[37], therefore, ideal FRET pairs that can prevent these problems are desired. To overcome these limitations, inorganic quantum dots[38] or luminescent lanthanide have been explored.

In this study, we have developed a series of trehalose based lanthanide-containing polycations for siRNA delivery and detection. In the previous study, polymers that are synthesized by polymerization of tetraethyleneamines or pentaethyleneamines and gadolinium or europium chelates had been reported to successfully deliver the pDNA to HeLa cells and reveal the property of MRI contrast capability[39]. The microscopy of the luminescent europium ion chelated polymers had shown the localization of the polyplexes in cytoplasma after successful cellular uptake, while the tranfection efficiency of pDNA as expression profiles were found to be low[39]. Therefore, we propose that the biodegradability and charge density of polymer backbones can be major factors that hinder the dissociation of the polyplexes, escaping from endosome and entering into the nucleus. In order to deliver siRNA, biodegradable and biocompatible polymers that can release the siRNA into the target sites are needed. Therefore, we sought to extend the polymer with trehalose motif in an alternating manner with lanthanide chelates and pentaethyleneamines. The trehalose domains are proposed to be a component in

increasing the biodegradability of the polymer and promoting the stability in the biological conditions; the lanthanide domain provides the imaging property and oligoamines domains provide the electrostatic interaction with negative charged siRNA. Further, we developed the lanthanide based FRET method to monitor the polyplexes packing and unpacking process in vitro using two FRET pairs: the Tb^{3+} chelated polymer (donor) with tetramethyl rhodamine(TMR) labeled siRNA (acceptor) and the Eu^{3+} chelated polymer (donor) with cyanine dye (Cy5) labeled siRNA (acceptors). Several research groups have also developed the FRET system to monitor siRNA, such as Anderson's group, who built the nanocomplexes that can aggregate the fluorophores locally to facilitate the FRET monitoring [40]. Kissel's group has developed triblock copolymers with quantum dots mediated FRET to monitor nucleic acid unpacking[41]. The lanthanide-organic dye FRET pairs have been reported to be used for examining protein conformational changes in biochemistry studies, while the use of lanthanide based FRET to study the polymer siRNA complexation and dissociation is reported for the first time. *In vitro* cell transfection studies have shown that all three trehalose containing lanthanide polymers can deliver siRNA into glioblastoma cells and achieve target gene knockdown. A significant enhancement of transfection efficiency was observed by inserting trehalose motif in the polymers. No apparent cytotoxicity was found throughout all the experiments with these type of polymers. The preliminary results of the experiments suggest that these structures could be applied for both siRNA delivery and imaging in the future development.

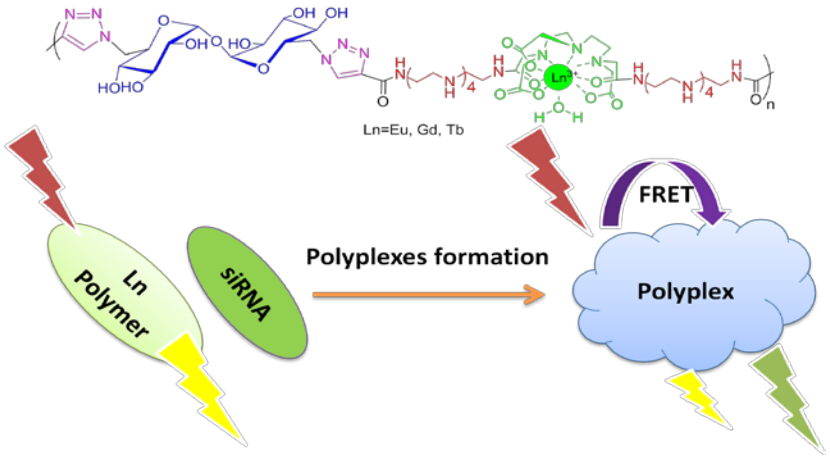

Figure 1. Structures of trehalose containing lanthanide click polycations and illustration of FRET for polymer and siRNA.

Experiments and results

Materials

U-87 MG-luc2 (U-87_luc2) cells, human glioblastoma cells genetically engineered to constitutively express luciferase, were obtained from Caliper LifeSciences, Inc. (Mountain View, CA). Luc2 siRNA, which targets luc2 luciferase, and a Cy5-labeled Luc2 siRNA were obtained from Integrated DNA Technologies, Inc. (Coralville, IA). The sequence of the sense strand of the Luc2 siRNA is 5'-GGACGAGGACGAGCACUUCUU-3', and the antisense strand sequence is 3'-UUCCUGCUCCUGCUCGUGAAG-5'. The Cy5 fluorophore within the Cy5-labeled Luc2 siRNA was conjugated to the 3' terminus of the sense strand (5'-GGACGAGGACGAGCACUUCUU-Cy5-3'). The TMR fluorophore within the TMR-labeled Luc siRNA was conjugated covalently to the 3' terminus of the sense strand (5'-GGACGAGGACGAGCACUUCUU-TMR-3'). (Scrambled siRNA (siCon) was

purchased from Dharmacon, Inc (Lafayette, CO). DMEM+GlutaMAXTM-I (DMEM), Opti-MEM I+GlutaMAXTM-I (Opti-MEM), UltraPureTM Agarose-1000, MTT (3-(4,5-dimethylthiazol-2-yl)-2,5-diphenyl tetrazolium bromide), propidium iodide (1.0 mg/mL solution in water), PBS pH=7.4, trypsin, antibiotic-antimycotic and Lipofectamine™2000 (Lipo) were obtained from Invitrogen, Inc. (Carlsbad, CA). DEPC-treated water for the RNA work was obtained from Fisher Scientific (Pittsburgh, PA). INTERFERin™ was a gift from Polyplus-Transfection (Strasbourg, France). The jetPEI™ was purchased from Polyplus-Transfection (above). The Luciferase Assay System was obtained from Promega Corporation (San Luis Obispo, CA). Bio-Rad DC Protein Assay Reagent A, Reagent B, and Reagent S were obtained from Bio-Rad Laboratories, Inc. (Hercules, CA). CellScrub™ Buffer was obtained from Genlantin, Inc. (San Diego, CA). Bovine albumin and all chemicals used in polymer synthesis were purchased from Sigma-Aldrich (St. Louis, MO) at the highest possible purity. Spectra/Por® dialysis membranes (MWCO: 1000) were obtained from Spectrum Laboratories, Inc. (Rancho Dominguez, CA). Glycofect Transfection ReagentTM, having a degree of polymerization of approximately 11 was donated by Techulon, Inc. (Blacksburg, VA).

Dry methylene chloride, dimethyl formamide and methanol were obtained using an MBRAUN MB solvent purification system manufactured by M. Braun Inertgas-Systeme GmbH (Garching, Germany), using HPLC grade solvents obtained from Fisher Scientific Co (Pittsburgh, PA). Thin layer chromatographies (TLC) were done using aluminum-backed silicagel plates (silicagel 60, F_{254}) obtained from Merck (Darmstadt, Germany) and visualized using UV light (254 nm) or staining agents: ninhydrin solution in ethanol for the visualization of amines, *p*-anisaldehyde solution in H_2SO_4/acetic

acid/ethanol for the visualization of carbohydrates. Preparative chromatographies were performed using a Buchi Separcore chromatography system, (Buchi Labortechnik AG, Switzerland) using Buchi plastic chromatography cartridges or homemade glass columns manually packed with 60-200 mesh Premium Rf silicagel (Sorbent Technologies Inc., Atlanta, GA). All solvents used for preparative chromatography were HPLC grade obtained from Fisher Scientific Co (Pittsburgh, PA). LC-MS data was obtained with an Agilent system, Agilent Technologies (Santa Clara, CA) with a time-of-flight (TOF) analyzer coupled to a Thermo Electron TSQ-LC/MS ESI mass spectrometer. NMR spectra were recorded using 400MR Varian-400 Hz spectrometer in deuterated solvents, namely D_2O, d_4-MeOD, d_6-DMSO, $CDCl_3$, CD_2Cl_2. All deuterated solvents were purchased from Cambridge Isotope Laboratories, Inc. (Andover, MA). ^{1}H-NMR spectra were recorded at 399.7 MHz and ^{13}C-NMR spectra were recorded at 101 MHz. Spectra were analyzed using MNova software (version 7.0.1-8414, Mestrelab Research S.L. (Santiago de Compostela, Spain)).

SEC was conducted using 1.0 wt% acetic acid/0.1 M Na_2SO_4 as the eluent at a flow rate 0.3 mL/min on size exclusion chromatography columns [CATSEC1000 (7μ, 50×4.6), CATSEC100 (5μ, 250×4.6), CATSEC300 (5μ, 250×4.6), and CATSEC1000 (7μ, 250×4.6)] obtained from Eprogen Inc. (Downers Grove, IL). Signals were acquired using Wyatt HELEOS II light scattering detector (λ = 662 nm), and an Optilab rEX refractometer (λ = 658 nm). SEC trace analysis was performed using Astra V software (version 5.3.4.18), Wyatt Technologies (Santa Barbara, CA). Biological sample fluorescence was measured with GENios Pro luminometer (TECAN US, Research Triangle Park, NC). Quartz Crystal Microbalance (QCM) experiments were performed on

Q-Sense E4 QCM (Q-sense; Vastra Frolunda, Sweden) instrument. Differential scanning calorimetery (DSC) was conducted on a TA Instruments Q100 under nitrogen.

Synthesis of the monomers and polymers

Synthesis of 2,3,4,2',3',4'-hexa-O-acetyl-6,6'-diazido-6,6'-dideoxyl-D-trehalose

Scheme 1. Synthesis of the hexa-O-acetyl-diazido -D-trehalose

The compound was synthesized according to a previously-published procedure. The final product was purified on a silica gel column using 10% (v:v) diethyl ether in DCM. Fractions containing the product were collected, the solvent was evaporated, and the products were further recrystallized from 10% (v:v) ethyl acetate in diethyl ether to yield fine white crystals. The total % yield from starting materials to final product was 33%.

^{1}H-NMR (400 MHz, $CDCl_3$) δ ppm: 5.49 – 5.40 (overlapping triplets, 2H, 3,3'), 5.39 – 5.29 (d, 2H,1,1'), 5.19 – 5.07 (dd, 2H, 2, 2'), 5.01 – 4.96 (t, 2H, 4,4'), 4.06-4.12(m,2H, 5,5'), 3.39-3.34, 3.19-3.15(dd, 4H, 6, 6'), 2.12-2.03 (m, 18H, $COCH_3$), ^{13}C-NMR (101 MHz, $CDCl_3$) δ ppm: 171.3, 104.5, 71.4, 70.3, 67.7, 49.3, 22.0. ESI-MS positive ion mode: found m/z $[M+Na]^+$ 667.18, $[M+NH_4]^+$662.21, $[M+H]^+$ 645.19.

a) b)

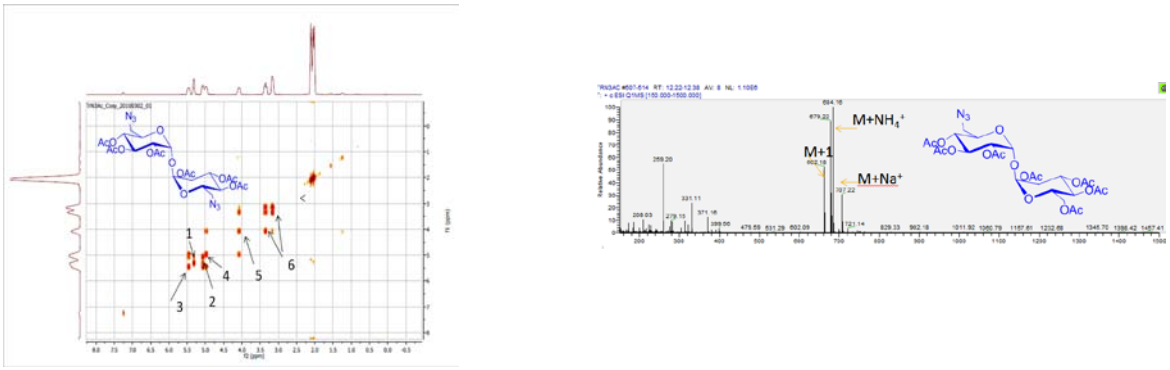

Figure 2. Structural determination of 2,3,4,2',3',4'-hexa-O-acetyl-6,6'-diazido-6,6'-dideoxyl-D-trehalose. a). ^{1}H-^{1}H COSY to assign the proton peaks on trehalose backbones. b). ESI-MS to confirm the mass of the compound.

Synthesis of trehalose Pentaethyleneamine click macromonomer

Scheme 2: Synthesis the Trehalose Pentaethyleneamine click macromonomer.

The pentaethylene amines were purified via reflux prior to the reaction. The primary amines of each side of pentaethylene amines were protected via reacting with ethyl trifluoroacetate, then di-*tert*-butyl dicarbonate were added dropwise under

room temperature to yield the fully protected pentaethylene amines. The deprotection of primary amines from fully protected pentaethylene amines were performed by refluxing with potassium carbonate in methanol. One of the primary amines is further protected with carboxybenzyl group at reaction ratio of 1:1.2, then the other primary amine reacted with propiolic acid via DCC (dicyclohexylcarbodiimide) coupling to yield 1-alkyne-6-carboxybenzyl-2,3,4,5-tetra(tert-butyloxycarbonyl)-pentaethylenetetraamine(compound g). The compound g then reacted with compound c (2,3,4,2',3',4'-hexa-O-acetyl-6,6'-diazido-6,6'-dideoxyl-D-trehalose) via copper(I) mediated azide– alkyne cycloaddition to yield dicarboxybenzyl pentaethylenetetraamine click trehalose macromonomers h. The products then underwent hydrogenation with Pd on carbon to remove the carboxybenzyl group from each side to yield the macromonomer I with primary amines on both sides.

1). 2,3,4,5-tetra (tert-butyloxycarbonyl)-pentaethylenetetraamine

The starting material (d) was purified via reflux in oxygen free condition. The purified d (yellowish oil like liquid) 62.23g (268.23mmol) was dissolved in 400 ml anhydrous MeOH processed via solvent purification system. The CF3COOEt 84.0g (591.4 mmol) was dissolved in 300 ml anhydrous MeOH. The so formed solution was added into reaction dropwise under N_2 for 24 hrs. The $(Boc)_2O$ 244.5g (1120 mmol) was dissolved in MeOH and added into the solution. The nitrogen was removed and the solution was stirred for another 4 hrs. Extra $(Boc)_2O$ of 10g was added into the solution and stirred for another 2 hrs. The solid was removed from the reaction and the solution was concentrated for flash column. The unreacted $(Boc)_2O$ was washed off as an oil like liquid. The solution was further concentrated, and the impurity was washed off by EtOAc to yield white solid. The whole mixture was dispensed in hexane and the solid was

collected, followed by using EA: hexane 1:1 to recrystalize the compound to yield white powder N6CF3Boc 55.34 g. 27.06 g of the N6CF3Boc was dissolved in 1000 ml round bottom flask and dissolved in MeOH, 20 ml water and 28.97 g K_2CO_3 was added into the solution. The mixture was refluxed at 80^{o}C for 12 hrs. The white solid was filtered off, then the solution was concentrated and the solvent was evaporated. The solid was dispensed in chloroform then the solid was filtered off. The solution was dried via addition of Na_2SO_4 then filtered and concentrated. The product was further recrystalized in EtOAc:hexane=3:1. The white solid was collected, dried and characterized. Yield of two steps is calculated to be 37%.

^{1}H-NMR (400 MHz, $CDCl_3$) δ ppm: 3.32-3.23 (overlapping d, 20H, -NBocCH_2-), 2.83-2.79 (dd, 4H, NH_2CH_2-), 1.61-1.45(s, 36H, -NCOO$(CH_3)_3$).

2). 1-carboxylbenzyl-2,3,4,5-tetra(tert-butyloxycarbonyl) pentaethyleneamines

The 2,3,4,5-tetra (*tert*-butyloxycarbonyl) pentaethyleneamines (compound e, N6Boc) 2.47g (3.92 mmol) and carboxylbenzyl chloride (CbzCl) 0.65 g(3.81 mmol) are dissolved in two flasks respectively with DCM. Then the CbzCl solution was added dropwisely into the N6Boc solution at -25^{o}C (the ice bath was prepared with NaCl mixed with ice) for 4 hrs. Then the solvent was evaporated, and the products was separated via silica gel chromatography with gradual polarity of mobile solution from Hexane:EA=3:1 to EA to EA:EtOH=5:1. Then the products were collected and concentrated, followed by recrystalization in Hexane: EA=1:1 to yield 1.59 g product f.

^{1}H-NMR (400 MHz, $CDCl_3$) δ ppm: 7.26-7.23 (m, 5H, -C6H5), 5.12-5.09 (s, 2H, -$COOCH_2$Ph), 3.38-3.22 (br, 20H, -CH2CH2-), 1.53-1.23 (br, 36H, -OC$(CH_3)_3$).

3).1-alkyne-6-carboxybenzyl-2,3,4,5-tetra(tert-butyloxycarbonyl) pentaethylenetetraamine

The product f (N6BocCbz) (50.2mg) was dissolved in DCM. The DCC (N,N'-Dicyclohexylcarbodiimide) (50mg) and propiolic acid (15 mg) were mixed in the DCM. Then the solution of N6BocCbz was added dropwise into the mixture of DCC and propiolic acid at 0oC. The ice bath was removed once the addition was over followed by an overnight reaction. The mixture was washed with water 3 times and organic layers were collected and dried with Na2SO4. Then the solvent was removed via evaporation, and the product was separated via chromatography using the gradient mobile phase of MeOH: DCM=0-0.2. Then 42.3 mg (% yield of 79.4%) of white powder was obtained and examined.

^{1}H-NMR (400 MHz, CDCl3) δ ppm: 7.32-7.24 (br, 5H, -C6H5), 5.07 (s, 2H, -COOCH2-), 3.41-3.30 (br, 20H, -CH2CH2-), 2.73 (s, 1H, -CCH), 1.46-1.43(br, 36H, -OC(CH3)3). ESI-MS: calculated mass: 819.0, found [M+H]+ : 819.49.

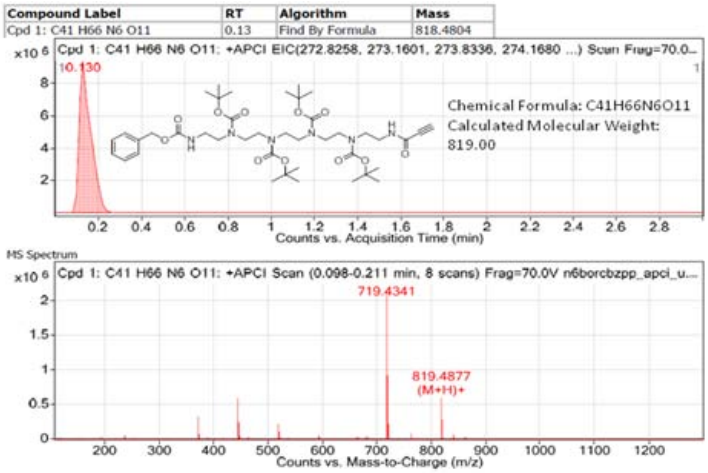

Figure 3. ESI-MS characterization of compound 1-alkyne-6-carboxybenzyl-2,3,4,5-tetra (tert-butyloxycarbonyl) pentaethylenetetraamine.

4). di-pentaethylenetetraamine click trehalose macromonomers (N4-Tr-N4)

The 1-alkyne-6-carboxybenzyl-2,3,4,5-tetra (tert-butyloxycarbonyl) pentaethylenetetraamine (compound g) (212.7 mg), 2,3,4,2',3',4'-hexa-O-acetyl-6,6'-diazido-6,6'-dideoxyl-D-trehalose (80 mg), sodium ascorbate (9.84 mg) were put into flask and 1ml ^{t}BuOH was added. $CuSO_4$ (18.9 mg) was dissolved in 1ml H_2O and added into the reaction. The mixture was stirred for 24hrs at 50^{o}C. The mixture was then dispensed in 1ml DMSO, followed by dispersed into 10 ml H_2O. The white solid was collected and dried to yield the product h 261.8 mg (% yield of 90.2%).

^{1}H-NMR (400 MHz, CDCl3) δ ppm: 8.02-8.01(s, 2H, triazole H), 7.20-7.19(m, 10H, -C_6H_5), 5.34(t, 2H, -1,1' trehalose H), 5.10-4.92 (s, 4H, -CH_2-Ph), 4.83-4.41 (m, 8H, -2,2',3,3',4,4',5,5'-trehalose H), 3.42-3.21(s, 40H, -CH_2CH_2-), 2.32-2.08(br, 18H, -$COCH_3$), 1.39-1.30(s, 72H, -$OC(CH_3)_3$).

ESI-MS: calculated mass: 2281.15, found $[M+Na]^+$: 2305.14.

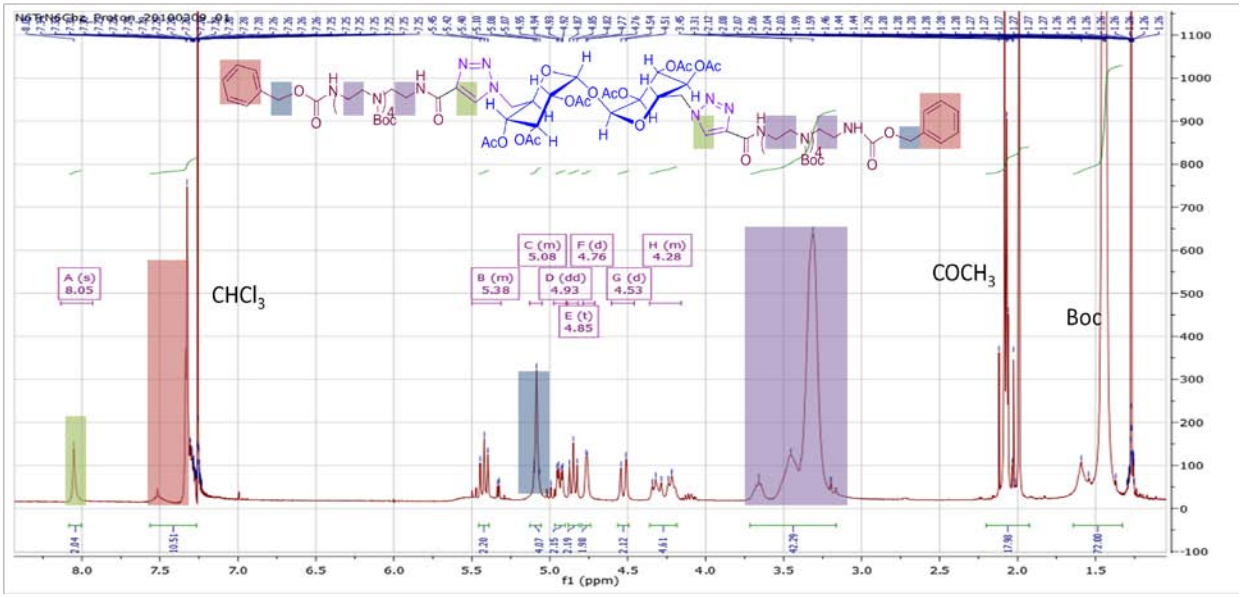

Figure 4. ^{1}HNMR characterization of di-carboxylbenzyl-di-pentaethylenetetraamine click trehalose macromonomers (h).

Then the di-carboxylbenzyl-di-pentaethylenetetraamine click trehalose macromonomers (0.208 g) and Pd/C 20 20mg were added into dry CH_2Cl_2. The hydrogen was kept bubbling using a balloon for 24 hrs at room temperature. Then the Pd/C was filtered out. The filtrate was concentrated and washed using flashing chromatography to remove the impurity to yield pale powder 0.15 g (% yield of 79.4%).

^{1}H-NMR (400 MHz, CDCl3) δ ppm: 8.02-8.00(s, 2H, triazole H, 5.38(t, 2H, -1,1' trehalose H), 4.78-4.46 (m, 8H, -2,2',3,3',4,4',5,5'-trehalose H), 3.42-3.24(s, 40H, -CH_2CH_2-), 2.34-2.03(br, 18H, -$COCH_3$), 1.38-1.32(s, 72H, -$OC(CH_3)_3$).

ESI-MS: calculated mass: 2013.07, found $[M+H]^+$: 2014.15.

Synthesis of DTPA-BA (diethylenetriaminepentaacetic acid bisanhydride) monomer

Scheme 3. Synthetic scheme of diethylenetriaminepentaacetic acid bisanhydride.

The diethylene triamine pentaacetic acid (5.50 g) was added into dry flask. The pyridine and acetic anhydride were added and stirred at 65^{o}C for 24 hrs. Then the solid was filtered out and washed with acetic anhydride and diethyl ether. The product was dried on a vacuum pump to yield white powder 4.35 g (% yield of 87.1%).

^{1}H-NMR (400 MHz, CDCl3) δ ppm: 3.68 (s, 8H, -NCH_2COOCO-), 3.28 (s, 2H,-NCH_2COOH), 2.74-2.71 (t, 4H, -CH_2N-), 2.59-2.56 (t, 4H,-NCH_2COOH).

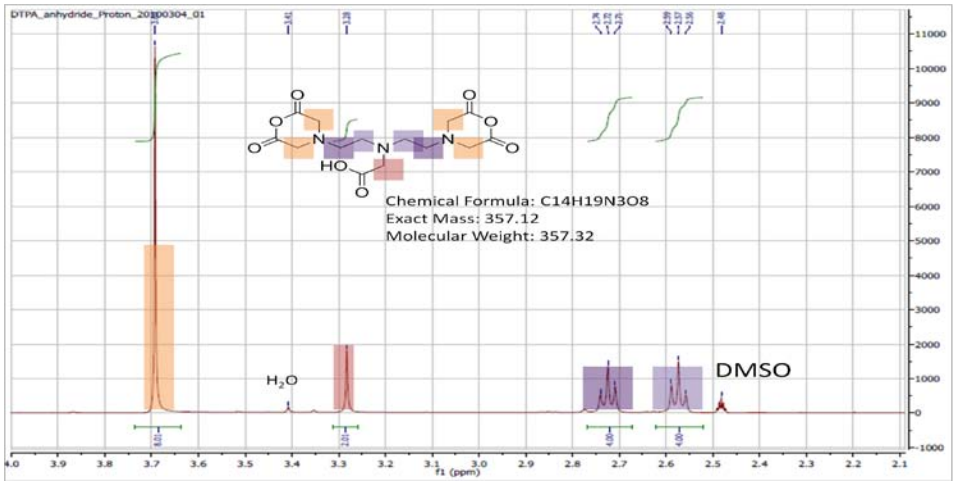

Figure 5. ^{1}HNMR characterization of DTPA-BA (diethylenetriaminepentaacetic acid bis anhydride).

Polymerization, polymer deprotection, and lanthanide chelation of the polymers

Scheme 4. Synthetic scheme of trehalose based lanthanide containing polymers.

The di-pentaethylenetetraamine click trehalose macromonomers (compound i) 201.3 mg and diethylenetriaminepentaacetic acid bisanhydride (compound k) 35.8 mg was dissolved in 1 ml dry DMSO respectively. Then the k solution was added dropwise into i solution using a syringe. The mixture was stirred for 18 hrs and put into dialysis against MeOH for 48hrs and dried on vacuum pump to yield pale powder TrN6DTPABocAc (compound l). Then TrN6DTPABocAc was added into MeOH. The pH was adjusted to 9 using NaOMe. The solution was dialysised against MeOH for 24 hrs and concentrated. Then the product was added into 5 ml DCM, and 5 ml acetic acid was added dropwise for 3 hrs. The solvent was evaporated and the product was dissolved in water for dialysis against ultra pure water for 48 hrs. Then the product was collected and dried to yield white solid. The products were characterized via NMR and SEC.

1H-NMR (400 MHz, DMSO) δ ppm: 8.31 (s, 2H, triazole H), 4.65-4.61(dd, 2H, 1,1'-trehalose), 4.53-4.50(s, 4H, 6,6'-trehalose), 4.15-4.0, 3.62-3.46(m, 8H, trehalose H),

3.39-3.31(s, 4H, triazole $CONHCH_2$), 3.25-3.09 (s, 10H, DTPA-NCH_2COOH), 3.07-2.65 (s, 40H, -NCH_2CH_2N-).

a).

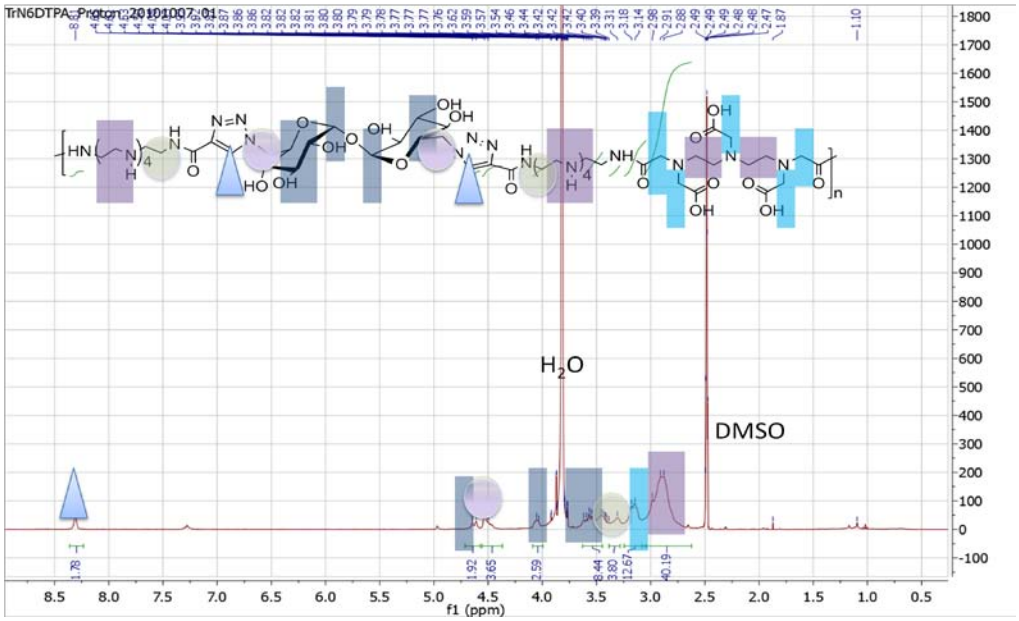

b).

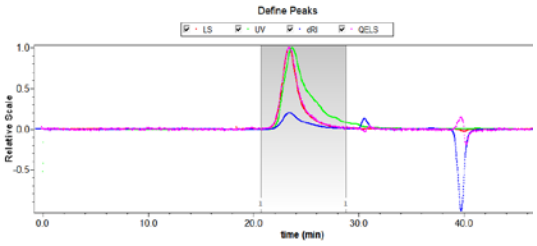

M_w=1.296×10^4 , M_n=1.233×10^4 , Đ=1.082, n_w= 10, n_{eq}=20, dn/dc=0.1350.

Figure 6. a). ^{1}HNMR spectra of trehalose pentaethylene polymers with lanthanide chelation domain. b). The SEC analysis of the polymer.

After deprotection, the polymers were chelated with europium, gadolinium and terbium ions at pH=5 to yield polymer TrN4Eu, TrN4Gd and TrN4Tb. The products were

dialyzed against ultra pure water for 48 hrs, and then dried on vacuum pump to yield white fluffy powder.

The synthetic scheme is guided by the criteria that allow the trehalose motif, lanthanide chelating domain and pentaethylene amines on the same polymer chain in an alternating manner. The crucial part of the synthesis is the trehalose pentaethyleneamine macromonomer. The synthesis started from difunctionalizing the primary hydroxyl on trehalose molecule and protected the rest of the hydroxyls with acetyl group to yield hexa-O-acetyl-diazido -D-trehalose. For the pentaethyleneamine part, after protecting the secondary amine with Boc (tert-Butyloxycarbonyl) and deprotecting the primary amine on each side, one of the primary amine was further protected by the Cbz (carboxylbenzyl) group, while the other primary amine was functionalized with propiolic acid via DCC (dicyclohexylcarbodiimide)coupling to yield mono functionalized pentaethyleneamine. The trehalose pentaethyleneamine click macromonomer was then synthesized via copper (I) catalyzed alkyne azide reaction with hexa-O-acetyl-diazido -D-trehalose followed by the deprotection of the Cbz groups. Then the macromonomer was copolymerized with DTPA-BA to yield the alternating polymers. After deprotection and chelating with lanthanide ions, the polymers were purified via exhaustive dialysis against ultrapure water for 48hrs, lyophilized, and analyzed on GPC, NMR, etc. The SEC analysis showed that the weight averaged number of repeating units is 10, for pentaethyleneamine block, it is equally 20 (n_{eq}=20), as one macromonomer has two pentaethylene blocks.

Investigation on properties of polymers

Determination of the number of water coordinate sites

The number of water coordination sites (q) per chelate was determined by measuring the luminescence lifetimes of the Tb^{3+} labeled polymer TrN4Tb in D_2O and H_2O (Table 1) using a Cary Eclipse fluorescence spectrometer (Agilent Technologies, USA; formerly Varian). The data was processed with Agilent Cary WinFLR software. The samples were prepared at 1 mM concentration (800µL) using D_2O and H_2O and deposited into a small-volume quartz cuvette. Lifetime measurements were performed with the excitation wavelength of 350 nm (slit 5nm), emission wavelength of 550 nm (slit 5 nm, a delay time of 0.1 ms, a gate time of 0.1 ms, and data were at number of cycles of 50. All the measurements were performed in triplicate.

Compound	Solution	Ave. lifetime (τ)
TrN4Tb	H_2O	1.265
TrN4Tb	D_2O	1.616
Calculated No. of Coordinate Sites		1.24

Table 1. Determination of number of water coordination sites (q) for polymer TrN4Tb via lifetime measurement in Uv-vis.

The revised Horrocks equation was applied to calculate the number of water coordination sites (q) per chelate unit. The number of coordinate sites was found to be 1.24, which is close to 1 for the polymers. The revised Horrocks equation is listed as follows:

$$q_{Tb} = 5\left[\left(\frac{1}{\tau_{H2O}} - \frac{1}{\tau_{D2O}}\right) - 0.06x\right]$$

x = number of N-H oscillators from amide groups coordinated to the Tb3+though the carbonyl.

Inductively coupled plasma optical emission spectroscopy

Inductively coupled plasma optical emission spectroscopy (ICP-OES) was performed (to determine lanthanide content of the polymers) at University of Illinois at Urbana-Champaign using PerkinElmer 2000DV ICP-OES system.

Element	*Theroretical*	*Found*	*Diff*
Eu	11.49%	7.86%	-3.63%
Gd	11.95%	8.65%	-3.30%
Tb	12.02%	8.32%	-3.70%

Table 2. ICP-OES analysis of the lanthanide content of polymers TrN4Eu, TrN4Gd and TrN4Tb respectively.

Three polymers chelated with different lanthanide ions were characterized via inductively coupled plasma optical emission spectroscopy (ICP-OES) for the content. The difference between theoretical values and found values is ranged from 3.30%-3.70% based on mass percentile. The value of percentile difference can attribute to the arrangement of the monomers in the polymer backbone as difference in ending group can lead to significant difference in content of chelating ions. These values provide useful structure information and are important for relaxivity calculation and comparisons with commercially available MRI contrast agent, which in this study is Magnevist.

Polymer siRNA binding assay

The polyplexes were prepared by adding 33 µL of polymer solution in RNase-free water to 33 µL of 2 µM siRNA solution in RNase-free water at room temperature at various N/P ratios.

Agarose gels [2% (w/v)] were prepared by dissolving 1 g agarose in 50 mL TAE buffer (40 mM Tris-acetate, 1 mM EDTA) while heating. Immediately before the gel solution was poured in the gel electrophoresis chamber and cooled to ambient temperature, 4 µL of ethidium bromide (10 mg/mL) was added. The polyplexes were formed by adding 10 µL of each polymer solution at various concentrations to 10 µL of 2 µM siRNA solution in RNase-free (DEPC-treated) water. The N/P ratio indicates the polymer/nucleic acid ratio for polyplex formulation (the number of secondary amines on polymer backbones to the number of phosphate groups on the nucleic acid backbones to form the polyplex solutions) as previously described. The polyplexes were incubated at room temperature for 30 min. 2 µL of Blue Juice™ loading buffer (Invitrogen) was added to each polyplex solution shortly before loading onto the gel. Electrophoresis was performed at 65 V for 45 min. The complexation of siRNA by the polymer was indicated by the lack of gel migration (or shift) of the siRNA-containing bands.

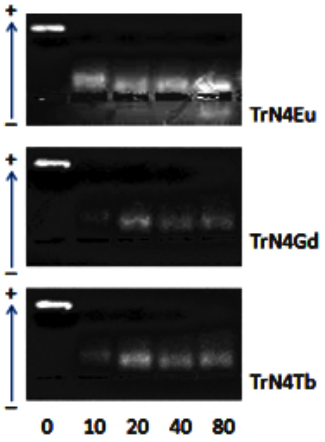

Figure 7. Gel electrophoresis analysis of TrN4Ln(Ln=Eu, Gd, Tb). The binding efficiency, which is reflected by the binding ratio, can be determined by the absence of siRNA band towards the positive electrode. The formulation ratios were varied from 0-80, which indicates the siRNA only.

After the purification and final deprotection of the polymers, TrN4Eu, TrN4Gd and TrN4Tb were examined on the gel electrophoresis to estimate the capability of the polymers to bind to siRNA. It was noticed that compared with trehalose polymers without chelating units, the binding between the polymers and siRNA is much stronger than the binding affinities between trehalose lanthanide containing polycations. The diminishment of the binding affinity can attribute to the negative properties of carboxylic groups on DTPA domain. All three polymers TrN4Eu, TrN4Gd and TrN4Tb can fully retard the siRNA migration at around N/P=20. Therefore, we chose N/P=40 to form polyplexes for the rest of the experiments.

Relaxivity of Gd chelated polymers

The effect on T_1 relaxation times of water in the presence of TrN4Gd polymers (chelated with Gd^{3+}) and their polyplexes was studied with a Bruker Minispec (20 mq,

0.47 T and 60 mq, 1.41 T series) using an inversion recovery pulse sequence (180^0- d_t- 90^0- acquire). Solutions of TrN4Gd polymers (5 different concentrations from 2.5 mg/ml to 0.5 mg/ml) and Magnevist® (a clinical contrast reagent) were prepared in ultrapure water (based on repeat unit molecular weight and on a per 'Gd^{3+}' basis analyzed on ICP-OES). All the measurements were performed in triplicate, and error bars represent the standard deviation of the three measurements.

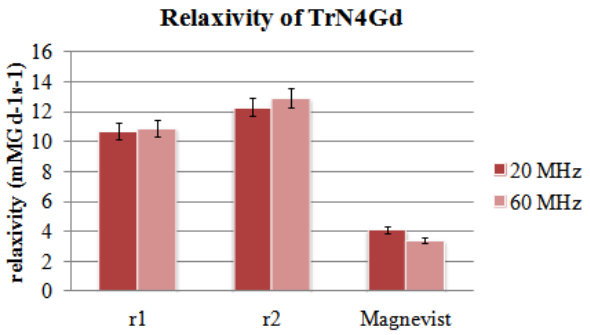

Figure 8. Relaxivity measurement of TrN4Gd according to water relaxation rate constants at 0.47 and 1.4 Tesla at 37 °C. Five polymer concentrations ranged from 2.5 mg/ml to 0.05 mg/ were used for the calculation. Each test was examined in triplicate.

The relaxivity has been adjusted according to Gd content percentile observed in ICP-OES. The r1 at both 0.47T and 1.4T is between 10.7-10.9 $mMGd^{-1}s^{-1}$, and the r2 is between 12.3-12.9 $mMGd^{-1}s^{-1}$. Compared with commercially available MRI contrast agent Magnevist, the polymer TrN4Gd achieved more than two times of relaxivity.

Dynamic light scattering study

Hydrodynamic diameters of the polymer-siRNA polyplex formulations were determined by dynamic light scattering (DLS) using a ZetaSizer (Nano ZS) instrument from Malvern, Inc. (Worcestershire, United Kingdom) equipped with a 633-nm laser. For each size measurement, polyplexes were formulated by addition of 33 µL of polymer solution in RNase-free water to 33 µL of 2 µM siRNA solution in RNase-free water at room temperature forming complexes at various N/P ratios. The formation of polyplexes was monitored by performing DLS measurements 60 min after solution mixing. Each polyplex solution was then diluted to a final volume of 750 µL with RNase-free water for zeta potential measurements of each sample in triplicate.

A) B)

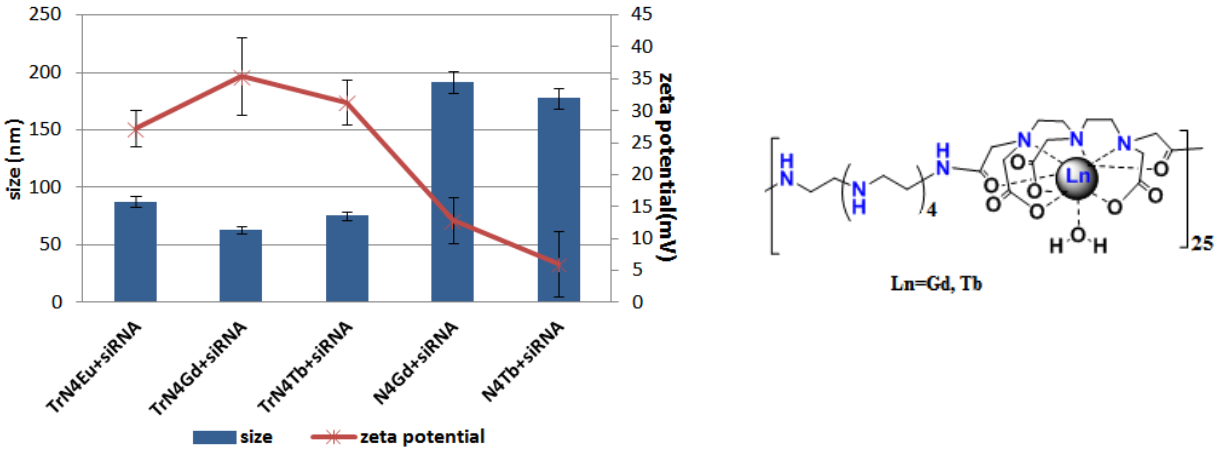

Figure 9. A). Dynamic light scattering study of polyplexes formed by lanthanide containing polymers with siRNA at N/P=40. The sizes of the polyplexes were shown as the bars, and the zeta potentials were expressed as star shaped dots connected with a red line. N4Gd and N4Tb were two polymers with mass averaged repeating unit of 25. All

the experiments were performed in water solution in triplicate. B). Structures of N4Gd and N4Tb.

In order to compare the polymers containing trehalose domains, two polymers without trehalose units was applied as reference: N4Gd and N4Tb. Since one repeating unit of trehalose containing polymer has two pentaethyleneamine domains, therefore the numbers of amine blocks of N4Gd and N4Tb are comparable with TrN4Eu, TrN4Gd and TrN4Tb. In the dynamic light scattering study, we can see that the trehalose containing lanthanide polymers TrN4Eu, TrN4Gd, TrN4Tb can form much smaller polyplexes than those formed with N4Gd and N4Tb. In contrast, the zeta potentials of polyplexes formed with TrN4Eu, TrN4Gd and TrN4Tb are with higher zeta potential compared with those formed with N4Gd and N4Tb respectively, which is a favorable optimization for siRNA delivery.

Stability of polyplexes upon addition of heparin

a) b)

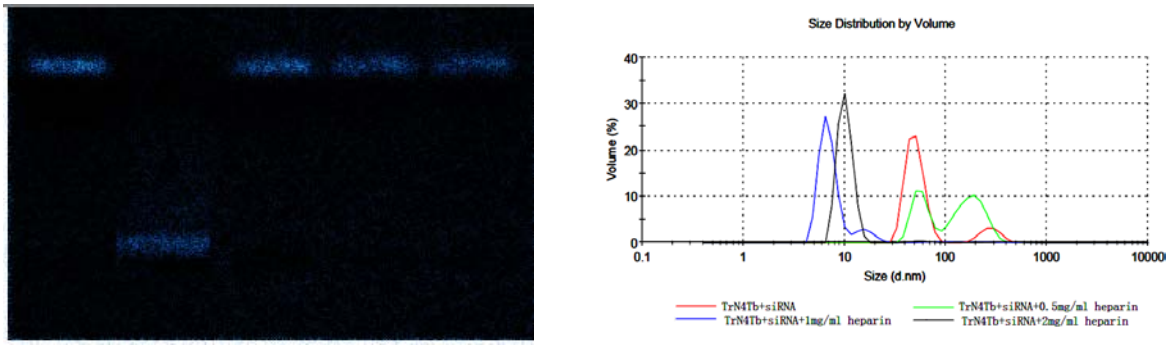

1 2 3 4 5

Figure 10. Stability of polyplexes upon addition of heparin. a) Gel electrophoresis of polyplexes formed by TrN4Tb and siRNA at N/P=40 in addition of different heparin concentrations. 1. siRNA only 2.TrN4Tb+siRNA 3. TrN4Tb+siRNA+0.5 mg/ml heparin

4.TrN4Tb+siRNA+1 mg/ml heparin 5. TrN4Tb+siRNA+2 mg/ml heparin. b) DLS study of size distribution of polyplexes upon addition of heparin in different concentrations.

The polyplexes were all prepared at N/P=40 followed by 30 min incubation, then concentrated heparin was added to yield different final concentration of heparin. The addition of heparin at different concentrations has been monitored via both gel electrophoresis and DLS. In the gel electrophoresis, we can observe that the polyplexes dissociate upon addition of heparin at a concentration of as low as 0.5 mg/ml. The dissociation at different concentrations was also monitored by DLS shown as in Figure 10B. In the figure, we can see that at the concentration of 0.5 mg/ml heparin, the polyplexes started to swell, then when the concentration increased to 1 mg/ml, the polyplexes collapsed and the size dropped significantly. Therefore, we chose 1 mg/ml heparin as the standard concentration for the following experiment to induce the dissociation of polyplexes.

FRET(Fluorescence resonance energy transfer) of polymer/siRNA complexation

Synergy™ H1 monochromator-based multi-mode microplate reader was applied in this study. 96 well plate (GENios Pro) was used for the measurement. The samples are prepared by adding 40 µl lanthanide chelated polymer solution into 40 µl 2 µM fluorescence labeled siRNA and incubated for 60 min. The addition of heparin (to yield 1 mg/ml final concentration) 20 µl was performed after the polyplexes formation and incubated for 15 min. The same amount of RNase free water 20 µl was added to other polyplexes in order to achieve same concentration of polyplexes. For the FRET pair of TrN4Eu/Cy5-siRNA, the sample was excited at 365 nm. For FRET pair TrN4Tb/TMR-

siRNA, the sample was excited at 345 nm. All spectrums were collected from 400 nm to 700 nm. The delay time is varied in order to monitor the dynamic of FRET.

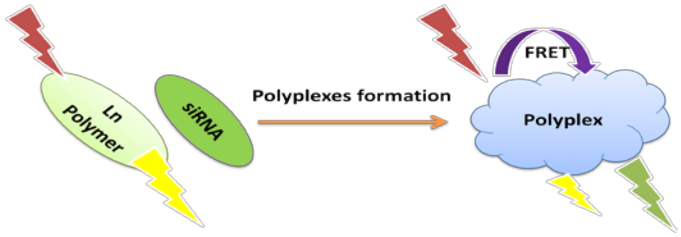

Figure 11. Illustration of monitoring polyplex formation via FRET.

FRET, a mechanism illustrating the energy transfer between two chromophores, has been successfully applied to aid the biomedical research. The donor chromophores, which in this study are europium and terbium ions, will transfer energy to adjacent acceptor chromophores via nonradiative interaction. The acceptors in this study are Cy5 and TMR that are labeled at the end of the siRNA chain. As shown in the illustration shown in Figure 11, before the polyplex formation, the donor and acceptor are far away, therefore, there is no increase in acceptor emission. Once the polyplexes formed, the donor and acceptor are close enough for the energy transfer through dipole-dipole interaction; therefore, we will observe the diminishment of excitation of donor accordingly.

a).

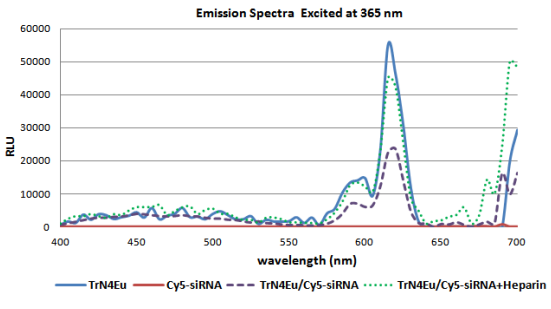

b).

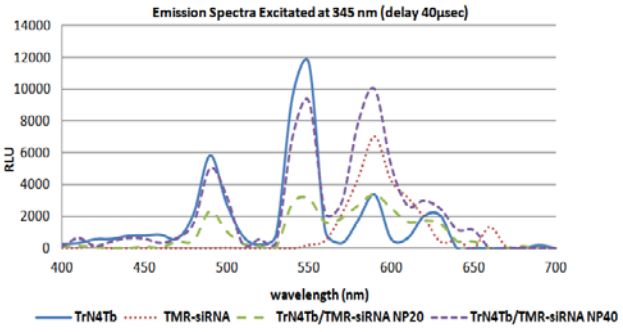

c). d).

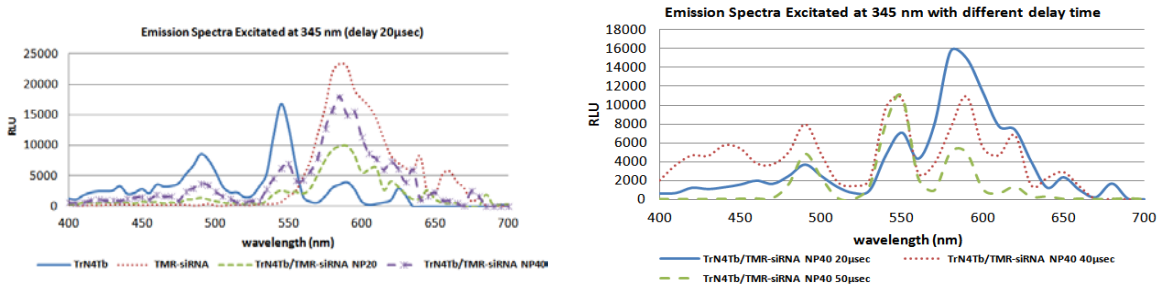

Figure 12. FRET study on the TrN4Eu/Cy5-siRNA and TrN4Tb/TMR-siRNA complexation and heparin mediated dissociation. a). Emission spectrum of TrN4Eu/Cy5-siRNA excited at 365 nm (TrN4Eu only: blue; Cy5-siRNA: red; TrN4Eu/Cy5-siRNA polyplexes: purple dash). b). Emission spectrum of TrN4Tb/TMR-siRNA at N/P=20 and 40 excited at 345 nm collected at delay time of 40µsec (TrN4Tb only: blue; TMR-siRNA: red dash; TrN4Tb/TMR-siRNA N/P=20: green dash; TrN4Tb/TMR-siRNA N/P=40: purple dash). c). Emission spectrum of TrN4Tb/TMR-siRNA at N/P=20 and 40 collected at delay time of 20 µsec (TrN4Tb only: blue; TMR-siRNA: red dash; TrN4Tb/TMR-siRNA N/P=20: green dash; TrN4Tb/TMR-siRNA N/P=40: purple star dash). d). Emission spectrum of TrN4Tb/TMR-siRNA excited at 345 nm and collected at different delay time.

The polyplexes complexation and dissociation were monitored via collecting the emission spectrum of solution formed in different conditions. Heparin, as mentioned in the study of stability of polyplexes, was used to induce the dissociation of polyplexes to illustrate the correlation of dissociation and restoration of emission from absence of FRET. The concentration used in the study is 1 mg/ml. In Figure 12. a) , we observe that after the TrN4Eu complexed with Cy5 labeled siRNA, the emission of Eu at 615 nm diminished dramatically due to FRET, then upon the addition of heparin, the emission of

Eu at peak of 615 nm was restored as indicated in the green dash line. In Figure 12 b), we formed the polyplexes in two different N/P ratios This time, the TMR-siRNA can also be excited and has an emission peak at 595 nm. The peak at 495 and 550 nm can attribute to the emission after exciting TrN4Tb at the N/P=20 as indicated in the green dash line, we can observe the peak at 495 and 550 nm decreased accordingly due to FRET, the peak at 595 nm also decreased, which could largely attribute to steric hindrance and bleach effect caused by complexation with polymer. In contrast, when the N/P ratio increased to 40, the emission at 495 and 550 nm is found restored, while the emission at 595 increased dramatically. We think at higher N/P ratio, the polyplexes composition may become more compact and have more free polymer chains in the solution, therefore the FRET is more prominent at emission peak of TMR-siRNA 595 nm than that of the lower N/P ratio. But the emission at 495 and 550 nm is restored, because of the more free polymer chains in the solution. We then tried to collect the data at a shorter delay time of 20 µsec (Figure 12 c)), and we saw that the peak at 595 nm for TMR-siRNA was higher than the polyplexes formed at N/P40. The phenomenon was just opposite from the experiment performed at a delay time of 40 µsec. In order to understand the correlation of delay time and FRET, we chose three different delay times 20 µsec, 40 µsec and 50 µsec. As indicated in Figure 12 d), FRET is more prominent at the earlier delay time, as we can observe the dramatic decrease in peak 550 nm and increase in peak 595 nm. The FRET effect was decreased dramatically as the delay time increased. Therefore, the choice of delay time is crucial for observation, because of the decay of the intensity as the collecting time point increased.

Cellular uptake of polyplexes and target gene knockdown in brain cancer cells

Cellular uptake for polyplexes via flowcytometry

Flow cytometry was performed to examine the cellular uptake of Cy5-labeled siRNA with various formulations at 3 h post-transfection. In general, U-87_luc2 glioblastoma cells were seeded at 300,000/well in 6-well plates 24 h prior to transfection. To transfect, 33 µL of each polymer solution was added to 33 µL of 2 µM Cy5-labeled siRNA solution. After a 30 min incubation at room temperature (to form the polyplexes), each polyplex solution was pipetted into 1584 µL of pre-warmed Opti-MEM to yield the final transfection solution. Each well was treated with 500 µL of the obtained transfection solution. After 3 h, the media was removed and cells were washed with 500 µL/well CellScrub™ Buffer for 15 min at room temperature. The CellScrub™ Buffer was then aspirated, and cells were exposed to trypsin (0.05% (w/v), 500 µL/well) for 3 min to provide detachment from the plate, then complete DMEM (500 µL/well) was applied to inhibit trypsin. The cell suspension was collected and centrifuged at 1000 rpm for 10 min at 4^{o}C. The supernatant was removed and cells were twice washed with 0.5 mL PBS and centrifuged to remove the extracellular polyplexes. Finally, 1 mL PBS was added and the suspensions were kept on ice prior to flow cytometry analysis. Propidium iodide (2.5 µL) was added prior to the analysis. The flowcytometer (FACSCalibur and FACSVerse, Becton Dickenson, San Jose, CA) equipped with a helium-neon laser to excite Cy5 at 633 nm was used to count twenty thousand events for each sample. The threshold fluorescence level was defined by manually adjusting the positive region such that <1% of negative control cells were positive for fluorescence. Each treatment was performed in triplicate.

Luciferase assay for siRNA mediated gene knockdown

Luciferase-expressing glioblastoma cells (U-87_luc2) were seeded at 50,000 cells/well in 24-well plates 24 h prior to transfection. In general, anti-luciferase (Luc2) siRNA, control (siCon) siRNA, and polymer stock solutions were diluted with RNase-free water, and the polyplexes were formed by the addition of 33 µL of polymer solution to 33 µL of siRNA solution, followed by incubation for 30 min at room temperature. The resulting polyplex solutions were then added to pre-warmed Opti-MEM or DMEM to yield transfection solutions. Cells were washed with PBS before the addition of 200 µL of the transfection solution. The formation of siRNA-containing lipoplexes using Lipofectamine™ 2000 were performed according to the manufacturer's protocol. Polyplexes with the carbohydrate polymers were formulated at various N/P ratios as we previously described.[42,43] The cells were incubated with polyplex/lipoplex solutions for 4 h before complete DMEM was added. Forty eight hours later, the cells were washed with 500 µL PBS and treated with 1x cell lysis buffer (Promega, Madison, WI) for 15 min at room temperature. Aliquots (5 µL) of cell lysate were examined on 96-well plates with a luminometer (GENios Pro, TECAN US, Research Triangle Park, NC) for luciferase activity over 10 s. For each well, 100 µL of luciferase assay substrate (Promega, Madison, WI) was added. The average of duplicate measurements on each individual replicate was utilized for calculation. The amount of protein (mg) in cell lysates was calculated using a standard curve generated with bovine serum albumin by following the protocol included in Bio-Rad DC protein assay kit. The relative light unit (RLU)/mg protein was then calculated and averaged across replicate wells. The protein and luciferase levels of non-

transfected cells were used for normalizing the data and calculating the extent of gene knockdown. Each treatment was tested in triplicate in 24-well plates.

A).

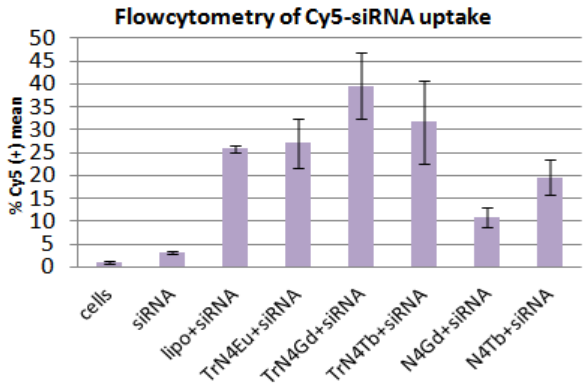

B).

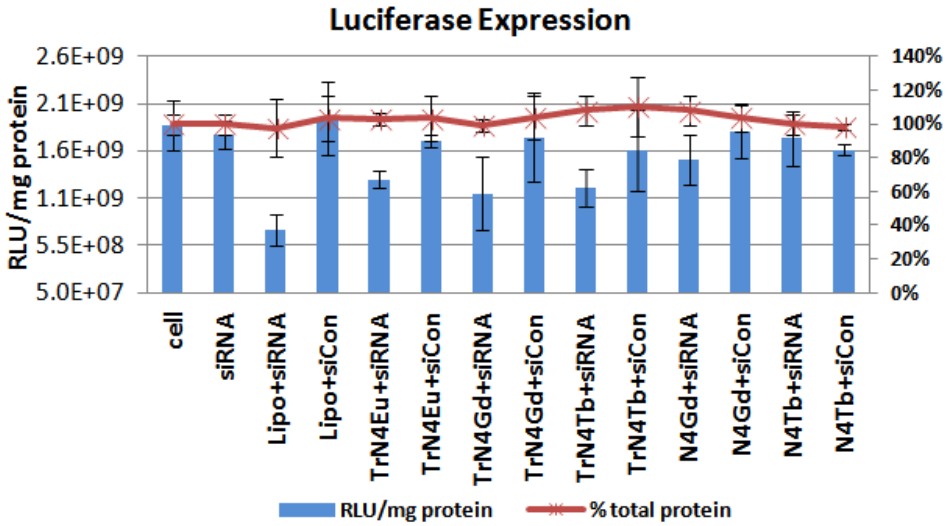

Figure 13. Cellular uptake and target gene knockdown studies of polyplexes formed from lanthanide polymers with siRNA. a). Flowcytometry study of polyplexes uptake 4 hrs after transfection using Cy5 labeled siRNA. b). Luciferase gene knockdown experiments to estimate the delivery efficiency of lanthanide containing polymers on

anti-luciferase siRNA into luciferase expressing U87 cells. The N/P ratio in both of the studies is chose to be 40 for all the polyplexes and lipofectamine was applied as positive control.N4Gd and N4Tb was used in the study for comparison. All the tests are in triplicate.

In order to estimate the efficiency of the polymers on siRNA delivery, flowcytometry and luciferase assay were conducted to monitor the cellular uptake and target gene knockdown in U87 glioblastoma cells. In Figure 13(a), the percentage of Cy5 positive cells were measured to show that trehalose containing lanthanide polycations can successfully deliver Cy5-siRNA into glioblastoma cells and achieved higher cellular uptake than those facilitated by N4Gd and N4Tb. In Figure 13(b), the luciferase gene knockdown experiments have shown that TrN4Eu, TrN4Gd and TrN4Tb all achieved moderate target gene knockdown in glioblastoma cells. The % extent of gene knockdown achieved by TrN4Eu, TrN4Gd and TrN4Tb are 31%, 40% and 37% respectively. On the other hand, the polyplexes formed with N4Gd and N4Tb didn't show significant gene knockdown. Therefore, the trehalose domains in the polymers play an important role in improvement of polymer performance. A similar phenomenon was observed in the study of structure and property relationships in carbohydrate containing polymers for siRNA delivery in systematic study in Chapter 2. The insertion of trehalose polymers can contribute to the biodegradability of the polymers in order to release the siRNA into cytoplasm. The detailed mechanism needs to be investigated in future studies.

Cytotoxicity study via MTT assay

MTT reagent (3-(4, 5-dimethylthiazol-2-yl)-2, 5-diphenyltetrazolium bromide) was used to estimate the cytotoxicity of the formulations. Typically, U-87_luc2

glioblastoma cells were seeded at 50,000 cells/well in 24-well plates 24 h prior to transfection. The polyplexes were formed following the procedure described above. 200 µL of transfection media was added to each well; 4 h later, complete DMEM was added at 1 mL/well. Then, 24 h later, the media was aspirated and the cells were washed with PBS (500 µL/well). 1 mL of serum-containing DMEM with 0.5 mg/mL of MTT (3-(4,5-Dimethylthiazol-2-yl)-2,5 Diphenyltetrazolium Bromide) was added to each well and cells were incubated for 1 h. The media was then replaced with 600 µL of DMSO for 15 min at room temperature. A 200 µL aliquot of the media was transferred to a well of a 96-well plate for analysis by colorimeter with wavelength at 570 nm. Samples of non-transfected cells were used for normalization.

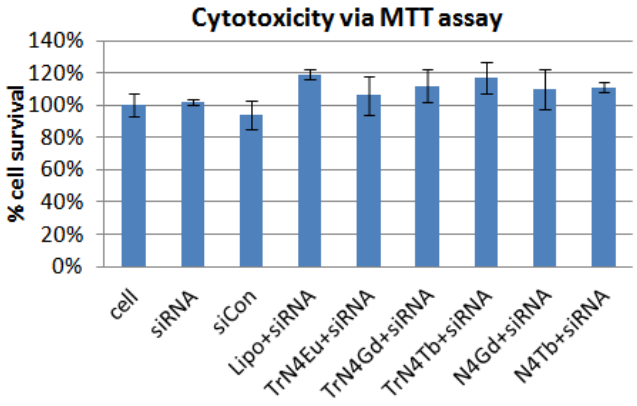

Figure 14. Cytotoxicity examined via MTT assay at 24 hrs incubation after transfection. All the polyplexes were formed at N/P=40. The transfection concentration of siRNA is 100 nM. All the tests are in triplicate.

Throughout all the tests, no cytotoxicity in U87 cells at N/P ratio of 40 was found. From the preliminary *in vitro* biosafety study of the polymer/siRNA complexes, the polymers are shown to be promising for future investigation to understand polyplexes dynamics.

Conclusion

In order to improve the performance of lanthanide containing cationic polymers for nucleic acid delivery, we have successfully synthesized a series of polymers with trehalose domain alternately distributed in the polymers with pentaethyleneamine and lanthanide chelating domains. The structure and molecular weight profiles have been verified via NMR and SEC respectively. Various properties of the polymers were examined upon the complexation with siRNA, including binding efficiency, dynamic light scattering studies, stability upon addition of heparin and FRET studies based on two pairs: TrN4Eu/Cy5-siRNA and TrN4Tb/TMR-siRNA. The relaxivity of the polymers TrN4Gd was examined and shown to be much larger than commercially available reagent Magnevist in two different magnetic fields. The number of water coordinate sites based polymer TrN4Tb were also examined via measuring the luminescence lifetime in H_2O and D_2O. The calculated number of water coordinate sites is 1.24, which is approximately 1 water coordinate site for each chelate. The FRET was monitored via using two different pairs TrN4Eu/Cy5-siRNA and TrN4Tb/TMR-siRNA. By adding the heparin into the polyplexes, we have observed the diminishment of FRET caused by dissociation of the polyplexes. The FRET has been demonstrated to be a strong time dependent event as we changed the delay times for spectra collection. The FRET decreased significantly while the delay time increased from 20 μsec to 50 μsec. The flowcytometry and luciferase gene knockdown experiments were conducted on luciferase expression cell line U87. The result showed that by incorporating the trehalose domains into the polymers, the performance on siRNA delivery is improved, which indicates the role of trehalose in improving the performance of the polymers. All the tests show no

cytotoxicity found. The polymer structure is also a good model to demonstrate the significant impact of carbohydrate on polymer performance for biomedical applications.

REFERENCES

(1) Yu, B.; Zhao, X.; Lee, L. J.; Lee, R. J. *AAPS J* **2009**, *11*, 195.

(2) Hammond, S. M.; Caudy, A. A.; Hannon, G. J. *Nat Rev Genet* **2001**, *2*, 110.

(3) Dorsett, Y.; Tuschl, T. *Nat Rev Drug Discov* **2004**, *3*, 318.

(4) de Fougerolles, A.; Vornlocher, H. P.; Maraganore, J.; Lieberman, J. *Nature Reviews Drug Discovery* **2007**, *6*, 443.

(5) Tang, X.; Maegawa, S.; Weinberg, E. S.; Dmochowski, I. J. *Journal of the American Chemical Society* **2007**, *129*, 11000.

(6) Soutschek, J.; Akinc, A.; Bramlage, B.; Charisse, K.; Constien, R.; Donoghue, M.; Elbashir, S.; Geick, A.; Hadwiger, P.; Harborth, J.; John, M.; Kesavan, V.; Lavine, G.; Pandey, R. K.; Racie, T.; Rajeev, K. G.; Rohl, I.; Toudjarska, I.; Wang, G.; Wuschko, S.; Bumcrot, D.; Koteliansky, V.; Limmer, S.; Manoharan, M.; Vornlocher, H.-P. *Nature* **2004**, *432*, 173.

(7) Whitehead, K. A.; Langer, R.; Anderson, D. G. *Nature Reviews Drug Discovery* **2009**, *8*, 516.

(8) Robbins, M.; Judge, A.; Maclachlan, I. *Oligonucleotides* **2009**, *19*, 89.

(9) Reischl, D.; Zimmer, A. *Nanomedicine* **2009**, *5*, 8.

(10) Tseng, Y. C.; Mozumdar, S.; Huang, L. *Adv Drug Deliv Rev* **2009**.

(11) Naldini, L.; Blomer, U.; Gallay, P.; Ory, D.; Mulligan, R.; Gage, F. H.; Verma, I. M.; Trono, D. *Science* **1996**, *272*, 263.

(12) Zimmermann, T. S.; Lee, A. C.; Akinc, A.; Bramlage, B.; Bumcrot, D.; Fedoruk, M. N.; Harborth, J.; Heyes, J. A.; Jeffs, L. B.; John, M.; Judge, A. D.; Lam, K.; McClintock, K.; Nechev, L. V.; Palmer, L. R.; Racie, T.; Rohl, I.; Seiffert, S.; Shanmugam, S.; Sood, V.; Soutschek, J.; Toudjarska, I.; Wheat, A. J.; Yaworski, E.; Zedalis, W.; Koteliansky, V.; Manoharan, M.; Vornlocher, H. P.; MacLachlan, I. *Nature* **2006**, *441*, 111.

(13) Oishi, M.; Nagasaki, Y.; Itaka, K.; Nishiyama, N.; Kataoka, K. *Journal of the American Chemical Society* **2005**, *127*, 1624.

(14) Kumar, P.; Wu, H.; McBride, J. L.; Jung, K.-E.; Hee Kim, M.; Davidson, B. L.; Kyung Lee, S.; Shankar, P.; Manjunath, N. *Nature* **2007**, *448*, 39.

(15) Liu, F.-F.; Ji, L.; Dong, X.-Y.; Sun, Y. *The Journal of Physical Chemistry B* **2009**, *113*, 11320.

(16) Pérez-Moral, N.; Adnet, C. l.; Noel, T. R.; Parker, R. *Biomacromolecules* **2010**, *11*, 2985.

(17) Imamura, K.; Murai, K.; Korehisa, T.; Shimizu, N.; Yamahira, R.; Matsuura, T.; Tada, H.; Imanaka, H.; Ishida, N.; Nakanishi, K. *Journal of Pharmaceutical Sciences* **2014**, *103*, 1628.

(18) Dráber, P.; Sulimenko, V.; Sulimenko, T.; Dráberová, E. In *Protein Downstream Processing*; Labrou, N. E., Ed.; Humana Press: 2014; Vol. 1129, p 443.

(19) Tonnis, W. F.; Amorij, J. P.; Vreeman, M. A.; Frijlink, H. W.; Kersten, G. F.; Hinrichs, W. L. J. *European Journal of Pharmaceutical Sciences* **2014**, *55*, 36.

(20) Men, N. T.; Kikuchi, K.; Nakai, M.; Fukuda, A.; Tanihara, F.; Noguchi, J.; Kaneko, H.; Linh, N. V.; Nguyen, B. X.; Nagai, T.; Tajima, A. *Theriogenology* **2013**, *80*, 1033.

(21) Tseng, W.-C.; Tang, C.-H.; Fang, T.-Y.; Su, L.-Y. *Biotechnology Progress* **2007**, *23*, 1297.

(22) Sizovs, A.; Xue, L.; Tolstyka, Z. P.; Ingle, N. P.; Wu, Y.; Cortez, M.; Reineke, T. M. *Journal of the American Chemical Society* **2013**, *135*, 15417.

(23) Chen, G.; Qiu, H.; Prasad, P. N.; Chen, X. *Chemical Reviews* **2014**.

(24) Fan, Z.; Senapati, D.; Singh, A. K.; Ray, P. C. *Molecular Pharmaceutics* **2012**, *10*, 857.

(25) Bardhan, R.; Lal, S.; Joshi, A.; Halas, N. J. *Accounts of Chemical Research* **2011**, *44*, 936.

(26) Murgia, S.; Bonacchi, S.; Falchi, A. M.; Lampis, S.; Lippolis, V.; Meli, V.; Monduzzi, M.; Prodi, L.; Schmidt, J.; Talmon, Y.; Caltagirone, C. *Langmuir* **2013**, *29*, 6673.

(27) Santra, S.; Perez, J. M. *Biomacromolecules* **2011**, *12*, 3917.

(28) Guo , Y.; Chen, W.; Wang, W.; Shen, J.; Guo, R.; Gong, F.; Lin, S.; Cheng, D.; Chen, G.; Shuai, X. *ACS Nano* **2012**, *6*, 10646.

(29) Liu, Q.; Zhu, H.; Qin, J.; Dong, H.; Du, J. *Biomacromolecules* **2014**, *15*, 1586.

(30) Jokerst, J. V.; Gambhir, S. S. *Accounts of Chemical Research* **2011**, *44*, 1050.

(31) Helms, V. *Principles of Computational Cell Biology*; Wiley, 2008.

(32) Zheng, J. In *Ion Channels*; Stockand, J., Shapiro, M., Eds.; Humana Press: 2006; Vol. 337, p 65.

(33) Jiang, R.; Lu, X.; Yang, M.; Deng, W.; Fan, Q.; Huang, W. *Biomacromolecules* **2013**, *14*, 3643.

(34) Schneider, S.; Lenz, D.; Holzer, M.; Palme, K.; Süss, R. *Journal of Controlled Release* **2010**, *145*, 289.

(35) Croissant, J.; Chaix, A.; Mongin, O.; Wang, M.; Clément, S.; Raehm, L.; Durand, J.-O.; Hugues, V.; Blanchard-Desce, M.; Maynadier, M.; Gallud, A.; Gary-Bobo, M.; Garcia, M.; Lu, J.; Tamanoi, F.; Ferris, D. P.; Tarn, D.; Zink, J. I. *Small* **2014**, *10*, 1752.

(36) Gautier, I.; Tramier, M.; Durieux, C.; Coppey, J.; Pansu, R. B.; Nicolas, J. C.; Kemnitz, K.; Coppey-Moisan, M. *Biophysical Journal* **2001**, *80*, 3000.

(37) Domingo, B.; Sabariegos, R.; Picazo, F.; Llopis, J. *Microscopy Research and Technique* **2007**, *70*, 1010.

(38) Kim, H.; Ng, C. Y. W.; Algar, W. R. *Langmuir* **2014**, *30*, 5676.

(39) Bryson, J. M.; Fichter, K. M.; Chu, W.-J.; Lee, J.-H.; Li, J.; Madsen, L. A.; McLendon, P. M.; Reineke, T. M. *Proceedings of the National Academy of Sciences* **2009**.

(40) Alabi, C. A.; Love, K. T.; Sahay, G.; Stutzman, T.; Young, W. T.; Langer, R.; Anderson, D. G. *ACS Nano* **2012**, *6*, 6133.

(41) Endres, T.; Zheng, M.; Kılıç, A.; Turowska, A.; Beck-Broichsitter, M.; Renz, H.; Merkel, O. M.; Kissel, T. *Molecular Pharmaceutics* **2014**, *11*, 1273.

(42) Liu, Y.; Reineke, T. M. *Bioconjugate Chemistry* **2006**, *17*, 101.

(43) Srinivasachari, S.; Reineke, T. M. *Biomaterials* **2009**, *30*, 928.

Chapter 5. Conclusions

siRNA has driven dramatic attention in search of alternative medicine in addition to conventional therapeutics. The major challenge is that siRNA has poor pharmacokinetic profile and can cause various side effects such as immunogenicity. Therefore, designing proper materials to facilitate the delivery and transport the siRNA to the RNAi machinery is the key requirement to achieve effective therapeutic outcomes.

In this research, we are driven by the ideal to obtain biocompatible and biodegradable materials that can encapsulate the siRNA into nanoparticles with proper surface parameters, to facilitate the cellular uptake and release them in the cytoplasm where the siRNA machinery locates. To examine the roles of carbohydrate in the polymer structures, we have synthesized and evaluated different structuralized carbohydrate containing polymers, including step growth polymers and RAFT diblock copolymers. In addition, alternating polymers containing lanthanide chelates are also synthesized and examined in order to obtain potential biocompatible theranostic agents.

In the structure-property relationship study for the step growth carbohydrate oligoamines polymers, we were surprised to discover that despite the high potency of T4 and Glycofect for pDNA delivery, both of these polymers were completely ineffective at forming polyplexes with and delivering siRNA *in vitro*. The dependence of potency on polymer type and length was more dramatic for siRNA delivery. Also, a dramatic dependence on molecular weight was observed with the trehalose and cyclodextrin polymers. Both the low molecular weight versions of these systems [Tr4(23) and CD4(10)] revealed no activity for siRNA delivery. However, as the degree of polymerization was further increased, the cyclodextrin polymers CD(26) and CD(39)

were very active for siRNA delivery, more so than the Tr4 polymer series. The two highest molecular weight analogs of the CD4 series were less effective for delivery. Upon the comparison, these data reveal two very important trends: i) length of the polymer has an effect on gene expression and gene knockdown and ii) the carbohydrate type/size plays a clear role in siRNA binding, compaction, and delivery. Cyclodextrin clearly promotes higher binding affinity, likely due to H-bonding via the hydroxyl groups and the polymerized nucleotides. In addition, cyclodextrin likely plays a role in promoting endosomal release of siRNA (as Tr4 analogs had lower affinity) possibly due to the known affinity of the hydrophobic cyclodextrin cup to extracting cholesterol out of the membrane, which could promote leaky endosomes. This was also clearly noticed when free polymer was added, which also clearly plays a role in promoting endosomal release of polyplexes carrying siRNA. While, the efficacy of step growth polymers was significantly reduced in serum, possibly due to the affinity of the carbohydrate to binding serum proteins, which likely coat the polyplexes. All the observations with these polymers illustrate that, knowledge based upon pDNA delivery cannot necessarily predict the performance of polymers for siRNA delivery. These findings also highlight the potential of utilizing the Tr4 and CD4 series of polymers as therapeutic pDNA and siRNA delivery agents and demonstrate the subtle effects of carbohydrate choice on the activity of pDNA and siRNA delivery.

Apart from the step growth polymers, we have obtained series of carbohydrate containing diblock copolymers via RAFT polymerization. The carbohydrate containing blocks were synthesized by polymerizing either glucose containing monomers or trehalose containing monomers. From the study on polyglucose polymers, we have found

that the effectiveness of siRNA mediated knockdown is dependent on the length of the length of the amine containing block. The proper chain length of primary amine block on polymers chains plays an important role to reach effective target gene knockdown. On the other hand, polytrehalose polymers have shown significant gene knockdown with all three different primary amines blocks. It was demonstrated that *poly*trehalose similarly to trehalose itself lowers the energy of phase transition (liquid to solid, and solid to liquid) of an aqueous solution and this property allowed us to lyophilize siRNA polyplexes without loss of biological function. Polytrehalose was shown to promote polyplex internalization by U-87 glioblastoma cells. The cellular uptake had zero order kinetics in both tested cell culture media and is directly proportional to the concentration of polytrehalose containing polyplexes in the media. Based on the results of the uptake experiments we speculate that a carbohydrate-binding receptor may be responsible for the high efficiency of uptake. The successful use of polytrehalose in polymers for siRNA delivery was demonstrated in luciferase expressing U-87 glioblastoma cells. This activity was preserved following the lyophilization of polyplexes, potentially enabling the storage of the therapeutic siRNA formulations as dry powders and simplifying transportation.

In order to improve the performance of lanthanide containing cationic polymers for nucleic acid delivery, we have successfully synthesized a series of polymers with trehalose domain alternately distributed in the polymers with pentaethyleneamine and lanthanide chelating domains. Various properties of the polymers were examined upon the complexation with siRNA, including binding efficiency, dynamic light scattering studies, stability upon addition of heparin and FRET studies based on two pairs: TrN4Eu/Cy5-siRNA and TrN4Tb/TMR-siRNA. The relaxivity of the polymers TrN4Gd

was examined and shown to be much larger than commercially available reagent Magnevist in two different magnetic fields. The number of water coordinate sites based polymer TrN4Tb were also examined via measuring the luminescence lifetime in H_2O and D_2O. The calculated number of water coordinate sites is 1.24, which is approximately 1 water coordinate site for each chelate. The FRET was monitored via using two different pairs TrN4Eu/Cy5-siRNA and TrN4Tb/TMR-siRNA. By adding the heparin into the polyplexes, we have observed the diminishment of FRET caused by dissociation of the polyplexes. The results showed that by incorporating the trehalose domains into the polymers, the performance on siRNA delivery is improved, which indicates the role of trehalose to improve the performance of the polymers. All the tests show no cytotoxicity found. The polymer structure is also a good model to prove the significant impact of carbohydrate on polymer performance for biomedical applications.

Above all the findings in the research, we have revealed the importance of incorporating carbohydrate units in the polymers to improve the performance of the polyplexes on siRNA delivery. The trehalose as a disaccharide has shown dramatic impact on siRNA delivery in both step growth polymers and diblock copolymers as coating block. The polytrehalose coating has been examined to be an effective technique to preserve the formulation during freeze drying cycle, and can be a potential coating block for other pharmaceutical approach for drug delivery and other biomedical applications.

In summary, the carbohydrate family plays an important role in search of biocompatible materials for siRNA delivery. The trehalose has been demonstrated to be effective component for developing coating materials for anti-aggregation, protection

from fierce environmental changes and essential to achieve quantitative siRNA delivery. The results from preliminary study *in vitro* tests suggest it is promising to further investigate on these carbohydrate based biomaterials.

Reference

1. Fire, A.; Xu, S.; Montgomery, M. K.; Kostas, S. A.; Driver, S. E.; Mello, C. C. *Nature* **1998**, *391*, 806.

2. Bernstein, E.; Caudy, A. A.; Hammond, S. M.; Hannon, G. J. *Nature* **2001**, *409*, 363.

3. Schwarz, D. S.; Hutvner, G.; Du, T.; Xu, Z.; Aronin, N.; Zamore, P. D. **2003**, *115*, 199.

4. Dykxhoorn, D. M.; Novina, C. D.; Sharp, P. A. *Nat Rev Mol Cell Biol* **2003**, *4*, 457.

5. Yu, B.; Zhao, X.; Lee, L. J.; Lee, R. J. *The American Association of Pharmaceutical Scientists.***2009**, *11*, 195.

6. Alexis, F.; Pridgen, E.; Molnar, L. K.; Farokhzad, O. C. *Molecular Pharmaceutics* **2008**, *5*, 505.

7. Maeda, H. *Adv Enzyme Regul* **2001**, *41*, 189.

8. Gilmore, I. R.; Fox, S. P.; Hollins, A. J.; Akhtar, S. *Current Drug Delivery* **2006**, *3*, 147.

9. Boussif, O.; Lezoualch, F.; Zanta, M. A.; Mergny, M. D.; Scherman, D.; Demeneix, B.; Behr, J. P. *Proceedings of the National Academy of Sciences of the United States of America* **1995**, *92*, 7297.

10. Judge, A. D.; Bola, G.; Lee, A. C. H.; MacLachlan, I. *Molecular Therapy* **2006**, *13*, 494.

11. Allerson, C. R.; Sioufi, N.; Jarres, R.; Prakash, T. P.; Naik, N.; Berdeja, A.; Wanders, L.; Griffey, R. H.; Swayze, E. E.; Bhat, B. *Journal of Medicinal Chemistry* **2005**, *48*, 901.

12. Dande, P.; Prakash, T. P.; Sioufi, N.; Gaus, H.; Jarres, R.; Berdeja, A.; Swayze, E. E.; Griffey, R. H.; Bhat, B. *Journal of Medicinal Chemistry* **2006**, *49*, 1624.

13. Soutschek, J.; Akinc, A.; Bramlage, B.; Charisse, K.; Constien, R.; Donoghue, M.; Elbashir, S.; Geick, A.; Hadwiger, P.; Harborth, J.; John, M.; Kesavan, V.; Lavine, G.;

Pandey, R. K.; Racie, T.; Rajeev, K. G.; Rohl, I.; Toudjarska, I.; Wang, G.; Wuschko, S.; Bumcrot, D.; Koteliansky, V.; Limmer, S.; Manoharan, M.; Vornlocher, H. P. *Nature* **2004**, *432*, 173.

14. de Fougerolles, A.; Vornlocher, H. P.; Maraganore, J.; Lieberman, J. *Nature Reviews Drug Discovery* **2007**, *6*, 443.

15. Oishi, M.; Nagasaki, Y.; Itaka, K.; Nishiyama, N.; Kataoka, K. *Journal of the American Chemical Society* **2005**, *127*, 1624.

16. Whitehead, K. A.; Langer, R.; Anderson, D. G. *Nature Reviews Drug Discovery* **2009**, *8*, 516.

17. Nguyen, H. K.; Lemieux, P.; Vinogradov, S. V.; Gebhart, C. L.; Guerin, N.; Paradis, G.; Bronich, T. K.; Alakhov, V. Y.; Kabanov, A. V. *Gene Ther* **2000**, *7*, 126.

18. Auguste, D. T.; Furman, K.; Wong, A.; Fuller, J.; Armes, S. P.; Deming, T. J.; Langer, R. *Journal of Controlled Release* **2008**, *130*, 266.

19. Rappaport, J.; Hanss, B.; Kopp, J. B.; Copeland, T. D.; Bruggeman, L. A.; Coffman, T. M.; Klotman, P. E. *Kidney International* **1995**, *47*, 1462.

20. Barquinero, J.; Eixarch, H.; Perez-Melgosa, M. *Gene Therapy* **2004**, *11*, S3.

21. Dalby, B.; Cates, S.; Harris, A.; Ohki, E. C.; Tilkins, M. L.; Price, P. J.; Ciccarone, V. C. *Methods* **2004**, *33*, 95.

22. Malone, R. W.; Felgner, P. L.; Verma, I. M. *Proceedings of the National Academy of Sciences of the United States of America* **1989**, *86*, 6077.

23. Frank-Kamenetsky, M.; Grefhorst, A.; Anderson, N. N.; Racie, T. S.; Bramlage, B.; Akinc, A.; Butler, D.; Charisse, K.; Dorkin, R.; Fan, Y.; Gamba-Vitalo, C.; Hadwiger, P.; Jayaraman, M.; John, M.; Jayaprakash, K. N.; Maier, M.; Nechev, L.; Rajeev, K. G.;

Read, T.; Rohl, I.; Soutschek, J.; Tan, P.; Wong, J.; Wang, G.; Zimmermann, T.; de Fougerolles, A.; Vornlocher, H. P.; Langer, R.; Anderson, D. G.; Manoharan, M.; Koteliansky, V.; Horton, J. D.; Fitzgerald, K. *Proceedings of the National Academy of Sciences of the United States of America* **2008**, *105*, 11915.

24. Chonn, A.; Semple, S. C.; Cullis, P. R. *Journal of Biological Chemistry* **1995**, *270*, 25845.

25. Papahadjopoulos, D.; Allen, T. M.; Gabizon, A.; Mayhew, E.; Matthay, K.; Huang, S. K.; Lee, K. D.; Woodle, M. C.; Lasic, D. D.; Redemann, C. *Proceedings of the National Academy of Sciences of the United States of America* **1991**, *88*, 11460.

26. Oh, Y. K.; Park, T. G. *Adv Drug Deliv Rev* **2009**.

27. Franchini, J.; Ranucci, E.; Ferruti, P.; Rossi, M.; Cavalli, R. *Biomacromolecules* **2006**, *7*, 1215.

28. Urban-Klein, B.; Werth, S.; Abuharbeid, S.; Czubayko, F.; Aigner, A. *Gene Therapy* **2005**, *12*, 461.

29. Tan, P. H.; Yang, L. C.; Shih, H. C.; Lan, K. C.; Cheng, J. T. *Gene Therapy* **2005**, *12*, 59.

39. Kim, S. H.; Jeong, J. H.; Lee, S. H.; Kim, S. W.; Park, T. G. *Journal of Controlled Release* **2008**, *129*, 107.

31. Ahn, C.-H.; Chae, S. Y.; Bae, Y. H.; Kim, S. W. *Journal of Controlled Release* **2002**, *80*, 273.

32. Petersen, H.; Martin, A. L.; Stolnik, S.; Roberts, C. J.; Davies, M. C.; Kissel, T. *Macromolecules* **2002**, *35*, 9854.

33. Malek, A.; Czubayk, F.; Aigner, A. *Journal of Drug Targeting* **2008**, *16*, 124.

34. Peng, Q.; Hu, C.; Cheng, J.; Zhong, Z.; Zhuo, R. *Bioconjugate Chemistry* **2009**, *20*, 340.

35. Kiang, T.; Wen, J.; Lim, H. W.; Leong, K. W. K. W. *Biomaterials* **2004**, *25*, 5293.

36. Artursson, P.; Lindmark, T.; Davis, S. S.; Illum, L. *Pharmaceutical Research* **1994**, *11*, 1358.

37. Roy, K.; Mao, H.-Q.; Huang, S. K.; Leong, K. W. *Nat Med* **1999**, *5*, 387.

38. Liu, X. D.; Howard, K. A.; Dong, M. D.; Andersen, M. O.; Rahbek, U. L.; Johnsen, M. G.; Hansen, O. C.; Besenbacher, F.; Kjems, J. *Biomaterials* **2007**, *28*, 1280.

39. Holzinger, M.; Bouffier, L.; Villalonga, R.; Cosnier, S. *Biosensors and Bioelectronics* **2009**, *24*, 1128.

40. Menuel, S.; Fontanay, S.; Clarot, I.; Duval, R. E.; Diez, L.; Marsura, A. *Bioconjugate Chemistry* **2008**, *19*, 2357.

41. Srinivasachari, S.; Fichter, K. M.; Reineke, T. M. *Journal of the American Chemical Society* **2008**, *130*, 4618.

42. Davis, M. E.; Brewster, M. E. *Nat Rev Drug Discov* **2004**, *3*, 1023.

43. Davis, M. E. *Molecular Pharmaceutics* **2009**, *6*, 659.

44. Srinivasachari, S.; Reineke, T. M. *Biomaterials* **2009**, *30*, 928.

45. Liu, Y.; Reineke, T. M. *Bioconjugate Chemistry* **2005**, *17*, 101.

46. Liu, Y.; Reineke, T. M. *Bioconjugate Chemistry* **2006**, *18*, 19.

47. Srinivasachari, S.; Liu, Y.; Zhang, G.; Prevette, L.; Reineke, T. M. *Journal of the American Chemical Society* **2006**, *128*, 8176.

48. Srinivasachari, S.; Liu, Y.; Prevette, L. E.; Reineke, T. M. *Biomaterials* **2007**, *28*, 2885.

49. Gullotti, E.; Yeo, Y. *Molecular Pharmaceutics* **2009**, *6*, 1041.

50. Suh, W.; Chung, J.-K.; Park, S.-H.; Kim, S. W. *Journal of Controlled Release* **2001**, *72*, 171.

51. Mok, H.; Park, T. G. *Macromolecular Bioscience* **2009**, *9*, 731.

52. Wu, G.; Barth, R. F.; Yang, W.; Chatterjee, M.; Tjarks, W.; Ciesielski, M. J.; Fenstermaker, R. A. *Bioconjugate Chemistry* **2003**, *15*, 185.

53. Qian, Z. M.; Li, H.; Sun, H.; Ho, K. *Pharmacol Rev* **2002**, *54*, 561.

54. Zugates, G. T.; Anderson, D. G.; Little, S. R.; Lawhorn, I. E. B.; Langer, R. *Journal of the American Chemical Society* **2006**, *128*, 12726.

55. W Suh, S. H., L Yu, SW Kim *Molecular Therapy* **2002**, *6*, 664.

56. Dharap, S. S.; Wang, Y.; Chandna, P.; Khandare, J. J.; Qiu, B.; Gunaseelan, S.; Sinko, P. J.; Stein, S.; Farmanfarmaian, A.; Minko, T. *Proceedings of the National Academy of Sciences of the United States of America* **2005**, *102*, 12962.

57. Kim, S. H.; Jeong, J. H.; Lee, S. H.; Kim, S. W.; Park, T. G. *Bioconjugate Chemistry* **2008**, *19*, 2156.

58. Cho, K. C.; Kim, S. H.; Jeong, J. H.; Park, T. G. *Macromolecular Bioscience* **2005**, *5*, 512.

59. Zhang, Y.; Holley, A. C.; Guo, Y.; Huang, F.; McCormick, C. L. *Biomacromolecules* **2009**, *10*, 936.

60. Buskas, T.; Ingale, S.; Boons, G.-J. *Angewandte Chemie International Edition* **2005**, *44*, 5985.

61. Ferkol, T.; Perales, J. C.; Mularo, F.; Hanson, R. W. *Proceedings of the National Academy of Sciences of the United States of America* **1996**, *93*, 101.

62. Lim, D. W.; Yeom, Y. I.; Park, T. G. *Bioconjugate Chemistry* **2000**, *11*, 688.

63. McNamara, J. O.; Andrechek, E. R.; Wang, Y.; Viles, K. D.; Rempel, R. E.; Gilboa, E.; Sullenger, B. A.; Giangrande, P. H. *Nat Biotech* **2006**, *24*, 1005.

64. Li, J.-M.; Wang, Y.-Y.; Zhao, M.-X.; Tan, C.-P.; Li, Y.-Q.; Le, X.-Y.; Ji, L.-N.; Mao, Z.-W. *Biomaterials* **2012**, *33*, 2780.

65. Jung, J.; Solanki, A.; Memoli, K. A.; Kamei, K.-i.; Kim, H.; Drahl, M. A.; Williams, L. J.; Tseng, H.-R.; Lee, K. *Angewandte Chemie* **2010**, *122*, 107.

66. Yezhelyev, M. V.; Qi, L.; O'Regan, R. M.; Nie, S.; Gao, X. *Journal of the American Chemical Society* **2008**, *130*, 9006.

67. Alabi, C. A.; Love, K. T.; Sahay, G.; Stutzman, T.; Young, W. T.; Langer, R.; Anderson, D. G. *ACS Nano* **2012**, *6*, 6133.

68. Moore, A. and Z. Medarova *Methods Mol Biol* **2009,** *487*, 93-110.

69. Bryson, J. M.; Fichter, K. M.; Chu, W.-J.; Lee, J.-H.; Li, J.; Madsen, L. A.; McLendon, P. M.; Reineke, T. M. *Proceedings of the National Academy of Sciences* **2009**.

70. Kelkar, S. S.; Xue, L.; Turner, S. R.; Reineke, T. M. *Biomacromolecules* **2014**, *15*, 1612.

71. Kamaly, N.; Kalber, T.; Ahmad, A.; Oliver, M. H.; So, P.-W.; Herlihy, A. H.; Bell, J. D.; Jorgensen, M. R.; Miller, A. D. *Bioconjugate Chemistry* **2007**, *19*, 118.

72. Dykxhoorn, D. M.; Novina, C. D.; Sharp, P. A. *Nat. Rev. Mol. Cell Biol.* **2003,** 4, (6), 457-467.

73. Hammond, S. M.; Caudy, A. A.; Hannon, G. J. *Nat. Rev. Genet.* **2001,** 2, (2), 110-119.

74. Whitehead, K. A.; Langer, R.; Anderson, D. G. *Nat. Rev. Drug Discov.* **2009,** 8, (2), 129-138.

75. Reischl, D.; Zimmer, A. *Nanomedicine* **2009,** 5, (1), 8-20.

76. Tseng, Y.-C.; Mozumdar, S.; Huang, L. *Adv. Drug Deliv. Rev.* **2009,** 61, (9), 721-731.

77. Herrero, M. A.; Toma, F. M.; Al-Jamal, K. T.; Kostarelos, K.; Bianco, A.; Da Ros, T.; Bano, F.; Casalis, L.; Scoles, G.; Prato, M. *J. Am. Chem. Soc.* **2009,** 131, (28), 9843-9848.

78. de Fougerolles, A.; Vornlocher, H.-P.; Maraganore, J.; Lieberman, J. *Nat. Rev. Drug Discov.* **2007,** 6, (6), 443-453.

79. Ding, W.; Hattori, Y.; Qi, X.; Kitamoto, D.; Maitani, Y. *Chem. Pharm. Bull.* **2009,** 57, (2), 138-143.

80. Gao, K.; Huang, L. *Mol. Pharm.* **2008,** 6, (3), 651-658.

81. Jiang, H.-L.; Kwon, J.-T.; Kim, E.-M.; Kim, Y.-K.; Arote, R.; Jere, D.; Jeong, H.-J.; Jang, M.-K.; Nah, J.-W.; Xu, C.-X.; Park, I.-K.; Cho, M.-H.; Cho, C.-S. *J Control Release* **2008,** 131, (2), 150-157.

82. Mintzer, M. A.; Simanek, E. E. *Chem. Rev.* **2008,** 109, (2), 259-302.

83. Boussif, O.; Lezoualc'h, F.; Zanta, M. A.; Mergny, M. D.; Scherman, D.; Demeneix, B.; Behr, J. P. *Proc. Natl. Acad. Sci. U.S.A.* **1995,** 92, (16), 7297-7301.

84. Werth, S.; Urban-Klein, B.; Dai, L.; Höbel, S.; Grzelinski, M.; Bakowsky, U.; Czubayko, F.; Aigner, A. *J Control. Release* **2006,** 112, (2), 257-270.

85. Davis, M. E. *Mol. Pharm.* **2009,** 6, (3), 659-668.

86. Srinivasachari, S.; Liu, Y.; Prevette, L. E.; Reineke, T. M. *Biomaterials* **2007,** 28, (18), 2885-2898.

87. Srinivasachari, S.; Reineke, T. M. *Biomaterials* **2009,** 30, (5), 928-938.

88. Lee, C. -C.; Liu, Y.; Reineke, T. M. Bioconjugate Chem. 2008, 19, 428-440.

89. Srinivasachari, S.; Liu, Y.; Zhang, G.; Prevette, L.; Reineke, T. M. *J. Am. Chem. Soc.* **2006,** 128, (25), 8176-8184.

90. Liu, Y.; Reineke, T. M. *J. Am. Chem. Soc.* **2005,** 127, (9), 3004-3015.

91. Liu, Y.; Wenning, L.; Lynch, M.; Reineke, T. M. *J. Am. Chem. Soc*. **2004,** 126, (24), 7422-7423.

92. Smith, A. E.; Sizovs, A.; Grandinetti, G.; Xue, L.; Reineke, T. M. *Biomacromolecules* **2011,** 12, (8), 3015-3022.

93. Scholz, C.; Wagner, E. *J Control Release* **2012,** 161, (2), 554-565.

94. Schallon, A.; Synatschke, C. V.; Jérôme, V.; Müller, A. H. E.; Freitag, R. *Biomacromolecules* **2012,** 13, (11), 3463-3474.

95. Salcher, E. E.; Kos, P.; Fröhlich, T.; Badgujar, N.; Scheible, M.; Wagner, E. J Controlled Release, 2012, 164, (3), 380-386.

96. Fröhlich, T.; Edinger, D.; Kläger, R.; Troiber, C.; Salcher, E.; Badgujar, N.; Martin, I.; Schaffert, D.; Cengizeroglu, A.; Hadwiger, P.; Vornlocher, H.-P.; Wagner, E. *J Control Release* **2012,** 160, (3), 532-541.

97. Liu, Y.; Wenning, L.; Lynch, M.; Reineke Theresa, M., Gene Delivery with Novel Poly(l-tartaramidoamine)s. In *Polymeric Drug Delivery I*, American Chemical Society: 2006; Vol. 923, pp 217-227.

98. Srinivasachari, S., Fichter, K. M., Reineke, T. M. *J. Am. Chem. Soc*. **2008,** 130, 4618-4627.

99. Grandinetti, G.; Reineke, T. M. *Mol. Pharm.* **2012,** 9, (8), 2256–2267.

100. Kwok, A.; Hart, S. L. *Nanomedicine* **2011,** 7, (2), 210-219.

101. Liu, Y., and Reineke, T. M. J. Am. Chem. Soc. 2005, 127, 3004-3015.

102. Reineke, T. M.; Davis, M. E., 9.26 - Nucleic Acid Delivery via Polymer Vehicles. In *Polymer Science: A Comprehensive Reference*, Editors-in-Chief: Krzysztof, M.; Martin, M., Eds. Elsevier: Amsterdam, 2012; pp 497-527.

103. Prevette, L. E., Kodger, T. E., Reineke, T. M., Lynch, M. L. *Langmuir* **2007,** 23, (19), 9773-9784.

104. Prevette, L. E.; Lynch, M. L.; Kizjakina, K.; Reineke, T. M. *Langmuir* **2008,** 24, (15), 8090-8101.

105. Boeckle, S.; von Gersdorff, K.; van der Piepen, S.; Culmsee, C.; Wagner, E.; Ogris, M. *J Gene Med* **2004,** 6, (10), 1102-1111.

106. Yancey, P. G.; Rodrigueza, W. V.; Kilsdonk, E. P. C.; Stoudt, G. W.; Johnson, W. J.; Phillips, M. C.; Rothblat, G. H. *J. Biol. Chem.* **1996,** 271, (27), 16026-16034.

107. Rodal, S. K.; Skretting, G.; Garred, O.; Vilhardt, F.; van Deurs, B.; Sandvig, K. *Mol. Biol. Cell* **1999,** 10, (4), 961-974.

108. van der Aa, M. A. E. M.; Huth, U. S.; Hafele, S. Y.; Schubert, R.; Oosting, R. S.; Mastrobattista, E.; Hennink, W. E.; Peschka-Suss, R.; Koning, G. A.; Crommelin, D. J. A. *Pharm. Res.* **2007,** 24, (8), 1590-1598.

109. Kline, M. A.; O'Connor Butler, E. S.; Hinzey, A.; Sliman, S.; Kotha, S. R.; Marsh, C. B.; Uppu, R. M.; Parinandi, N. L., Methods Mol. Biol. 2010, 610, 201-211.

110. Malmo, J.; Sørgård, H.; Vårum, K. M.; Strand, S. P. *J Controlled Release* **2012,** 158, (2), 261-268.

111. Knop, K.; Hoogenboom, R.; Fischer, D.; Schubert, U. S. *Angewandte Chemie International Edition* **2010**, *49*, 6288.

112. Ting, S. R. S.; Chen, G.; Stenzel, M. H. *Polymer Chemistry* **2010**, *1*, 1392.

113. Götz, H.; Harth, E.; Schiller, S. M.; Frank, C. W.; Knoll, W.; Hawker, C. J. *Journal of Polymer Science Part A: Polymer Chemistry* **2002**, *40*, 3379.

114. Matyjaszewski, K.; Xia, J. *Chemical Reviews* **2001**, *101*, 2921.

115. Moad, G.; Rizzardo, E.; Thang, S. H. *Australian Journal of Chemistry* **2005**, *58*, 379.

116. Ahmed, M.; Deng, Z.; Liu, S.; Lafrenie, R.; Kumar, A.; Narain, R. *Bioconjugate Chemistry* **2009**, *20*, 2169.

117. Albertin, L.; Stenzel, M.; Barner-Kowollik, C.; Foster, L. J. R.; Davis, T. P. *Macromolecules* **2004**, *37*, 7530.

118. Wu, Y.; Wang, M.; Sprouse, D.; Smith, A. E.; Reineke, T. M. *Biomacromolecules* **2014**, *15*, 1716.

119. Roy, A.; Kim, Y.-B.; Cho, K. H.; Kim, J.-H. *Biochimica et Biophysica Acta (BBA) - General Subjects*.

120. Paneni, F.; Costantino, S.; Cosentino, F. *Curr Atheroscler Rep* **2014**, *16*, 1.

121. Teramoto, N.; Sachinvala, N.; Shibata, M. *Molecules* **2008**, *13*, 1773.

122. Benaroudj, N.; Lee, D. H.; Goldberg, A. L. *J. Biol. Chem.* **2001**, *276*, 24261.

123. Hagen, S. J.; Hofrichter, J.; Eaton, W. A. *Science* **1995**, *269*, 959.

124. Clegg, J. S.; Seitz, P.; Seitz, W.; Hazlewood, C. F. *Cryobiology* **1982**, *19*, 306.

125. Adams, R. P.; Kendall, E.; Kartha, K. *Biochem. Syst. Ecol.* **1990**, *18*, 107.

126. Ramlov, H.; Westh, P. *Cryobiology* **1992**, *29*, 125.

127. Sømme, L. *Eur. J. Entomol.* **1996**, *93*, 349.

128. Du, J.; Liang, Y.; Xu, F.; Sun, B.; Wang, Z. *Journal of Pharmacy and Pharmacology* **2013**, *65*, 1753.

129. Autiero, I.; Langella, E.; Saviano, M. *Molecular BioSystems* **2013**, *9*, 2835.

130. Crowe, J. H.; Crowe, L. M.; Oliver, A. E.; Tsvetkova, N.; Wolkers, W.; Tablin, F. *Cryobiology* **2001**, *43*, 89.

131. Srinivasachari, S.; Liu, Y.; Zhang, G.; Prevette, L.; Reineke, T. M. *J. Am. Chem. Soc.* **2006**, *128*, 8176.

132. Xue, L.; Ingle, N. P.; Reineke, T. M. *Biomacromolecules* **2013**, *14*, 3903.

133. Tseng, W. C.; Tang, C. H.; Fang, T. Y.; Su, L. Y. *Biotechnol. Prog.* **2007**, *23*, 1297.

134. Sarkar, S.; Davies, J. E.; Huang, Z.; Tunnacliffe, A.; Rubinsztein, D. C. *J. Biol. Chem.* **2007**, *282*, 5641.

135. Casarejos, M.; Solano, R.; Gómez, A.; Perucho, J.; de Yébenes, J.; Mena, M. *Neurochem. Int.* **2011**.

136. Wada, M.; Miyazawa, Y.; Miura, Y. *Polym. Chem.* **2011**, *2*, 1822.

137. Mancini, R. J.; Lee, J.; Maynard, H. D. *J. Am. Chem. Soc.* **2012**, *134*, 8474.

138. Crowe, J. H.; Carpenter, J. F.; Crowe, L. M. *Annu. Rev. Physiol.* **1998**, *60*, 73.

139. Jensen, R. L.; Chkheidze, R. *Tumors of the Central Nervous System* **2011**, *1*, 99.

140. MacLaughlin, F. C.; Mumper, R. J.; Wang, J.; Tagliaferri, J. M.; Gill, I.; Hinchcliffe, M.; Rolland, A. P. *J Control Release* **1998**, *56*, 259.

141. Branca, C.; Magazù, S.; Maisano, G.; Migliardo, F.; Migliardo, P.; Romeo, G. *J Phys Chem B* **2001**, *105*, 10140.

142. Freed, K. F.; Edwards, S. *J Chem Phys* **1974**, *61*, 3626.

143. Uhlmann, D. *J Non Cryst Solids* **1972**, *7*, 337.

144. Buckwalter, D. J.; Sizovs, A.; Ingle, N. P.; Reineke, T. M. *ACS Macro Lett* **2012**, *1*, 609.

145. Manel, N.; Kim, F. J.; Kinet, S.; Taylor, N.; Sitbon, M.; Battini, J. L. *Cell* **2003**, *115*, 449.

146. Elsas, L. J.; Longo, N. *Annu. Rev. Med.* **1992**, *43*, 377.

147. Airley, R.; Loncaster, J.; Davidson, S.; Bromley, M.; Roberts, S.; Patterson, A.; Hunter, R.; Stratford, I.; West, C. *Clin. Cancer Res.* **2001**, *7*, 928.

148. Airley, R. E.; Loncaster, J.; Raleigh, J. A.; Harris, A. L.; Davidson, S. E.; Hunter, R. D.; West, C. M. L.; Stratford, I. J. *Int. J. Cancer* **2003**, *104*, 85.

149. Jensen, R. L. *J. Neurooncol.* **2009**, *92*, 317.

150. Yu, B.; Zhao, X.; Lee, L. J.; Lee, R. J. *AAPS J* **2009**, *11*, 195.

151. Hammond, S. M.; Caudy, A. A.; Hannon, G. J. *Nat Rev Genet* **2001**, *2*, 110.

152. Dorsett, Y.; Tuschl, T. *Nat Rev Drug Discov* **2004**, *3*, 318.

153. de Fougerolles, A.; Vornlocher, H. P.; Maraganore, J.; Lieberman, J. *Nature Reviews Drug Discovery* **2007**, *6*, 443.

154. Tang, X.; Maegawa, S.; Weinberg, E. S.; Dmochowski, I. J. *Journal of the American Chemical Society* **2007**, *129*, 11000.

155. Soutschek, J.; Akinc, A.; Bramlage, B.; Charisse, K.; Constien, R.; Donoghue, M.; Elbashir, S.; Geick, A.; Hadwiger, P.; Harborth, J.; John, M.; Kesavan, V.; Lavine, G.; Pandey, R. K.; Racie, T.; Rajeev, K. G.; Rohl, I.; Toudjarska, I.; Wang, G.; Wuschko, S.; Bumcrot, D.; Koteliansky, V.; Limmer, S.; Manoharan, M.; Vornlocher, H.-P. *Nature* **2004**, *432*, 173.

156. Whitehead, K. A.; Langer, R.; Anderson, D. G. *Nature Reviews Drug Discovery* **2009**, *8*, 516.

157. Robbins, M.; Judge, A.; Maclachlan, I. *Oligonucleotides* **2009**, *19*, 89.

158. Reischl, D.; Zimmer, A. *Nanomedicine* **2009**, *5*, 8.

159. Tseng, Y. C.; Mozumdar, S.; Huang, L. *Adv Drug Deliv Rev* **2009**.

160. Naldini, L.; Blomer, U.; Gallay, P.; Ory, D.; Mulligan, R.; Gage, F. H.; Verma, I. M.; Trono, D. *Science* **1996**, *272*, 263.

161. Zimmermann, T. S.; Lee, A. C.; Akinc, A.; Bramlage, B.; Bumcrot, D.; Fedoruk, M. N.; Harborth, J.; Heyes, J. A.; Jeffs, L. B.; John, M.; Judge, A. D.; Lam, K.; McClintock, K.; Nechev, L. V.; Palmer, L. R.; Racie, T.; Rohl, I.; Seiffert, S.; Shanmugam, S.; Sood, V.; Soutschek, J.; Toudjarska, I.; Wheat, A. J.; Yaworski, E.; Zedalis, W.; Koteliansky, V.; Manoharan, M.; Vornlocher, H. P.; MacLachlan, I. *Nature* **2006**, *441*, 111.

162. Oishi, M.; Nagasaki, Y.; Itaka, K.; Nishiyama, N.; Kataoka, K. *Journal of the American Chemical Society* **2005**, *127*, 1624.

163. Kumar, P.; Wu, H.; McBride, J. L.; Jung, K.-E.; Hee Kim, M.; Davidson, B. L.; Kyung Lee, S.; Shankar, P.; Manjunath, N. *Nature* **2007**, *448*, 39.

164. Liu, F.-F.; Ji, L.; Dong, X.-Y.; Sun, Y. *The Journal of Physical Chemistry B* **2009**, *113*, 11320.

165. Pérez-Moral, N.; Adnet, C. l.; Noel, T. R.; Parker, R. *Biomacromolecules* **2010**, *11*, 2985.

166. Imamura, K.; Murai, K.; Korehisa, T.; Shimizu, N.; Yamahira, R.; Matsuura, T.; Tada, H.; Imanaka, H.; Ishida, N.; Nakanishi, K. *Journal of Pharmaceutical Sciences* **2014**, *103*, 1628.

167. Dráber, P.; Sulimenko, V.; Sulimenko, T.; Dráberová, E. In *Protein Downstream Processing*; Labrou, N. E., Ed.; Humana Press: 2014; Vol. 1129, p 443.

168. Tonnis, W. F.; Amorij, J. P.; Vreeman, M. A.; Frijlink, H. W.; Kersten, G. F.; Hinrichs, W. L. J. *European Journal of Pharmaceutical Sciences* **2014**, *55*, 36.

169. Men, N. T.; Kikuchi, K.; Nakai, M.; Fukuda, A.; Tanihara, F.; Noguchi, J.; Kaneko, H.; Linh, N. V.; Nguyen, B. X.; Nagai, T.; Tajima, A. *Theriogenology* **2013**, *80*, 1033.

170. Tseng, W.-C.; Tang, C.-H.; Fang, T.-Y.; Su, L.-Y. *Biotechnology Progress* **2007**, *23*, 1297.

171. Sizovs, A.; Xue, L.; Tolstyka, Z. P.; Ingle, N. P.; Wu, Y.; Cortez, M.; Reineke, T. M. *Journal of the American Chemical Society* **2013**, *135*, 15417.

172. Chen, G.; Qiu, H.; Prasad, P. N.; Chen, X. *Chemical Reviews* **2014**.

173. Fan, Z.; Senapati, D.; Singh, A. K.; Ray, P. C. *Molecular Pharmaceutics* **2012**, *10*, 857.

174. Bardhan, R.; Lal, S.; Joshi, A.; Halas, N. J. *Accounts of Chemical Research* **2011**, *44*, 936.

175. Murgia, S.; Bonacchi, S.; Falchi, A. M.; Lampis, S.; Lippolis, V.; Meli, V.; Monduzzi, M.; Prodi, L.; Schmidt, J.; Talmon, Y.; Caltagirone, C. *Langmuir* **2013**, *29*, 6673.

176. Santra, S.; Perez, J. M. *Biomacromolecules* **2011**, *12*, 3917.

177. Guo, Y.; Chen, W.; Wang, W.; Shen, J.; Guo, R.; Gong, F.; Lin, S.; Cheng, D.; Chen, G.; Shuai, X. *ACS Nano* **2012**, *6*, 10646.

178. Liu, Q.; Zhu, H.; Qin, J.; Dong, H.; Du, J. *Biomacromolecules* **2014**, *15*, 1586.

179. Jokerst, J. V.; Gambhir, S. S. *Accounts of Chemical Research* **2011**, *44*, 1050.

180. Helms, V. *Principles of Computational Cell Biology*; Wiley, 2008.

181. Zheng, J. In *Ion Channels*; Stockand, J., Shapiro, M., Eds.; Humana Press: 2006; Vol. 337, p 65.

182. Jiang, R.; Lu, X.; Yang, M.; Deng, W.; Fan, Q.; Huang, W. *Biomacromolecules* **2013**, *14*, 3643.

183. Schneider, S.; Lenz, D.; Holzer, M.; Palme, K.; Süss, R. *Journal of Controlled Release* **2010**, *145*, 289.

184. Croissant, J.; Chaix, A.; Mongin, O.; Wang, M.; Clément, S.; Raehm, L.; Durand, J.-O.; Hugues, V.; Blanchard-Desce, M.; Maynadier, M.; Gallud, A.; Gary-Bobo, M.; Garcia, M.; Lu, J.; Tamanoi, F.; Ferris, D. P.; Tarn, D.; Zink, J. I. *Small* **2014**, *10*, 1752.

185. Gautier, I.; Tramier, M.; Durieux, C.; Coppey, J.; Pansu, R. B.; Nicolas, J. C.; Kemnitz, K.; Coppey-Moisan, M. *Biophysical Journal* **2001**, *80*, 3000.

186. Domingo, B.; Sabariegos, R.; Picazo, F.; Llopis, J. *Microscopy Research and Technique* **2007**, *70*, 1010.

187. Kim, H.; Ng, C. Y. W.; Algar, W. R. *Langmuir* **2014**, *30*, 5676.

188. Bryson, J. M.; Fichter, K. M.; Chu, W.-J.; Lee, J.-H.; Li, J.; Madsen, L. A.; McLendon, P. M.; Reineke, T. M. *Proceedings of the National Academy of Sciences* **2009**.

189. Alabi, C. A.; Love, K. T.; Sahay, G.; Stutzman, T.; Young, W. T.; Langer, R.; Anderson, D. G. *ACS Nano* **2012**, *6*, 6133.

190. Endres, T.; Zheng, M.; Kılıç, A.; Turowska, A.; Beck-Broichsitter, M.; Renz, H.; Merkel, O. M.; Kissel, T. *Molecular Pharmaceutics* **2014**, *11*, 1273.

191. Liu, Y.; Reineke, T. M. *Bioconjugate Chemistry* **2006**, *17*, 101.

192. Srinivasachari, S.; Reineke, T. M. *Biomaterials* **2009**, *30*, 928.